ISSN-0039-2502

Journal of the Association of Lunar & Planetary Observers

The Strolling Astronomer

ALPO – Association of Lunar & Planetary Observers
Founded in 1947

Volume 63, Number 2 Spring 2021

Now in Portable Document Format (PDF) for
Macintosh and PC-compatible computers
Online and in COLOR at http://www.alpo-astronomy.org

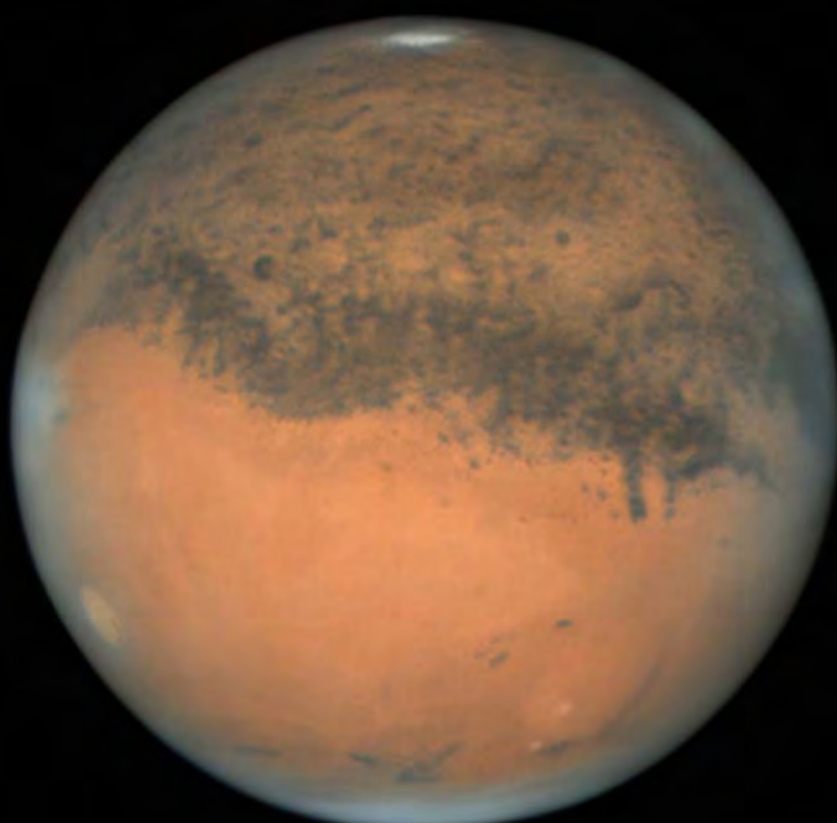

Mars: Almost within arm's reach
(See page 3 for image details.)

CELESTRON

THE FINISHING TOUCHES

Your telescope setup is as unique as you are. Take it to the next level by adding some of **Celestron's latest accessories.**

NEW! ULTIMA EDGE™

FLAT FIELD EYEPIECES

See the whole picture with the Ultima Edge. The proprietary lens configuration ensures a flat, clear image all the way to the edge of the field of view. All five models have fully multi-coated lenses, and all but one are parfocal, so there's no need to refocus when switching between them. Available in 10mm, 15mm, 18mm, 24mm and 30mm focal lengths.

NEW! TELESCOPE AND TRIPOD

CARRYING BAGS

Keep your telescope protected and arrive in style with this **NEW** line of custom bags designed to fit your optical tube, accessories, and tripod perfectly.

HIGH-TECH ACCESSORIES

STARSENSE AUTOALIGN

Automatically align your computerized telescope to the night sky in about 3 minutes with no user input needed.

SKYPORTAL WIFI MODULE

Control your telescope wirelessly via the SkyPortal mobile app for your smartphone or tablet.

POWERTANK LITHIUM

PORTABLE BATTERIES

Power your telescope for up to 17 hours with our safe, reliable line of rechargeable lithium batteries.

Explore all our telescope accessories at celestron.com/accessories

CELESTRON PREMIER SELECT DEALERS

B&H Photo – 800.947.9970 – bhphotovideo.com
High Point Scientific – 800.266.9590 – highpointscientific.com
Optics Planet – 800.504.5897 – opticsplanet.com
Astronomics – 800.422.7876 – astronomics.com
OPT Telescopes – 800.483.6287 – optcorp.com
Woodland Hills – 888.427.8766 – telescopes.net
Adorama – 800.223.2500 – adorama.com
Focus Camera – 800.221.0828 – focuscamera.com
Agena AstroProducts – 562.215.4473 – agenaastro.com

Journal of the Association of Lunar & Planetary Observers

The Strolling Astronomer

Volume 63, No.2, Spring 2021
This issue published in March 2021 for distribution in both portable document format (pdf) and hardcopy format. Hard copy printing and distribution by Sheridan Press.

This publication is the official journal of the Association of Lunar & Planetary Observers (ALPO).

The purpose of this journal is to share observation reports, opinions, and other news from ALPO members with other members and the professional astronomical community.

© 2021, Association of Lunar & Planetary Observers (ALPO). The ALPO hereby grants permission to educators, academic libraries and the professional astronomical community to photocopy material for educational or research purposes as required. There is no charge for these uses provided that credit is given to *The Strolling Astronomer*, the "JALPO" or the ALPO itself. All others must request permission from the ALPO.

For membership or general information about the ALPO, contact:

Matthew Will
ALPO Membership Secretary/Treasurer
P.O. Box 13456
Springfield, Illinois 62791-3456

E-mail to: matt.will@alpo-astronomy.org

Visit the ALPO online at:
http://www.alpo-astronomy.org

Founded in 1947

Inside the ALPO

Papers & Presentations

ALPO Resources

Inside the ALPO
Member, section and activity news

Association of Lunar & Planetary Observers (ALPO)

Founded by Walter H. Haas, 1947

Board of Directors

Executive Director (Chair); Julius L. Benton, Jr.
Associate Executive Director; Carl Hergenrother
Member of the Board; Sanjay Limaye
Member of the Board; Ken Poshedly
Member of the Board; Timothy J. Robertson
Member of the Board; Richard W. Schmude, Jr.
Member of the Board & Secretary/Treasurer; Matthew Will

Primary Interest Section & Observing Section Staff

(See full listing in *ALPO Resources*)
Publications: Ken Poshedly
Online Section: Larry Owens
Outreach Section:
Lunar& Planetary Training, Timothy J. Robertson
YouTube Channel & Podcasts, Timothy J. Robertson
Youth Activities, Pamela Shivak
Eclipse Section: Keith Spring
Mercury & Venus Transit Section: Keith Spring
Meteors Section: Robert D. Lunsford
Meteorites Section: Dolores Hill
Comets Section: Carl Hergenrother
Solar Section: Rik Hill
Mercury Section: Frank Melillo
Venus Section: Julius L. Benton, Jr.
Mercury/Venus Transit Section: Keith Spring
Lunar Section:
Lunar Topographical Studies & Selected Areas Program; David Teske
Lunar Meteoritic Impact Search; Brian Cudnik
Lunar Transient Phenomena; Anthony Cook
Lunar Domes Studies Program, Raffaello Lena
Mars Section: Roger Venable
Minor Planets Section: Frederick Pilcher
Jupiter Section: (Open)
Saturn Section: Julius L. Benton, Jr.
Remote Planets Section: Richard W. Schmude, Jr.
Exoplanets Section: Jerry Hubbell

Point of View:

Who Writes for the Journal? You Do!

By Ken Poshedly, coordinator, ALPO Publications Section

Regular readers of this Journal — at least those of you who read more than just a page or two — are surely familiar with the names Julius Benton, Richard Schmude, Rik Hill and Raffaello Lena. And that's because they are the ones who consistently provide you, the membership, with top-notch apparition reports, which is pretty much the bread-and-butter of this Journal's content.

Julius, besides serving as our current executive director, is head of both the Venus and the Saturn observing sections. Richard Schmude also heads two observing sections, that is, the Jupiter Section and the Remote Planets Section. And Rik Hill? Well, even though he heads only the ALPO Solar Section, that's also a mighty task. Take a look at the extremely detailed descriptions and interpretations he offers in this issue with his report on Carrington Rotations 2231 thru 2235. Raffaello, a geologist by profession, and his assistant Jim Phillips, a retired physician, consistently provide us with extremely scientific analysis of those itty-bitty lunar domes.

But this time, we include works by others whose names may not be familiar to you:

- In his "Personal Reflections on Observational Astronomy", Stephen Tzikas, a chemical engineer who enjoys radio astronomy and who first came upon the scene in the ALPO when he completed our Lunar & Planetary Training Program under Tim Robertson, tells us how he approaches an observing session, from the kind of equipment he uses to the observing techniques he uses. Is it just "find something and then move on"? Nope, not Steve. He actually observes and sketches. Now THERE'S a time-taker if there ever was one. And the sketches he produces are most dazzling. See what you think.
- Darryl Wilson, a retired scientist, became interested in astronomy at the age of 12 and still has his observing log from that time when his equipment consisted of a Jason-Empire 60 mm refractor on an alt-azimuth mount. He has been an affiliate faculty member with the Physics and Astronomy Department at George Mason University since 2011. In this Journal, Darryl offers the third in a series of papers on "Basic Interpretation and Analysis of Lunar Thermal Images" — what may become the next step in lunar imaging techniques for amateurs, given the right equipment, of course.
- And finally, we have Richard Wilds, a member of both the ALPO and IOTA (the Intl. Occultation Timing Assn), whose scholarly work in this issue details to the smallest degree with "luna incognita". Hint: get your cup of coffee ready and be prepared for an in-depth look at grazing occultations of the Moon.

So you see? Our pages are open to all who have papers of interest to we, the Earthbound observers of the solar system.

Inside the ALPO
Member, section and activity news

News of General Interest

Our Cover: A Most Attractive Mars

By Roger Venable, coordinator, ALPO Mars Section

Our cover image of Mars for this issue of your Journal was made by Damian Peach with the assistance of the Chilescope team on October 17, 2020, centered on 03:06 UT. The opposition of Mars was three days earlier and closest approach was 11 days earlier. The apparent subtended diameter of the planet was 22.1 seconds of arc when this image was made. South is up and east is to the left.

The image shows the white South Polar Cap at the top of the image to be nearing its smallest residual size, as Mars was in early southern summer (LS = 298°). Near the lower left edge of the image is a bright oval corresponding to Olympus Mons, the largest volcano in the Solar System. It is bright due to mild frosting on its upper slopes. Many of the speckles in the darker, southern (upper) half of the planet are impact craters, and many of them have names that can be individually identified if you have a detailed geological map of the planet.

The dark, irregular streak across the middle of the planet comprises Mare Sirenum on the left, Mare Cimmerium in the center and Mare Tyrrhenum on the far right. The blue-white North Polar Hood, a dense cloud that covers the North Polar Region during its winter, is prominent at the bottom of the image. At the middle of the left, afternoon edge of the image there is a cloud composed of water-ice particles, typical of the late afternoon clouds that are often visible.

Pranvera Hyseni, recipient of the first *Michael D. Reynolds Astronomy Award* "In Appreciation and Recognition for Your Outstanding Contributions to Further Worldwide Interest in Astronomy". Ms. Hyseni was our keynote speaker at the ALPO online conference held October 2 and 3. Her remarks included her efforts to establish an observatory and planetarium in her home country of Kosovo. A GoFundMe page has been established with the goal of raising funds for that facility. She is currently working towards her master's degree in astronomy at San Jose State University in California.

The entire right, morning edge of the planet shows a haze of the type that sublimates during the Martian morning. At the lower right are two small, bright spots. The larger one is Elysium Mons, and the other is Hecates Tholus, which are two immense volcanos in the Elysium area. To their upper left are three small dark spots that together compose Trivium Charontis. This trio conveyed the descriptor "Trivium" to the spots 125 years ago, though most Earth-based observations show them as a single spot, due to insufficient resolution.

The image shows remarkable detail, consistent with the use of the Chilescope in excellent seeing. This instrument is of the Richey-Chretien design, of 1-meter aperture, located at an altitude of 1,560 meters in the Andes Mountains, 330 kilometers north of Santiago, Chile. The Rayleigh resolution limit of the telescope is approximately 0.14 seconds of arc, while the use of its ASI290MM camera at 0.06 seconds of arc per pixel meets the Nyquist criterion for displaying maximum resolution. Accordingly, the resolution of detail in the image is about 0.14 seconds of arc, which corresponds to about 1 millimeter on the cover page. To make this image, Damian made images in infrared and blue over a period of about an hour. He made synthetic green images by combining the infrared and blue images and then used the *WinJUPOS* program to combine the images made at slightly different times, in the program's "derotation" method.

The Chilescope is available to amateur astronomers on a rental basis, and you can schedule observing time on it at https//chilescope.com.

Mars is also available to amateur astronomers, and if your sky is clear you do not need an appointment.

Inside the ALPO

Member, section and activity news

ALPO 2021 Conference News

By Tim Robertson & Ken Poshedly, ALPO Conference coordinators

Overview

Due to the continuing nearly worldwide quarantining caused by the Covid-19 pandemic, the 2021 Conference of the ALPO will be held online on Friday and Saturday, August 13 and 14. (This is to prevent a scheduling conflict with the 2021 Astronomical League Convention (ALCON 2021) which will be held in Albuquerque, NM, on August 4 thru 7, 2021.)

The ALPO conference times will be:

- Friday from 1 p.m. to 5 p.m. Eastern Time (10 a.m. to 2 p.m. Pacific Time)
- Saturday from 1 p.m. to 6 p.m. Eastern Time (10 a.m. to 3 p.m. Pacific Time).

The ALPO Conference is free and open to all via two different streaming methods:

- The free online conferencing software application, Zoom.
- On the ALPO YouTube channel at *https://www.youtube.com/channel/UCEmixiL-d5k2Fx27Ijfk41A*

Those who plan to present astronomy papers or presentations must (1) already be members of the ALPO, (2) use Zoom, and (3) have it already installed on their computer prior to the conference dates. Zoom is free and available at *https://zoom.us/*

Those who have not yet joined the ALPO may do so online, so as to qualify to present their work at this conference. Digital ALPO memberships start at only $18 a year. To join online, go to *http://www.astroleague.org/store/index.php?main_page=product_info&cPath=10&products_id=39*, then scroll to the bottom of that page, select your membership type, click on "Add to Cart" and proceed from there.

There will be different Zoom meeting hyperlinks to access the conference each of the two days of the conference. Both links will be posted on social media and e-mailed to those who wish to receive it that way on Thursday, August 12, 2021. The Zoom virtual (online) "meeting room" will open 15 minutes prior to the beginning of each day's activities.

Those individuals wishing to attend via Zoom should contact Tim Robertson at *cometman@cometman.net* as soon as possible.

Agenda

The conference will consist of initial welcoming remarks and general announcements at the beginning each day, followed by papers and research findings on astronomy-related topics presented by ALPO members.

Following a break after the last astronomy talk on Saturday will be presentations of the Walter Haas Observing Award, the Peggy Haas Service Award and the Michael D. Reynolds Astronomy Award. The last one is brand new and was presented to Ms. Pranvera Hyseni several months ago in recognition for her work over the past several years to advance the public's awareness and appreciation of astronomy.

A keynote speaker will then follow the awards presentations on Saturday. The selection of a keynote speaker is in progress and the final decision will be announced in the summer issue of this Journal (JALPO63-3).

Presentation Guidelines

All presentations should be no more than 15 minutes in length; the preferred method is 12 minutes for the presentation itself plus 3 minutes for follow-up questions. The preferred format is Microsoft PowerPoint.

Send all PowerPoint files of the presentations to Tim Robertson at *cometman@cometman.net* .

Suggested Topics

Participants are encouraged to present research papers and experience reports concerning various aspects of Earth-based observational astronomy including the following.

- New or ongoing observing programs and studies, specifically, how those programs were designed, implemented and continue to function.
- Results of personal or group studies of solar system or extra-solar system bodies.
- New or ongoing activities involving astronomical instrumentation, construction or improvement.
- Challenges faced by Earth-based observers such as changing interest levels, deteriorating observing conditions brought about by possible global warming, etc.

Information about paper presentations, the keynote speaker and other conference data will be published in this Journal and online as details are learned.

Search Continues for Jupiter Section Lead Coordinator

Interested individuals should contact the ALPO executive director for more information.

Inside the ALPO
Member, section and activity news

Hardcopy JALPO Issues Still Available

Please note that for those who still wish to add to their library of hardcopy ALPO Journals, we still have a healthy number of various issues left, some dating back to 1962. One oft overlooked thing about these early Journals is that they pre-date the age of satellite exploration of the Moon, the Sun, the planets and comets. Thus, the observing reports are full of the enthusiasm that comes with knowing that we were not competing with high tech gadgets already orbiting these celestial bodies.

And while the photos in those pages are crude when compared to the CCD and webcam images of today, the text captions that accompany them express how much work went into trying to squeeze out every little detail, no matter how grainy.

Please check the list of available issues in the back of this Journal to see what might suit your own interests.

ALPO Website Updates

Various announcements have been posted to the ALPO website home page.

Book Review Ideas Needed

Bob Garfinkle, our book review editor, states that it's been quite awhile that since he's received suggestions for an astronomy book review.

Surely there have been such books published over the past year or so. And it is Bob himself, who authored the highly prized three-volume "Luna Cognita" (available from Amazon at *https://www.amazon.com/Luna-Cognita-Comprehensive-Observers-Handbook/dp/1493916637*).

Bob can be reached via e-mail at *ragarf@earthlink.net*

Call for JALPO Papers

The ALPO encourages its members to submit written works (with images, if possible) for publication in this Journal.

As with other peer-reviewed publications, all papers will be forwarded to the appropriate observing section or interest section coordinator.

Thus, the best method is to send them directly to the coordinator of the ALPO section which handles your topic.

A complete list of ALPO section coordinators and their contact information can be found in the *ALPO Resources* section of this Journal.

ALPO Interest Section Reports

ALPO Online Section

Report by Jim Tomney, acting assistant section coordinator
jim@tomney.com

The ALPO website (*http://alpo-astronomy.org*) was up and available for the 4th quarter of 2020 (Oct-Dec) with no reported issues. During that time, approximately 40,000 visits were made to the website, with October being the busiest month with almost 17,000 visits (likely stimulated by the Mars opposition.)

Several updates to the content of various sections, such as documenting the change over from Yahoo groups to Groups.io were completed, as well as handling the discontinuation of Adobe Flash (which was used to upload images to the ALPO section galleries).

During this quarter, 41 observers from 10 different countries submitted 1,669 files representing their solar and major planet observations to the ALPO gallery.

We encourage everyone to continue to submit their observations for inclusion in the ALPO gallery by sending them to the appropriate e-mail address listed on the website's Gallery Submission Guidelines page (*http://www.alpo-astronomy.org/alpo/?page_id=952*). A crucial aspect of the guideline is for the file name to contain the UT date and time of the observation, since it is cumbersome and

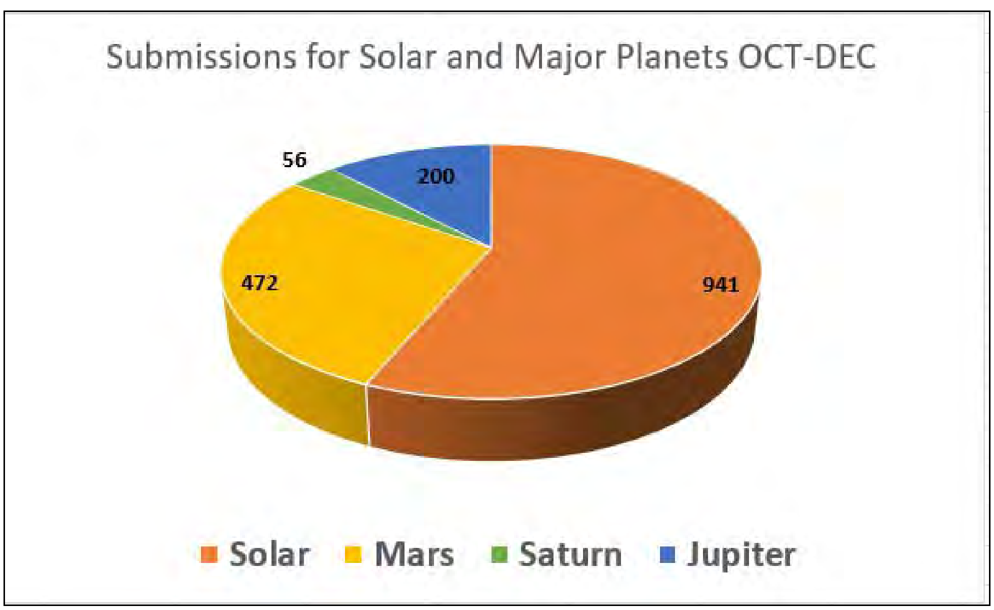

Inside the ALPO
Member, section and activity news

error-prone to locate that value by examining the image.

We are continuing to look at the website in terms of quality, seeking to do things such as correcting / removing links and outdated content. Section coordinators should let us know of any corrections or changes needed for their portion of the website. If any section coordinator needs an ID for your section's blog, contact Larry Owens at Larry.Owens@alpo-astronomy.org.

If you'd like to offer any comments or feedback about the site please reach out to the ALPO Online Section coordinators using the contact information found at *http://www.alpo-astronomy.org/alpo/?page_id=179*.

Follow us on Twitter, "friend" us on FaceBook or join us on MySpace.

Outreach Section

Lunar & Planetary Training Program

Report by Tim Robertson, program coordinator
cometman@cometman.net

The ALPO Training Program currently has four active students at various stages of the program.

The ALPO Lunar & Planetary Training Program is a two-step program, and there is no time requirement for completing the steps. I have seen that those students who are motivated usually complete the steps in a short amount of time. The motivation comes from the desire to improve their observing skills and contribute to the pages of the Journal of the ALPO.

This program is open to all members of the ALPO, beginner as well as the expert observer. The goal is to help make members proficient observers. The ALPO revolves around the submission of astronomical observations of members for the purposes of scientific research. Therefore, it is the responsibility of our organization to guide prospective contributors toward a productive and meaningful scientific observation.

The course of instruction for the Training Program is two-tiered:

- The first tier is the "Basic Level" and includes reading the *ALPO Novice Observers Handbook* and mastering the fundamentals of observing. These fundamentals include performing simple calculations and understanding observing techniques.
- When the student has successfully demonstrated these skills, he or she can advance to the "Novice Level" for further training where one can specialize in one or more areas of study. This includes obtaining and reading handbooks for specific lunar and planetary subjects. The novice then continues to learn and refine upon observing techniques specific to his or her area of study and is assigned to a tutor to monitor the novice's progress in the Novice Level of the program.

When the novice has mastered this final phase of the program, that person can then be certified to "Observer Status" for that particular field.

For more information on the ALPO Training Program, contact Tim Robertson at 195 Tierra Rejada Rd #148, Simi Valley CA, 93065; e-mail to cometman@cometman.net

YouTube & 'Observers Notebook' Podcasts

Report by Tim Robertson, program coordinator
cometman@cometman.net

The ALPO now has a *YouTube* channel continues to include instructional videos, lectures. We used it to livestream the ALPO 2020 Conference held last fall. Check it out and subscribe to the channel!

https://www.youtube.com/channel/UCEmixiL-d5k2Fx27Ijfk41A?

December 2020 was an interesting month for the *Observers Notebook* podcast. On 4 December, I posted an image on our Facebook page of the progression of the planetary conjunction between Jupiter and Saturn. On that date, the *Observers Notebook* Facebook page had just 110 members. That one image, however, was shared over 3,000 times, with over 237,000 people seeing the post.

Now (early 2021), we have over 440 members of that Facebook page, and our daily podcast downloads dramatically increased by over 20%.

The *Observers Notebook* podcast continues to remain strong. I have recorded over 115 podcasts with various members of the ALPO, mostly section coordinators to highlight the programs within each section. The length of the podcast averages around 30 minutes in length. The longest podcast thus far is over 1 hour and 30 minutes. But we can record longer, there is no time limit — the hosting service we use has unlimited space available for podcasts.

It takes a great amount of time and money to make and produce the podcast, thus far it has been done with the help of service called "Patreon", and

Inside the ALPO
Member, section and activity news

we currently have 12 supporters, two of which are NOT members of the ALPO!

We have two generous Patreon supporters who each donate $35 a month to the podcast. Thanks to Steve Siedentop and Michael Moyer for their generous support of the *Observers Notebook*.

You, too, can support the *Observers Notebook* podcast by giving as little as $1 a month. For a $5 monthly contribution, you receive early access to the podcast before it goes public; for a monthly donation $10, you receive a copy of the *Novice Observers Handbook*, and for $35 a month, you receive "producer" credits on the podcast and a year's membership to the ALPO. You can help us out by going to the link below:

https://www.patreon.com/ObserversNotebook

New podcasts are released the 1st and 15th of every month, and if you subscribe to it via iTunes, it will automatically be downloaded to your device.

The podcast will also be used to "get the word out" on any breaking astronomy news or events happening in the night sky. So, let me know if you have any breaking news that you want out there.

If you have a topic that you want covered in the podcast, please drop me a note – I'm also looking for member-profile pieces where we get to know the members of the ALPO.

Here are a few interesting statistics you might be interested in as well:

- Number of downloads as of January 10, 2021: 45,000+
- Number of Subscribers (all formats): 275+
- Average of number daily downloads (last month): 100
- iTunes rating: 5 Stars!
- Locations of most downloads: USA, UK, Japan, Canada, New Zealand, and Poland.

You can hear the podcast on iTunes, Stitcher, iHeart Radio, Amazon Echo, and Goggle Play just search for *Observers Notebook*, you can listen to it at the link below:

https://soundcloud.com/observersnotebook

The *Observers Notebook* is also on Facebook-

https://www.facebook.com/groups/ObserversNotebook/

Thanks for listening!

Thanks for listening! For more information about the ALPO Lunar & Planetary Training Program or the *Observers Notebook*" podcasts, contact Tim Robertson at195 Tierra Rejada Rd #148, Simi Valley CA, 93065; e-mail to cometman@cometman.net

So What IS Up with Don?

Besides Tim Robertson's *Observers Notebook* podcasts, we wish to also point out the weekly 20-minute *What's Up With Don* podcasts done by ALPO member and noted comet discoverer Don Machholz. A new one is released every Wednesday and they are available at all the usual podcast sources.

Don is rated number one in the world for visual comet discoveries and has a long and valued history with the ALPO. He joined the ALPO in 1968 and now has "Lifetime" member status by way of longevity. He was the ALPO Comets Section Recorder (now called "coordinator") from August 1988 through June 2000, when he received the *ALPO Peggy Haas Service Award*.

So far, Don is credited with the discovery of 12 comets that include the periodic comets 96P/Machholz, 141P/Machholz, the non-periodic C/2004 Q2 (Machholz) which were visible with binoculars in the northern sky in 2004 and 2005, C/2010 F4 (Machholz), and most recently C/2018 V1 (Machholz-Fujikawa-Iwamoto). In 1985, he discovered Comet Machholz 1985-e using a homemade cardboard telescope with a wide (10 inches) aperture that gave it a broader field of view than most commercial telescopes. Don utilizes a variety of methods in his comet discoveries; for instance, in 1986 he used 29×130 binoculars to discover 96P/Machholz.

And besides his comet-hunting activities, he is also one of the inventors of the "Messier Marathon" event, which is a race to observe all the Messier objects in a single night.

Inside the ALPO
Member, section and activity news

Youth Activities Program

Report by Pamela Shivak, program coordinator
pamelashivak@yahoo.com

As of 15 January 2021, the ALPO Youth Program Facebook Group has welcomed 260 contributors domestically and internationally, including astronomy clubs, planetariums, educators, astronomy magazines, astrophotographers and space enthusiasts of all kinds to the group.

I will continue to add content and members to the group. Once star parties and other activities start up again, more content will be added to educate and encourage young people to become interested in astronomy, space and STEM (science, technology & math).

I will be promoting “International SUNday”, which I founded in 2014 and will be celebrated on the 20 June 2021 summer solstice (that is, the first day of summer). “International SUNday” is a worldwide celebration of the Sun and the solstice, which can be enjoyed either virtually or at a safe public or private event. Get on board! Join the group, plan an event and post a link back to your page on the “International SUNday” Facebook group. For details about “International SUNday”, see the link below:

https://www.facebook.com/groups/IntlSUNday/

Visit us at *https://www.facebook.com/groups/ALPOYOUTHPROGRAM/*

ALPO Observing Section Reports

Eclipse Section

Report by Keith Spring, section coordinator
star.man13@hotmail.com

The 2021 Eclipse viewing season is fast approaching, and with it comes new opportunities to observe these wonders of nature!

On Wednesday, May 26, 2021, the West Coast of the United States will experience a Total Lunar Eclipse at 4:11:25 a.m. Pacific Daylight Time. (It will also be visible from South-East Asia, Australia, Pacific and Antarctica.) This will be a perfect opportunity to make observations of this rare phenomenon.

Inside the ALPO
Member, section and activity news

The next chance to view a Total Lunar Eclipse will not be for another year, in May 2022.

Besides the May 26 event, please note the following:

- 2021 Jun 10; **Annular Solar Eclipse**; Visible from Canada,
- Russia; Partial in North America, Europe, North Asia
- 2021 Nov 19; **Partial Lunar Eclipse**; Visible from Asia, Australia, Pacific, North America, South America
- 2021 Dec 4; **Total Solar Eclipse**; Duration 1 minute, 54 seconds; Visible from Antarctica.

Be sure to make many observations for archival and consideration for publication in the Eclipse Section of the ALPO Journal!

The ALPO Eclipse Section is looking forward to seeing all of your submissions! Please send your reports via e-mail to *eclipse@alpo-astronomy.org* or via regular mail to Keith Spring, 2173 John Hart Circle, Orange Park, FL 32073.

Visit the ALPO Eclipse Section online at *www.alpo-astronomy.org/eclipseblog*

Mercury / Venus Transit Section

Report by Keith Spring, section coordinator
star.man13@hotmail.com

Past Transits

This section is still accepting reports for the November 11, 2019 Mercury Transit for archival. Please send your reports via *eclipse@alpo-astronomy.org* or regular mail to the contact information in the *ALPO Resources* section of this Journal.

Future Mercury Transits

- November 12-13, 2032 - Visible from Europe, much of Asia, Australia, Africa, South/some coastal areas of East North America, South America, Pacific, Atlantic, Indian Ocean and Antarctica.
- November 6-7, 2039 - Europe, much of Asia, Australia, Africa, much of South America, Pacific, Atlantic, Indian Ocean and Antarctica.

Inside the ALPO
Member, section and activity news

- May 7-8, 2049 - Europe, Asia, Africa, North America, South America, Pacific, Atlantic, Indian Ocean, Arctic, Antarctica.

Future Venus Transits

- December 10-11, 2117
- December 8, 2125

Please send your reports via e-mail to *eclipse@alpo-astronomy.org* or regular mail to Keith Spring, 2173 John Hart Circle, Orange Park, FL 32073.

Visit the ALPO Mercury/Venus Transit Section online at *www.alpo-astronomy.org/transit*

Meteors Section

Report by Robert Lunsford, section coordinator
lunro.imo.usa@cox.net

We have just passed the doldrums of winter, when meteor activity in the northern hemisphere is at its lowest point of the year. During the spring months, we can look forward to two major meteor displays and warmer temperatures. Usually moonlight will spoil one of the two springtime displays, but in 2021, both displays peak with little lunar interference.

This would be a great time for those new to meteor observing to hone their skills prior to the arrival of the Perseids this August. Practice is necessary to separate random meteors from those actually associated with the Lyrids and the eta Aquariids. Look for detailed articles on how to view these two displays on the ALPO website in April.

Visit the ALPO Meteors Section online at *www.alpo-astronomy.org/meteorblog/* Be sure to click on the link to viewing meteors, meteor shower calendar and references.

Meteorites Section

Report by Dolores H. Hill, section coordinator
dhill@lpl.arizona.edu

The ALPO Meteorites Section received communications from Randy Tatum on new specimens he has acquired: carbonaceous chondrites Allende (CV3), NWA 7454 (CV3), and NWA 12322 (CV3); HED meteorites NWA 11342 diogenite and NWA 12265 eucrite melt breccia, ordinary chondrite NWA 869 (L3-6), Sericho pallasite, and an interesting shrapnel-shaped piece of the Sikhote Alin IIAB iron (which fell in Russia in 1947).

As of January 16, 2021, the *Meteoritical Bulletin* contains a total of 65,104 meteorites. Eleven new and updated meteorite falls have been

Inside the ALPO
Member, section and activity news

approved since 7 October 2020, including 4 historical falls from Bulgaria:

- Silistra 1917 (achondrite-ungr),
- Pavel 1966 (H5),
- Virba 1873 (L6),
- Konovo 1931 (LL5).

Other interesting falls include Tarda, Morocco (C2-ungr) that arrived as a "yellow fireball with green edges" with a whistle and multiple detonations. Some stones display fusion crust with blue iridescent areas and distinctive "charcoal-like odor". Tiros, Brazil 2020 (eucrite); Madura Cave, Australia 2020 (L5) recovered by the Desert Fireball Network; Auckland, New Zealand that fell through a roof in 2004 (L5); Santa Filomena, Brazil 2020 (H5-6); Tihigrin, Mali (L4); Narashino, Japan 2020 (H5).

The Meteoritical Society's Nomenclature Committee approved or revised 1,038 new meteorites between 7 October 2020 and 16 January 2021. There are particularly interesting ungrouped and anomalous meteorites in this list.

Newly approved meteorites include 868 ordinary chondrites (203 H, 630 L, 31 LL, 3 mixed OC brec, 1 OC5-anom); 1 EH; 55 carbonaceous chondrites (1 C2, 4 C2-ungr, 15 CK, 2 CM, 15 CO, 13 CV; 2 CV-ox; 1 CV-red; 2 CR); 7 R chondrites; 2 acapulcoites; 2 brachinites: 6 mesosiderites; 1 IID iron; 3 pallasites; 2 ureilites; 48 HEDs (6 Howardites, 38 Eucrites, 3 Diogenites; 1 Diogenite-anom); 1 lodranite; 10 ureilites; 3 achondrites-ungrouped; 16 Lunar; 13 Martian.

More information and official details on particular meteorites can be found at: *https://www.lpi.usra.edu/meteor/metbull.php*

Visit the ALPO Meteorites Section online at *www.alpo-astronomy.org/meteorite/* for a very detailed explanation of all facets of meteorite studies.

Comets Section

Report by Carl Hergenrother, section coordinator
carl.hergenrother@alpo-astronomy.org

The second quarter of 2021(April to June) continues a relatively slow period for bright comets. Barring a surprise discovery or outburst, the quarter's brightest comet may be C/2020 R4 (ATLAS), an intermediate-period object with an orbital period of ~940 years.

The ATLAS (Asteroid Terrestrial-Impact Last Alert System) project discovered C/2020 R4 on 2020 September 12 with a 0.5-m, f/2 astrograph located on Mauna Loa in Hawai'i. At discovery, the comet was located at 2.71 au from the Sun, 1.95 au from Earth, and was a faint 18th magnitude. As of early January, observers placed the comet between 10th and 12th magnitude. As of the writing of this report (mid-February), the comet is too close to the Sun to be observed. It should become visible again in the morning sky around the time of perihelion (March 1 at 1.03 au). Due to the lack of observations over the recent weeks, its brightness in the April-June timeframe is uncertain. The comet could start April at magnitude 9.9 and brighten to magnitude 9.1 near closest approach to Earth on April 23 at 0.46 au. It then rapidly fades to 14th magnitude by the end of June as it moves away from both the Earth and Sun.

While no other comets are expected to be brighter than 10th magnitude, there are a few fainter objects of interest.

- Jupiter-family comet 7P/Pons-Winnecke was discovered in 1819 by Jean Louis Pons of Marseille, France. It was one of Pons' 37 discoveries. The comet would then go unseen until rediscovered by Friedrich August Theodor Winnecke of Bonn, Germany in 1858. Winnecke would also discover 9 other comets. In the past, 7P had a smaller perihelion that allowed very close approaches to Earth with the comet often reaching 6th magnitude. The closest approach occurred in 1927 at 0.039 au when the comet reached 3rd magnitude. This year perihelion occurs on May 27 at 1.23 au with a closest approach to Earth on June 12 at 0.44 au, its closest since 1945. Due to the current larger perihelion distance, the comet is only expected to peak around magnitude 11. After this return, Pons-Winnecke's perihelion will decrease allowing brighter returns in the future.
- Another short-period comet of interest is 15P/Finlay, an 1886 discovery made at the Royal Observatory at Cape of Good Hope in South Africa by William Henry Finlay. 2021 marks the 16th observed return of 15P. Its best return was in 1906 when it passed 0.27 au from Earth and reached 6th magnitude. During its last return in 2014/2015, it experienced two outbursts where it increased by 2-3 mag with the overall brightest reaching 7th magnitude. Finlay may still be a very faint object at the start of April (18-19th magnitude) but should rapidly brighten to magnitude 11 at the end of June on its way to a July 13 perihelion at 0.99 au. At its brightest in early August is should be around magnitude 9.9. If it experiences additional outbursts, it could be even brighter.

Inside the ALPO
Member, section and activity news

Table of Ephemerides for Comets 7P/Pons-Winnecke, 15P/Findlay, C/2020 R4 (ATLAS) and C/2021 A1 (Leonard)

Date	R.A.	Decl.	r (au)	d (au)	Elong (deg)	Mag	Const	Max El 40N	Max El 40S
7P/Pons-Winnecke									
2021 Apr 01	17 51.0	+09 04	1.410	0.813	101M	14.3	Oph	56	41
2021 Apr 11	18 22.7	+08 09	1.357	0.726	102M	13.8	Oph	54	42
2021 Apr 21	18 56.1	+06 33	1.311	0.648	102M	13.3	Aql	51	44
2021 May 01	19 31.5	+04 00	1.276	0.580	103M	12.8	Aql	47	46
2021 May 11	20 09.1	+00 19	1.250	0.524	104M	12.4	Aql	42	50
2021 May 21	20 48.2	-04 39	1.237	0.481	106M	12.0	Aql	36	55
2021 May 31	21 28.2	-10 45	1.235	0.454	108M	11.6	Cap	30	61
2021 Jun 10	22 07.5	-17 37	1.246	0.442	111M	11.4	Aqr	23	68
2021 Jun 20	22 43.9	-24 38	1.269	0.447	114M	11.3	Aqr	17	75
2021 Jun 30	23 15.5	-31 16	1.303	0.465	118M	11.2	Scl	12	81
15P/Finlay									
2021 Apr 01	20 33.3	-25 11	1.703	1.824	66M	19.1	Cap	6	48
2021 Apr 11	21 05.9	-23 26	1.609	1.665	69M	18.2	Cap	6	50
2021 Apr 21	21 40.8	-21 05	1.515	1.518	70M	17.3	Cap	6	51
2021 May 01	22 18.0	-18 02	1.423	1.388	70M	16.4	Aqr	5	51
2021 May 11	22 57.6	-14 13	1.334	1.277	70M	15.4	Aqr	5	50
2021 May 21	23 39.4	-09 37	1.249	1.189	68M	14.5	Aqr	5	47
2021 May 31	00 23.1	-04 21	1.172	1.128	66M	13.5	Psc	6	43
2021 Jun 10	01 08.2	+01 20	1.104	1.095	62M	12.6	Cet	7	38
2021 Jun 20	01 54.1	+07 02	1.049	1.088	59M	11.7	Psc	10	33
2021 Jun 30	02 40.1	+12 21	1.011	1.106	56M	11.0	Ari	13	28
C/2020 R4 (ATLAS)									
2021 Apr 01	19 49.2	-01 19	1.144	0.918	73M	9.9	Aql	32	39
2021 Apr 11	18 58.8	+07 53	1.225	0.645	93M	9.4	Aql	51	41
2021 Apr 21	16 59.8	+24 26	1.318	0.472	122M	9.1	Her	75	25
2021 May 01	13 53.1	+33 14	1.421	0.540	130E	9.7	CVn	83	17
2021 May 11	12 07.2	+29 15	1.530	0.796	115E	10.9	Leo	79	21
2021 May 21	11 24.5	+25 04	1.644	1.115	101E	11.9	Leo	65	25
2021 May 31	11 05.8	+22 05	1.760	1.450	89E	12.8	Leo	51	28
2021 Jun 10	10 57.4	+19 52	1.878	1.784	79E	13.5	Leo	39	30
2021 Jun 20	10 54.3	+18 06	1.997	2.109	69E	14.1	Leo	28	30
2021 Jun 30	10 54.3	+16 38	2.116	2.419	60E	14.7	Leo	20	27

- While there are always dozens of comets within reach of imagers at any time, the last comet we'll discuss will be faint during the 2nd quarter of 2021, but may brighten into a nice object at the end of the year. Comet C/2020 A1 (Leonard) was found on 2021 January 3 by Catalina Sky Survey astronomer Greg Leonard with the Mount Lemmon 1.5m reflector. At discovery, the comet was around magnitude 19 and located at a distance of 5.1 au from the Sun. Pre-discovery observations were found back to April 2020 (when the comet was 7.5 au from the Sun). Between April 1 and June 30, C/Leonard will move from 4.2 to 3.1 au from the Sun and brighten from magnitude 17.6 to 16.7.
- The real excitement, though, occurs around the end of the year when the comet will reach a closest approach to Earth on December 12 at 0.233 au, closest approach to Venus on 2021 December 18 at 0.028 au, and perihelion on 2022 January 3 at 0.62 au. While forecasting the brightness of any comet nearly a year before perihelion is problematic, C/Leonard has a few things going for it. It is a dynamically old comet with an orbital period of ~70,000 years. This means it has visited the inner solar system before and is not likely to disintegrate, though two recent disintegrators in 2020 may have been dynamically old [C/2019 Y4 (ATLAS) and possibly C/2020 P1 (NEOWISE)].

Assuming a conservative brightening rate, C/Leonard would brighten to around magnitude 6 in mid-December. But another thing in C/Leonard's favor is a very high phase angle of ~160 degrees. If the comet proves to be dust-rich, it could see an additional 3-4 magnitudes of brightening in mid-

Inside the ALPO
Member, section and activity news

Table of Ephemerides for Comets 7P/Pons-Winnecke, 15P/Findlay, C/2020 R4 (ATLAS) and C/2021 A1 (Leonard) (Continued)

C/2021 A1 (Leonard)									
2021 Apr 01	12 49.5	+60 33	4.152	3.629	114M	17.6	UMa	70	0
2021 Apr 11	12 23.3	+61 33	4.041	3.595	109E	17.5	UMa	69	0
2021 Apr 21	11 56.7	+61 49	3.929	3.581	102E	17.4	UMa	68	0
2021 May 01	11 31.9	+61 24	3.815	3.582	95E	17.3	UMa	69	0
2021 May 11	11 10.9	+60 25	3.701	3.592	88E	17.2	UMa	68	0
2021 May 21	10 54.3	+59 00	3.584	3.607	80E	17.1	UMa	63	0
2021 May 31	10 42.3	+57 20	3.467	3.621	73E	17.0	UMa	55	0
2021 Jun 10	10 34.3	+55 31	3.347	3.631	65E	16.9	UMa	48	0
2021 Jun 20	10 29.8	+53 39	3.226	3.630	58E	16.8	UMa	40	0
2021 Jun 30	10 28.1	+51 46	3.104	3.617	52E	16.7	UMa	34	0

December due to forward scattering of light by dust (with a peak brightness more like magnitude 2 to 3). As exciting as that sounds, the comet will be at a small elongation of only 15 degrees at that time so a difficult object to observe. Let's hope C/Leonard brightens at a faster rate and is a dust-rich object. In the meantime, imagers will be able to follow its development without interruption this year.

As always, the Comet Section is happy to receive all comet observations, whether images, drawings, magnitude estimates, and even spectra. Please send your observations via e-mail to *carl.hergenrother@alpo-astronomy.org*

Drawings and images of current and past comets are being archived in the ALPO Comets Section image gallery at *http://www.alpo-astronomy.org/gallery/main.php?g2_itemId=4491*

Visit the ALPO Comets Section online at *www.alpo-astronomy.org/comet*

Solar Section

Report by Rik Hill, section coordinator & scientific advisor
rhill@lpl.arizona.edu

NASA announced on September 17, 2020 that we have passed through Solar Minimum and are now officially in Solar Cycle 25. The minimum was statistically determined to have occurred in December 2019 with the last maximum having been April 2014.

Solar Section Assistant Coordinator Kim Hay has taken over the writing of summaries for each rotation as they end and these are posted on the Solar Section webpage. She also cites much of the work that Theo Ramakers has done and is doing on reverse polarity sunspot regions. Observers are encouraged to check this out from time to time to keep up with current activity.

I am happy to report that staffing in the ALPO Solar Section remains stable and we look forward to more activity as we put 2020 behind us (thank God!) and move on into 2021!

For information on solar observing – including the various observing forms and information on completing them – go to *www.alpo-astronomy.org/solar*

Mercury Section

Report by Frank J. Melillo, section coordinator
frankj12@aol.com

This coordinator hopes that 2021 will be a good year, or at least better than last year. I did some great observations of Mercury last November and will do a write-up that includes a description of ground-based imaging in addition to the 2020 apparition report. This year, I would like to see more people observing Mercury because there will be three great apparitions: two morning appearances later in the year and an evening appearance very soon.

As you read this in March, Mercury is visible in the morning sky, but its visibility is poor and it is heading for the Superior Conjunction with the Sun on April 19.

Mercury will then appear in the evening sky after sunset and the view will be the best of the year. By April 26, Mercury will be visible north of Venus about 30 minutes after sundown. A pair of binoculars will be needed for a fine view. It will shine brilliantly at -1.6 magnitude! The entire month of May will be the best to view Mercury with the naked eye, as well as through binoculars and telescopes.

On May 16, Mercury will reach its greatest eastern elongation, 22 degrees east of the Sun. A naked-eye view will be interesting while Venus shines below. It will be a rare sight because Mercury is always seen closer to the horizon than any planets nearby. Telescopically, it will display a nearly half-phase at 7.8 seconds of arc disk diameter. Another interesting night to see Mercury will be May 28, when it will be less than 0.5

Inside the ALPO
Member, section and activity news

degree from Venus! The pair will set about an hour and 15 minutes after the Sun. But Mercury will dim to a second-degree magnitude! A pair of binoculars is a must in order to see Mercury with brilliant Venus nearby.

Mercury will go through inferior conjunction with the Sun on June 10. But take note: it will have a favorable morning apparition from late June into most of July. More about that in the next issue of this Journal. Please take a look at Mercury and send in your observations!

Please, send in your observations of Mercury. Visit the ALPO Mercury Section online at *www.alpo-astronomy.org/mercury*

Venus Section

Report by Julius Benton, section coordinator
jlbaina@msn.com

Venus reached Inferior Conjunction on March 26, 2021, thereby ending the 2020-21 Western (Morning) apparition. During the current 2021-22 Eastern (Evening) apparition, Venus is passing through its waning phases (a progression from a nearly fully illuminated disk and ultimately to its crescent phases). Thus, observers are witnessing the leading hemisphere of the planet as it increases its apparent diameter at the time of sunset on Earth.

Venus is predicted to reach theoretical dichotomy (half phase) on October 28 and then subsequently attain its greatest illuminated extent by December 7, 2021 at visual magnitude -4.8. Venus will reach Inferior Conjunction with the Sun on January 8, 2022, thereby ending the 2021-22 Eastern (Evening) apparition.

For the convenience of observers, the accompanying table of Geocentric Phenomena in Universal Time (UT) pertains to the current 2020-21 Western) Morning) apparition and is included here for the convenience of interested observers.

As of the date of this report (January 2021), ALPO Venus observers had submitted over 550 separate observations in the form of digital images of the planet at UV, visual and near IR wavelengths, as well as numerous drawings in integrated light (no filter) and with different color filters. Observational reports for the current 2021-22 Eastern (Evening) apparition are expected to be received regularly throughout the new apparition.

Regular readers of this Journal should be familiar with our continuing collaboration with professional astronomers as exemplified by our sharing of visual observations and digital images at various wavelengths during ESA's previous Venus Express (VEX) mission that ran for about nine years, from 2006 until the mission ended in 2015. It remains as one of the most successful Pro-Am efforts to date, involving ALPO Venus observers around the globe. Such observations will remain important for further study and will continue to be analyzed for several years to come as a result of this endeavor.

For reference, the VEX website is *http://sci.esa.int/science-e/www/object/index.cfm?fobjectid=38833&fbodylongid=1856.*

A follow-up collaborative Pro-Am effort remains underway during the 2020-21 Western (Morning) Apparition in continuing support of Japan's (JAXA) *Akatsuki* mission that began full-scale observations starting back in April of 2016. The website for the *Akatsuki* mission remains active so interested and adequately equipped ALPO observers can still register and start submitting images if they have not already done so.

Frank Melillo of Holtsville, NY submitted this UV image of Venus on December 3, 2020, taken at 14:16 UT with a 25.4 cm (10.0 in.) SCT showing the roughly horizontal V, Y, or ψ (psi)-shaped dusky clouds that are typically seen aligned along the planet's terminator on Venus in good seeing conditions. The seeing conditions here were rated 6.0 on the normally used ALPO seeing scale of 0 to 10, with 10 representing perfect seeing. The apparent diameter of Venus in this image is 11.7", a gibbous phase with k=0.892 (89.2% illuminated), and visual magnitude –3.8. South is at the top in this image.

As always, more information will continue to be provided on the progress of the mission in forthcoming reports in this Journal. It is extremely important that all observers participating in the programs of the ALPO Venus Section always first contribute their observations to the ALPO Venus Section at the same time submittals are sent to the Akatsuki mission.

Breaking recent news from the *Akatzuki* mission at the time of this report is the mission's discovery of some interesting atmospheric phenomena on Venus in the form of a giant discontinuity and

Inside the ALPO
Member, section and activity news

disruption rapidly propagating along the middle and lower clouds of Venus that is not readily visible in the upper clouds of the planet. This atmospheric phenomenon is comparable with other planetary patterns spotted at the super-rotating upper cloud levels like the horizontal V, Y, or ψ (psi)-shaped dusky clouds that are roughly aligned along the planet's terminator typically seen in images captured UV wavelengths. A study of past observations with ground-based telescopes and data from the earlier Venus Express mission shows evidence that this is a quasi-permanent feature of the atmosphere of Venus that presumably has been missed since at least the year 1984.

While this phenomenon is very challenging to observe on the dayside upper clouds with usual UV imaging techniques, it may be that the dayside middle clouds could be marginally noticeable on images taken at visible and near-IR wavelengths). In fact, wavelengths longer than 700nm seem to be better suited for earth-based observers participating in our pro-Am efforts to see what they can accomplish with perhaps detecting the middle cloud phenomena reported by Akatsuki scientists. More on these developments will be forthcoming in a subsequent update.

We are continuing our full coordination and strong teamwork with the *Akatsuki* mission team in collection and analysis of all observations. If anyone has questions about our Pro-Am efforts, please do not hesitate to contact the ALPO Venus Section for guidance and assistance. Those still wishing to register to participate in the coordinated observing effort between the ALPO and Japan's (JAXA) *Akatsuki* mission should utilize the following link:

https://akatsuki.matsue-ct.jp/

The observation programs of the ALPO Venus Section are listed on the Venus page of the ALPO website at http://www.alpo-astronomy.org/ as well as in considerable detail in the author's *ALPO Venus Handbook* available free as ALPO Monograph 15 on the ALPO website. (Go to www.alpo-astronomy.org, click on the ALPO home page, lick on the *ALPO Section Galleries* link near the top-right corner of the page, click on Publication Section, click on ALPO Monographs, then click on "ALPO Monograph 15 - Venus Handbook (Revised Edition 2016)".)

Observers are urged to attempt to make simultaneous observations by performing digital imaging of Venus at the same time and date that others are imaging or making drawings of the planet at visual wavelengths. Regular imaging of Venus in both UV, near-IR and other wavelengths is important, as are visual numerical relative intensity estimates and reports of features seen or suspected in the atmosphere of the planet (e.g., dusky atmospheric markings, visibility of cusp caps and cusp bands, measurement of cusp extensions, monitoring the Schröter phase effect near the date of predicted dichotomy, and looking for terminator irregularities). Routine use of the standard ALPO Venus observing forms will help observers know what should be reported in addition to supporting information such as telescope aperture and type, UT date and time, magnifications and filters used, seeing and transparency conditions, etc.

Under favorable circumstances during future apparitions, Venus observers should monitor the dark side of Venus visually for the Ashen Light and use digital imagers to capture any illumination that may be present on the planet as a cooperative simultaneous observing endeavor with visual observers. Also, observers should undertake imaging of the planet at near-IR wavelengths (for instance, 1000 nm) around the dates on either side of inferior conjunction, whereby the hot surface of the planet becomes apparent and occasionally mottling shows up in such images attributable to cooler dark higher-elevation terrain and warmer bright lower surface areas in the near-IR.

The ALPO Venus Section encourages readers worldwide to join us in our projects and the many challenges ahead.

Routine use of the standard ALPO Venus observing form will help observers know what should be reported in addition to supporting information such as telescope aperture and type, UT date and time, magnifications and filters used, seeing and transparency conditions, etc. The ALPO Venus observing form is located online at:

http://alpo-astronomy.org/gallery3/var/albums/Publications-Section/Observing-Section-Publications/Venus/VenusReportForm.pdf?m=1521162039

Table Geocentric Phenomena of the 2020-21 Western (Morning) Apparition of Venus in Universal Time (UT)

Inferior Conjunction	2020 Jun 03^d 00^h UT (angular diameter = 58.3″)
Greatest Illuminated Extent	2020 July 10^d 08^h UT ($-4.7m_V$)
Theoretical Dichotomy	2020 August 12.88^d UT (Venus is predicted to be exactly half phase)
Greatest Elongation West	2020 August 13^d 00^h UT (46.0°)
Superior Conjunction	2021 March 26^d 00^h UT (angular diameter = 9.8″)

Inside the ALPO
Member, section and activity news

Individuals interested in participating in the programs of the ALPO Venus Section are encouraged to visit the ALPO Venus Section online *http://www.alpo-astronomy.org/venusblog/*

Lunar Section

Lunar Topographical Studies / Selected Areas Program

Report by David Teske, program coordinator
drteske@yahoo.com

The ALPO Lunar Topographic Studies Section (ALPO LTSS) received a total of 225 observations from 29 observers in 8 countries during the October-December 2020 quarter. The countries represented by observers were Argentina (10), USA (6), Italy (2), Columbia (1), Uruguay (5), France (1), Bolivia (1), Mexico (2) and unreported (1).

It is most impressive to have so many high-quality lunar observations submitted from so many observers throughout the world, particularly Latin America. A total of 27 articles were published in addition to numerous commentaries on images selected in the monthly newsletter *The Lunar Observer,* which had an average page count of 71 pages per issue during the quarter. It was placed on the *Cloudy Nights* website and viewed an average of 161 times in each month of the quarter.

Throughout the quarter, *The Lunar Observer* included a section called "By the Numbers," which looked at observer's locations and telescopes used for Moon gazing. In all three months, Schmidt-Cassegrain telescopes were the most common telescope for lunar observations, followed by Maksutov-Cassegrain telescopes.

The "Focus-On" series continued under Jerry Hubbell, with the continuation of the "Lunar 100" observing program during this quarter. Every other month starting in May 2020 explores 10 of the "Lunar 100" targets. In November 2020, the fourth 10 items on the "Lunar 100" list were featured, and in January 2021 the fifth set of 10 were explored. We have had an incredible response from across the globe, including contributions images and drawings of these lunar subjects.

Pastel drawing of the Moon-and-Mars conjunction on September 9, 2020, at 06:00 UT by Michel Deconinck (Aquarellia Observatory, Verdon, France). Observed with a 152 mm (6.0 in.), f/8 Bresser refractor; magnification 32x. Time span to complete this drawing, 05:50 to 07:00 UT.

Future "Focus-On" articles will highlight observations from the Lunar 100 observing list. The "Lunar 100" observing list was originally compiled by Charles Wood as a list of 100 targets to observe on the Moon from very easy (Lunar 100 number 1, the Moon) to very challenging (Lunar 100 number 100, Mare Marginus swirls). Every other month will feature 10 of the "Lunar 100" targets in the "Focus-On" series. March 2021 will feature "Lunar 100"

Inside the ALPO
Member, section and activity news

targets 51-60, and in May we will explore targets 61-70.

Each month *The Lunar Observer* also features an in-depth article from Dr. Anthony Cook on the Lunar Geologic Change Detection Program, which is the BAA's equivalent of the ALPO's Lunar Transient Phenomena program. Other articles are about lunar features, including lunar domes and images of recent lunar topographic studies.

Electronic submissions can now be made by emailing to the coordinator. See the most recent issue of *The Lunar Observer* on the ALPO website ((*http://www.alpo-astronomy.org/gallery3/index.php/Lunar*) for instructions. Hard copy submissions should continue to be mailed to the coordinator at the address listed in the ALPO Resources Section of the Journal.

The lunar image gallery/archive is also now active. Wayne Bailey continues to submit archived images to the Lunar Gallery. This coordinator is now adding current lunar image submissions to the Lunar Gallery. Also, all issues of *The Lunar Observer*, including those from its beginning in 1997 as an American Lunar Society publication to June 2004 when it became the newsletter of this ALPO program, are now available on the ALPO website due to hard work by Theo Ramakers. Also, in the ALPO Lunar Gallery images and reports can be found in the Lunar Dome section.

For more info, including current and archived issues of *The Lunar Observer*, go to *moon.scopesandscapes.com*.

Lunar Meteoritic Impacts

Report by Brian Cudnik, program coordinator
cudnik@sbcglobal.net

Please visit the ALPO Lunar Meteoritic Impact Search site online at *http://alpo-astronomy.org/lunarupload/lunimpacts.htm*

Lunar Transient Phenomena

Report by Dr. Anthony Cook, program coordinator
tony.cook@alpo-astronomy.org

The following reports have been received since the last summary, however they should not necessarily be regarded as LTP reports:

- 2020 Nov 22 UT 18:15-18:45 Trevor Smith (UK - 16" Newtonian) saw a grey streak across the floor of Stofler.
- 2020 Dec 20 Burg, Plinius and Proclus UT 19:00-2998 Trevor Smith (UK - 16" Newtonian) noted red on the western floor and rims of the first two craters and red on the western rim of Proclus. No color was seen on other craters. No filters used.

The first report maybe natural illumination, but can be checked out easily through our repeat illumination program. The latter could be atmospheric spectral dispersion or chromatic aberration, but it is interesting that color was not visible on other craters checked. All our observers are encouraged to use red and blue filters to check out any "visual" detections of color in future or to attempt to use cameras (even camera phones) to back up their visual sightings.

We continue to have success, though, in eliminating some past LTP reports, though, via our repeat illumination program *http://users.aber.ac.uk/atc/lunar_schedule.htm*, though, others remain unresolved.

General Information: For repeat illumination (and a few repeat libration) observations for the coming month - these can be found on the following web site: *http://users.aber.ac.uk/atc/lunar_schedule.htm* . By re-observing and submitting your observations, only this way can we fully resolve past observational puzzles. To keep yourself busy on cloudy nights, why not try "Spot the Difference" between spacecraft imagery taken on different dates? This can be found on: *http://users.aber.ac.uk/atc/tlp/spot_the_difference.htm* . If in the unlikely event you do ever see a LTP, firstly read the LTP checklist on *http://users.aber.ac.uk/atc/alpo/ltp.htm* , and if this does not explain what you are seeing, please give me a call on my cell phone: +44 (0)798 505 5681 and I will alert other observers. Note when telephoning from outside the UK you must not use the (0). When phoning from within the UK please do not use the +44! Twitter LTP alerts can be accessed on *https://twitter.com/lunarnaut* .

Dr Anthony Cook, Department of Physics, Aberystwyth University, Penglais, Aberystwyth, Ceredigion, SY23 3BZ, Wales, United Kingdom. E-mail to *atc@aber.ac.uk*

Monthly summaries of the observations received as well as the best observation from each observer that can provide useful science on re-evaluation past LTP reports are published in the ALPO Lunar Section newsletter *The Lunar Observer* (*http://moon.scopesandscapes.com/tlo.pdf*) – often 10 or more pages per month.

We receive repeat illumination reports from astronomers across the world, most notably the UAI in Italy, the BAA in the UK, the AEA and SLA in Argentina, and LIADA members in Bolivia and Uruguay. In the U.S., our most active ALPO

Inside the ALPO
Member, section and activity news

contributors are Jay Albert, Rik Hill and Gary Varney.

We welcome observations from visual observers, and also astronomers with color imaging capability, who are able to record subtle natural colors on the lunar surface.

We also welcome new participants, whether they are experienced visual observers or high-resolution lunar imagers.

LTP observational alerts are given on the Twitter page: *https://twitter.com/lunarnaut*

Please visit the ALPO Lunar Transient Phenomena site online at *http://users.aber.ac.uk/atc/alpo/ltp.htm*

Lunar Domes Studies

Report by Raffaello Lena, program coordinator
raffaello.lena@alpo-astronomy.org

We have received 101 images, including some by Michael Barbieri, Alessandro Bianconi, Jean Pierre Brahic, Howard Eskildsen, Guy Heinen, Richard Hill, Luigi Morrone, Davide Pistritto, K.C. Pau, Jim Phillips, Frank Schenck, Martin Stenke, Michael Sweetman, Maximilian Teodorescu, Andrea Vannoni, Christian Viladrich, Ivica Zajac and Carmelo Zannelli. Many images are of high resolution and of great interest for our program.

- Morrone has imaged the dome Meton 1.
- Heskildsen has imaged the Cauchy domes field, Fracastorius dome, Piccolomini dome, Valentine domes, Mairan T domes, Gruithuisen domes, Rümker volcanic complex and Grimaldi dome. He has also submitted images of Herodotus omega dome and the Marius hills.
- Sixty high-resolution images taken by Viladrich have been examined. He has imaged the Fracastorius dome, Hyginus domes, Sinus Aestuum region, the dome Schröter 1, the region near Gambart including the domes named Gambart 1-3 and Sommering, Mare Insularum with Milichius - T. Mayer and Hortensius domes, Maraldi domes in different solar illumination angle.
- The wide region including the domes in Cauchy and Maraldi D, displays some additional domes, which have been recently reported in an our preliminary report (see: *http://www.alpo-astronomy.org/lunarblog/wp-content/uploads/2020/01/domes-maraldi.pdf*).
- Hill has imaged Capuanus and Kies domes, Petavius dome and Hyginus domes.
- Bianconi has imaged the dome Teneriffe 1 and the Gassendi region. Bianconi, Brahic and Barbieri have submitted images of the dome Laplace 1, first identified by Teodorescu (see *http://www.alpo-astronomy.org/lunarblog/wp-content/uploads/2019/10/dome-sinus-iridum-alpo.pdf*).
- Pau has imaged a prominent Kipuka east of Taruntius in Mare Fecunditatis.
- Pistritto has imaged Gruithuisen highland domes, domes in Milichius region, Teneriffe 1 dome, Laplace 1 dome and the domes in Arago region.
- Sweetman has imaged the Hortensius domes.
- Schenck has imaged the domes near Luther crater, the domes in Messier designated Messier 1 to Messier 5, and Aristillus 1.
- Zajac has imaged Mons Rümker. Stenke has imaged the dome Teneriffe 1 and the Milichius Hortenius domes field.
- Teodorescu has imaged the dome Herodotus omega and has submitted images of Mare Crisium.

A campaign to encourage lunar observers to image the domical object in Mare Crisium named “Cr1” under waning Moon phase was organized and started on November 1, 2020. This was done completely through the internet, specifically through the use of e-mails and astronomical forums. The goal of this project was to image Cr1 under low solar illumination angles and to describe the relationship between Cr1 and the nearby topography of the Mare Crisium

New telescopic images taken by Bianconi, Teodorescu, Pau and Vannoni display a connection with the southern ridge when the region is imaged under grazing lighting conditions. Moreover, two features like scarps traversing the surface of Cr1 are noted, oriented SW and NS, respectively.

This complex bulge may have formed when magma, or volcanic gases, rose under a lava flow near the surface and inflated it. Thus, based on the new acquired data described above, the most likely explanation could be that Cr1 is an inflation of the upper surface layers associated with the formation of the wrinkle ridges that cross the mare margins. This possible explanation is described in our report:

http://www.alpo-astronomy.org/gallery3/var/albums/Lunar/Lunar-Domes/2020-Images/Observing%20Crisium%201%20%28second%20preliminary%20report%29

Inside the ALPO
Member, section and activity news

%20Is%20an%20inflation%20of%20the%20upper%20surface%20layers%20associated%20with%20the%20formation%20of%20wrinkle%20ridges.pdf?m=1605478624

During a survey, we identified a dome in Posidonius crater, termed Posidonius 1. Our data based on measurements carried out using the LOLA DEM, photoclinometry, and shape-from-shading analysis indicate that the dome Pos1 is related to a magmatic body rising near the surface, with a low intrusion depth. The dome has been imaged by Teodorescu, Viladrich, Zannelli, Phillips, Heinen, Schenck. A preliminary report is available at: http://www.alpo-astronomy.org/gallery3/var/albums/Lunar/Lunar-Domes/2021/server_upload/posidonius%20swell%20ALPO.pdf?m=1610296995

The presence of a small-scale graben detectable only on NAC imagery is an example of the “traces” of the laccolith-forming intrusion of pressurized magma between rock layers of the lunar crust. The dome Posidonius 1 is located at 28.26° E and 32.02° N, with a diameter of 8.0 x 11.2 km ± 0.3 km, height of 74 ± 10 m, yielding an average flank slope of 0.8° ± 0.08°. Our data suggest that the most probable formation mechanism of Posidonius 1 is a shallow magmatic intrusion.

As a note of general interest, China's Chang'e-5 mission touched down on the lunar surface near the Mons Rümker's domes on December 1, 2020. On December 3 the ascent stage of the spacecraft left the Ocean Procellarum carrying about 2 kilograms of lunar material, and safely returned to Earth.

Finally, I have recently published a description of the minerals associated with eruptive volcanos to broaden ALPO lunar observer's knowledge of the geology (including mineralogy and petrology) of these features. It can be found at: http://www.alpo-astronomy.org/gallery3/var/albums/Lunar/Lunar-Domes/2021/volcanic%20material.pdf?m=1611336197&fbclid=IwAR3KzhAggiXZW2NwcdJVpbOv3cM0mppS5B__RKWTur9rsHWrzrtlAtCRnMY

Interested observers can publish their newly acquired images using the e-mail lunar-domes@alpo-astronomy.org . Preference for the filename would be to start with the date as YYYY-MM-DD-HHMM with leading zeros where appropriate. This than could follow with the Observer's ID. This than could be followed with the name(s) of the features shown.

Images received are also shared in our Facebook group Lunar Dome Atlas Project: https://www.facebook.com/groups/814815478531774/.

Interested observers can also participate in the lunar domes program by contacting and e-mailing their observations to both Raffaello Lena, Lunar Dome Studies Program coordinator, at (raffaello.lena@alpo-astronomy.org) and Jim Phillips, assistant coordinator, at (thefamily90@gmail.com).

Mars Section

Report by Roger Venable, section coordinator
rjvmd@hughes.net

On April 1, Mars' diameter will subtend only 4.6 arc seconds, a tiny size that will render the observation of planetary detail very challenging. However, it will still be at a solar elongation of 65° in the evening sky with a magnitude of 1.3, so that you may wish to ascertain how much detail you can see with such a small, bright object. Autumn began in the Martian Southern Hemisphere on February 7, and for a few weeks around that time, the South Polar Region was seen to become increasingly cloudy while the North Polar Hood dissipated to reveal the large, seasonal North Polar Cap (NPC). The NPC and the clouds of the South Polar Hood (SPH) will be prominent by the time you read this. Mars will have a northern declination and, for northern observers, it will linger in the evening sky through the summer.

The observing season is coming to an end, after an apparition that has allowed the best views and some of the best images ever made of the Red Planet. (Though the 2018 opposition was closer, a global dust storm obscured the planet that year around the time of closest approach to Earth, frustrating observers who wished to see more details of the albedo features.) The ALPO Mars Section is very appreciative of the many hours of work that imagers and artists have committed to documenting the planet's appearance during the 2020 apparition.

Courting the Residual South Polar Cap

The residual SPC is displaced from the South Pole. It is of oval shape, about 7 latitudinal degrees in its long dimension, and positioned such that one end of the oval is at the South Pole and the other end is 7 degrees away toward meridian 60° west longitude. That is approximately the longitude of Juventae Fons and Ophir. Consequently, when the SPC has shrunk to its smallest size in late southern summer, and the Earth is near the celestial equator of the Martian sky, we can see the SPC best when meridian 60° faces Earth. Moreover, it will be hardest to detect when the opposite

Inside the ALPO
Member, section and activity news

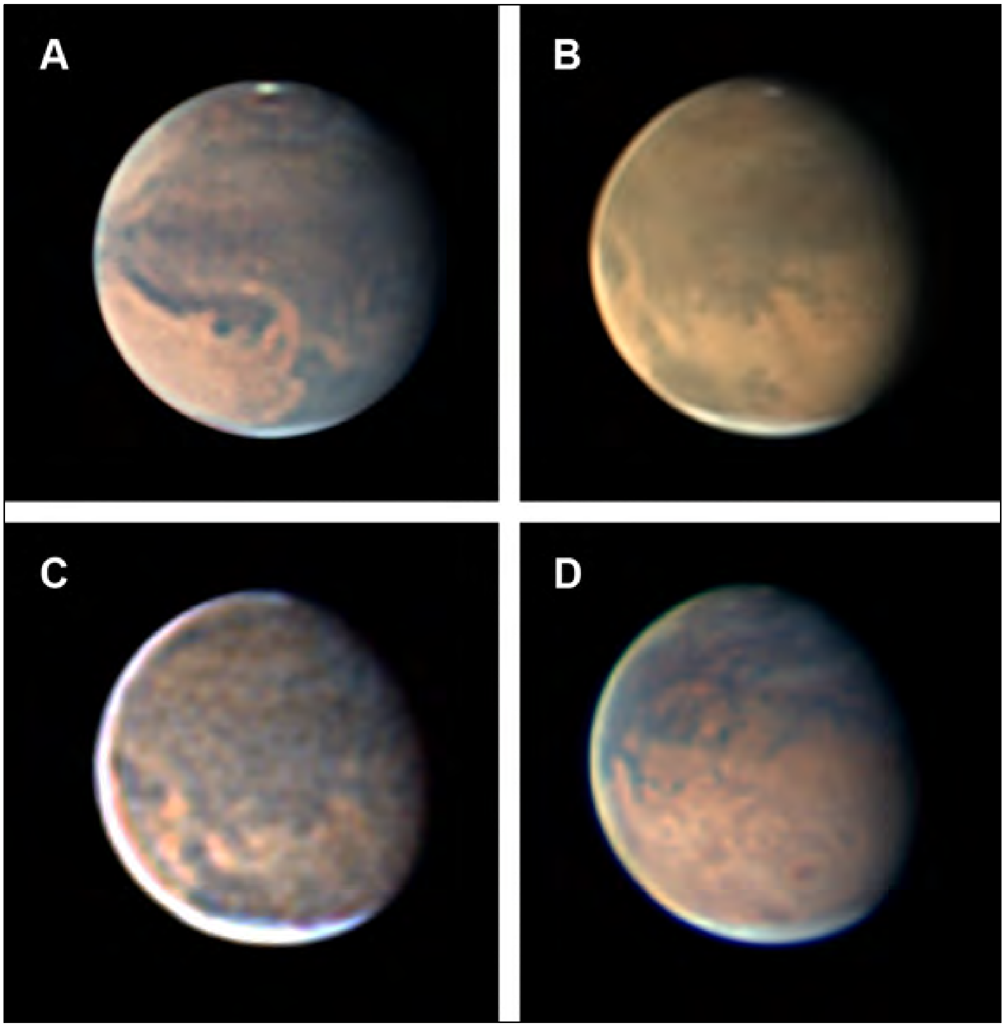

Figure 1. South is up in these images. Notice that the illumination defect – the dark, unseen crescent that gives the planet an oval appearance – extends beyond or "behind" the SPC. In the following image descriptions, CM is central meridian, Ls is areocentric longitude of the Sun whereby 0° is the start of northern spring, DS is areocentric declination of the Sun, and DE is areocentric declination of Earth.
A. Image by Gary Walker of Macon, Georgia, USA, on December 11, 2020, at 00:21 UT. He used a Maksutov telescope of 254 mm (10 in.) aperture, a monochrome camera with R, G and B filters, and the derotation technique of processing. Apparent diameter 13.0". Seeing 6/11, transparency 4.5/6. CM = 9°, Ls = 329°, DS = -12.7°, DE = -24.3°.
B. Image by Martin Lewis of Hertfordshire, UK, on January 6, 2021, at 21:00 UT. He used a Newtonian reflector of 444 mm (18 in.) aperture, a color camera and a luminance filter, and the derotation technique of processing. Apparent diameter 9.8". CM = 62°, Ls = 344°, DS = -6.9°, DE = -22.3°.
C. Image by Paul Maxson of Arizona, USA, on January 15, 2021, at 01:18 UT. He used a Dall-Kirkham telescope of 250 mm (10 in.) aperture, and a monochrome camera with R, G, and B filters. Apparent diameter 9.1". Seeing III/V. CM = 48°, Ls = 348°, DS = -5.1°, DE = -21.2°.
D. Image by Tiziano Olivetti of Bangkok, Thailand, on January 23, 2021, at 11:52 UT. He used a Dall-Kirkham telescope of 505 mm (20 in.) aperture, and a monochrome camera with R, G, and B filters. Apparent diameter 8.4". CM = 125°, Ls = 352°, DS = -3.25°, DE = -19.9°.

meridian - that is, 240° - is facing us. Anticipating that the seasonal terminator would cross the South Pole on February 7 (at the beginning of southern autumn), your coordinator expected that images would show the SPC in early February only if a meridian near 60° was facing Earth. Was this correct? When was the SPC last seen?

Gary Walker's image in panel A of Figure 1 shows the bright, residual SPC as it looked when in full sunlight on December 11, 2020. The last view of the SPC by European observers may be that of Michael Lewis on January 6, 2021, shown in Figure 1, panel B. Paul Maxson's image of January 15, shown in panel C of Figure 1, is the last clear view of the SPC as seen from North America, although Paul's image of the next day might be showing it vaguely. A number of observers in the Far East were able to detect the SPC after January 15, and the last clear detection was by Olivetti on January 23 (Figure 1, panel D). Recall that the terminator was nearing the South Pole with the approach of southern autumn, so that the angle of sunlight on it the pole was very low. This caused the dimness of the SPC in panels B, C, and D in comparison to its former brightness seen in panel A. The declination of the Sun in the Martian sky on January 23, when the SPC was last detected, was 3.25° south. The declination of the Earth in the Martian sky was 19.9° south. At all Earth longitudes, the SPC became undetectable two to three weeks prior to the terminator's reaching the South Pole. The progression of the SPC's invisibility - first invisible from Europe, then from North America, and lastly from the Far East - is due to the progression of the 240° meridian of invisibility around the planet due to the interplay of the rotation periods of Earth and Mars.

Inside the ALPO
Member, section and activity news

Experienced Mars observers know that the 37.5-minute difference between the synodic rotation periods of Earth and Mars causes us to see a lower-numbered meridian of Mars each night, if we observe regularly at the same time of our nights. This enables us to see every face of Mars in a cycle of about 38 days. Accordingly, the time between meridian 60° facing Earth and meridian 240° facing earth is about 19 days. As the start of Martian southern autumn nears, is it possible that we can see the SPC on some nights, but find it to be invisible about 19 days later, and then see it again after another 19 days have passed? I looked for such an occurrence among the many images made this apparition, but I was unable to find a convincing example using the images of any one observer. Therefore, I conclude that the progression of the SPC's invisibility due to the seasonal advance of the terminator slightly outpaces the change in its visibility due to the night to night march of the central meridian.

Be sure to send your observations to *mars@alpo-astronomy.org* and to the section coordinator at *rjvmd@hughes.net*.

We invite you to join the 1,000 members of the marsobservers group of groups.io (*https://groups.io/g/marsobservers*). Observers upload their images or drawings to the photos section there, and share their thoughts about their observations.

To check the ALPO Mars image gallery on the ALPO website, first, go to *http://www.alpo-astronomy.org*, then click on the "ALPO Section Galleries" link at the upper right corner of the screen. Next click on the "Mars images and observations" icon, then click on the Mars image folder for the desired year.

Minor Planets Section

Report by Frederick Pilcher, section coordinator
pilcher35@gmail.com

Following here are highlights published in the *Minor Planet Bulletin*, Volume 48, No. 1, 2021 January-March. which represent recent achievements of the ALPO Minor Planets Section.

The usual procedure for minor planet lightcurve work is to use solar-colored stars in the field to calibrate the magnitude of the moving asteroid as its magnitude varies with rotation. As the asteroid moves from one star field to another, a different set of calibration stars must be used for each session. Due to catalog inaccuracies, aligning the lightcurves on different nights requires zero-point adjustments. This procedure has produced reliable results for many projects.

For some work, it is not sufficient – in particular HG plots, rotations with small amplitude or very long period, binary asteroid events, and tumbling behavior.

The recent online availability of catalogs with magnitudes consistent within about 0.02 magnitudes across the sky, including ATLAS, Pan-STARRS, and GAIA2, has enabled great improvements in these latter studies. The staff of the ALPO Minor Planets Section recommends that observers switch to their use as soon as is feasible. W. Romanishin explains how to achieve this high level of accuracy with the ordinary R filter and the Pan-STARRS catalog.

Brian Warner and Robert Stephens find evidence for satellites of asteroids 4030, 16970, 39282, 85275, 119356, 159402, 420302, and 2019 AN5. For 4030, 85275 and 159402, well-defined dips in the rotational lightcurve caused when the satellite transits or is eclipsed or occultated by the larger body establish the period of revolution around the main body. The existence of the satellite is considered secure. For the others the evidence is more tenuous and the satellite's existence is only tentative.

Peter Birtwhistle has photometrically observed four very small asteroids, 2018 CB, 2018 GE3, 2020 KK7, and 2020 SW, moving closer to the Earth than the Moon. He describes all the difficulties in tracking an asteroid moving very rapidly across the sky background. For all four asteroids he finds rotation periods much shorter than the centrifugal limit at which small pieces detach from the surface and move away. All four of these objects are solid rocks without significant regolith.

Brian Warner and Robert Stephens find tumbling behavior for asteroids 13162 and 19764. Tumbling occurs when the rotation axis itself precesses around a second axis in space and is detected when the rotational lightcurve does not repeat, even approximately, from one rotational cycle to the next.

Brian Warner and Robert Stephens publish spin-shape models for 1626 Sadeya and (68134) 2001 AT18 and also present new high-quality lightcurves for both objects.

In addition to asteroids specifically identified above, lightcurves with derived rotation periods are published for 149 other asteroids as listed here: 49, 57, 188, 191, 236, 261, 270, 375, 383, 424, 426, 444, 469, 499, 530, 570, 572, 584, 586, 605, 716, 737, 764, 805, 911, 921, 936, 994, 999, 1108, 1143, 1146, 1157, 1162, 1180, 1269, 1306, 1346, 1404, 1439, 1537, 1576, 1582, 1594, 1656, 1748, 2034, 2050, 2151, 2246, 2299, 2334, 2341, 2409, 2577, 2665, 2684, 2760, 2927, 2962, 3022, 3068, 3086, 3453, 3519, 3548,

Inside the ALPO
Member, section and activity news

3578, 3895, 3913, 3970, 4055, 4353, 4491, 4738, 4956, 5222, 5408, 5433, 5870, 5996, 6259, 6434, 6792, 7234, 7910, 8278, 9162, 10403, 10419, 11059, 11220, 12112, 12494, 13035, 13186, 13195, 14211, 14793, 14923, 15710, 17711, 18879, 19019, 19186, 19562, 19764, 21663, 23482, 23989, 24177, 25332, 27057, 28565, 35371, 41653, 51534, 52768, 53435, 54441, 56086, 65936, 87684, 96341, 129480, 136900, 137108, 137199, 145656, 146134, 162173, 164755, 285990, 380128, 411165, 450648, 480936, 498066, 2003 BK47, 2005 QS10, 2006 HB, 2006 NL, 2006 UD63, 2007 VX137, 2014 LW21, 2016 NV38, 2016 PN, 2018 LM4, 2020 PL2, 2020 SN.

Secure periods have been found for some of these asteroids, and for others only tentative or ambiguous periods. Some are of asteroids with no previous lightcurve photometry, others are of asteroids with previously published periods that may or may not be consistent with the newly determined values.

Newly found periods that are consistent with periods previously reported are of more value than the uninitiated may realize. Observations of asteroids at multiple oppositions widely spaced around the sky are necessary to find axes of rotation and highly accurate sidereal periods.

I congratulate the authors of all of these papers for excellent writing of the technical details of all of these projects. Their competent explanations will reward careful reading of their *Minor Planet Bulletin* papers.

The Minor Planet Bulletin is a refereed publication and that it is available online at *"http://www.MinorPlanet.info/MPB*

Annual voluntary contributions of $5 or more in support of the publication are welcome.

Please visit the ALPO Minor Planets Section online at *http://www.alpo-astronomy.org/minor*

Jupiter Section

Report compiled by Richard Schmude and Craig MacDougal

Jupiter will be visible in the early morning sky in April. It will be in Capricorn in early April but will shift into Aquarius by the end of that month. Since its equator will be facing Earth, all four Galilean moons will transit this year.

I am hoping several individuals will submit near-infrared images of Calisto transiting Jupiter this year. These images may give us more information about surface features on that moon.

Craig MacDougal reports the ALPO Jupiter e-mail group has moved to Groups.io. To subscribe to this group, send a blank e-mail to:

ALPO-JUPITER+subscribe@groups.io

Craig also reports that 120 images have been shared with this group. This is new, since members were not able to share images in the previous (Yahoo) e-mail group.

The 2020-2021 Jupiter apparition report has been submitted it to the editor for inclusion in a future JALPO issue. A few of the highlights of the 2020-21 apparition include shrinking of the Great Red Spot and emergence of the South Temperature Current D, which may be the fastest current on Jupiter.

A continuing request from the ALPO Jupiter Section staff: The NASA Juno mission is currently enthusiastically accepting images of Jupiter from amateur observers. And because Juno is not primarily an imaging mission, the mission coordinators are especially interested in our (ALPO member) contributions. Please check this article for general background: *https://skyandtelescope.org/astronomy-news/observing-news/juno-pro-am-workshop-05252016/* . After sending your images to us, you're invited to also send your Jupiter images to the JunoCam homepage at: *https://www.missionjuno.swri.edu/junocam* . The JPL hopes the Juno mission will be extended for another three years past July of 2021.

Finally, this is to reminds all that the updated Jupiter manual, "Observing Jupiter in the 21st Century" is now available from the Astronomical League. Because there are several important updates in this revised version, all who observe or image Jupiter are strongly urged to obtain a copy.

It is available at *https://store.astroleague.org/index.php?main_page=index&cPath=1*

Another reminder, all contributors are advised to send all images ONLY to *Jupiter@alpo-astronomy.org* where they will be scanned for viruses before being forwarded on to me. Those received images will also be posted in the ALPO Jupiter Images and Observations gallery.

Visit the ALPO Jupiter Section online at *http://www.alpo-astronomy.org/jupiter*

Inside the ALPO
Member, section and activity news

Saturn Section

Report by Julius Benton, section coordinator
jlbaina@msn.com

The 2020-21 apparition of Saturn concluded when the planet reached conjunction with the Sun on January 24, 2021, thus the 2021-22 apparition is now underway.

The accompanying Table of Geocentric Phenomena for the 2021-22 Apparition in Universal Time (UT) is included here for the convenience of observers.

As of this writing (January 2021), the ALPO Saturn Section had received more than 950 individual visual observations and multi-wavelength images for the previous 2020-21 observing season. Observers contributing digital images had consistently been reporting considerable discrete atmospheric phenomena in Saturn's northern hemisphere, including small white spots in the EZn (northern half of the Equatorial Zone) interacting with the adjacent EB (Equatorial Band), plus sporadic small white spots in the EZs (southern half of the Equatorial Zone), as well as a curious persistent white ripple or streak midway within the EB (Equatorial Belt).

Another strange-looking narrow white streak has also been imaged regularly within the NEBs (North Equatorial Belt, southern component). Small white and dark spots continue to appear the NNNTeB (North North North Temperate Belt as well as in the NPR (North Polar Region).

The aforementioned atmospheric phenomena have shown up well in most images captured using RGB, red, and 685nm IR filters. It is extremely important for observers to continue to monitor Saturn and capture images with the same multi-wavelength filters to determine if the same or similar features will persist and change morphologically with time during the current 2021-22 apparition. Observers should be watchful for any new atmospheric phenomena that might suddenly evolve.

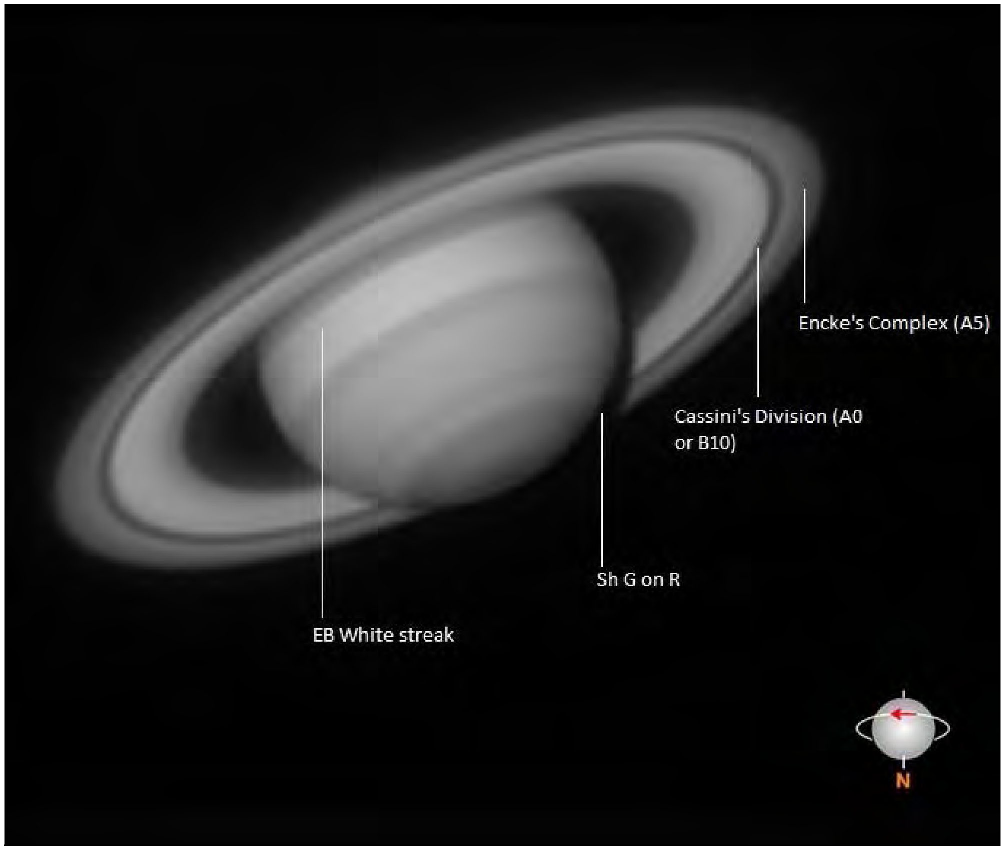

Detailed RGB image of Saturn taken by Trevor Barry of Broken Hill, Australia on December 8, 2020, at 09:564 UT. His image was captured in good seeing using a 685nm IR filter with a 40.6 cm (16.0 in.) Newtonian and it reveals the curious elongated white streak or ripple within the EB (Equatorial Belt) which had been rather conspicuous most of the apparition but appears somewhat vague in the image in poorer seeing conditions. He rated the seeing at 4.0 using the traditional 0 to 10 ALPO seeing scale, where 10 represents perfect seeing. The Sh G on R (Shadow of the Globe on the Rings is visible in this image as well as Cassini's Division (A0 or B10) and Encke's Complex (A5). The apparent diameter of Saturn's globe in this image is 15.5" with a ring tilt of +21.6°. and CMI = 230.7°, CMII = 75°, CMIII = 146.3°. The apparent visual magnitude = +0.6. South is at the top of the image.

With the rings tilted by about +18° toward our line of sight from Earth in 2021-22, observers still have reasonably favorable opportunities to view, draw, or image the northern hemisphere of the globe and north face of the rings even though the inclination of the rings toward Earth is diminishing slowly and with Saturn's southerly declination of -18° for Northern Hemisphere observers.

Pro-Am cooperation actively continues uninterrupted during the 2021-22 apparition of Saturn, and our team of observers are routinely monitoring Saturn for atmospheric phenomena and actively sharing our results and images with the professional community. This maintains our collaborative historical

Inside the ALPO
Member, section and activity news

efforts with the Cassini mission that started its amazing odyssey back on April 1, 2004 until the spacecraft plunged into Saturn's atmosphere on September 15, 2017. For many years to come, planetary scientists will be carefully studying the vast database of images and data gleaned from the Cassini mission, including images provided during the mission by ALPO observers. Therefore, anyone around the globe who wants to join us in our observational endeavors is highly encouraged to submit systematic observations and digital images of the planet at various wavelengths throughout the current observing season.

Observers are also reminded that visual numerical relative intensity estimates (also known as visual photometry) remain an extremely important part of our visual observing program and are badly needed to ascertain recurring brightness variations in the belts and zones on Saturn as well as the major ring components.

ALPO Saturn observing programs are listed on the Saturn page of the ALPO website at http://www.alpo-astronomy.org/saturn as well as in more detail in the author's book, *Saturn and How to Observe It*, available from Springer, Amazon.com, etc., or by writing to the ALPO Saturn Section for further information.

Also consult "ALPO Monograph 14 - Theory and Methods for Visual Observations of Saturn" available online at http://alpo-astronomy.org/gallery3/index.php/Publications-Section/ALPO-Monographs/ALPO-Monograph-14-Theory-and-Methods-for-Visual-Observations-of-Saturn

Observers are urged to pursue digital imaging of Saturn at the same time that others are imaging or visually monitoring the planet (i.e., simultaneous observations).

The ALPO Saturn Section thanks all observers for their dedication and perseverance in regularly submitting so many excellent reports and images in recent years. The professional community continues to solicit drawings, digital images, and supporting data from amateur observers around the world in our active ALPO Pro-Am cooperative effort.

Table of Geocentric Phenomena for the 2021-22 Apparition of Saturn in Universal Time (UT)

Conjunction	2021 Jan 24^d 00^h UT
Opposition	2021 Aug 02^d 06^h UT
Conjunction	2022 Feb 04^d 00h UT
Opposition Data for August 2, 2021	
Equatorial Diameter Globe	18.5″
Polar Diameter Globe	16.3″
Major Axis of Rings	42.0″
Minor Axis of Rings	13.0″
Visual Magnitude (m_v)	+0.2
B = Declination Constellation	+18.1° +18.4° Sagittarius

Information on ALPO Saturn programs, including observing forms and instructions, can be found on the Saturn pages on the official ALPO Website at www.alpo-astronomy.org/saturn

All are invited to also subscribe to the Saturn e-mail discussion group at Saturn-ALPO@yahoogroups.com

Remote Planets Section

Report by Richard W. Schmude, Jr., section coordinator
schmude@gordonstate.edu

Uranus and Neptune will not be well-placed in the sky in April, but by May 1, at least Neptune rises shortly after 3:30 a.m. in Aquarius and should be visible before sunrise. Uranus is located in Aries and rises about the same time as the Sun.

Both planets have albedo features which can be imaged with a near-infrared filter. Uranus has a bright North Polar Region while Neptune may have irregular bright spots.

Pluto rises shortly before 1 a.m. in early May in Sagittarius and, hence, will be visible most of the night.

To find any of the remote planets for telescopic observations, it is suggested that you first use a star chart which shows the position of the target, then use binoculars to find the target. Note that skyandtelescope.org is a great source to find specific locations of sky objects.

Next, locate the target in the finder scope of your telescope. Finally, center your target in the field of view using a low-power eyepiece. You may need a dark site to locate Neptune both in binoculars and in your finder scope.

Both planets have albedo features which can be imaged with a near-infrared filter.

Inside the ALPO
Member, section and activity news

Uranus has a bright North Polar Region while Neptune may have irregular bright spots.

During late 2020, several individuals recorded images of the bright north polar region of Uranus. Christophe Pellier recorded Uranus images in blue, green, red and near infrared light. The north polar region became progressively clearer from blue to near infrared light.

The writer has recorded a few new V-filter brightness measurements. According to these results, both planets are close to their 2019 brightness levels.

The 2019-2020 Remote Planets Apparition Report has been submitted for publication and should appear in this Journal later this year. The writer plans to prepare the 2020-2021 apparition report in this summer.

Finally, my usual reminder that the book *Uranus, Neptune and Pluto and How to Observe Them* is available from Springer at *www.springer.com/astronomy/popular+astronomy/book/978-0-387-76601-0* or elsewhere (such as *www.amazon.ca/Uranus-Neptune-Pluto-Observe-Them/dp/0387766014*).

Visit the ALPO Remote Planets Section online at *www.alpoastronomy.org/remote*

Exoplanets Section

Report by Jerry Hubbell
acting section coordinator
jerry.hubbell@alpo-astronomy.org

Starting a brand-new observing section for a very well-respected organization with a long and rich history of providing information to the greater astronomical community can be a challenge. This is somewhat new to me and I want to assure the ALPO leadership, staff and members that my primary goal is to create a section that lives up to this long history and provides value over and above what already exists in the wider astronomical community. There are several challenges and opportunities that are unique to the ALPO Exoplanet Section which I will discuss. We will be relying on our existing members who are very experienced in doing related observations of minor planets, variable stars and other celestial objects to get the best data possible using small telescopes with advanced instrumentation.

Over the past few months, there has been some discussion on why we need a new exoplanet section and what real benefits might be realized by forming such a section. I covered this in the previous issue of the JALPO (Volume 63, Number 1, Winter 2020), but there has been additional discussion on this since then. One of the questions that I have received is "What is going to make our program different from any of the other groups that already have exoplanet sections or programs such as the American Association of Variable Star Observers (AAVSO) and the British Astronomical Association (BAA)?". The answer to this question forms the design basis for the ALPO Exoplanet Section.

The challenge in doing exoplanet observations is that it requires us to re-examine our instruments and equipment used to acquire the necessary data, the procedures currently being used, and our analysis processes. All these need to be updated to be successful in doing transit photometry. Since this is the case, I have designed the structure of the ALPO Exoplanet Section to focus on these fundamental differences and needed improvements. This is depicted in the new exoplanet section logo provided by my daughter (Figure 1.)

Since the exoplanet section is currently in a two-year probation period where the ALPO leadership is monitoring the progress of the section, the initial goals will be related to these three fundamental areas: Instrumentation, Observation and Analysis. My plan includes creating the following groups within the section and have assistant coordinators assigned to each of these groups within the section:

- Instrumentation Group
- Observing Program Group
- Analysis & Modeling Group
- Exoplanet Data Reporting Group
- Exoplanet Observation Training Group

My goal is to get each of these groups up and operational within the next six months – by the end of the Summer 2021. Once we have identified and appointed the assistant coordinators, I would like to suggest we create some type of exoplanet section "vision statement" and "mission statement" that will make it clear how and why this section operates the way it does. This will help answer those questions that have been asked over the past few months.

Instrumentation Group

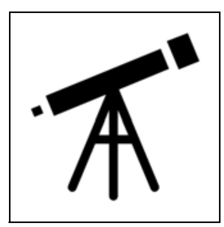

I put the Instrumentation Group first on the list because instrument performance is a fundamental driver in obtaining the necessary high-precision data to successfully observe, measure and model exoplanet transits. This does not necessarily mean that the equipment that the section members already have will not do the job… it will. What members need to think about in terms of their instruments is how they configure and use these instruments in a unique way to observe and record the exoplanet transits versus other similar objects. To obtain the

Inside the ALPO
Member, section and activity news

highest precision measurements will require additional components, processes and procedures to get the most precise data. By creating an instrumentation group within the ALPO Exoplanet Section, we put needed focus on the requirement to maximize the performance of the instruments used to acquire the best exoplanet transit data.

The primary goal of the Instrumentation Group is to define and demonstrate valid instrument configurations and components, including the selection of off-the-shelf instruments, the determination of configuration settings and parameters, and researching the use and application of new instrument systems, sub-systems and components. Additional work is needed to understand and measure the different sources of error due to the instruments used for the observation of exoplanet transits.

The members contributing to the Instrumentation Group will help further define and help other members of this section learn what a successful instrument system configuration looks like and what is needed to get the best results.

Observing Program Group

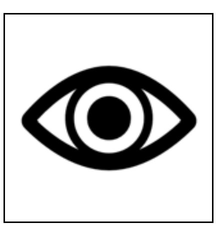

The Observing Program Group is mainly concerned with developing and refining the observing plans, processes and procedures used by members to obtain the best exoplanet transit data. The primary goal of the group is to provide the needed resources for members to be able to easily identify exoplanets to observe and develop the information needed to acquire the observations and do the analysis of the observations for specific exoplanets.

Processes and procedures will also be developed to coordinate observations of specific exoplanet transit events between our members.

The Observing Program Group members can use the information developed by the Instrumentation Group to build their astronomical imaging systems and acquire the best data possible. The Observing Program Group members will also have a way to submit their data to members of the Analysis and Modeling Group (described below) to perform the analysis and develop results based on their data. In this way, we can create a collaborative structure across the different groups of the exoplanet section.

Analysis and Modeling Group

The Analysis and Modeling Group members are interested in learning how to process the data acquired during their own observation runs or may be interested in processing and analyzing other member's data. It is expected that these group members will develop and improve data processing and analysis techniques and perhaps develop new and improved exoplanet transit modeling tools. A large part of this group's members may be dedicated to computer-based analysis and modeling automation tools in the future.

The Analysis and Modeling Group will provide resources and services to other members of the ALPO Exoplanet Section for their use. These resources will include currently freely available analysis to configuration files, data analysis examples and training materials.

Exoplanet Data Reporting Group

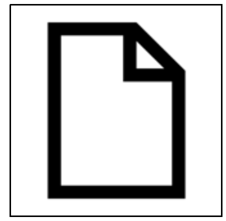

The primary role of the Exoplanet Data Reporting Group members is to coordinate the transfer of data and analysis results to those external professional and other organizations that want and need the exoplanet observation data our members create. This group will also manage and archive all member data and analysis results in a standard format suitable for searching and for the development of papers based on the section member's observations. Finally, the reporting group will coordinate the work of our members with professional exoplanet observing programs to provide Pro-Am opportunities, to contribute to real research and to realize the opportunity to get published in professional papers.

Members of this group will facilitate all section members in creating data sets and narrative reports for publication in the section newsletter *The Exoplanet Observer* (aka TEO), and in the quarterly JALPO publication. The reporting group will also be responsible for publication of the section newsletter every month and in the management of the ALPO web page for the ALPO Exoplanet Section. *The Exoplanet Observer* will cover the following items every month:

- Discussion of latest exoplanet developments and discoveries
- Online and in-person meetings scheduled
- Observation reports from members
- Instrumentation and equipment
- Observing and analysis procedures and techniques

Inside the ALPO
Member, section and activity news

- Education Corner: Discussion of exoplanet transit observing terminology, methods and resources
- Member presentations and paper submissions

Additional areas to report will be developed and changes to this basic outline may occur over time based on suggestions submitted by the members.

Exoplanet Observation Training Group

The Exoplanet Observation Training Group will provide members with documents, procedures, presentations and other training material developed by this section needed to learn how to observe and analyze transit data and report exoplanet transit observations. Additional resources from the other section groups will be aggregated by the training group for archiving and distribution to section members as needed. The training group members will also maintain contact with the larger exoplanet observing community to share results and to bring "best practices" and relevant information back to the exoplanet section for implementation as desired.

The training group members will also develop multi-media training materials including videos and presentations and may hold live training sessions to foster a more collaborative and active training environment. The training group members will be directly involved with and contribute to the other groups on an as needed basis.

In Summary

As you can see, I have developed a very ambitious plan to provide a comprehensive program and section to support all our ALPO members interested in learning about and observing exoplanet transits. I am honored to be selected to lead this effort and I welcome all feedback on how I am doing. It will take a dedicated team of section group assistant coordinators to bring this section to full fruition and to ensure that it will serve the ALPO general membership long into the future. I think that with this structure in place, we can move forward very quickly over the next few months and provide some resources for our fellow members to get started in this exciting field during these both challenging and exciting times in astronomy and in the world in general.

I think being an active member of the new ALPO Exoplanet Section will provide a good challenge and an excellent learning opportunity along with contributing to cutting-edge astronomical observing techniques for small telescope systems. I would encourage those wishing to join this section to please contact me at jerry.hubbell@alpo-astronomy.org and please let me know if you would like to be considered for an assistant coordinator position. And don't forget to let me know which group you are interested in coordinating. Finally, I welcome questions about this new section and would like everyone's thoughts on this approach to creating the new exoplanet section.

Errata

- An incorrect spelling of the first name of our Exoplanets Section appeared in JALPO63-1 (Winter 2021). The correct spelling is Jerry Hubbell and he holds a Sponsoring Membership in the ALPO. Jerry's e-mail address is *jerry.hubbell@alpo-astronomy.org*
- The URL for the MSRO Science site in the *Point of View* column in JALPO63-1 (Winter 2021) was misspelled. It should be *https://msroscience.org*
- The second in a series of papers by Darryl Wilson which appeared in JALPO62-4 (Autumn 2020) was incorrectly titled. The correct title should have been "Introduction to Thermal Imaging of the Moon."

Be a part of the In Crowd at ALPO 2021!

Online sessions Friday and Saturday, August 13 and 14 in the comfort of your own home (or wherever).

See page 4 of this Journal for complete details

Inside the ALPO
Member, section and activity news

Introducing Michel Deconinck

Michel is the newly appointed acting assistant coordinator for the ALPO Comets Section and works with that section's lead coordinator, Carl Hergenrother. Below is how he entered the world of astronomy and the ALPO:

A retired nuclear engineer, Michel worked first for different nuclear medicine projects and then as senior principal consultant at Oracle.

He's been a fan of the cosmos since the very beginning of the space conquest. "I still remember, I was age 5, the 'bip-bip' of the first Sputnik. And then follows the different missions with 'supermen' on board of incredible spaceships."

He joined the CAB (the Brussel Astronomical Club) as member and quickly moved up to being president. "I worked for some specific jobs at the Royal Belgium Observatory, mainly around the solar specialties (Wolf number estimation, corona polarization during eclipse, spectroscopy, solar interferometry...). Jannik (my wife) helps me with this passion; she is very motivating and this is a huge help!"

He first learned of the ALPO by way of his interest in meteors. "I've active in naked-eye meteor observation since 1970. At that time, I joined the past IUAA (a sort of an IAU branch for the amateur, as coordinator for the meteor section). For example I'm in contact with Robert Lunsford (of the ALPO Meteors Section and the American Meteor Society). On the cloudynights.com forum, I regularly read Carl Hergenrother's great comets notes, so the link with ALPO was natural."

Michel also is an avid sketcher, as well as an observer. "As a long-time astro-sketcher, I was interested first in the huge database of comet images maintained in ALPO. For me, this is "THE" world's best reference. In parallel, I'm interested in information about the Lunar, Mercury and Venus sections of the ALPO, where I send my sketches, as well.

As an imager, he had a chance to catch a good photo of the comet West 1975. That photo was used in national newspapers and some books and "was probably the starting point for my comet passion." In 1986, Michel joined the International Halley Watch in order to collect observations from Belgian astronomers and also organized a specific exhibition for the Université libre de Bruxelles (a research university in Brussels).

His mobile observatory (a lovely California van) is equipped with the following: a pair of Vixen 126mm, f/5 binoculars; a 102mm, f/10 refractor on an EQ3 mount motorized for right ascension; a 70mm, f/5 refractor on an altazimuth mount. In addition, Michel's backyard home observatory includes: a 152mm. f/8 refractor equipped with a white light filter and is dedicated mainly to daily sunspot counting and is used alongside a 35mm H-alpha Lunt solar telescope (both of which are on an EQ5 mount motorized for declination and right ascension; and 250mm, f/10 and f/15 Takahashi Mewlon (Dall-Kirkham) telescopes on GoTo EQ6 mounts. All are used only for observation and sketching.

I'm a navigator, sailing for years with my wife on our two-mast sailing boat in the Atlantic, the North seas and the med seas, and... using stars with a sextant to know where I was.

I'm an artist, today I teach art in different painting schools in Provence. Since years I specialize myself in night watercolors. I put in scene (with precision), the stars, planets and comets, this is the scientific part of the view, and in the foreground, I like to paint houses, trees, mountains and sometime an observer (with less precision but creativity) for the artistic counterpart.

I send astronomical alerts to the French speaking community. New objects as cataclysmic stars, aurora, meteors, etc... and of course new comets. I ask the contacts I have now, to share their photos, sketches and observations to ALPO.

I share to ALPO my own observations of comets, estimation of magnitude, coma diameter, DC, tails characteristics as well as the sketches done.

Papers & Presentations

Interpretive Observing: Personal Reflections on Observational Astronomy

By Stephen Tzikas,
ALPO Member
Tzikas@alum.rpi.edu

To our hard-copy readers: This paper can be viewed in full-color in the online (pdf) version of this Journal.

Overview

As a chemical engineer, I often think in terms of chemistry, and analytical chemistry is one of the four main branches in that science, the others being physical, organic and inorganic. There is no commonly used similar term in astronomy, though of course, analytical concepts exist. I joined the Association of Lunar & Planetary Observers (the ALPO) and the Society of Amateur Radio Astronomers (SARA) about the same time, in late 2012. Since I had a great interest in observational astronomy, I wanted to be part of any organization that offered an analytical approach to astronomy, whether it be in the optical or radio segments of the electromagnetic spectrum, which are generally the only two broad segments in astronomy for study as a ground observer.

When one uses a radio telescope, the target is observed via a signal that is generated by the receiver after it is captured by an antenna. Usually the signal is displayed on a laptop or desktop screen. It's not so different in optical astronomy, where the antenna is replaced by a telescope and the receiver is replaced by our direct vision. While it can be a great and satisfying accomplishment to visually observe or obtain a signal in radio astronomy, both the radio signal and the viewed image in optical astronomy are where many observers stop. I was once one of those observers who "stopped."

For years I looked at the Moon and planets thinking my casual but "live" view of them was all that there was. For example, Venus is covered in clouds and is a bright white disk at various phases. That is all one can glean from the view, I thought. I could say something similar about the other planets and lunar craters. You look at the observing target for a minute or two, marvel at it, and that was all. No other details were noticed. In radio astronomy, the collected signals on the computer screen were similar.

Over the years, though, I began obtaining more in those views and signals. I wish I could give the reader a set of simple instructions that they could reproduce instantly, but I can't. I call this article "Interpretive Observing" and there is no internet term for this, nor similar terms such as "perceptual observing." This type of observing is not only about maximizing the view of fine details in an observation (which can be challenging), but also about how it is recorded.

I once wrote an article in the April 2017 ALPO Lunar Section newsletter *The Lunar Observer* titled "Analysis of a 1609 Galileo Lunar Sketch," whereby I estimated that in my lunar sketch, "250 *daylight features could be seen, 500 features in twilight, perhaps even more in night conditions. Even at a rate of sketching a feature every minute, approximately 10 hours would be required for an accurate sketch. Hence with this time limitation and other restrictions such as weather and changing colongitude, Galileo, like myself, had to decide on styling shortcuts."*

Focused Experiential and Training Opportunities

Unfortunately, gleaning details from an observation is a long-term skill that requires many hours of practice, even though the steps are rather simple. A lot of parameters are involved. How is sunlight reflecting off the target object? What are the conditions on the target object? What are the local observing conditions of the observer? What types of instruments are used, and how well does the observer use his or her often sub-par instruments and accessories? No one starts with quality instruments, nor does anyone have the fortune of excellent observing conditions night after

Online Features

Left-click your mouse on:

• The author's e-mail address in blue text to contact the author of this article.

• The references in blue text to jump to source material or information about that source material (Internet connection must be ON).

Observing Scales

Standard ALPO Scale of Intensity:

0.0 = Completely black

10.0 = Very brightest features

Intermediate values are assigned along the scale to account for observed intensity of features

ALPO Scale of Seeing Conditions:

0 = Worst

10 = Perfect

Scale of Transparency Conditions:

Estimated magnitude of the faintest star observable near Venus, allowing for daylight or twilight

IAU directions are used in all instances.

night. I recognized that and took it one step at a time over many years and I still have much more to room to develop.

When it comes to radio astronomy, I recognize how much of it can challenge a professional with a Ph.D. in electrical engineering. Moreover, in this age of unlimited internet information, it becomes an endless and futile pursuit of knowledge as we chase astronomical experiences. I've been forced to constantly and continuously narrow my fields of focus to the long terms goals I have. Sometimes I think about how nice it was when the state of science was still manageable to an observer with fewer unproductive distractions and temptations.

The ALPO is an organization where one can still learn great observational skills, but it takes a commitment of time. In my opinion, it's a worthwhile commitment. A few years ago I graduated from the ALPO Lunar & Planetary Training Program, which focuses on observational sketching of the lunar surface. Many of those sketches appeared in past issues of *The Lunar Observer*. Some of the skills I developed in the training program are today proving useful for planetary observing. Having good observational skills enhances the real time view of the Moon or a planet. After all, if one doesn't know what to view, it is not seen. Bringing awareness assists in these interpretive skills and will help observers record better observations. If those observations are provided to databases, they will help science.

My first sketches of the lunar craters were not much more than line-and-shadow figures, taking less than a minute to sketch. They eventual became higher quality, taking about three hours to sketch. The requests from my mentor, Tim Robertson, for ever-increasing observational details required that I adopt some best practices. I discuss these further in this article. By no means are these tips comprehensive. However, they do offer a beginner advice on observing that may not be so obvious.

In my opinion, the best enjoyment of an observation comes with understanding the observation and being able to interpret it in full. Similarly in radio astronomy, understanding a signal tells one what that signal really means. In radio astronomy, one must discern radio frequency interference (RFI) from galactic hydrogen, both of which are ubiquitous. Radio interference also includes the noise from the components of the radio telescope itself.

A task such as calculating the spectral flux density (somewhat equivalent to a visual

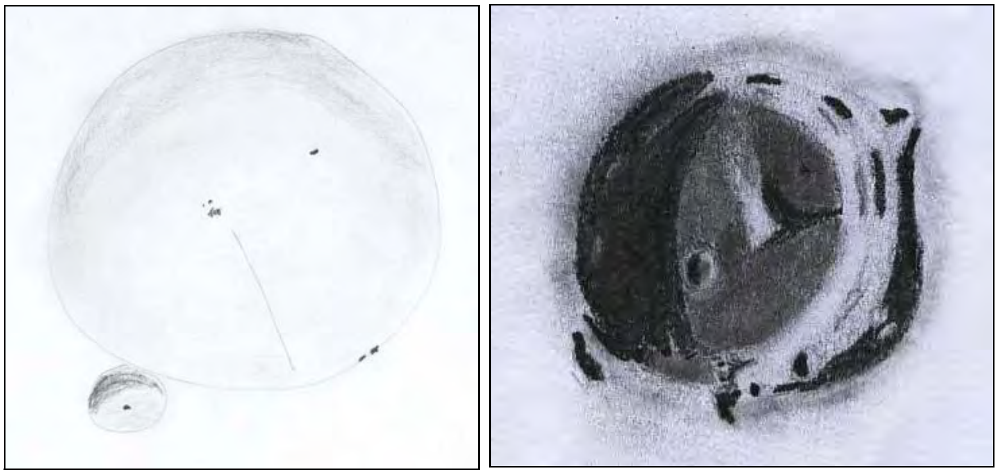

Figure 1. A comparison of one of the author's early sketches with a later, more skilled effort. At **LEFT** is a March 5, 2014 sketch of the lunar crater Petavius at the commencement of my time in the ALPO Lunar & Planetary Training program. At **RIGHT** is my August 4, 2014 sketch of the lunar crater Arzachel, just past the half-way mark in the time in the ALPO training program.

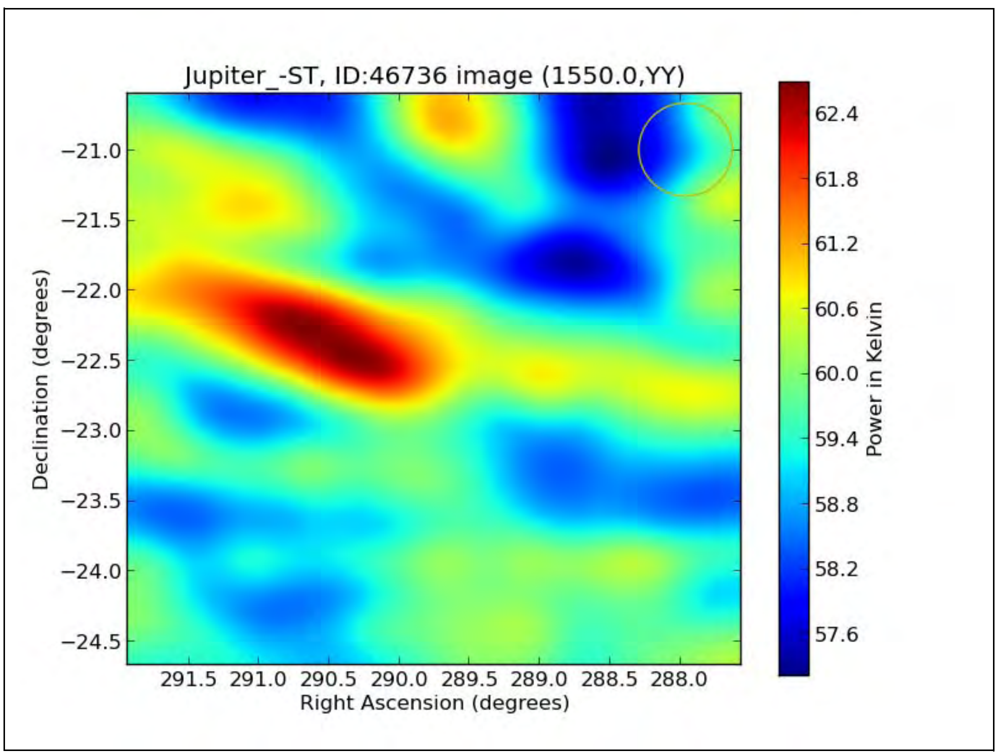

Figure 2. Radio telescopes can be used to observe the Sun, Moon and planets. Above is a raster map of Jupiter; the reddish oval includes the planet's magnetic field synchrotron emissions. The image was taken by the author via the Society of Amateur Radio Astronomers (SARA) 20m radio telescope program account available to SARA members. Radio Observation Skynet 59130 Jupiter-ST 46736-56280; October 8, 2020, 22:50 UT (Jupiter in Sagittarius); Low Resolution, 1350-1750 MHz, Center Frequency 1150 MHz; Raster Map: 0.3 second integration time, 1024 channels.

Figure 3. Solar, planetary and lunar filters exist for the enhancement of certain details. **Above left**, this Thousand Oaks solar filter fits over the front aperture of an 8-inch telescope. This one is used for visual observing, but others exist for photographic purposes. **Above center**, small eyepiece 0.965-inch solar filters are rarely seen anymore because of safety concerns. These filters, such as the one above at the left, screw into the threads on the back of eyepieces. Rather than the filter being fitted to the aperture end of the telescope, the filter receives the focused concentrated solar rays. Smaller type low-cost eyepieces are still readily found and can be used with adapters on all telescopes. **Above right**, this set of various size eyepiece filters can be used for lunar and planetary viewing.

magnitude in optical astronomy) is difficult. Obtaining a flux density measurement within 10% is considered good for an amateur not performing a detailed statistical analysis. A stricter (within 1% accuracy) is expected of professionals and is possible with advances in technology and computational power.

When I joined ALPO, the greatest incentive was its observational training program. That was the most enlightening program I ever attended for an observational skill. It lasted an entire year and I realized at the end of the course actually how "blind" the common observer is. After the ALPO observation program, the trained human eye can spend hours sketching a feature such as a crater. In my opinion, these sketches can sometimes document the object better than a photograph of similar resolution. A photograph is a static, two-dimension image, and not a live experience. The colors and tones can be false or poorly distinguished. The resolution at the instant a single photograph is taken is set, and not given the benefit to improve as the atmospheric condition fluctuates with moments of superior "seeing" that the human eye can wait and see.

Figure 4. A basic knowledge of eyepieces is required for useful observing. Smaller focal length eyepieces offer greater magnification over higher focal length eyepieces. Eyepieces also vary in field of view, lens quality and eye relief. Shown here is an assortment of 2-inch barrel eyepieces.

Knowing how to interpret a radio frequency signal and how to optically observe a lunar and planetary object are both criteria for an analytical record of the event and can be applied towards the research of interest. Just take a look at the ALPO observation forms and the requested details on them. Many observers won't understand the terms, let alone how to observe them. In radio astronomy, such detailed and various measurements are critical as well, in order to understand how radio object properties change with time, whether that is with fading supernova remnants like Cassiopeia A, or observations of slowing pulsars.

When observing astronomical targets, it is important to select an appropriate target that is within the means of the observer. The right instrument and parameters must be determined for optimization. When to observe can play an important role. What to expect and how to record it are critical. If sketching, knowing a 10-step tone scale for an intensity diagram is essential. In radio astronomy, one uses an appropriate frequency-based receiver and the appropriate antenna for those frequencies. In optical astronomy the proper telescope and accessories are important. A common piece of advice is that aperture is paramount, which often means using a reflecting telescope. But that is only true in some cases. For lunar and planetary observing, a refractor is more essential in my opinion. My achromatic 120mm (4.7 inch) refractor gives better results than the 8-inch, 13.1-inch, and 16-inch reflecting telescopes that I use for other types of observations. Sometimes better viewing is due to better atmospheric conditions, but not always.

My preference is for lenses instead of mirrors due to their quality, even if the reflecting telescopes are reasonably collimated. In my opinion, lenses are like high-definition television compared to the "snowy" images of larger reflectors, where aperture is not needed for bright lunar and planetary objects. There is a very valid reason serious and trained observers opt to buy smaller and more expensive apochromatic refractors over much larger and more affordable reflectors.

Choosing a Suitable Target

In the ALPO training program I was asked to choose a target, such as a crater, for long-term observation. That wasn't so simple. I sketched a variety of features before learning some craters and features were more conducive to detail than others, and that some had longer observation

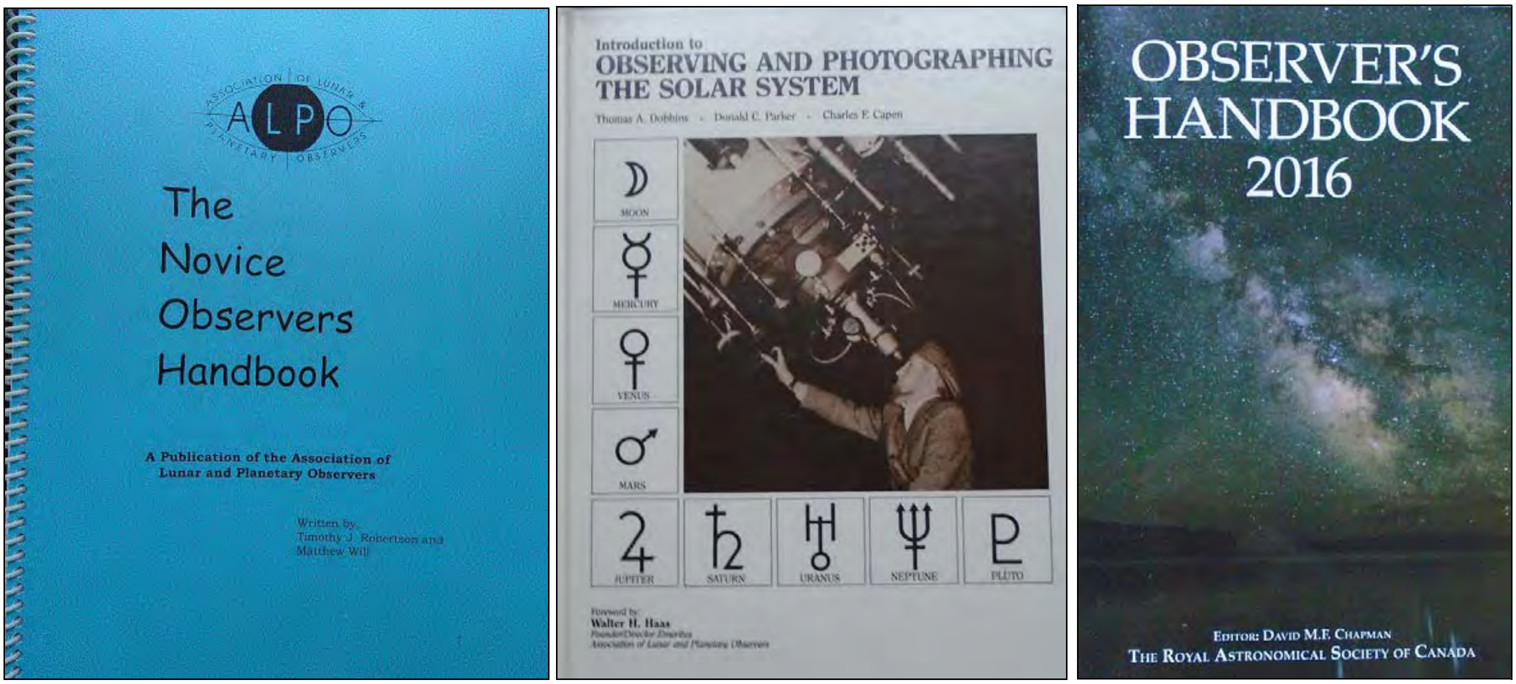

Figure 5. Numerous guidebooks and annual observer guides are available for purchase, new or second-hand. *The Novice Observers Handbook* and the *Introduction to Observing and Photographing the Solar System* are used in ALPO training. The *Observer's Handbook*, published annually and sold through the Astronomical League, is a great guide for the new astronomical observer on upcoming events for a specific year.

windows that others. I eventually settled on Arzachel for its richness of detail, and Proclus for its richness in tones over a long observational period. The later was especially convenient for a backyard with a good view of the western sky, as it stayed visible for most of the waxing period and some waning. Whenever observing choices were made, I learned about the features and their geology. Astronomical League observing programs are useful as well in teaching the types of solar, planetary, and lunar features that can be seen. If observing the Sun, get to know the various types of filters and telescopes. Companies such as Coronado, Daystar, and Lunt make dedicated solar telescopes in the H-Alpha or Calcium K wavelengths.

Choosing the Instrumentation Parameters

Obviously, one wants a telescope that can provide a high enough magnification to see sufficient detail. If you want to squeeze the most out of your optical instruments, you need to understand how they function. “Aperture” is a term one hears a lot in astronomy, but it is not so important in lunar or planetary observing when objects are inherently bright. Large apertures are more suited to faint deep space objects, but are limited in their usefulness in bright suburban areas. For lunar and planetary observing, focal length and proper eyepieces are important. Both play a critical role in the useful magnification of an object. The focal length of the telescope divided by the focal length of the eyepiece provides the magnification. This is one reason why classic professional observatories had such long majestic telescopes, even though the aperture was relatively small. A set of eyepieces has useful roles but there is a lower limit to a small focal length eyepiece before the magnified image it provides become too blurry and dim. Higher focal length eyepieces provide less magnification, but help in pinpointing a small object, from where you can eyepiece “hop” to ever-increasing magnification, boosting it further with a barlow lens. A resolution limit of 1 arc second due to atmospheric instability issues makes a 4 to 5 inch refractor ideal for lunar and planetary observing. Filters too, that can be screwed into the eyepiece have different roles for improving contrast. Optical quality makes a great difference in planetary viewing. A refracting telescope can have excellent quality with its superior optics and fixed collimation. Even if one knows how to collimate optics in a reflecting large-aperture telescope, the contrast is never quite like a refractor. This is why advanced observers are willing to pay thousands of dollars for a smaller refractor instead of buying a larger aperture reflector at a fraction of the price. My 120mm achromatic refractor, in my opinion, has better and sharper views of Mars and Jupiter than my 8-inch and 13.1-inch scopes, as well as a 16-inch aperture telescope for which I have access. Think of it as a difference between two television screens - a sharp digital image versus the old snowy analog television. Schmidt-Cassegrain Telescopes (SCTs) and their catadioptric variants have very long focal lengths. This make for excellent magnification. I have achieved some good views of Mars with only a 90mm Maksutov. One great way to learn further about instrumentation is to attend a star party. A great variety of instrumentation and accessories are usually displayed at star parties, from the simple to the sophisticated. Owners are often very pleased to discuss the capabilities of their

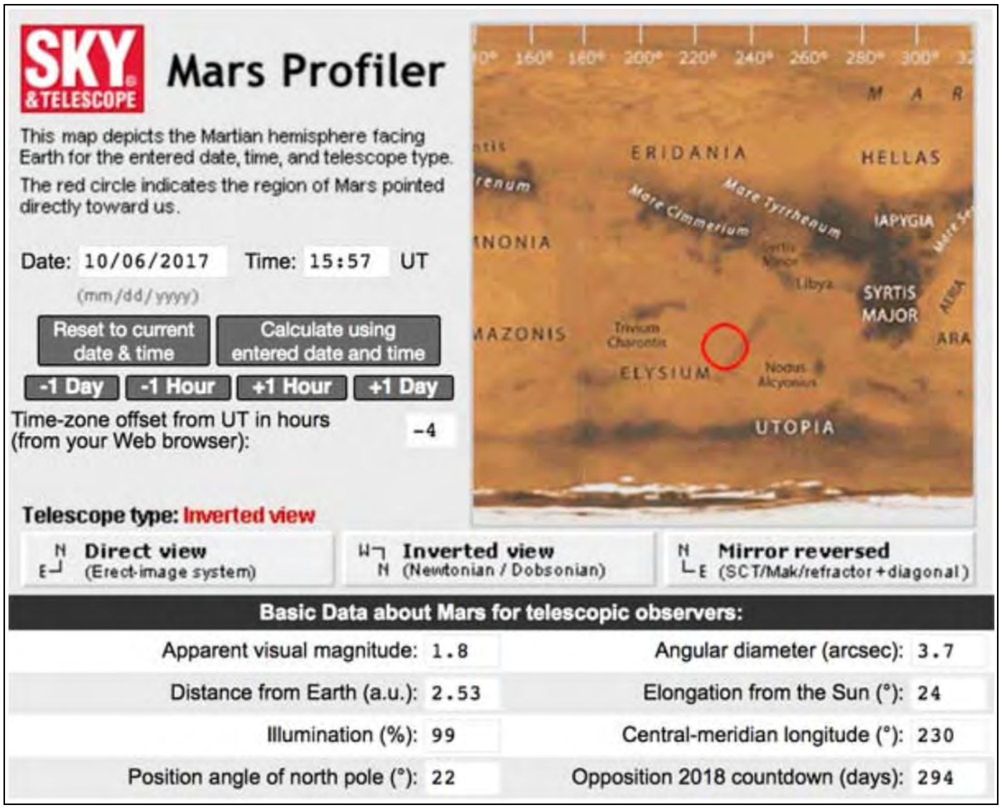

Figure 6. Numerous websites specialize in services providing useful information and simulated views for observers. Above is a screen capture of *Sky & Telescope* magazine's *Mars Profiler* app. The NASA Jet Propulsion Laboratory's *Solar System Simulator* also provides excellent apparent views of Mars and other planets.

set-up and provide observational tips. Additionally, some educational-based observatories, and other observatories with public viewing nights, often seek volunteers to assist in their public outreach efforts. This is another great way to learn about observing.

Choosing the Appropriate Time

The Moon has phases and a target will not be seen when it is not illuminated. It is also important to understand co-longitude and when a target is in view. Maximum contrast is when a target is near the terminator, but every other illuminated time may have different and subtle tones to sketch. The Moon traverses the sky quite rapidly. During a recent conjunction of the Moon and Mars, I watched the Moon's position change from being west of Mars to east of Mars in just a few hours! This has impacts for sketching if the object is near the terminator, and the subtle shifting of shadow can be seen in as little as an hour.

For planets it is important to know an appropriate time to view them, especially so for Mars. During Mars' closest approach it is far easier to examine than when it is at its farthest distance from Earth. Mercury and Venus are inner planets with phases, and for their closest approaches, will always appear as crescents. Viewing always improves for Jupiter, Saturn, Uranus and Neptune when they are at their nearest points, but the variability is not as pronounced the further out a solar system planet is, given the large distance. Viewing Jupiter is best during its opposition, but even then, atmospheric seeing (stability) conditions play a big role. Multiple nights with the same instrument could bring greatly varying detail. Knowing key terminology is important. The ALPO observation forms are a good place to learn these key terms and can be found online at the following site:

http://www.alpo-astronomy.org/publications/ALPO%20Observing%20Forms.html

Reviewing the ALPO Novice Observers Guide and finding a copy of the Introduction to Observing and Photographing the Solar System on the internet are also helpful. Acquaint yourself with various websites that offer information such as positional data calculated down to the second.

Managing Expectations

I always try to get an idea of what to expect before I view it. Unfortunately there is no guide that shows every co-longitude shadowing of each feature on the Moon. However, an atlas will give some basic detail of what on expect on a crater floor or rim. Knowing these key features will help you try to hone in. If you know they exist, you have a chance of seeing them especially if you are eyepiece “hopping” with ever-increasing magnification. With Mars, for example, getting an idea of the tonal variations of its surface through an apparent view tool such as the “Mars Profiler” will help you pinpoint your focus in areas that may have subtle tonal variations, where otherwise you might be oblivious to such features. Be aware of often overlooked bright limb features of Venus and Mars, since they are often overlooked. Also be aware of terminator effects. Often times Martian surface features can be obscured with clouds that blend the apparent view to seem similar to other light areas of the Martian surface. Look for changes in tones on Jupiter that denote the bands of zones and belts, as well as the types of spots within them. Look for the shadow of Saturn's rings on its surface. These are all common features that many observers overlook.

Recording the Observation

Everyone has their own style of drawing and recording. Earlier, I noted it would be impossible to draw the entire full lunar surface in one night, even at low power and fully within the field of view of the telescope eyepiece. There is just too much detail if you look for that detail. Sometimes one need needs to compensate in their sketching styles for this. Are small features ignored? Are they somehow blended with techniques? It's somewhat subjective, but there is plenty of material on the internet including historical professional drawings of the Moon that will provide you with many interpretive styles. Even a small crater can be a challenge. When I first entered the ALPO Lunar & Planetary Training Program, it took me only seconds to sketch my simplistic chosen crater; now it can take me two or three hours. I usually start with a simple draft intensity diagram sketch. Next, I hone into each quadrant with a more detailed draft intensity diagram. After the observation is complete, I will go back and redraw the draft intensity diagram with a little more skill. I never do the actual final sketch while observing. The draft sketches and collected thoughts written in my observational notes are the most time-consuming part of the overall observation.

Get to know your instruments. Many local astronomy clubs have loaner equipment, and star parties allow you to see other telescopes. Sometimes observers have radio telescopes set up. Radio telescopes can be modest set-ups and cost an investment of only $100 to $200 dollars, much like the cost of optical telescopes. Unlike optical telescopes, there is a wider variety of antennas and receivers, all geared to do different types of observations at different radio frequencies. At star parties ask owners about their telescopic mounts and tripods, their finder scopes, eyepiece focal lengths and the type of telescope they are using. As you learn more, you'll discover many more observational tips for lunar and planetary observing. You can spend years observing the same target and never run out of new experiences if you keep seeking to learn more about it and invest in the experience.

The Tone Scale

When you select a target to sketch, it is not difficult to see how a 10-tone scale can be roughly applied. As you seek more detail and compare pinpoint features and small sub-features, the full 10 tone scale is easily consumed. When you further hone into details, it is not unusual at all to start seeing half tones and quarter tones, especially as you sketch farther out from the target.

A thorough observer should take advantage of all instruments available to study a Solar System target. In optical observing, spectroscopy shows the composition of the target in the visible range. Consider the "RSpec Real Time Spectroscopy" website and their link to observational projects at *https://www.rspec-astro.com/sample-projects/*. One project provides an example of detecting the methane atmosphere on Neptune or Uranus. In radio astronomy, spectroscopy is used to study specific molecules in the radio frequency ranges. In radio astronomy there are many affordable home telescopes, as well as publicly accessible remote professional radio dishes like those available through Skynet. By using these various instruments one can study the Sun (SuperSid), Jupiter (Radio Jove), radio meteors, and the radio signals and maps of the Sun, Moon, and other planetary objects. Goldstone Apple Valley Radio Telescope has a special Uranus observing program for students. With the American Radio Relay League (ARRL), one can bounce signals off the Moon. Though less frequent, one can even partake in observations of radio eclipses and occultations. The Society of Amateur Radio Astronomers (SARA) helps the interested person to see the invisible radio universe. Exploring the opportunities that ALPO provides will help the interested person recognize an amazing universe of optical detail that is perceptually invisible to the untrained observer. These "hidden" radio and optical views will give the patience observer an entire lifetime of rewarding challenges.

Many observers consider accurate sketching, astrophotography, photometry, spectroscopy, exoplanet observing, and radio astronomy to be challenging. No doubt they require a commitment of time and often a financial investment. It's a choice not to make lightly with so many competing astronomy observational programs for pleasure and citizen science pursuit. Add to this a growing number of universities offering astronomical certificates and graduate level academic programs welcoming adults and retirees, both via online and on-site. It can become overwhelming, but that's just astronomy. There are other branches of science that are just as conducive to observation at both amateur and university levels of sophistication. These include geology, ecology, and electronics. May your enjoyment of scientific observing outweigh the frustration of decision-making over the immense number of choices for what to observe and study.

Figure 7. Typical sketching pencils, blending stumps and a kneaded eraser can be found at all common arts and crafts shops. These supplies help a sketcher properly record the proper tones within an observation.

Papers & Presentations:

A Report on Carrington Rotations 2231 through 2235 (2020 01 06.3826 UT to 2020 05 21.8750 UT)

By Richard (Rik) Hill,
Coordinator & Sc10ientific Advisor,
ALPO Solar Section
rhill@lpl.arizona.edu

Overview

> *To our hard-copy readers: This paper can be viewed in full-color in the online (pdf) version of this Journal.*

*This reporting period was characterized by very low to extremely low activity with only three active regions exceeding 100 millionths of the disk in area and none going beyond 160 millionths. The greatest development of these groups was Cao, Cso, and Dso (for one day), but they still produced some nice B and C class flares. The plot of activity (R_I) for the rotations in this reporting period looks like there was good activity, but one needs to take a look at the small numbers themselves! (**Plot "Rotational R_I for This Report"**).*

*For several years, people have asked, "Are we there yet?" concerning the solar minimum. As explained in the last report, we can't know that until we have been through it. I'm glad, however, to now report that solar minimum was officially determined by NASA to be December 2019 during CR 2223: https://science.nasa.gov/solar-cycle-25-has-begun and Cycle 25 is now underway. This can be seen in a plot of the last half of Cycle 24 (**Plot "R_I by Carrington Rotation"**) and in this report all the active regions discussed are Cycle 25 as Cycle 24 regions will likely become rarer from now on.*

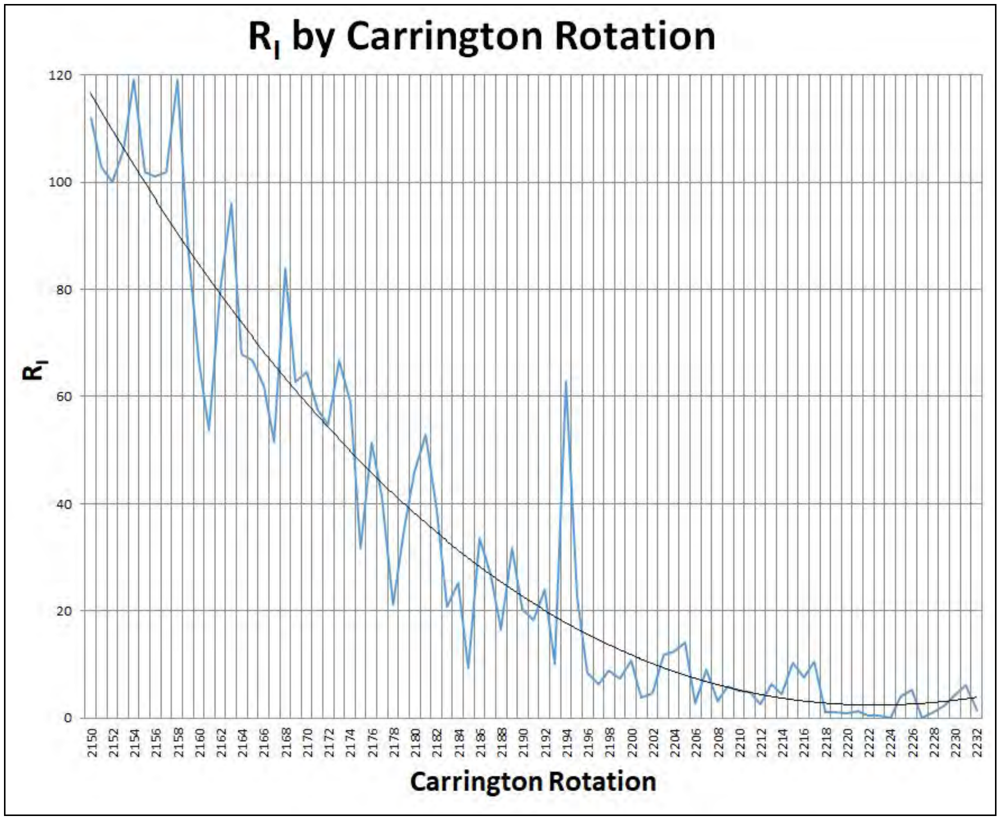

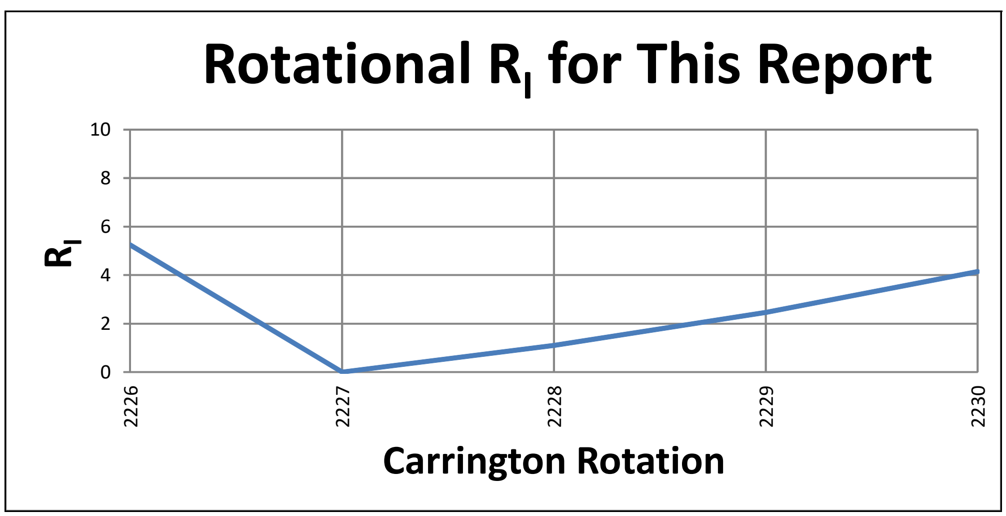

Observers contributing to this report, and their modes of observing are summarized in the table on page 37. It is not possible to present work from every observer, but everyone's work contributed. Readers should use this as a reference throughout this report rather than this information being repeated on every image or in each mention.

Terms and Abbreviations

Readers are encouraged to return here as needed for definitions of any unfamiliar terms and abbreviations.

AR = Active Regions, that is, areas which include all activity in all wavelengths for that area of the Sun as designated by NOAA; only the last four digits of the full identification number is used here

CaK = Calcium K-line observations

CM = Central Meridian of the visible disk

CR = Carrington Rotations

faculae = bright regions of the Sun's photosphere seen most easily near the Sun's edge

groups = visible light or "white light" sunspots associated with an Active Region

H-a = hydrogen-alpha observations

"leader" and "follower" = "east" and "west" on the Sun; using the "right-hand rule" where, using your right hand, your thumb pointing up is the North Pole and the rotation follows the curl of your fingers. Orientation of all images is with north up and celestial west to the right.

Na-D = Sodium-D observations

Naked-eye sunspots = those spots visible on the Sun without amplification but through proper and safe solar filtration; never look at the Sun, however briefly, without such filtration even at sunrise/sunset.

NOAA = National Oceanic and Atmospheric Administration

N, S, E and W = north, south, east, west

plage = a luminous area in the Sun's chromosphere that appears in the vicinity of an active region

W-L = white light observations

****

Statistics compiled by this author have their origin in the finalized daily International Sunspot Number data published by the World Data Center - Solar Index and Long Term Solar Observations (WDC-SILSO) at the Royal Observatory of Belgium. All times used here are Coordinated Universal Time and dates are reckoned from that and will be expressed numerically with month/day (for example, "9/6" and "10/23"). Carrington Rotation commencement dates are obtained from the table listed on the ALPO Solar Section web page at:

http://www.alpo-astronomy.org/solarblog/?page_id=3423

Areas of regions and groups are expressed in the standard units of millionths of the solar disk, with a naked-eye spot generally being about 900-1,000 millionths for the average observer. The McIntosh Sunspot Classification used here is the one defined by Patrick McIntosh formerly of NOAA (McIntosh 1981, 1989) and detailed in an article in the Journal of the ALPO, Volume 33 (Hill 1989). This description is also included in an online article on white-light flare observation located at:

http://www.alpo-astronomy.org/solarblog/?page_id=200

This will be referred to as the McIntosh Class. The magnetic class of regions is assigned by NOAA and will be entered parenthetically after the McIntosh Class unless specifically referred to as "mag. class".

Lastly, due to the constraints of publishing, most of the images in this report have been cropped, reduced or otherwise edited. The reader is advised that all images in this report, and a hundred times more, can be viewed at full resolution in the ALPO Solar Archives. The archives can be accessed by going to www.alpo-astronomy.org, then clicking on the ALPO Section Galleries link near the top-right corner of the page, then clicking on "Solar Observations Archive". You can also access the archives directly through this link: http://alpo-astronomy.org/gallery3/index.php/Solar-Observations-Archive .

Table of Contributors to This Report

Observer	Location	Telescope (aperture, type)	Camera	Mode	Format
Paul Andrew	Dover, Kent, UK	152mm RFR	ZWO ASI 290	H-a	Digital Images
Raffaello Braga	Milano, Italy	112mm RFR	PGR Chameleon mono	H-a	
Tony Broxton	Launceston, Cornwall, UK	127mm SCT	N/A	W-L	Drawings
Jeffery Carels	Bruges, Belgium	100mm, RFR	ZWO-ASI 120MM	W-L	Digital Images
Vlamir da Silva	Sao Palo, Brazil	40mm H-a PST	DMK21AU04.AS	H-a	
Michel Deconinck	Artignosc-sur-Verdon, Var, France	152mm RFR	N/A	W-L	Drawings
Howard Eskildsen	Ocala, FL, USA	80mm RFR	DMK41AF02	W-L wedge	Digital Images
Guilherme Grassmann	Curitiba, Brazil	60mm RFR	Lumenera Skynyx 2.0	H-a	
Ewan Hobbs	Hastings, East Sussex, UK	152mm RFR	Point Grey IMX174	W-L / H-a	
Monty Leventhal	Sydney, New South Wales, Australia	250mm SCT	N/A	W-L / H-a	Drawings
			Canon Rebel T3i EOS	H-a	I
Tom Mangelsdorf	Wasilla, AK, USA	120mm RFR	N/A	W-L	Drawings
Frank Mellilo	Holtsville, NY, USA	200mm SCT	DMK21AU03AS	H-a	Digital Images
Luigi Morrone	Benevento, Italy	356mm SCT	ZWO ASI290M	W-L	
Theo Ramakers	Oxford, GA, USA	80mm RFR	ZWO ASI174MM	H-a	
		279mm SCT	DMK41AU02AS	W-L	
		40mm H-a PST	DMK21AU03AS	H-a	
		40mm CaK PST		CaK	
Randy Tatum	Bon Air, VA, USA	180mm RFR	DFK31AU	W-L / pentaprism	
David Teske	Louisville, MS, USA	60mm RFR	N/A	W-L / H-a	Drawings
		100mm RFR	ZWO-ASI120mm	H-a	Digital Images
David Tyler	Buckinghamshire, UK	178mm RFR	ZWO ASI 120	W-L	
		90mm RFR	ZWO ASI 120	H-a	
Geert Vandenbulcke	Koksijde, Belgium	80mm RFR	ZWO ASI 290	H-a	
Christian Viladrich	Nattages, France	300mm RFN	Basler 1920-155	W-L	

Telescope types: Refractor (RFR), Newtonian Reflector (RFN), Schmidt Cassegran (SCT), Personal Solar Telescope (PST)
Mode Types: White Light (W-L), Hydrogen Alpha Filter (H-a), Calcium Potassium Filter (CaK)

Carrington Rotation 2231

Dates: 2020 05 21.8750 to 2020 06 18.0764
Avg. R_I = 6.15
High R_I = 17 (6/8)
Low R_I = 0 (12 days)
(see plot on page 5)

There were only two active regions during this rotation, AR 2764 and AR 2765, with the latter being larger and longer lived. AR 2765 officially rotated onto the disk on 6/4 but was seen in numerous images by Section observers the day before. In fact, Teske noted a loop prominence on the limb on 6/1 in his combination w-l/H-a drawing at 14:58 UT, at the latitude where this region was located. It is typical that Section observers catch these regions a day or two before official designation is made. Ramakers imaged the region in both w-l (13:23 UT) and CaK (13:53 UT) on 6/3. (**Figure 1**). It was highly foreshortened at the time but it was still obvious that a sizable region was coming into view with much attendant faculae. Maximum development of this region was rapidly reached as Cao class on 6/6 with 110 millionths area shown well in a w-l image by Vandenbulcke at 08:07 UT (**Figure 2**), and then Dso class on 6/7 when it reached 130 millionths area.

However, some of the best images were obtained during meridian passage on 6/9. Andrew got a spectacular H-a image at 08:48 UT showing a long dark filament extending east like a trailing tail. (**Figure 3**). Then Tyler got an excellent w-l image at 10:30 UT showing the region now at 100 millionths area Cso class, with the main leader spot, consolidating and becoming more circular (**Figure 4**). This is typical of a

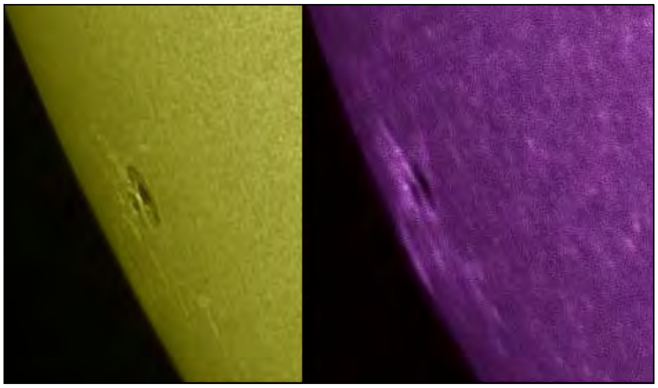

Figure 1. A two-pane view of AR 2765 by Ramakers on 6/3. Right pane is CaK at 13:23 UT and the left is a w-l at 13:53 UT.

Figure 2. A w-l view of AR 2765 by Vandenbulcke on 6/6 at 08:07 UT.

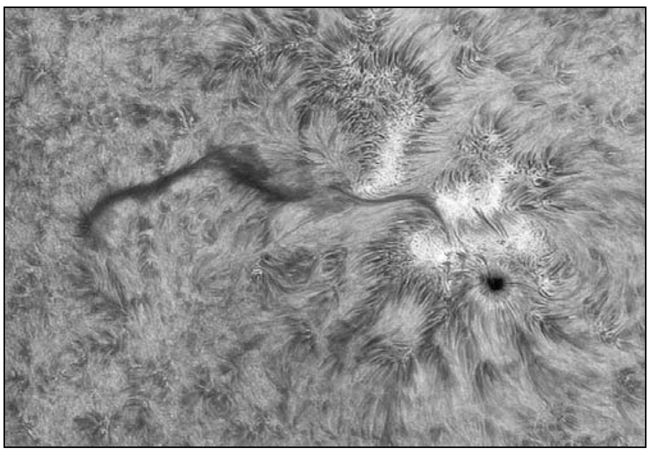

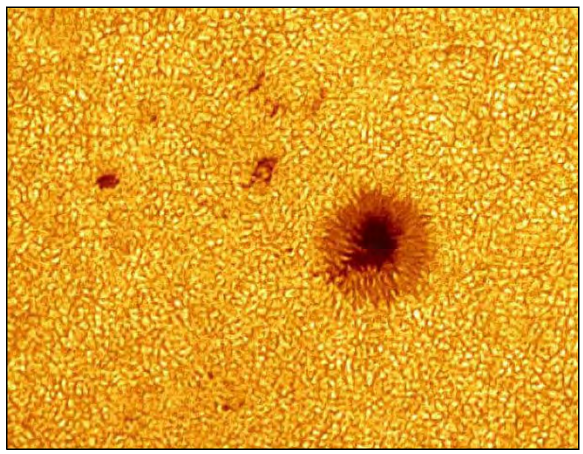

Figure 3. An H-a image of AR 2765 showing a large dark filament to the south by Andrew on 6/9 at 08:48 UT.

Figure 4. A Tyler w-l view of AR 2765 on 6/9 at 10:30 UT.

Figure 5. AR 2765 near the limb as seen in w-l by Tatum on 6/14 at 17:07 UT.

spot group that is past its peak, and from here it decreased in area as it neared the limb with the umbra breaking up within the penumbra. Tatum got a good w-l last look at it near the limb with the region now just a small Hsx lone spot of 60 millionths area (**Figure 5**).

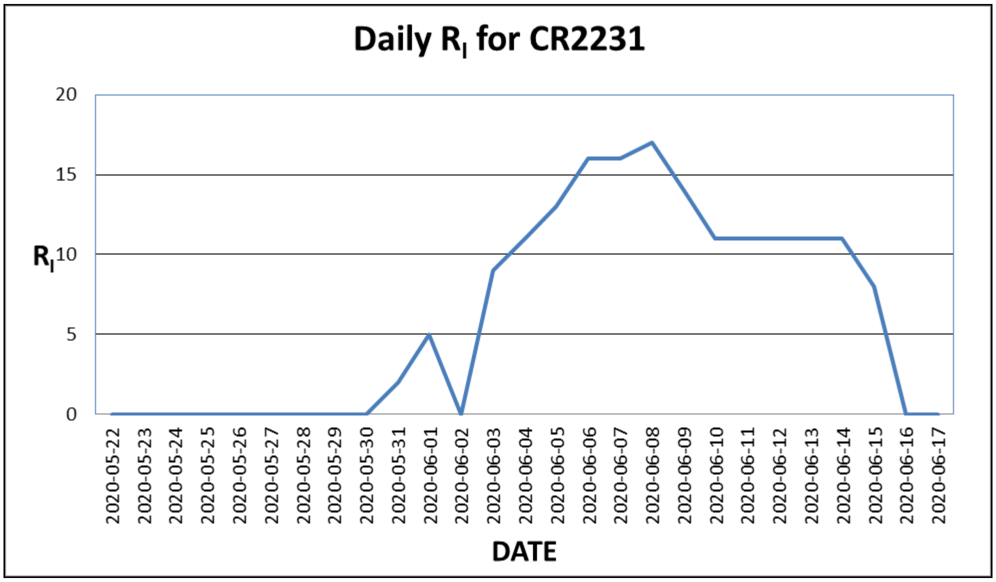

Carrington Rotation 2232

Dates: 2020 06 18.0764 to 2020 07 15.2750
Avg. R_I = 1.48
High R_I = 07 (7/4)
Low R_I = 0 (20 days)
(see plot on this page)

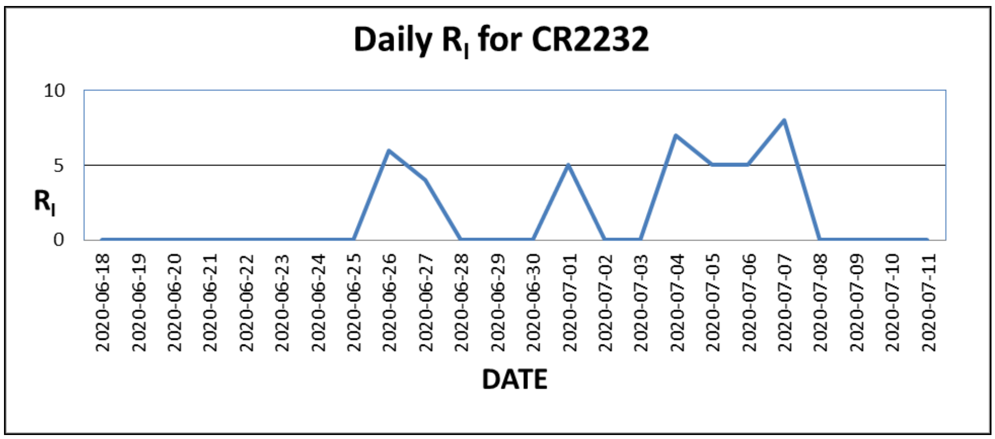

This rotation had very low activity. The one region AR 2766 (7/5-7/6) never got over 10 millionths and was classed as only Bxo-Axx. Even so, there were some impressive limb prominence observations like the one by Grassmann at 12:37 UT on 6/18 (**Figure 6**). Then a beautiful forest of prominences was recorded by Andrew on 6/29 at 09:44 UT (**Figure 7**). Finally, Ramakers caught another cluster of small prominences on the SE limb on 7/14 at 13:02 UT (**Figure 8**).

Carrington Rotation 2233

Dates: 2020 07 15.2750 to 2020 08 11.4931
Avg. R_I = 11.5
High R_I = 27 (8/1)
Low R_I = 0 (5 days)
(see plot on page 7)

This rotation had the highest R_I for the reporting period, 11.5, and the lowest number of zero spot days (5) since CR 2195 of October, 2017. Even so this is still characterized as low activity. Four ARs were designated, AR 2767 to AR 2770, during this rotation with AR 2767 and AR 2770 being the largest.

AR 2767 was first seen by Grassmann in CaK on 7/21 at 13:16 UT (**Figure 9**). The next day it was seen as an Hsx of 120 millionths area as imaged by Carels in w-l at 08:43 UT (**Figure 10**). It did not change for the next 5 days then began to reduce in size to 50 millionths while remaining Hsx as it left the disk on 8/3.

By contrast, AR 2770 appeared on the disk on 8/4 and by the second day was seen as a Cso region of 50 millionths. Ramakers got a first good look at this region in w-l on 8/3 at 14:14 UT (**Figure 11**). At that point it was just a couple of very foreshortened spots connected by faculae. On 8/5 it had grown to 160 millionths when Ramakers again observed it in w-l at 13:06 UT (**Figure 12**). As suddenly as it had grown, it dropped back down to 70 millionths on 8/7. Even so we have two remarkable images of the region, one CaK image by Viladrich at 07:49 UT (**Figure 13**), and another in w-l by Tyler at 09:42 UT (**Figure 14**). Eskildsen made observations of AR 2770 on 8/9 in w-l at 12:37 UT, H-a at 12:28 UT and CaK at 12:39 UT giving us a good look at this decaying region (**Figure 15**).

AR 2770 reduced in area from this point on and by 8/10, the day of Central Meredian (CM) passage, this region was clearly on its way out being Cso of only 30 millionths disk area. The umbra had broken into two major pieces and each piece was getting smaller. By 8/14 it was completely gone.

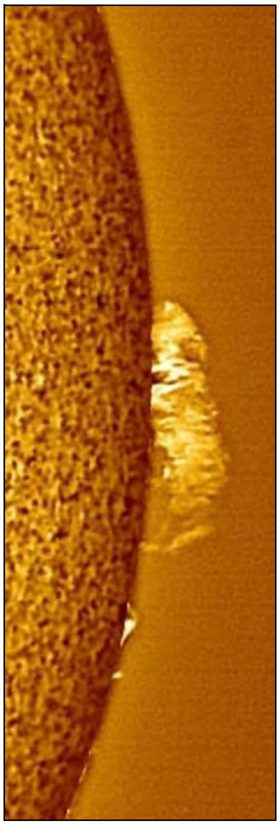

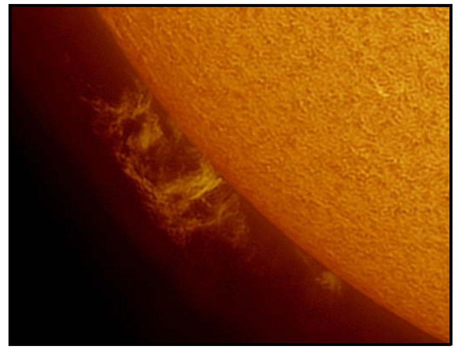

Figure 6 (Side left). SW limb prominence in H-a by Grassmann at 12:37 UT on 6/18.

Figure 7. (Above left) NE limb prominences by Andrew on 6/29 at 09:44 UT.

Figure 8. (Above right) SE limb prominences on 7/14 by Ramakers at 13:02 UT.

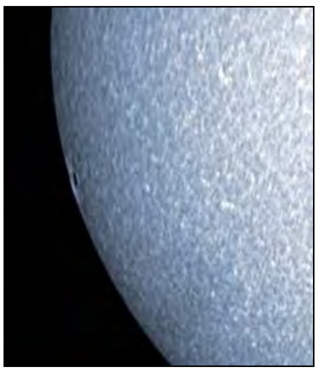

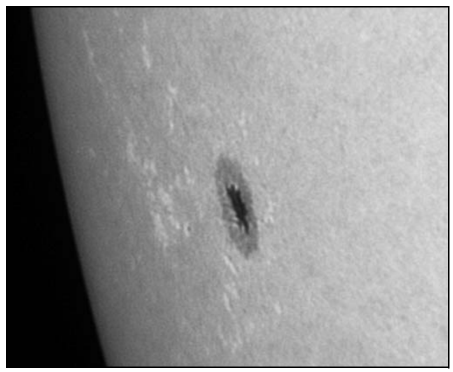

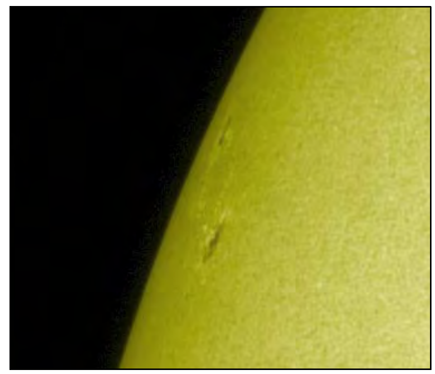

Figure 9. (Above left) AR 2767 first seen by Grassmann in CaK on 7/21 at 13:16 UT as a yet undesignated spot on the limb.

Figure 10. (Above center) A w-l image of AR 2767 near the limb on 7/22 at 08:43 by Carels.

Figure 11. (Above right) A w-l image of AR 2770 by Ramakers on 8/3 at 14:14 UT.

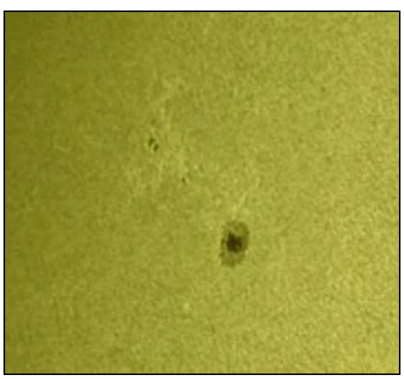

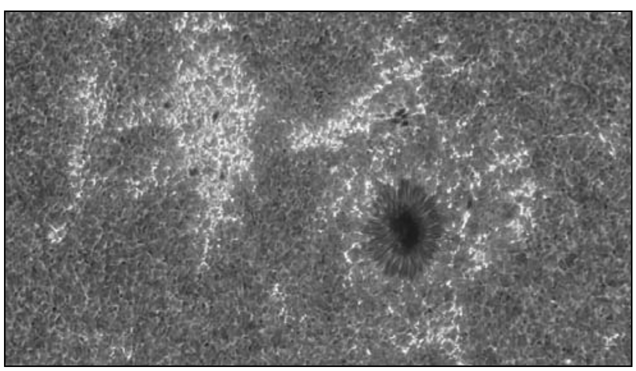

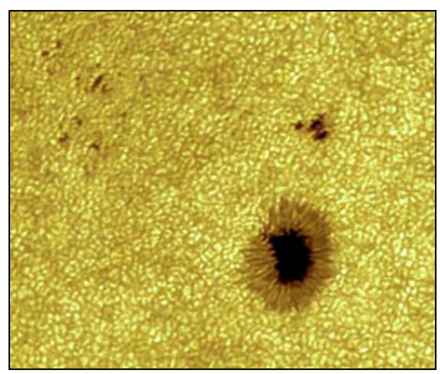

Figure 12. (Above left) Another w-l image of AR 2770 on 8/5 at 13:06 UT by Ramakers.

Figure 13. (Above center) A spectacular CaK image of AR 2770 on 8/7 at 07:49 UT by Viladrich with a scale of ~0.1 arcsec/pixel.

Figure 14. (Above right) Another sub-arc-second w-l view of AR 2770 by Tyler on 8/7 at 09:42 UT.

Carrington Rotation 2234

Dates: 2020 08 11.4931 to 2020 09 07.7396

Avg. R_I = 3.52

High R_I = 17 (8/12)

Low R_I = 0 (17 days)

(see plot on this page)

Again, we had low activity for this rotation. Two regions designated AR 2771 and AR 2772 were small Bxo groups typified by a Ramakers image of AR 2772 on 8/18 at 12:44 UT (**Figure 16**). The same day this region produced a coronal mass ejection that missed the Earth on 8/20. Each of these two regions only lasted 3 days. Observers submitted some images of the small prominences seen like the one by Ramakers on 8/11 at 13:03 UT. The features were not associated with a particular active region (**Figure 17**).

Lastly, we have a beautiful montage of prominences by Andres on 8/13 at the times noted on the images (**Figure 18**).

Carrington Rotation 2235

Dates: 2020 09 07.7396 to 2020 10 05.0125

Avg. R_I = 0.88

High R_I = 8 (9/23)

Low R_I = 0 (19 days)

(see plot on page 8)

This CR had the lowest average R_I (0.88) for the entire reporting period. There was only one active region and it lasted only 3 days, never attaining an area greater than 10 millionths or a class more evolved than Axx. Andrew got a nice field of NW limb prominences and spicules on 9/15 at 08:53 UT (**Figure 19**).

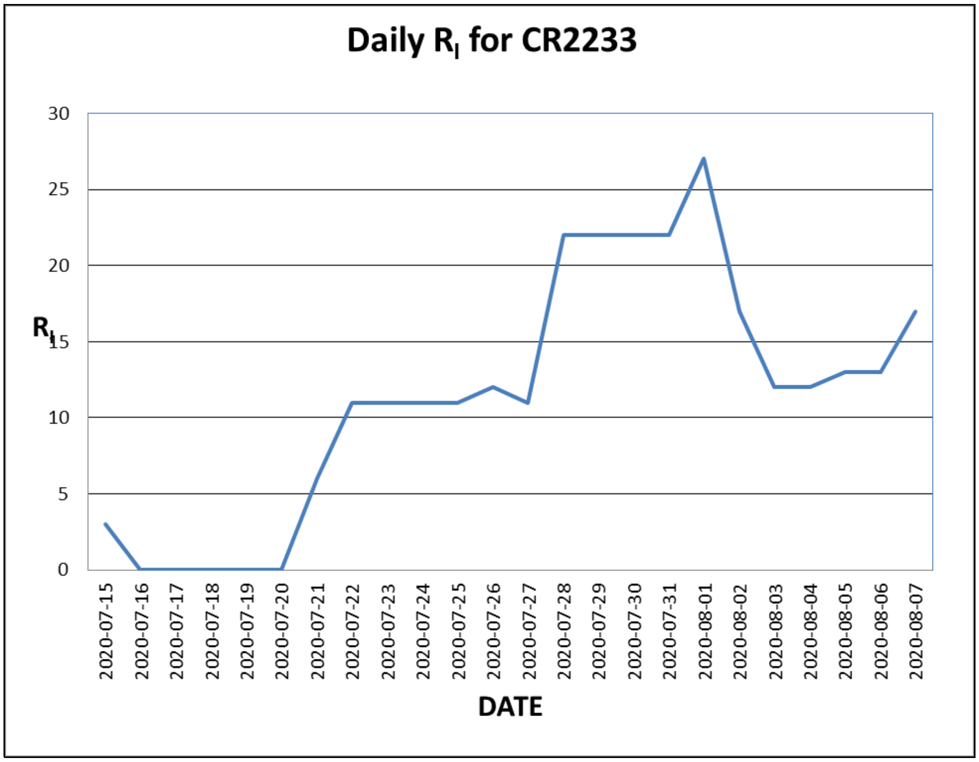

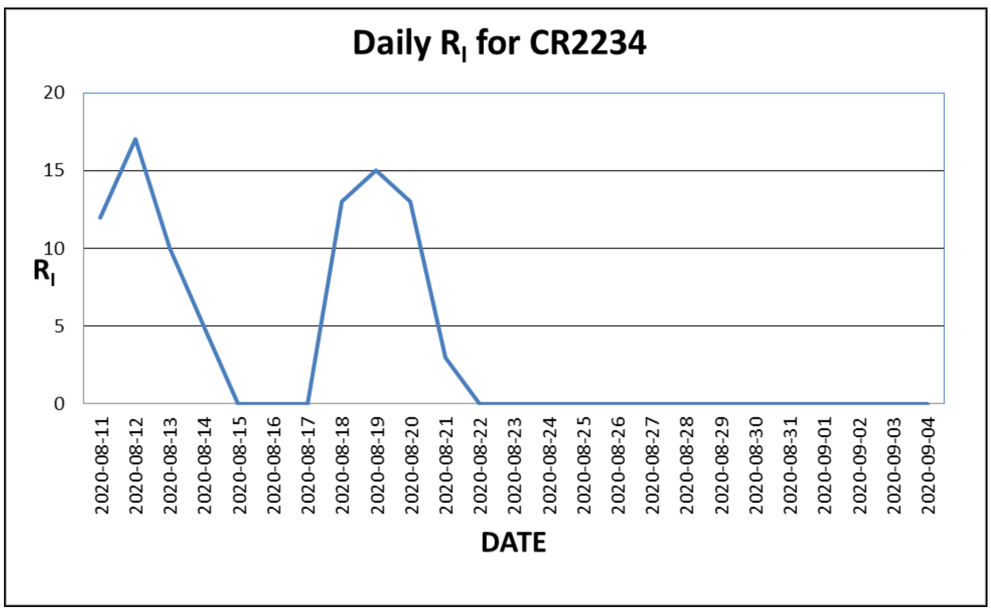

Conclusion

This reporting period was in the doldrums of solar minimum. But even at this writing, only two months after the end of this period, activity is starting to pick up. The question now is what will be the nature of the increase? There are two competing models, one showing a slow ramping up over the next year or two and the other showing a very rapid increase in just the next few months! We can document this with our observations and help determine which model is more accurate.

If you enjoyed this sampling of images you are encouraged to go to the Solar Section Gallery where you can enjoy many more that will hopefully serve as inspiration for your own observing. Join the ALPO (and thereby the Solar Section) and add your efforts to this gallery that they might be included in future reports!

Sunny skies to all!

For more information go to: *http://www.alpo-astronomy.org/member/ALPO_Standard_Memberships.html*

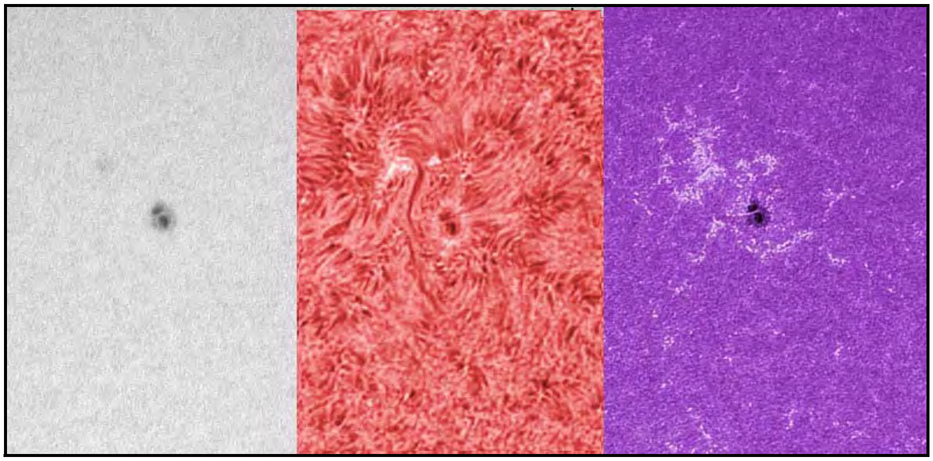

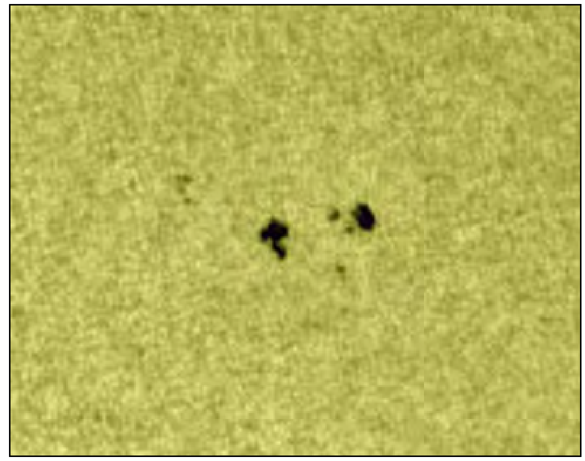

Figure 15. (Above left) A three pane Eskildsen image of AR 2770 on 8/9 in w-l at 12:37 UT (left), H-a at 12:28 UT (center) and CaK at 12:39 UT (right).

Figure 16. (Above right) An image of AR 2772, a Bxo group that was representative of the two regions that were on the sun in CR 2234, taken by Ramakers on 8/18 at 12:44 UT.

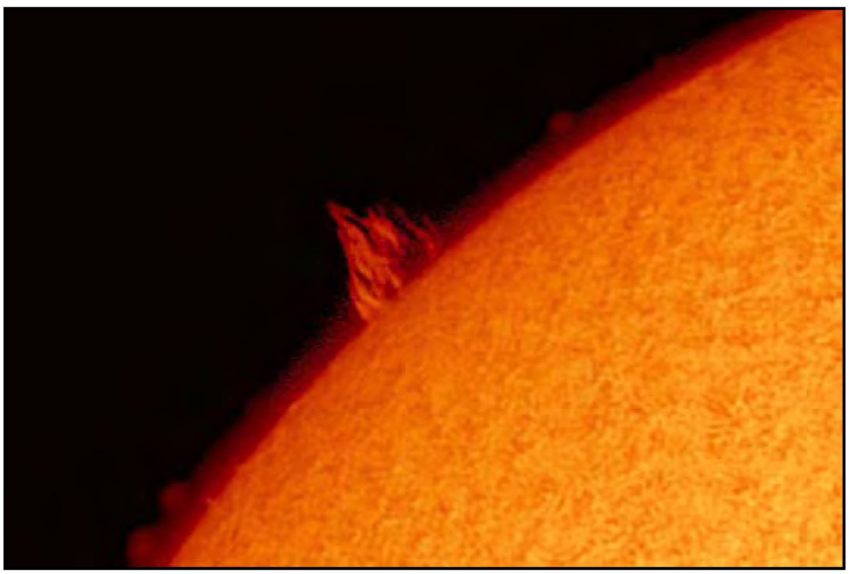

Figure 17. (Above) A Ramakers image of a delicate limb prominence on 8/11 at 13:03 UT.

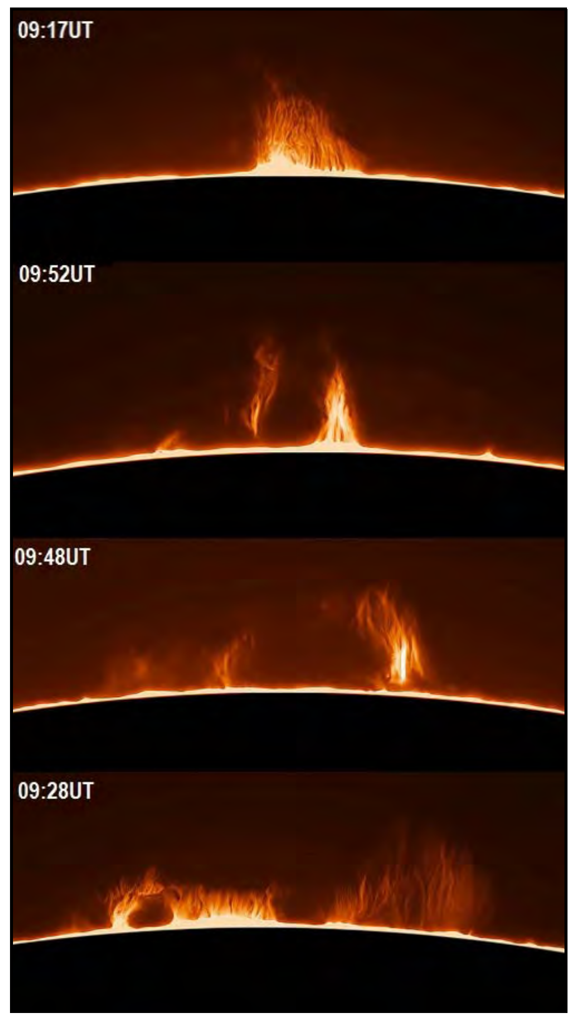

Figure 18. (Right) A spectacular 4 pane H-a montage of limb prominences by Andrew on 8/13 at 09:40 UT.

Figure 19. (Bottom) Another beautiful limb prominence image by Andrew on 9/15 at 08:53 UT not associated with an active region.

References

Hill, R.E., (1989) "A Three-Dimensional Sunspot Classification System" *Journal of the Assn of Lunar & Planetary Observers*, Vol. 33, p. 10.*http://www.alpo-astronomy.org/gallery3/var/albums/Publications-Section/ALPO-Journals/DJALPO-Volume-33/DJALPO%20Vol_%2033%20Nos_%201-3%20January%201989.pdf?m=1578431360*

Hill, R. E. (2021) "A Report on Carringtion Rotations 2226 through 2230", Journal of the Assn of Lunar and Planetary Observers Vol. 63, No. 1, p. 52.

Livingston, W., Penn, M.; (2008) "Sunspots may vanish by 2015." *https://wattsupwiththat.files.wordpress.com/2008/06/livingston-penn_sunspots2.pdf*

McIntosh, Patrick S., (1981) "The Physics Of Sunspots". Sacramento Peak National Observatory, Sunspot, NM; L.E. Cram and J.H.Thomas (eds.), p.7. *https://ui.adsabs.harvard.edu/abs/1981phss.conf.....C/abstract*

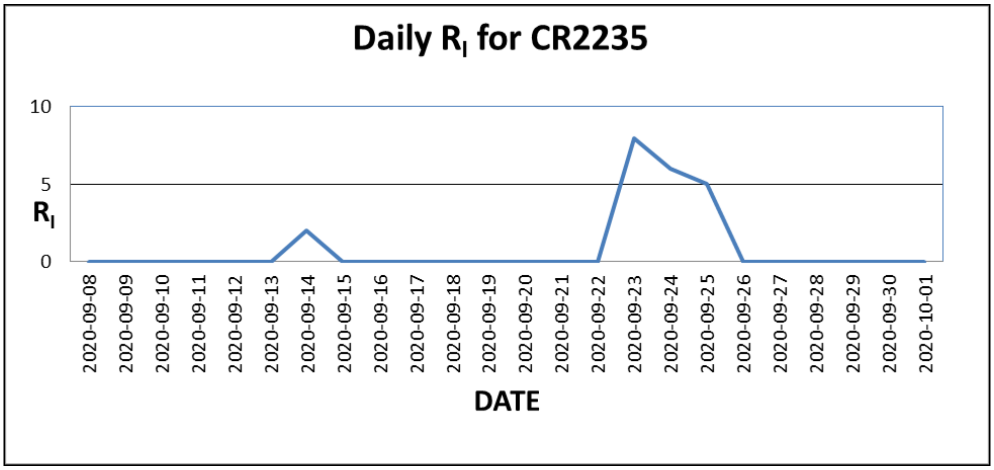

McIntosh, Patrick S., (1989) "The Classification of Sunspot Groups" *Solar Physics*, Vol. 125, Feb. 1990, pp. 251-267. *http://adsabs.harvard.edu/abs/1990SoPh..125..251M*

Solar Map of Active Regions *https://www.raben.com/maps/date*

SILSO World Data Center *http://sidc.be/silso/home*

SILSO Sunspot Number *http://www.sidc.be/silso/datafiles*

The Mass Time-of-Flight spectrometer (MTOF) and the solar wind Proton Monitor (PM) Data by Carrington Rotation. *http://umtof.umd.edu/pm/crn/*

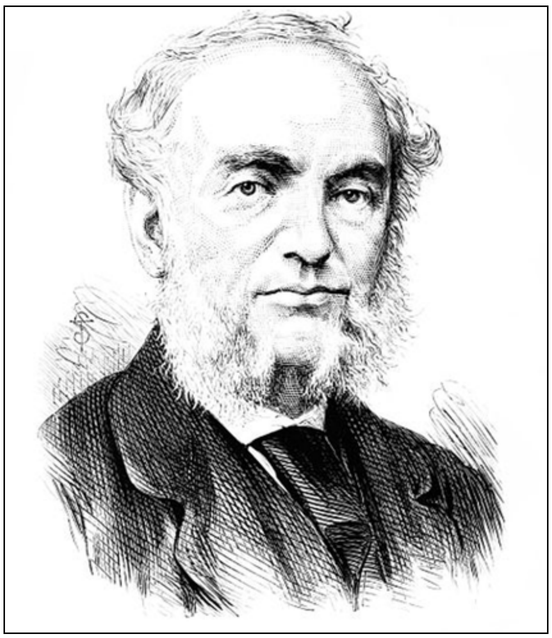

Richard Christopher Carrington and His Legacy

Carrington (26 May 1826 – 27 November 1875) was an English amateur astronomer whose 1859 astronomical observations demonstrated the existence of solar flares as well as suggesting their electrical influence upon the Earth and its aurorae; and whose 1863 records of sunspot observations revealed the differential rotation of the Sun.

The "Carrington Rotation" is a system for comparing locations on the Sun over a period of time, allowing the following of sunspot groups or reappearance of eruptions at a later time.

Because a Solar rotation is variable with latitude, depth and time, any such system is necessarily arbitrary and only makes comparison meaningful over moderate periods of time. Solar rotation is arbitrarily taken to be 27.2753 days for the purpose of Carrington rotations. Each rotation of the Sun under this scheme is given a unique number called the Carrington Rotation Number, starting from November 9, 1853.

Richard Carrington determined the solar rotation rate from low latitude sunspots in the 1850s and arrived at 25.38 days for the sidereal rotation period. Sidereal rotation is measured relative to the stars, but because the Earth is orbiting the Sun, we see this period as 27.2753 days.

It is possible to construct a diagram with the longitude of sunspots horizontally and time vertically. The longitude is measured by the time of crossing the central meridian and based on the Carrington rotations. In each rotation, plotted under the preceding ones, most sunspots or other phenomena will reappear directly below the same phenomenon on the previous rotation. There may be slight drifts left or right over longer periods of time.

ALPO Solar Section

OBSERVER____

ADDRESS____

DATE/TIME____________________________________UT

SEEING__________ CLOUDS__________ WIND__________

APERTURE________mm FOCAL LENGTH________mm TYPE_____

EYEPIECE______mm FILTRATION____________________

OBSERVATION: *DIRECT* OR *PROJECTED*? (CIRCLE ONE)

ROTATION____________

P_____ B_____ L_____

GROUPS: N_____ + S_____ =_____

SPOTS: N_____ + S_____ =_____

R = 10G + S = __________

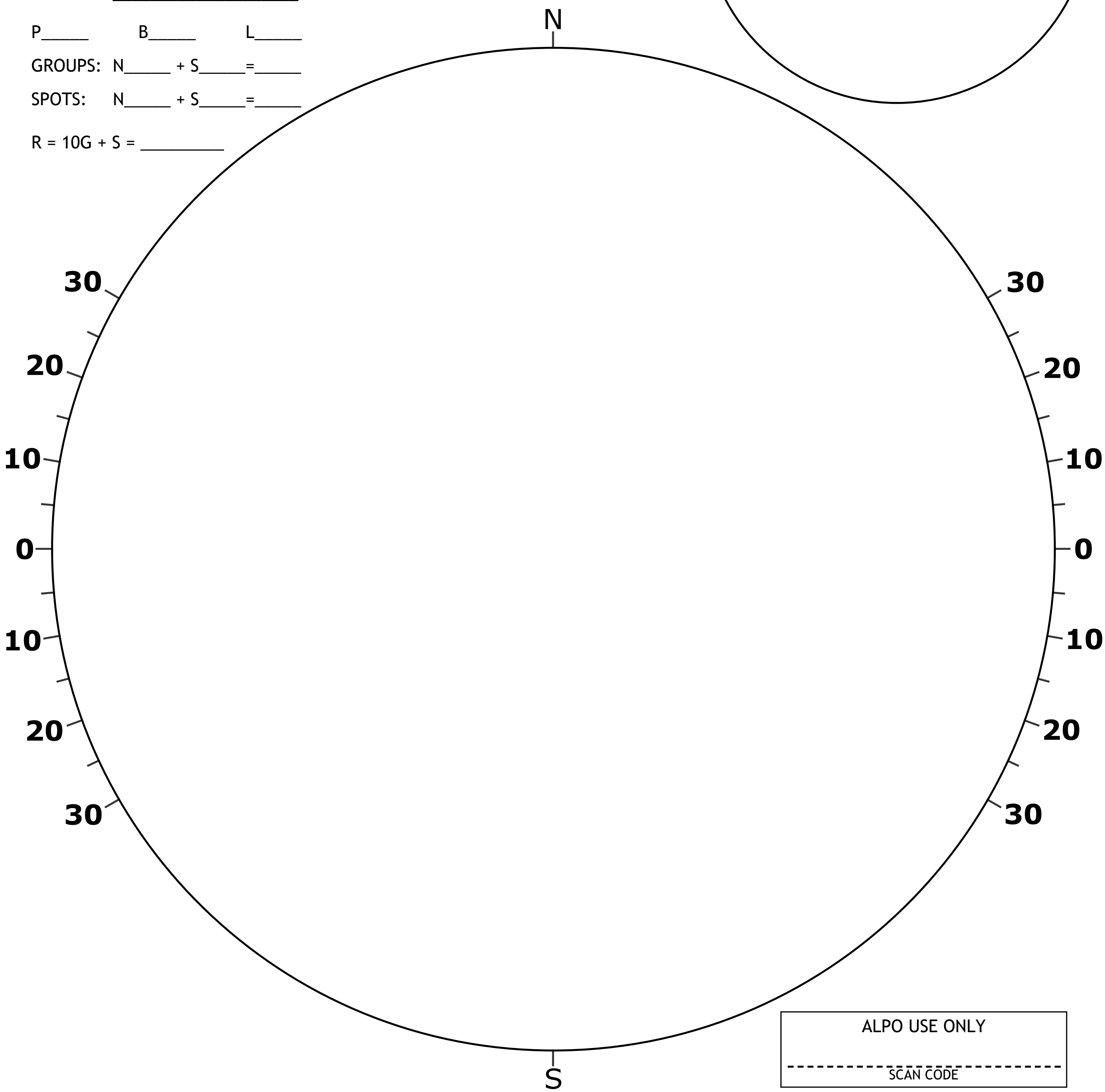

ALPO USE ONLY

SCAN CODE

Papers & Presentations

J and H filter Brightness of Venus: 2014-2020

By Richard W. Schmude, Jr.,
schmude@gordonstate.edu

Abstract

This paper summarizes over 200 new J- and H-filter brightness measurements of Venus made since 2016. The reduced magnitudes are described by: $J(1, \alpha) = -5.072 - 0.468\alpha + 2.4287\alpha^2 - 0.6264\alpha^3$ *and* $H(1, \alpha) = -5.1616 - 0.1434\alpha + 2.015\alpha^2 - 0.5852\alpha^3$ *where* α *is the phase angle in degrees divided by 100 and* $J(1, \alpha)$ *and* $H(1, \alpha)$ *are reduced magnitudes. There is evidence the* $H(1, \alpha)$ *value is dimmer when the longitude of the central meridian lies between 0 and 90° W than between 90 and 180° W or 270 and 0° W. More measurements, with a lower scatter, are needed before more definite conclusion can be made.*

Introduction

The writer carried out J- and H-filter brightness measurements of Venus between 2014 and early 2016 (Schmude, 2017a). The results presented here are a continuation of that study. The J and H filters are sensitive to wavelengths of 1.15-1.35 µm and 1.5-1.8 µm, respectively. A historical review of near-infrared brightness studies of Venus has already been given (Schmude, 2017).

Brightness measurements in near-infrared wavelengths are useful for several reasons. They may help provide useful constraints on the heat budget of Venus. Furthermore, they may lead to the detection of large volcanic hot spots. Finally they may yield information on how the lower atmosphere interacts with the hot surface.

Purpose of This Work

One objective of this study is to report the reduced magnitudes of Venus in the J and H filters covering a wider phase angle range than in (Schmude, 2017a). The J – H color index values are reported for phase angles of between 30° and 150°. A second objective is to determine if the longitude of Venus' central meridian affects the planet's near infrared brightness. Finally, predicted dates of when Venus will be brightest in late 2021 are presented.

Methods and Materials

The method of obtaining brightness values is described elsewhere (Schmude, 2017a). Comparison star magnitudes are from Henden (2002). All measurements are corrected for color transformation and extinction based on the procedure in Hall and Genet (1988). Secondary extinction coefficients are assumed to equal zero. The normalized magnitude is described by Shephard (2017) and is the brightness Venus would have if its Sun and Earth distances equal 1.0 astronomical unit. Values of the phase angle and other necessary values are from the JPL Ephemeris at (*https://ssd.jpl.nasa.gov/horizons.cgi*).

Results

New $J(1, \alpha)$ and $H(1, \alpha)$ measurements are summarized in tables 1 and 2, respectively. The range of phase angles for the J filter is 17.9° to 159.8°. The corresponding range for the H filter is 17.7° to 161.4°. Figure 1 shows graphs of the reduced magnitude values plotted against the phase angle divided by 100 for both filters. The phase angle of Venus is measured from the observer to that planet (Venus) with the Sun at the vertex. (Shephard, 2017)

All reduced magnitude values (between 2014 and 2020) were fitted to a cubic equation and the results are shown in Figure 1. The standard error of estimate (Larson & Farber, 2006) for the $J(1, \alpha)$ values is 0.056 magnitudes. The corresponding value for $H(1, \alpha)$ values is 0.055 magnitudes. These are close to the expected uncertainty of J and H filter magnitudes (Henden, 2002).

Computed reduced magnitudes for both filters and J – H color indexes are shown in Table 3 for selected phase angles. These values are based on the equations in Figure 1. Essentially, Venus' J – H color index increases as the phase angle increases.

Online Features

Left-click your mouse on:

• The author's e-mail address in blue text to contact the author of this article.

• The references in blue text to jump to source material or information about that source material (Internet connection must be ON).

Observing Scales

Standard ALPO Scale of Intensity:

0.0 = Completely black

10.0 = Very brightest features

Intermediate values are assigned along the scale to account for observed intensity of features

ALPO Scale of Seeing Conditions:

0 = Worst

10 = Perfect

Scale of Transparency Conditions:

Estimated magnitude of the faintest star observable near Venus, allowing for daylight or twilight

IAU directions are used in all instances.

The atmosphere of Venus is more transparent to near-infrared than to visible light. Taylor (2014) reports light with a wavelength of 1.2 µm penetrates to an altitude of ~5 km whereas light with a wavelength of 1.7 m penetrates to an altitude of ~20 km. These are much lower altitudes than for "reflected solar" light (~75 km).

Does the brightness of Venus change with the central meridian longitude? To answer this question, I computed the difference between the measured and predicted reduced

Table 1. Reduced Magnitude Measurements for the J-filter Made Between Sep. 2016 and May 2020

Date	$J(1, \alpha)$ (–)	Date	$J(1, \alpha)$ (–)	Date	$J(1, \alpha)$ (–)	Date	$J(1, \alpha)$ (–)
2016		**2017**		**2017**		**2019**	
Sep. 16.01	4.80	Feb. 4.00	3.64	Jun. 9.39	3.99	Feb. 25.48	4.49
Sep. 29.01	4.72	Feb. 4.02	3.63	Jul. 4.37	4.25	Mar. 7.46	4.55
Oct. 6.99	4.76	Feb. 4.05	3.64	Jul. 4.40	4.36	Mar. 20.45	4.82
Oct. 17.99	4.72	Feb. 9.01	3.50	Jul. 22.38	4.50	**2020**	
Oct. 22.99	4.70	Feb. 9.03	3.48	Jul. 22.41	4.48	Jan. 21.01	4.73
Nov. 14.99	4.57	Feb. 16.01	3.25	Aug. 17.41	4.68	Feb. 15.02	4.50
Nov. 15.00	4.60	Feb. 17.02	3.27	Aug. 17.43	4.68	Feb. 15.05	4.50
Nov. 17.99	4.50	Feb. 17.04	3.25	Aug. 24.40	4.73	Feb. 22.03	4.46
Nov. 18.01	4.51	Feb. 17.07	3.23	Aug. 24.42	4.73	Feb. 28.04	4.38
Nov. 21.97	4.52	Feb. 19.02	3.20	Sep. 7.40	4.82	Mar. 1.02	4.36
Nov. 21.99	4.53	Feb. 19.04	3.19	Sep. 25.45	4.85	Mar. 1.05	4.34
Nov. 22.01	4.54	Feb. 24.02	3.05	Oct. 5.45	4.92	Mar. 8.04	4.27
Dec. 1.99	4.47	Feb. 24.04	3.02	Oct. 5.46	4.95	Mar. 26.04	4.08
Dec. 2.02	4.46	Feb. 25.03	3.00	Oct. 20.46	5.08	Mar. 27.04	4.09
Dec. 10.01	4.39	Feb. 25.05	2.99	Oct. 20.46	5.07	Mar. 27.06	4.08
Dec. 10.03	4.42	Feb. 26.00	2.96	Oct. 25.45	5.03	Apr. 2.04	3.93
Dec. 10.98	4.38	Feb. 26.03	2.95	Oct. 25.46	5.06	Apr. 2.07	3.94
Dec. 11.01	4.38	Feb. 26.05	2.95	**2018**		Apr. 12.05	3.75
Dec. 11.04	4.38	Feb. 26.07	2.91	Mar. 4.01	5.01	Apr. 14.05	3.69
2017		Mar. 4.01	2.75	Mar. 15.02	5.08	Apr. 14.08	3.69
Jan. 8.03	3.99	Mar. 4.03	2.74	Apr. 5.03	5.05	Apr. 16.06	3.68
Jan. 13.00	3.98	Mar. 9.01	2.55	Apr. 19.04	5.03	Apr. 22.07	3.50
Jan. 13.02	3.97	Mar. 9.03	2.54	Apr. 21.05	4.89	Apr. 25.05	3.43
Jan. 13.04	3.99	Mar. 11.01	2.44	Apr. 29.04	4.83	Apr. 25.07	3.43
Jan. 14.01	3.99	Mar. 16.01	2.30	Jun. 7.07	4.67	Apr. 28.06	3.37
Jan. 14.04	4.00	Mar. 18.03	2.07	Aug. 5.06	4.02	Mar. 1.06	3.28
Jan. 27.01	3.74	Apr. 7.45	2.52	Nov. 28.48	3.25	May 3.06	3.17
Jan. 27.03	3.74	Apr. 26.42	3.19	**2019**		May 8.05	3.08
Jan. 27.06	3.77	May 8.41	3.46	Jan. 11.49	4.08	May 12.06	2.91
						May 16.06	2.87

Table 2. Reduced Magnitude Measurements for the H-filter for Sep. 2016 to May 2020

Date	H(1, α) (–)	Date	H(1, α) (–)	Date	H(1, α) (–)	Date	H(1, α) (–)
2016		**2017**		**2017**		**2019**	
Sep. 29.00	4.83	Feb. 17.03	3.51	Sep. 4.42	4.81	Nov. 25.97	4.88
Oct. 7.00	4.79	Feb. 17.06	3.44	Sep. 7.42	4.86	**2020**	
Oct. 18.00	4.84	Feb. 17.08	3.48	Sep. 16.43	4.86	Jan. 21.00	4.69
Oct. 23.00	4.75	Feb. 19.03	3.42	Sep. 18.44	4.86	Feb. 15.01	4.52
Nov. 14.98	4.59	Feb. 24.03	3.28	Sep. 25.44	4.88	Feb. 15.04	4.54
Nov. 15.00	4.61	Feb. 24.05	3.28	Oct. 4.45	4.95	Feb. 22.02	4.52
Nov. 17.98	4.53	Feb. 24.06	3.28	Oct. 4.45	4.97	Feb. 28.03	4.40
Nov. 18.00	4.54	Feb. 25.02	3.27	Oct. 19.46	5.11	Feb. 28.05	4.48
Nov. 21.98	4.51	Feb. 25.04	3.26	Oct. 19.46	5.11	Mar. 1.02	4.46
Nov. 22.00	4.52	Feb. 25.06	3.26	Oct. 24.46	5.15	Mar. 1.04	4.51
Dec. 1.98	4.50	Feb. 26.02	3.23	Oct. 31.46	4.99	Mar. 8.03	4.37
Dec. 2.01	4.51	Feb. 26.04	3.23	Nov. 3.47	5.07	Mar. 26.03	4.15
Dec. 9.99	4.41	Feb. 26.06	3.18	Nov. 10.48	5.15	Mar. 26.05	4.14
Dec. 10.02	4.43	Mar. 4.02	3.08	Nov. 11.47	5.15	Mar. 27.03	4.20
Dec. 11.00	4.42	Mar. 4.04	3.07	Nov. 17.48	5.17	Mar. 27.05	4.15
Dec. 11.02	4.43	Mar. 9.02	2.96	**2018**		Apr. 2.03	4.06
Dec. 11.05	4.44	Mar. 9.05	2.94	Mar. 8.01	5.20	Apr. 2.06	4.08
2017		Mar. 11.02	2.90	Apr. 5.02	4.97	Apr. 12.04	3.89
Jan. 8.04	4.10	Mar. 11.03	2.90	Apr. 19.03	4.93	Apr. 12.08	3.95
Jan. 13.01	4.07	Mar. 16.02	2.76	Apr. 21.04	4.96	Apr. 14.04	3.86
Jan. 13.03	4.08	Mar. 17.02	2.64	Apr. 29.05	4.90	Apr. 14.07	3.86
Jan. 13.05	4.07	Apr. 1.45	2.53	Jun. 7.06	4.69	Apr. 16.04	3.86
Jan. 14.02	4.10	Apr. 7.44	2.92	Aug. 5.05	4.16	Apr. 22.06	3.68
Jan. 14.05	4.09	May 8.40	3.68	Aug. 26.03	3.81	Apr. 26.04	3.63
Jan. 27.00	3.90	Jun. 9.40	4.09	Nov. 28.47	3.46	Apr. 25.06	3.67
Jan. 27.02	3.90	Jul. 4.38	4.36	**2019**		Apr. 28.05	3.59
Jan. 27.04	3.91	Jul. 4.41	4.44	Jan. 11.47	4.20	May 1.04	3.51
Feb. 4.01	3.75	Jul. 22.39	4.50	Feb. 25.47	4.64	May 3.04	3.35
Feb. 4.03	3.77	Jul. 22.42	4.52	Mar. 7.47	4.57	May 8.04	3.33
Feb. 4.06	3.76	Aug. 17.40	4.71	Mar. 20.47	4.76	May 12.05	3.24
Feb. 9.02	3.67	Aug. 17.42	4.71	Apr. 4.03	4.77	May 12.07	3.23
Feb. 9.04	3.68	Aug. 24.39	4.72	Apr. 11.43	4.78	May 16.05	3.10
Feb. 16.02	3.50	Aug. 24.41	4.73	Apr. 16.43	4.82		

Table 3. The J - H color Indexes of Venus for Different Phase Angles

Phase Angle (degrees)	J(1, α) (magnitudes)	H(1, α) (magnitudes)	J – H value (magnitudes)
30	–5.011	–5.040	0.03
60	–4.614	–4.658	0.04
90	–3.983	–4.115	0.13
120	–3.227	–3.151	0.30
150	–2.424	–2.957	0.53

Table 4. Predicted Date and Phase Angles of Maximum Brightness of Venus for the J and H Filters

Date of Max. Brightness	Corr. for Extinction	Filter	α (degrees)	Max. brightness
Dec. 12, 2021	No	J	128	–5.935
Dec. 19, 2021	No	H	138	–6.232
Dec. 5, 2021	Yes	J	119	–5.511
Dec. 10, 2021	Yes	H	125	–5.855

magnitude value. Essentially, the predicted reduced magnitude is from the appropriate equation in Figure 1. Since the central part of Venus' disc is in darkness for phase angles greater than 90°, I selected only brightness value differences for phase angles less than 70°. These are plotted against the longitude of the central meridian and are shown in Figure 2.

The brightness value differences for the J- and H-filters show some scatter. There are no 0.1 magnitude or higher changes for the J-filter covering a 90° longitude range. There may be a ~0.05 magnitude change for the H-filter. Respective mean H-filter magnitudes and standard deviations (σ) when the central meridian is between 0-90° W, 90-180° W and 270-0° W are 0.039 (σ = 0.031), –0.025 (σ = 0.044) and –0.003 (σ = 0.050) magnitudes, respectively.

The writer carried out t-tests at the 95% confidence level (Larson and Farber, 2006). The most significant result is a statistically significant difference between the mean value for 0-90° W compared to the means for 90°-180° W and 270°-0° W. (This difference is even significant at the 99% confidence level.)

Essentially, the mean measured magnitude difference for 0°-90° W is greater than for the other two longitude ranges. The 0°-90° W area includes Maxwell Montes and half of the large elevated area Ishtar Terra. It is not clear if these features affect the measured H-filter magnitudes. More data are needed, to make firmer conclusions.

When is Venus brightest in near-infrared light? Venus has a low orbital eccentricity and, hence, its distance from the Sun does not change much from one elongation to the next. The distances and phase angles for late November and December of 2021 (JPL Horizons) were used in computing apparent magnitudes. Brightness values are shown in Figure 3. Dates of maximum brightness without atmospheric extinction along with maximum brightness values are given in Table 4.

Atmospheric extinction will also affect brightness values. The extinction coefficients vary. I chose the mean extinction coefficients (magnitude/air mass) of 0.088 and 0.066 for the J and H filters, respectively (Schmude, 2017b). I carried out a second calculation taking atmospheric extinction into account for 0:00 UT. This is about when Venus is obvious in the western sky for the central time zone. The results are shown in Figure 3. Dates of maximum brightness are given in Table 4. In the no-extinction case, Venus reaches a peak brightness at phase angles of 128° and 138° for the J- and H-filters, respectively. With atmospheric extinction, peak brightness occurs at lower phase angles.

Acknowledgements

The writer thanks Bryson Smith and his wife for their assistance.

References

Hall, D. S., Genet, R. M. "Photoelectric Photometry of Variable Stars, Second, Revised and Expanded Edition, Willmann-Bell, Inc. Richmond, VA, 1988. *https://www.alibris.com/Photoelectric-Photometry-of-Variable-stars-A-Practical-Guide-for-the-Smaller-Observatory-Douglas-S-Hall/book/5109450*.

Henden, A. A. "JHK Standards for Small Telescopes", *Journal of the American Assn of Variable Star Observers*, 31, 11-20, 2002. *http://adsabs.harvard.edu/full/2002JAVSO..31...11H*

JPL Horizons at *https://solarsystem.nasa.gov/planets/venus/overview/*

Larson, R., Farber, B. "Elementary Statistics Picturing the World", 3rd edition, Pearson, Upper Saddle River, NJ, 2006. *https://www.alibris.com/Elementary-Statistics-Picturing-the-World-Ron-Larson-Captain/book/1998720*

Schmude, R. W. Jr. "Near-Infrared Photometry of Venus", *Journal of the Royal Astronomical Society of Canada*, 111, pp. 104-110 (2017a). *http://articles.adsabs.harvard.edu/pdf/2017JRASC.111..104S*

Schmude R. W., Jr., "ALPO Observations of Mars During the 2005 Apparition", *Journal of the Assn of Lunar & Planetary Observers*, 59(1), pp. 58-72 (2017b). *http://alpo-astronomy.org/gallery3/index.php/Publications-Section/ALPO-Journals/DJALPO-2017/DJALPO59-1-Winter2017*

Shepard, M. K. "Introduction to Planetary Photometry." Cambridge: Cambridge University Press, Cambridge, 2017. *https://www.amazon.com/Introduction-Planetary-Photometry-Michael-Shepard/dp/110713174X*

Taylor, F.W. "The Scientific Exploration of Venus", Cambridge University Press, Cambridge, U.K., 2014. pp. 314. *https://www.amazon.com/Scientific-Exploration-Venus-Fredric-Taylor/dp/1107023483*

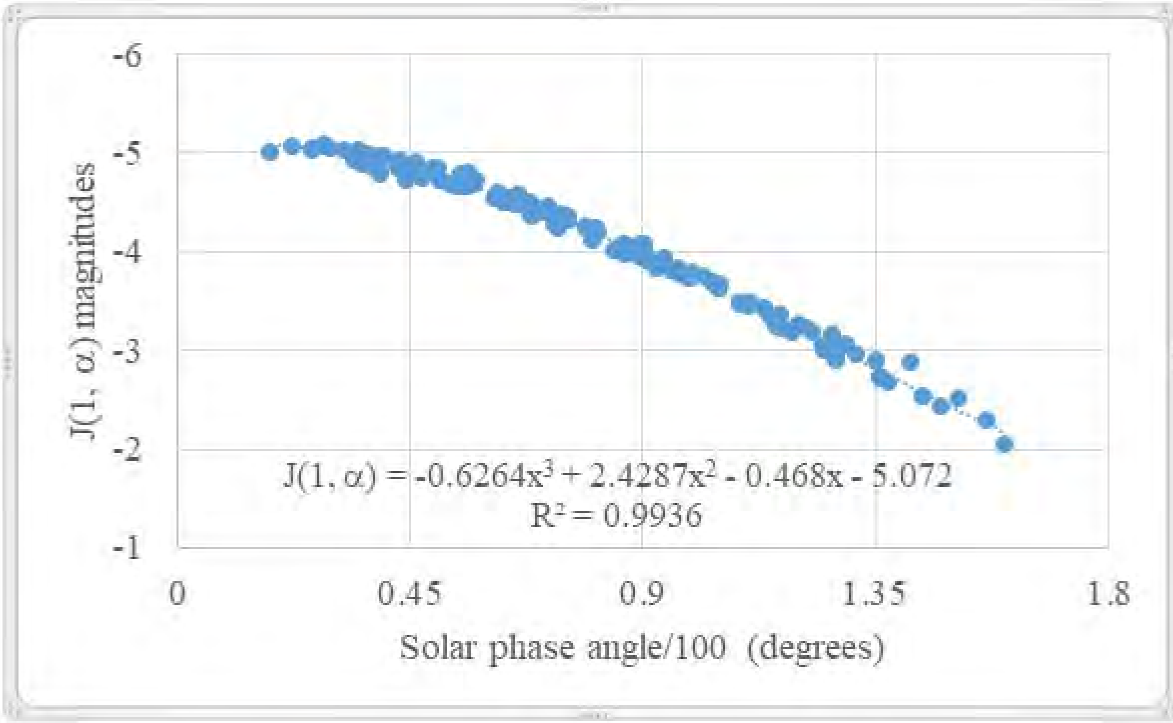

-6
-5
-4
-3
-2
-1
J(1, α) magnitudes
J(1, α) = -0.6264x³ + 2.4287x² - 0.468x - 5.072
R² = 0.9936
0
0.45
0.9
1.35
1.8
Solar phase angle/100 (degrees)

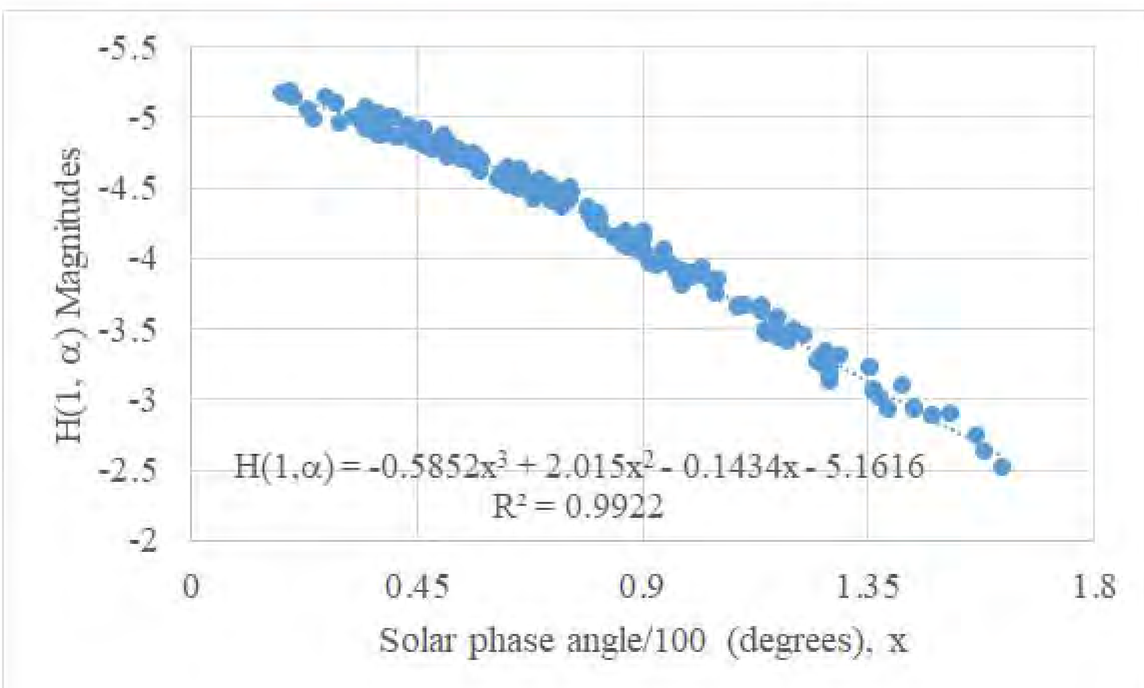

-5.5
-5
-4.5
-4
-3.5
-3
-2.5
-2
H(1, α) Magnitudes
H(1,α) = -0.5852x³ + 2.015x² - 0.1434x - 5.1616
R² = 0.9922
0
0.45
0.9
1.35
1.8
Solar phase angle/100 (degrees), x

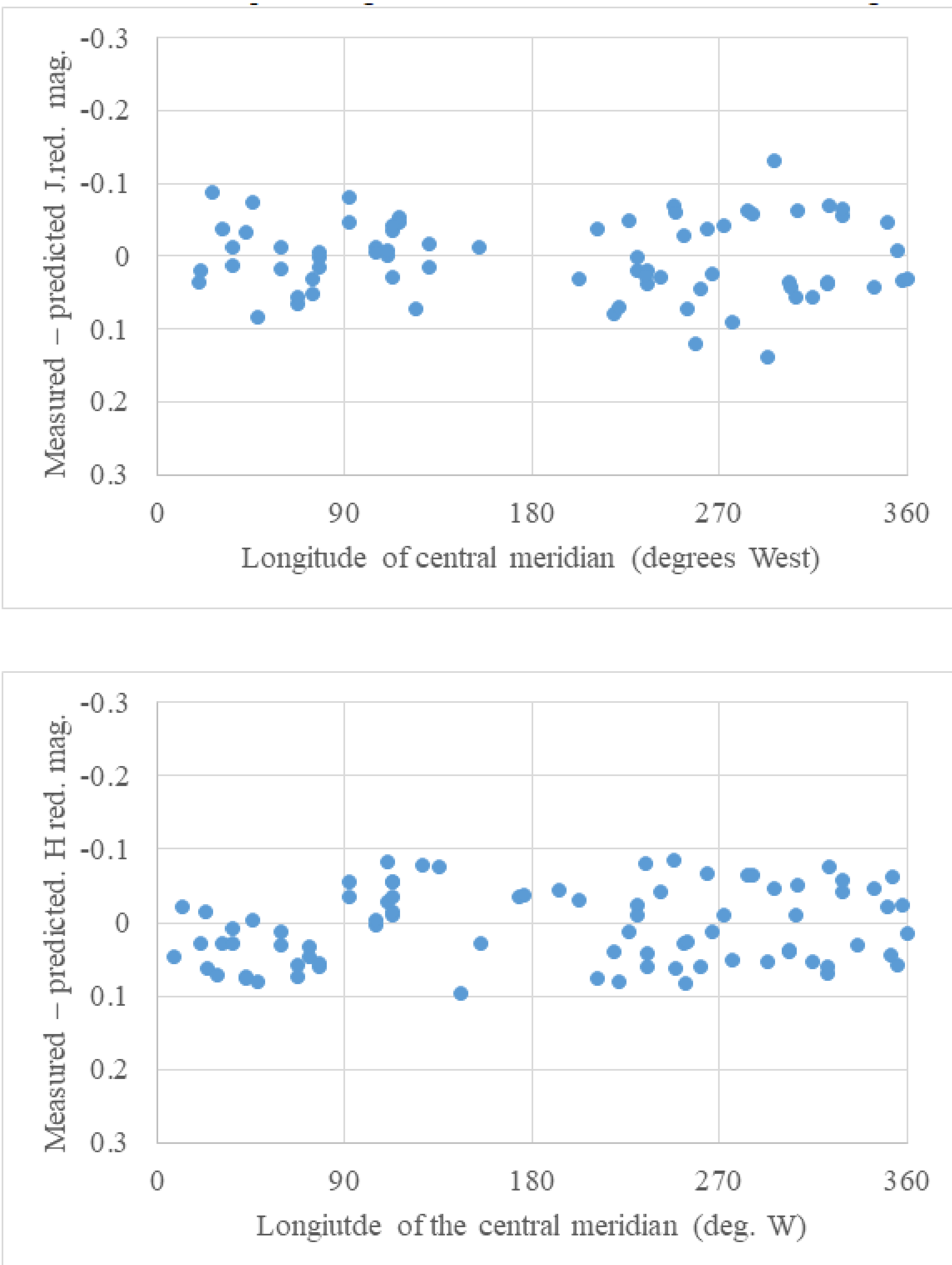

Figure 2. The measured minus predicted reduced magnitude values plotted against the longitude of the central meridian for the J filter (top) and H filter (bottom). In all cases, only measurements made when the phase angle was below 70° were used in these figures.

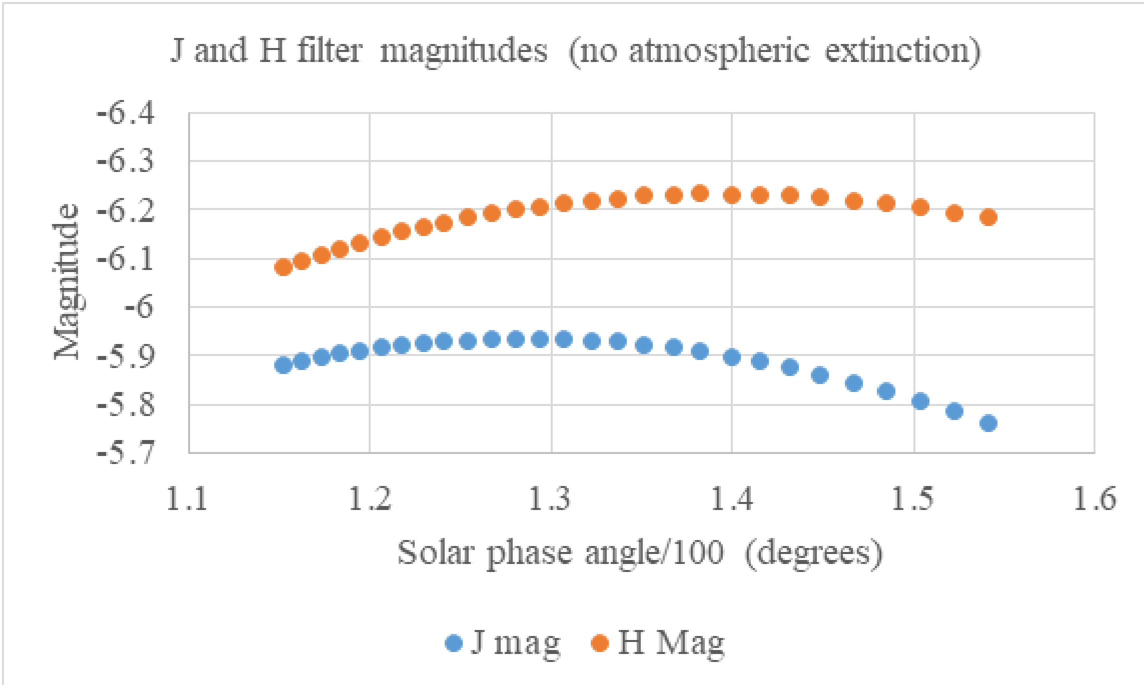

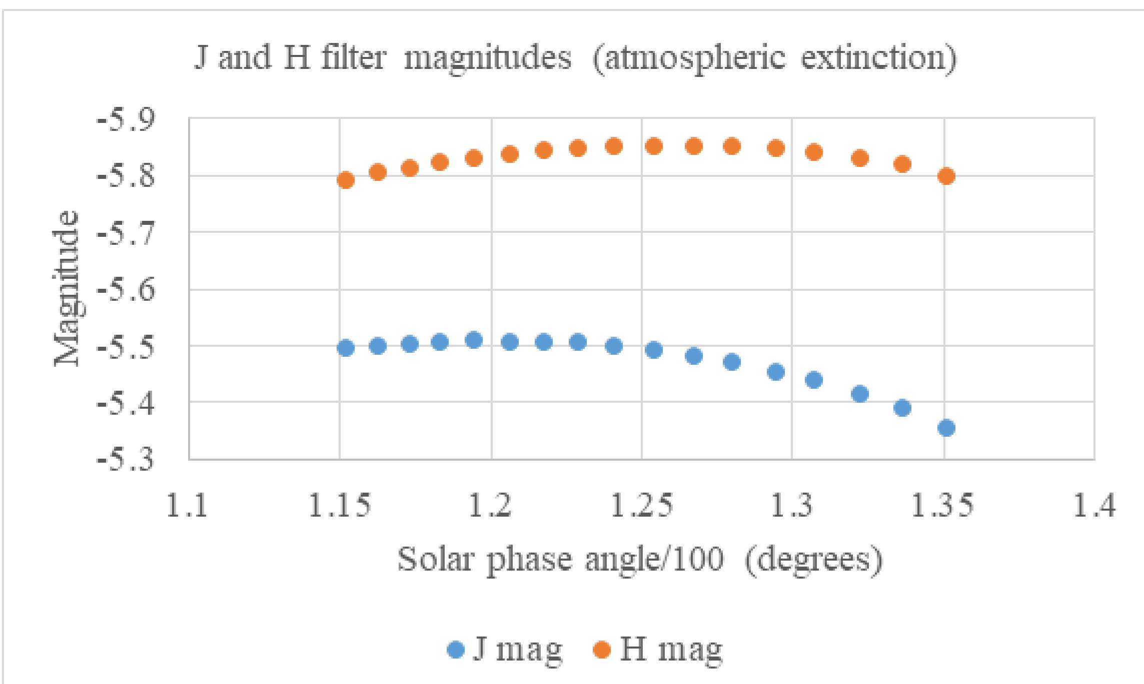

Figure 3. Predicted magnitudes of Venus for different phase angles occurring in November and December of 2021. The predicted magnitudes are based on the equations in Figure 1. The top graph shows the case when the atmosphere does not absorb any light and the bottom graphs shows the situation when there are extinction coefficients of 0.088 and 0.066 magnitudes/air mass for the J and H filters, respectively.

Papers & Presentations

Basic Interpretation and Analysis of Lunar Thermal Images

Darryl Wilson
stargazer_guy@juno.com
(See "About the Author" at the end of this paper)

This paper is the third of three papers by Mr. Wilson on this topic. The first paper appeared in JALPO62-3 (Summer 2020) and the second paper appeared in JALPO62-4 (Autumn 2020).

Abstract

This paper is an introduction to the interpretation of thermal images of the Moon that can be taken by amateur astronomers using commercially available, uncooled thermal imagers in 2020.

It explains how you can use a few simple heuristics to interpret features that are visible in the images. It also introduces the reader to some of the analysis techniques that were used to develop the interpretation rules. Since thermal infrared (TIR) imaging of the Moon is a relatively new field, amateur astronomers will undoubtedly make observations that are not clearly explained by the rules-of-thumb presented here. Research opportunities exist in areas such as detection of meteor impacts, outgassing events and other phenomena. Because further analysis will be necessary if the new observations are to be understood, this article covers a basic set of math and physics tools that can be used to analyze new issues as they arise.

Overview

This article assumes that you have seen TIR images of the Moon on the internet, or that you have taken your own. You probably have a number of questions about the features you see in the images.

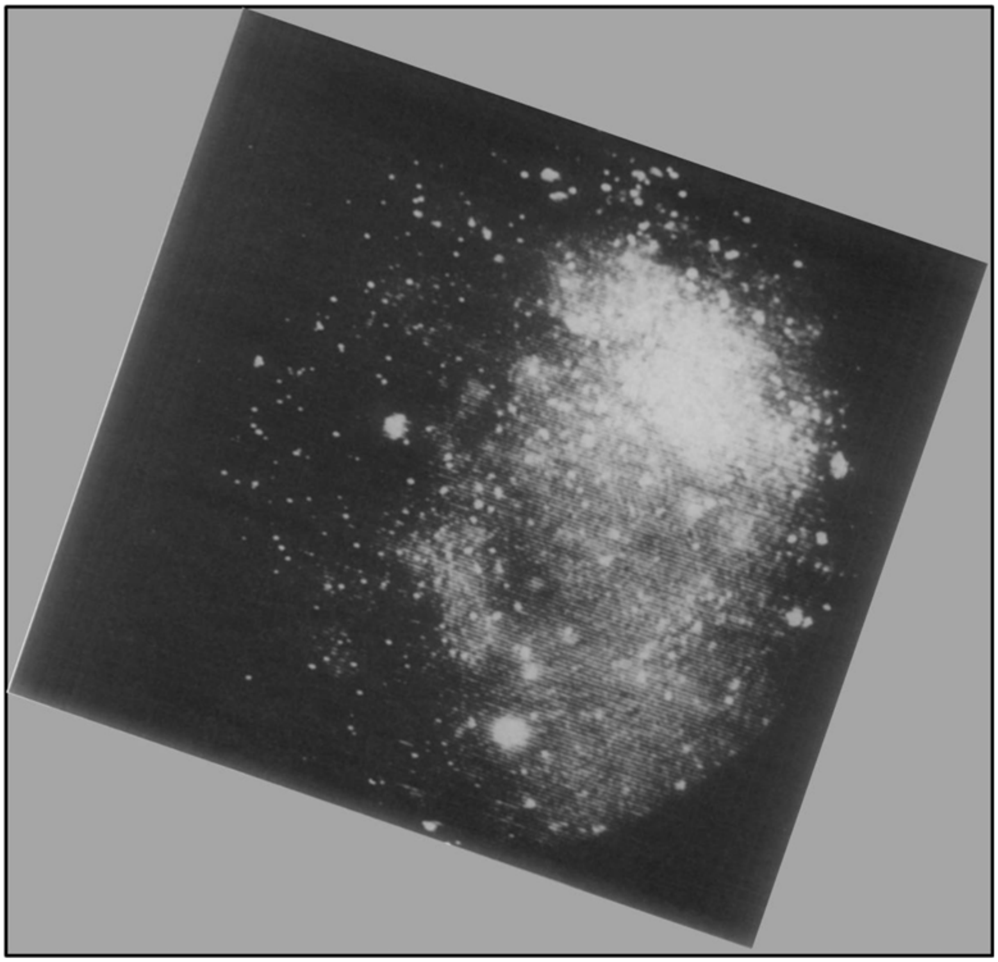

Figure 1. TIR image of lunar eclipse December 19, 1964; 10 - 12 micron wavelength; Shorthill and Saari, 1965.

This paper provides four rules of thumb for interpreting what we see when we look at a lunar thermal image. It goes further to describe the physical basis used to establish these heuristics by relating the observable phenomena to thermo-physical properties of the lunar surface.

It is useful to frame this discussion by introducing two separate but interrelated concepts, processes and observables. They correspond to causes and effects. The observables are the effects that we see in the images. The processes are the causal, physics-based phenomena that are responsible for what we can image.

The following observables, listed in alphabetical order, are discussed and explained:

1. Copernicus' floor is darker than surrounding mare.

2. Crater rays are darker than the maria.

3. Crater rims appear rounded during the day.

4. Crater walls are visible all day.

5. High albedo craters are darker.

6. Many small craters glow after sunset.

7. Mare topography is visible.

8. Maria are only slightly brighter than the highlands.

9. Telescope resolving power is poor in the TIR.

10. The lunar surface cools rapidly after sunset.

11. The subsolar point is where the temperature is highest.

12. Tycho is an anomalous large glowing crater.

The following physics-based processes, listed in alphabetical order, are relevant to our discussion and are discussed:

1. Albedo-temperature relationship

2. Atomic and molecular energy transfer processes

3. Cavity effect

4. Emissivity

5. Radiative cooling

6. Radiometric balance

7. Radiometric calibration

8. Regolith insulation

9. Solar elevation angle effect

10. Telescope resolving power

11. Thermal crossover

12. Thermal inertia (P)

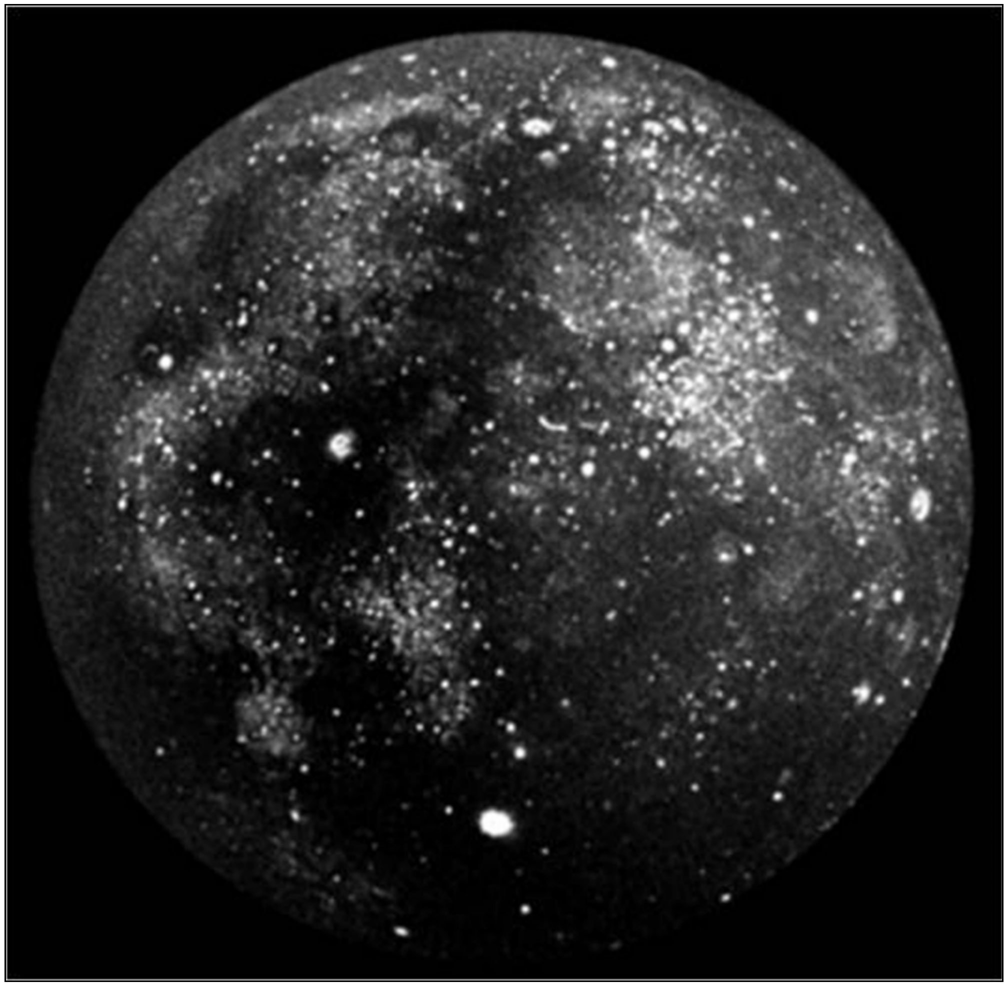

Figure 2. Lunar eclipse January 21, 2019, 05:12 UT; Austin Richards, Goleta, California; Midwave Infrared (MWIR) FLIR RS8303 telescope; 3 - 5 micron wavelength.

The mathematical treatment presented is intentionally brief and casual. It is intended to aid understanding of many of the facts presented, and to point the interested reader in productive directions for quantitative analysis of some of the processes listed above without striving for completeness. If a first order effect is known to cause an observable (e.g., solar flux heats the surface to thermal equilibrium), a governing equation is presented. Second order effects, though relevant, may be omitted. Their inclusion would be appropriate for an engineering document, but this is intended to be less formal. The main goal here is to provide the reader with a qualitative understanding of the features that can be seen in lunar TIR images, and a set of analysis techniques that will enable the motivated reader to explore further.

Finally, a set of four concise interpretation rules that explain most of what is visible in lunar TIR images is presented. They are essentially the quick-start guide to interpretation of thermal images of the Moon.

An Abbreviated History of Lunar Thermal Imaging

As the U.S. space program was building towards the Apollo Moon landings during the 1960s, the thermal properties of the lunar surface were studied extensively. A report by W. M. Sinton titled “Eclipse temperatures of the lunar crater Tycho”

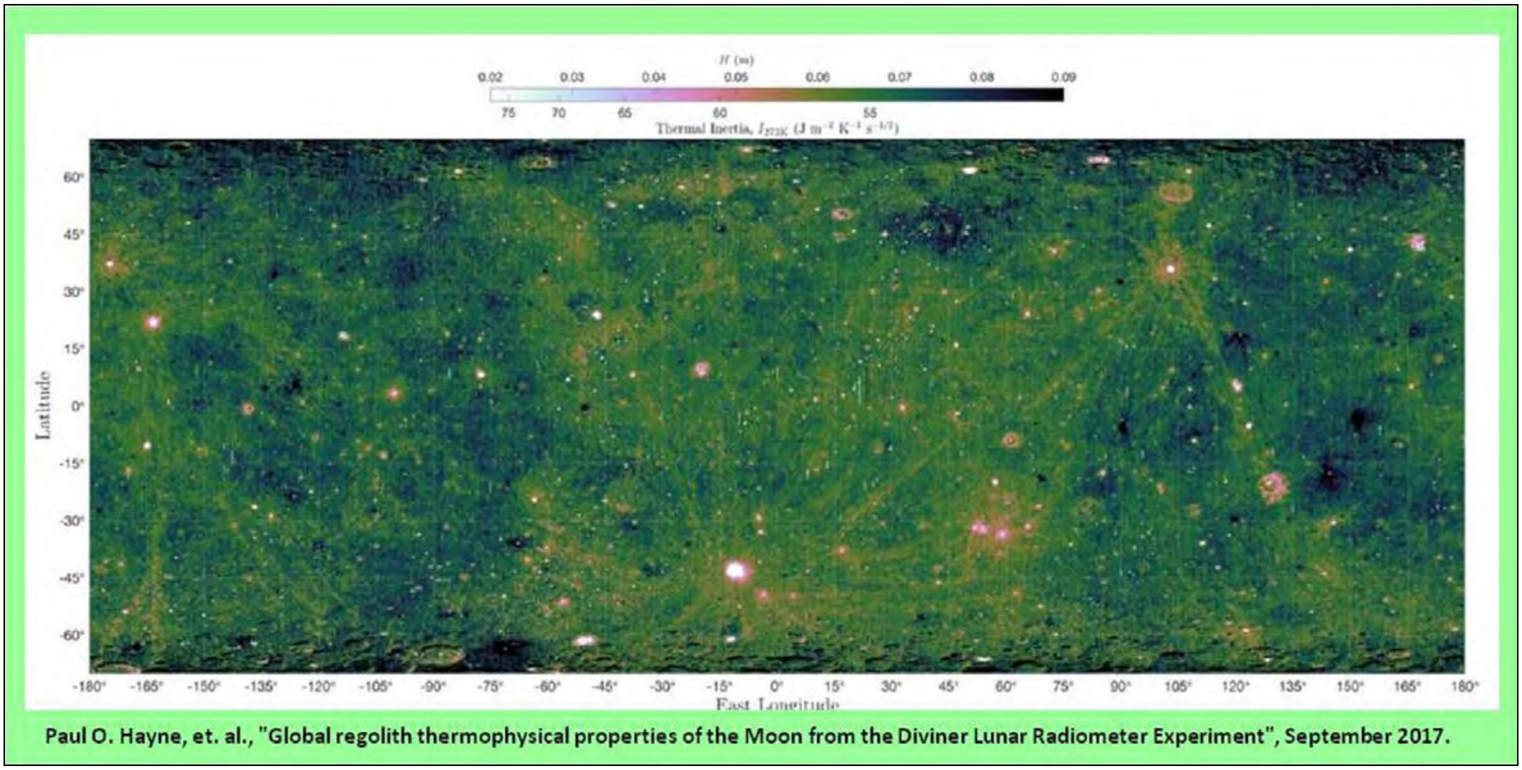

Figure 3. Thermal inertia map of the Moon; Paul O. Hayne, et. al.; "Global regolith thermophysical properties of the Moon from the Diviner Lunar Radiometer Experiment", September 2017.

was published in *Lowell Obs. Bull*. 5, 25-26 as early as 1960 (Saari, 1964). A TIR image of the totally eclipsed Moon on December 19, 1964 is reproduced in **Figure 1** (Saari, 1964). A 74-inch telescope and a liquid-neon-cooled thermal detector, state-of-the-art technology at the time, were required to achieve this result. It showed many thermal hotspots on the lunar disk for the first time. Most of them correspond to the locations of small craters. With a few exceptions, large craters are generally unremarkable. Among those, Tycho seems to be the hottest, with Copernicus, Langrenus, Aristoteles, Aristarchus and Atlas also anomalously warm.

Dr. Anthony Cook, coordinator of the ALPO Lunar Transient Phenomena program, imaged the Moon at TIR wavelengths during the March 3, 2007 lunar eclipse. He republished the thermal image that he took for the December 2019 issue of *The Lunar Observer* (*TLO*) (Cook, 2019). Although the spatial and radiometric resolution of his image was limited, it definitely showed that Tycho was an anomalous hotspot on the lunar disk as the surface was cooling during the eclipse.

An online search revealed an image of the Moon taken by Austin Richards in Goleta, California, with a medium-wave infrared (MWIR, wavelengths from 3 to 5 microns) FLIR RS8303 telescope during the eclipse on January 21, 2019 at 05:12 UT (flir.com). The image is reproduced here in **Figure 2**. Although his imager was sensitive to a somewhat different temperature range than the TIR imagers used by Shorthill and Saari, and the author, it shows many of the same thermal features.

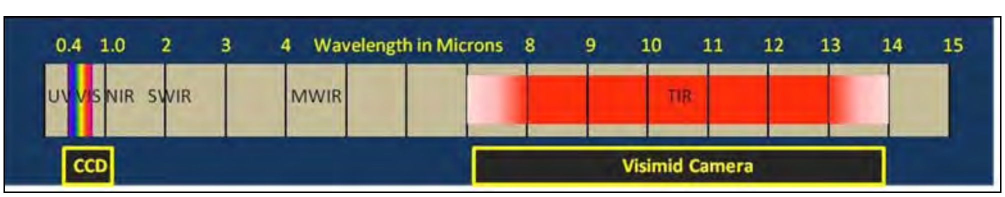

Figure 4. Electromagnetic spectrum coverage of CCD imagers and thermal infrared cameras.

It should be noted that the aforementioned images were all acquired during lunar eclipses. The sudden reduction in heat load that occurs at the lunar surface during an eclipse is significantly different from the regular diurnal heating and cooling processes that are discussed in this paper. Nevertheless, some of the same observable lunar features are prominent.

The November 2019 issue of TLO included an article titled "Lunar Nighttime Thermal Analysis" (Wilson, 2019). In it, this author noted that many craters in the 5 to 10 mile diameter size range continue to glow visibly in the TIR region of the spectrum for as long as 72 hours after lunar sunset. A diffuse bright area corresponding to the interior of Atlas was also noted. Unbeknownst to the author at the time, he had rediscovered thermal features noted by Salisbury and Hunt more than 50 years ago (Salisbury, 1966).

In recent years, the Diviner Lunar Radiometer Experiment, a part of the Lunar Reconnaissance Orbiter (LRO) program, has shed light on spatial and temporal thermal patterns on the lunar surface. **Figure 3** is a global thermal inertia (P) map of the lunar regolith based on this data (Williams et al., 2016), (Hayne, 2017). The papers referenced by Williams and Hayne are excellent sources of scientific and technical information that can extend the reader's understanding of some of the material presented in this paper.

Introduction

If you have used a thermal camera to take your own images of the Moon, congratulations. You are part of a small group of amateur astronomers that, like those who embraced CCD imaging in the early 1990s, have an opportunity to make novel observations that will advance our field. Extended observations of the effects of meteoroid impacts and detection of plumes as a result of outgassing are two possible areas of discovery. Even if you have no intention of trying to make new discoveries, you will still see the Moon (Venus and Mars, too, if you look) as human eyes never have. **Figure 4** compares the region of the electromagnetic spectrum covered by TIR technology with the region covered by CCD cameras and visible light. It can be seen that TIR wavelengths are roughly 20 times longer than those of visible light.

If you don't own a thermal imager, that's fine too. Perhaps you have seen thermal images of the Moon and you are intrigued. This should offer some understanding of the types of information provided by thermal images that cannot be obtained by visible light images. The thermal images presented in this article were taken with a Visimid X-640 thermal camera. It is the author's hope that you may eventually be interested enough to purchase a thermal imager and give it a try yourself.

It should be noted that the TIR region of the electromagnetic spectrum, as referenced in this paper, is not the same as that covered by observatories such as SOFIA and ESO that are commonly referenced to on the internet as the source of published TIR images. They operate at wavelengths that are about five times shorter than those we can capture with commercially available TIR cameras. They image physical processes

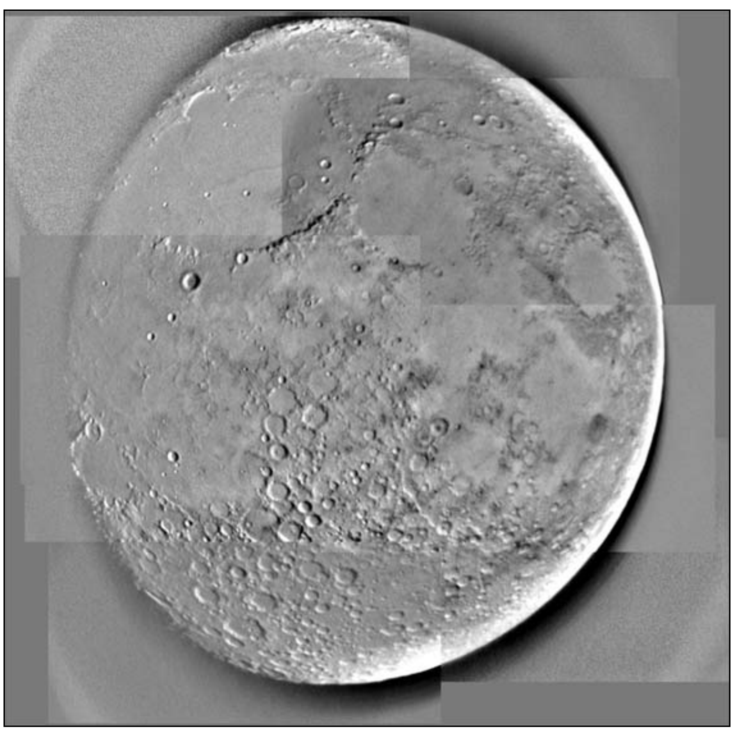

Figure 5 (above left). Thermal image mosaic of a 12-day old Moon; August 12, 2019, 08:12 to 02:30 UT; Darryl Wilson; 18" Obsession Newtonian, Visimid X-640 thermal camera.

Figure 6 (above right). Visible light reference image of a 12-day old Moon; August 12, 2019, 03:33 UT; Darryl Wilson; 80 mm APO refractor, Celestron Skyris 274C, 270 1/1712 s exposures; Registax Linear Default, X^0.7 power law stretch.

that TIR cameras cannot see, and TIR cameras image temperatures below the range they can detect. In this paper, TIR means the range of wavelengths that are emitted by natural objects on the Earth's surface -- from Antarctica to the hot springs of Yellowstone National Park.

Before we begin our detailed discussion of many of the phenomena that are visible in TIR images, let's get straight to the point and cover four simple rules-of-thumb that will explain most of what we see in lunar thermal images.

Interpretation Rule Number One

Lunar surface temperature variations are primarily due to variations in the solar elevation angle. Over long distances, this is proportional to the distance from the subsolar point, where maximum surface temperature occurs. Over smaller distances, surface topography effects dominate.

Interpretation Rule Number Two

Albedo effects cause differences in rates of heating which result in noticeable temperature differences that can persist well into the lunar day.

Interpretation Rule Number Three

Given two objects at the same temperature, the one with the higher emissivity will appear brighter in a TIR image.

Interpretation Rule Number Four

If rules one through three don't explain what you see, it might be an exposed outcrop of exposed silicates, free of insulating regolith, that has a higher thermal inertia than the surroundings.

With the above interpretation rules in mind, we can explore the interrelationships between the response of the lunar surface to incoming solar radiation (insolation), and the physical processes that cause the surface to warm enough to radiate electromagnetic energy that our TIR camera can detect.

Differing Atomic Physics Processes Cause TIR and Visible Radiation

Let's begin with a simple question. Is IR radiation from the Sun bouncing back to the TIR camera to form the TIR image the same way visible light does to form an image with CCD cameras? The answer requires a discussion at the level of atoms and molecules, at the boundary between observational astronomy and atomic physics.

When we image the Moon in visible light, we are collecting photons that have hit the Moon and almost instantaneously been re-radiated back in our direction.

TIR imaging is different. Here's how it happens. Imagine that you're the first solar photon to land on a rock at lunar sunrise. It's likely that you have a wavelength in the range of visible light since that's where the Sun radiates most strongly. One atom at the surface of the rock is the most affected by your energy. The albedo is 10%, so there's a 10% chance that you'll be bounced back into space, but 90% of the time you'll be absorbed. When that happens, one of the atom's electrons takes the energy that you brought and uses it to change its orbit to a different one – one that has a higher energy level. The atom now has a single electron in a high energy state.

It is surrounded by several other (cold) atoms that can easily accept some of the energy. They are so close that their electron clouds partially overlap. They are essentially in constant contact. The absorbed energy is transferred to the nearby atomic bonds such that several bonds each gain a fraction of it. In the process, it is transformed from electron

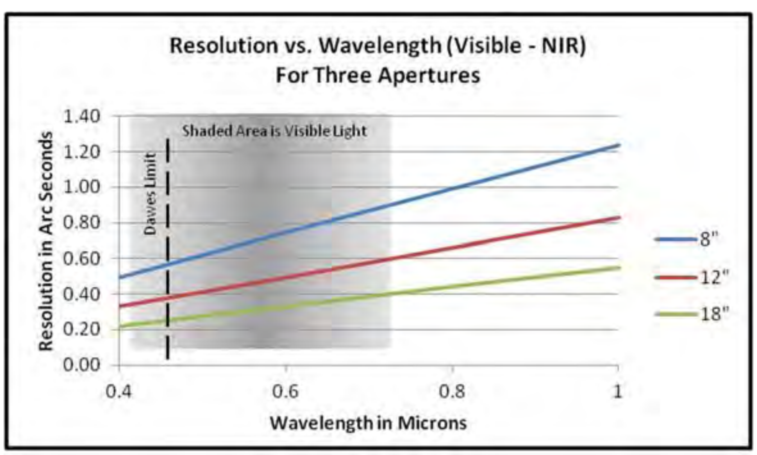

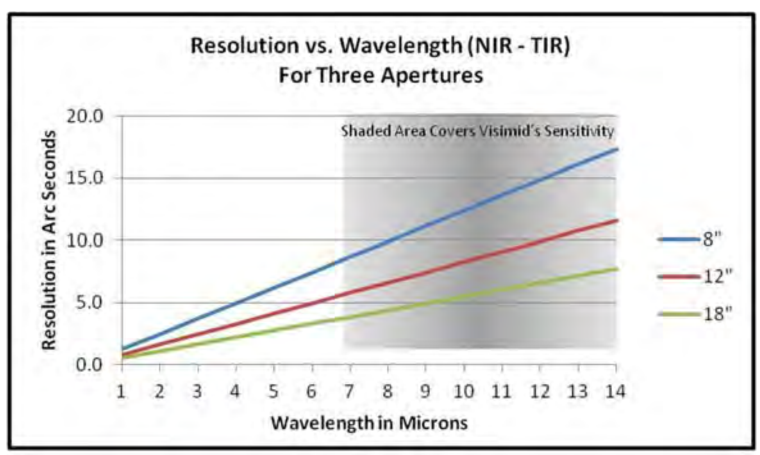

Figure 7 (above left). Telescope resolution from visible to NIR.

Figure 8 (above right). Telescope resolution from NIR to TIR.

energy into vibrational motion of the adjacent atoms. This happens so fast that there is usually not enough time to bounce a photon back into space. The vibrational motion that remains is thermal energy.

As other photons land on the rock, their energy is also absorbed. Thermal energy gradually builds, causing the atoms to vibrate more vigorously. After enough photons have been absorbed by the rock, the atoms near its surface will all be vibrating enough (have enough energy) to radiate in the wavelength region that the thermal infrared camera can sense (7 to 14 microns). This range includes room temperature photons.

It takes a while for this process to occur. That's another way of saying that it takes a while for the Sun to warm a Moon rock from -250 degrees F to 0 degrees F. So we shouldn't use the term “bounce” when a series of atomic energy acceptance and transfer processes that take considerable time -- perhaps many minutes -- must occur before a return photon with enough energy is dispatched towards our detector.

So what results from this process? After solar energy is transferred from a photon, to an excited electron, to an excited molecular bond, and then back to a lower energy photon, what does the result resemble when it lands on our TIR detector at the focal plane? Exit atomic physics, enter observational astronomy.

First Light With a Thermal Imaging Camera

Thermal images of the sunlit side of the Moon display many of the same features that are present in visible light images. **Figure 5** is a mosaic of several thermal images that were taken August 12, 2019. **Figure 6** is a visible light image taken at the same time for comparison. Craters, maria, and mountain ranges are all plainly visible and identifiable in the thermal image. At first glance, you might even think that you were looking at a visible image -- except that it doesn't look quite right. Crater rims look a little too rounded; their shadows are too soft. The rays are mostly missing. A few appear only as faintly dark shadows. Gently sloping features are present on the floors of the maria far from the terminator - where you expect that they shouldn't be visible at all. And the spatial resolution seems to be much worse than you recall from your first 60 mm refractor, even though you are now imaging through a Newtonian with several times as much aperture. The lunar landmarks are all familiar, but many things seem strangely different. What's going on here?

TIR Wavelengths Cause Poor Resolution

Let's first discuss the lack of spatial detail. Most amateur astronomers are introduced to the concept of telescope resolution through the use of Dawes' equation, $R = 4.56 / D$, where D is the aperture (in inches) of the objective optic and R is the telescope's resolution in arc seconds. **Figure 7** plots telescopic resolution for three apertures as a function of the wavelength of light from violet to the near-infrared (NIR). The shaded region is visible light, and the vertical dashed line denotes where the Dawes formula applies. Dawes' equation is simple and works well, but it implicitly assumes that the *eye* is the detector, and visible light is being observed. Since TIR imaging is done far outside the visible spectrum, we need something else. **Figure 8** plots telescopic resolution for three apertures as a function of longer

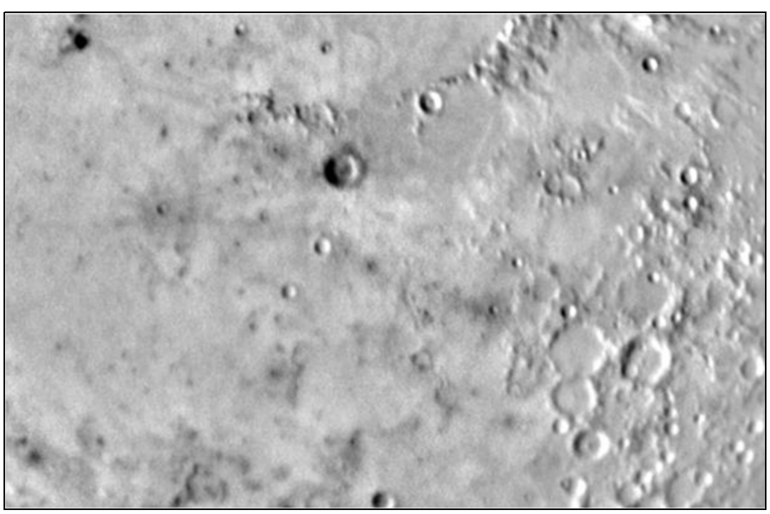

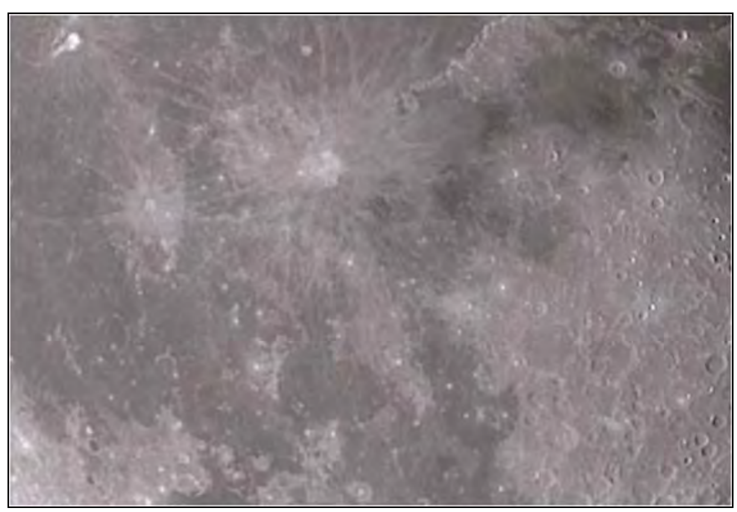

Figure 9 (above left). Lunar thermal image; September 18, 2019, 06:31 UT; Darryl Wilson; 18" Obsession Newtonian, Visimid X-640 thermal camera.

Figure 10 (above right). Visible light image; September 18, 2019, 04:17 UT; Darryl Wilson; 80 mm APO refractor, Celestron Skyris 274C.

wavelength of light - from the NIR to the TIR. The shaded region denotes the range of wavelengths that are detected by a TIR sensor. It is easy to see from a comparison of the two plots that the resolving power of a telescope is much worse in the TIR than in the visible spectrum.

The resolving power (**Equation 1**) was used to generate the two plots. It says that the resolving power of a telescope is equal to 1.22 times the wavelength (λ) of electromagnetic radiation, divided by the aperture of the primary optic. The units for λ and the diameter of the primary mirror (D) must be the same, and resolution (R) will be in units of radians. Multiply R by 206,265 arcseconds per radian to get the answer in arc seconds.

$$R = 1.22\ \lambda / D \qquad (1)$$

Since spatial resolution is clearly not the forte of TIR imaging, there must be some other compelling reason to do it. There is. We can learn about the thermo-physical properties of the surface of the Moon by analyzing the relative brightness of features throughout the lunar day. This information is not available in visible light images.

Albedo is an Important Factor

How should we interpret the brightness patterns we see in thermal images? A common sense approach would seem to be a sensible start. Imagine the lunar surface is like a parking lot on a summer day. There are three categories of surface features - asphalt, concrete and white painted lines. By mid-morning, the low albedo asphalt will have absorbed enough solar energy to be hot. The high albedo white lines will still be cool since they are highly reflective. A nearby concrete sidewalk will be at an intermediate temperature. A thermal image of the parking lot would look like a photographic negative. The asphalt would appear bright, the lines dark and the concrete would be of intermediate brightness.

The surface of the Moon follows that pattern through most of the lunar day. Bright craters like Aristarchus, and prominent ray systems like those of Copernicus and Kepler, warm more slowly and appear darker than the surrounding mare in the thermal image, as illustrated in **Figure 9**. **Figure 10** is a visible light image taken at the same time, 4.2 days after full Moon, showing the familiar rays and bright spots that correspond to small craters. Many of the bright spots in the visible light image appear as dark spots in the TIR.

Albedo is defined as the fraction of solar flux reflected by a surface at visible wavelengths. **Equation 2** expresses the relevant energy balance relationship. It states that the amount of radiation reflected (R) plus the amount absorbed (A) must equal the total incoming solar flux (F). Surface areas with high albedo (reflectance in the visible, R_{vis}) reflect more solar energy than low albedo areas. Since they reflect more, they absorb less, and they warm more slowly and remain at a lower temperature for a long time after local sunrise. This albedo-temperature relationship explains much of what we observe during the lunar morning.

$$F = R + A \qquad (2)$$

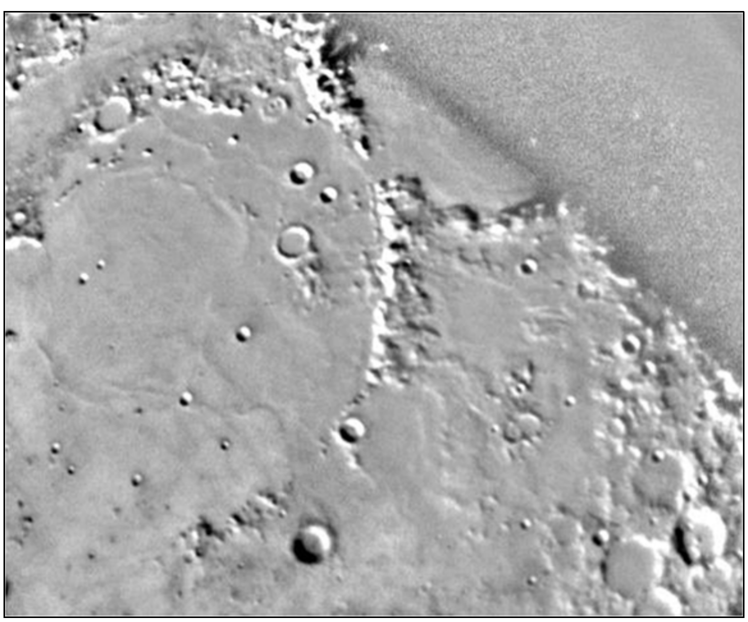

Figure 11 (above left). Lunar thermal image; September 20, 2019, 07:07 UT; Darryl Wilson; 18" Obsession Newtonian, Visimid X-640 thermal camera.

Figure 12 (above right). Visible light image; September 20, 2019, 07:59 UT; Darryl Wilson; 80 mm APO refractor, Celestron Skyris 274C.

This albedo effect is easy to understand, it applies over most of the visible disk for most of the lunar day, and it's exactly what most people expect. Surprisingly however, it's not the dominant cause of variability in thermal emittance from the lunar surface. If it were, thermal images would primarily be contrast-reversed versions of their visible light counterparts. We'll get to the main cause of thermal emittance variability shortly, but first let's touch on some reasons that the albedo interpretation may not apply when you might expect that it should.

Albedo Does Not Explain Everything

Early in the lunar day, exceptions to the albedo-temperature pattern can occur in some places because of shadowing effects caused by surface roughness. Crater rays that contain large quantities of boulder-sized ejecta are a likely example.

In the lunar afternoon, the common sense pattern no longer applies due to a phenomenon known as thermal crossover. A low albedo feature absorbs more solar energy during the day, reaching its maximum temperature more quickly. Low albedo often means slightly higher emissivity. A more emissive object radiates more strongly, thereby losing thermal energy more rapidly as solar irradiation decreases. Its higher temperature also causes greater emittance. At lower Sun angles, insolation becomes less than emission, and the surface begins to cool. By late afternoon, the initially warmer area has cooled to the same temperature as the cooler one. Thermal contrast is lost and they become indistinguishable to the thermal sensor. This is illustrated in **figures 11** and **13**, which were taken about 49 hours after **Figure 9**. Copernicus' rays, still visibly cooler than the surrounding mare four days after Full Moon, have become invisible two days later. This happens because the warmer mare cooled more rapidly, reached the same temperature, and thermal contrast was lost. The corresponding visible light images in **figures 12** and **14** show the Copernican ray system clearly.

Nature Seeks Thermal Equilibrium

The time-delay of temperature response to applied heat described above persists for a limited time. Thermal equilibrium must eventually occur because in the long run, what is absorbed (A) must be emitted (E), as stated in Equation 3. If that were not true, then the temperature would either approach absolute zero or infinity.

$$A = E \qquad (3)$$

Another exception to the common sense pattern involves a few large craters (for instance, Copernicus) that remain cooler throughout most of the day. The albedo of the interior of Copernicus is high, and it appears cooler in the thermal image Figure 9. It is tempting to conclude that high albedo is responsible for the lower temperature, but evidence to the contrary is easy to find. The interior of Archazel appears to have a similar albedo, and its interior is not cooler than its surroundings. The two craters are similar in size and they seem to be morphologically similar. Something is different there. What is it? The explanation involves two interrelated ideas.

Regolith is the Moon's Blanket

First, most of the lunar surface is covered by what is called regolith. Regolith is the

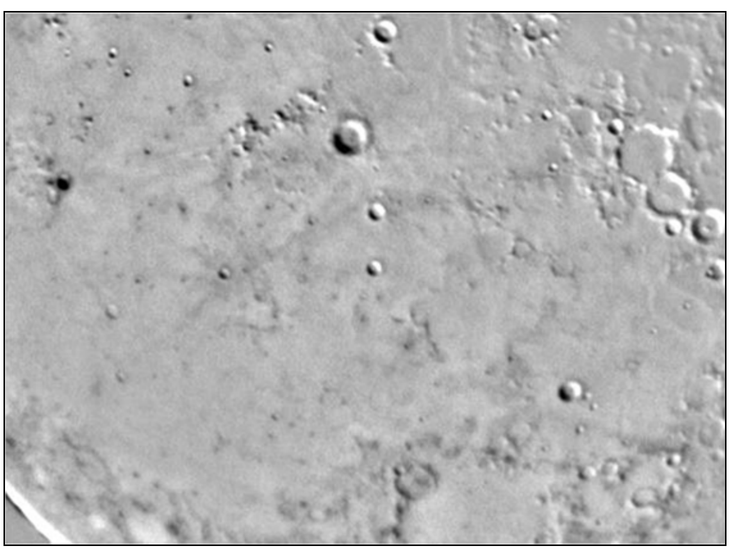

Figure 13 (above left). Lunar thermal image; September 20, 2019, 07:47 UT; Darryl Wilson; 18" Obsession Newtonian, Visimid X-640 thermal camera.

Figure 14 (above right). Visible light image; September 9, 2020, 07:59 UT; Darryl Wilson; 80 mm APO refractor, Celestron Skyris 274C.

result of space weathering of the lunar surface. Micrometeoroid bombardment over billions of years has slowly pulverized the surface rock, turning it into tiny bits of fine-grained particles - like a powder. Recall pictures of the footprints of the Apollo astronauts. It is highly insulating, and it prevents most solar heat from penetrating into the lunar surface. Because absorption of thermal energy is minimized during the lunar day, there's not much to radiate away after sunset. That explains why most of the surface cools rapidly to a temperature below the limit of detection from Earth.

Second, when a large cratering event occurs, as occurred when Copernicus was formed, the insulating surface layer is blasted away, and the underlying rock is exposed. Fresh, exposed silicate rock has very different thermal properties than regolith. Its thermal conductivity and heat capacity are greater, so it absorbs more solar energy during the day.

Regolith insulates the Moon. Young craters are essentially holes in the regolith that allow heat to flow in and out more efficiently. During the day, the enhanced absorbtance of solar energy by regolith-free areas causes the temperature to remain lower than the surroundings. After sunset, the lack of an insulating layer allows them to radiate more efficiently than the regolith. As we shall soon see, this causes some craters to literally glow in the night. Copernicus is one of a few large craters that are young enough so that their interior surfaces still contain exposed silicates, not yet covered by the regolith that results from eons of micrometeoroid bombardment of the lunar surface - a process known as known as space weathering. It is also the reason that Copernicus is a visible hotspot in **figures 1** and **2**.

Thermal Inertia

The thermo-physical property that distinguishes regolith from exposed silicate rock is known as thermal inertia (P). Exposed silicate rock has a high thermal inertia. Regolith has a low thermal inertia. As expressed in **Equation 4**, P is defined as the square root of the product of a material's thermal conductivity (K), heat capacity (C_p), and density (ρ). It is a measure of the ability of a substance to accept and release thermal energy. In remote sensing and planetary science it is calculated by analyzing diurnal temperature change measurements. Unfortunately, confusion surrounds the use of the term "thermal inertia" in much of the literature.

$$P = (KC_p\rho)^{1/2} \quad (4)$$

The confusion seems to arise from two reasons; 1) the failure to clearly discriminate between surface temperature and bulk temperature, and 2) a lack of clarity regarding the timeframe of applied heat and temperature measurements.

Low thermal conductivity leads to a rapid rise in surface temperature, and delays a rise in bulk temperature. High thermal conductivity resists a rise in surface temperature, and causes a more rapid increase in bulk temperature.

Low heat capacity leads to a rapid rise in both surface and bulk temperatures. High heat capacity resists a rise in both surface and bulk temperatures when heat is applied.

An analogy can be made between **Equation 5** (Newton's Second Law of Motion), which states that force equals mass times acceleration (the rate of velocity (v) change per unit time (t)), and **Equation 6**, which states that the

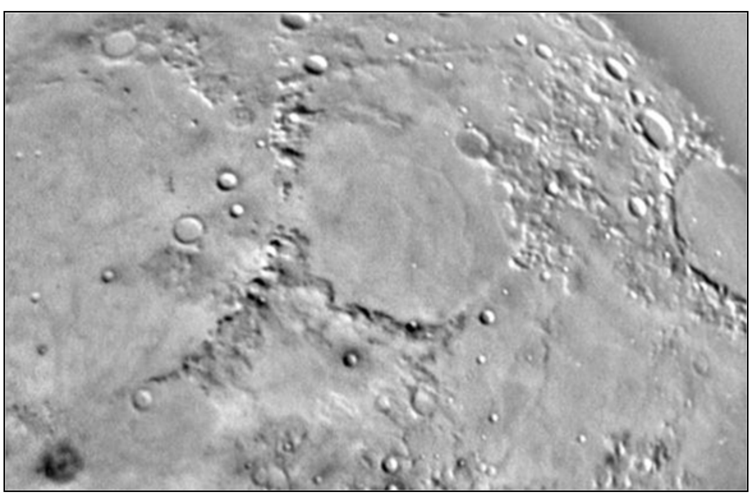

Figure 15 (above left). Lunar thermal image; September 16, 2019, 04:11 UT; Darryl Wilson; 18" Obsession Newtonian, Visimid X-640 thermal camera.

Figure 16 (above right). Visible light image; September 16, 2019, 05:21 UT; Darryl Wilson; 80 mm APO refractor, Celestron Skyris 274C.

applied heat (Q) is equal to thermal inertia (P) times the rate of temperature (T) change per unit time (t). For a given flow of heat, a small value for P will result in a rapid change in temperature. A high thermal inertia will cause a slow change in temperature.

Just as inertia is the physical property of an object that resists acceleration when a force is applied, P is the physical property of a material that resists a rise in surface temperature when heat is applied. Just substitute "heat" for "force", and "rise in surface temperature" for "acceleration".

$$F = m * a = m * \Delta v/\Delta t \quad (5)$$

$$Q = P * \Delta T/\Delta t \quad (6)$$

Regolith covers most of the lunar surface. Its loose agglomeration of particles of various sizes results in low thermal conductivity, and a correspondingly low value of P. When it absorbs sunlight, the surface is warmed much faster than heat can be conducted downward and away. This results in a rapid, steady rise in temperature until equilibrium is established between insolation and re-radiation to space.

In isolated areas on the lunar surface, materials with high thermal conductivity and high heat capacity, such as exposed silicates, have high thermal inertias. The interior of young craters often contain regolith free silicates that were exposed during the impact. If the silicate bedrock is more than a few meters deep, its relatively high thermal conductivity results in a constant downward heat flow during the day from the surface to the cooler layers below. This heat flow happens fast enough to keep the surface cooler than it is on the regolith, where the downward flow does not occur.

High thermal inertia materials delay surface temperature rise and the re-emittance of electromagnetic radiation for us to detect. The higher the thermal inertia, the greater the time-lag.

Solar Elevation Angle Effect is Dominant

All of the effects mentioned to this point are easily observed in thermal images of the Moon, but the most important factor influencing the brightness patterns that are recorded by our TIR camera is the angle that the incoming radiation makes with the surface. The solar elevation angle effect is so strong that the varying slopes of crater walls cause most of them to remain clearly defined even at Full Moon. Even small changes in the solar angle cause relatively large changes in detected thermal radiation. Thermal contrast is lost only in the equatorial region near the subsolar point, where temperatures reach maximum values. In the TIR, most of the lunar surface looks like a relief map, regardless of lunar phase.

Although the walls of craters far from the terminator can be traced all around their circumference, they are not sharply defined. Figures 11 and 13 have numerous examples of crater walls that appear rounded compared to the visible light images we are used to seeing. The solar elevation angle effect is again responsible. As one proceeds from the crater center to the wall, and beyond, the temperature of the surface changes gradually depending on the average angle of sunlight received by each patch of surface. There are no sharp shadows to be imaged as there are in visible light images.

The maria are so flat that their gentle slopes do not generate shadows in visible light images except when the Sun is within a few degrees of the horizon. TIR images reveal their topography even when the terminator is far away. Subsidence of the crust that occurred

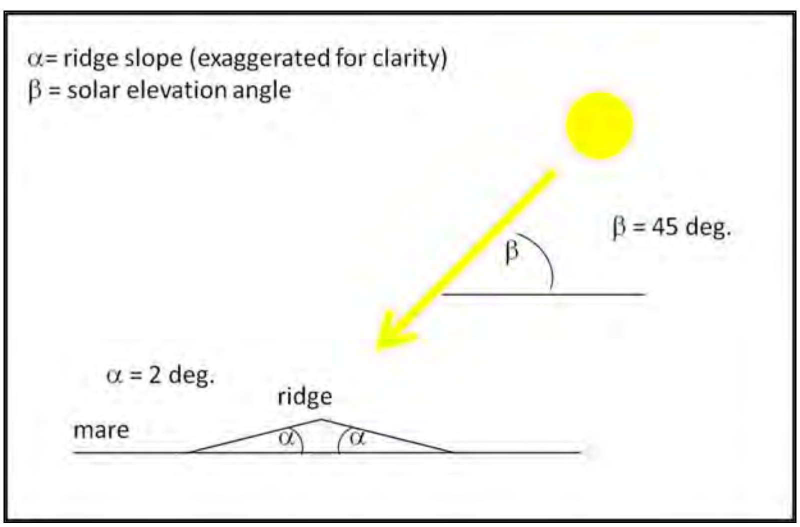

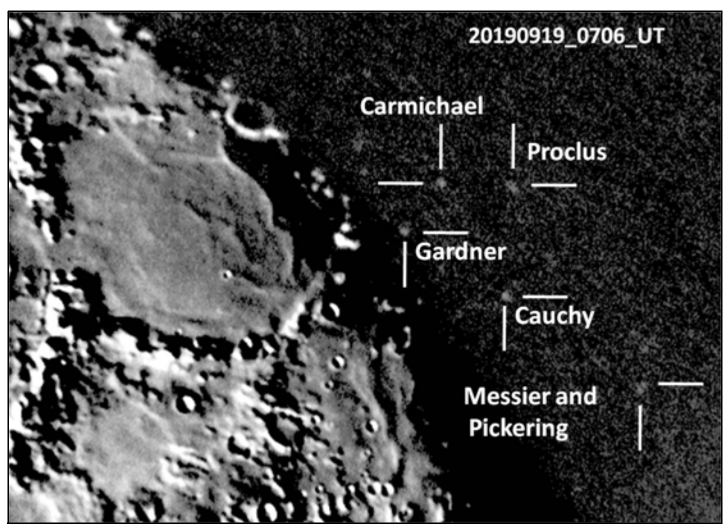

Figure 17 (above left). Solar illumination of shallow slopes on mare.

Figure 18 (above right). Night glow of craters; September 19, 2019, 07:06 UT; Darryl Wilson; 18" Obsession Newtonian, Visimid X-640 thermal camera.

billions of years ago caused wavelike ripples in the surface. These are easily visible in TIR images because even small differences in the angle of solar irradiation causes detectable temperature differences. **Figure 15** shows relief variations in the maria several hundred miles from the terminator. **Figure 16**, the visible light image taken simultaneously, shows the flat appearance with which we are all familiar. The effect of interpretation rule number one is strong.

We can calculate the strength of this effect easily enough. **Figure 17** illustrates the situation when the solar elevation angle (β) is 45 degrees, and a ridgeline perpendicular to the direction of insolation has a slope (α) of 2 degrees on either side. This is a typical slope for wrinkles in the maria. For this example, we assume the Moon is a blackbody with emissivity (ε) = 1.0 for ease of calculation. **Equation 7** quantifies the amount of radiative flux emitted by such an object. It says that the amount of energy radiated by each square meter of surface area is proportional to Boltzman's constant ($\sigma = 5.67 \times 10^{-8}$ W / m^2 K^4) times the fourth power of the absolute temperature times by the emissivity (ε). We begin with the knowledge that the solar flux (F_s) at the Earth's, and Moon's, distance from the Sun is 1,340 W/m^2. At thermal equilibrium, **Equation 8** says that flux in must be equal to flux out ($F_{in} = F_{out}$). F_{in} for the sunward facing side of the ridge (F_1) is

$$F_1 = F_s \sin(\beta+\alpha) = 980 \text{ W/m}^2$$

F_{in} for the other facing side of the ridge (F_2) is

$$F_2 = F_s \sin(\beta-\alpha) = 914 \text{ W/m}^2$$

Now that we know the flux values for each side of the ridge, we can invert **Equation 7** to solve for the temperatures on either side. We get:

$$T_1 = (F_1 / \varepsilon\,\sigma)^{1/4} = 366 \text{ K, and}$$

$$T_2 = (F_2 / \varepsilon\,\sigma)^{1/4} = 360 \text{ K}$$

A 6 K temperature difference is detectable in TIR images. That means that a wrinkle ridge in the mare with a 2 degree downward slope on either side of the ridge can be imaged even when it is 45 degrees from the terminator. Lesser slopes can be detected closer to the terminator.

$$F = \varepsilon\,\sigma\,T^4 \qquad (7)$$

$$F_{in} = F_{out} \qquad (8)$$

While we're discussing the maria, let's ask a simple question. Why don't they appear much brighter in the thermal images? Due to their lower albedo, as seen in **Figure 6**, we reason that they should absorb solar radiation much faster, and become much hotter. The TIR image of **Figure 5** shows that they're a little warmer than the highlands, but it's barely noticeable. There must be a flaw in our reasoning. Can we find it?

The maria surely absorb energy from the Sun faster than the highlands, but not for long. The albedo (R_{vis}) of the maria is roughly 0.07, and that of the highlands is roughly 0.16. That means that the maria absorb about 93% of the incident radiation, and the highlands absorb about 84%. Those numbers are not dramatically different, and both areas are covered with insulating regolith, so they warm at similar, albeit slightly different, rates. Although the maria do warm faster, before a large temperature difference can develop they approach their highest possible temperature, and the rate of warming slows to a stop. Soon afterwards, the temperature in the highlands reaches that of the maria. At any instant in fact, the maximum temperature on the lunar surface is always close to the subsolar point. It is nearly independent of surface material type and albedo.

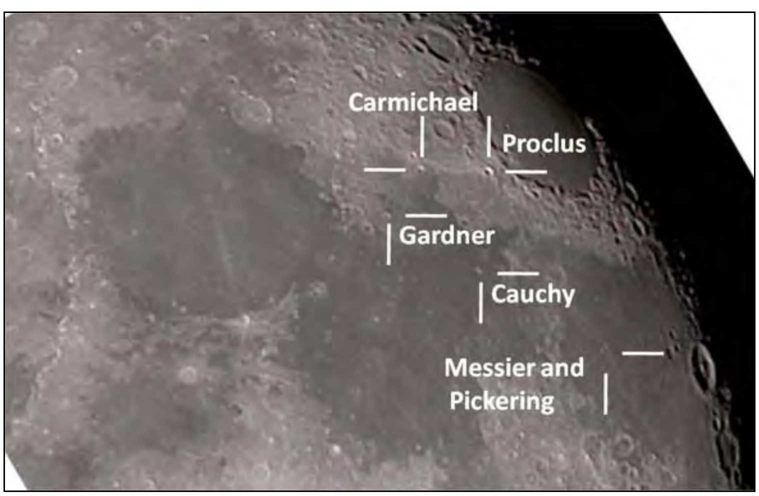

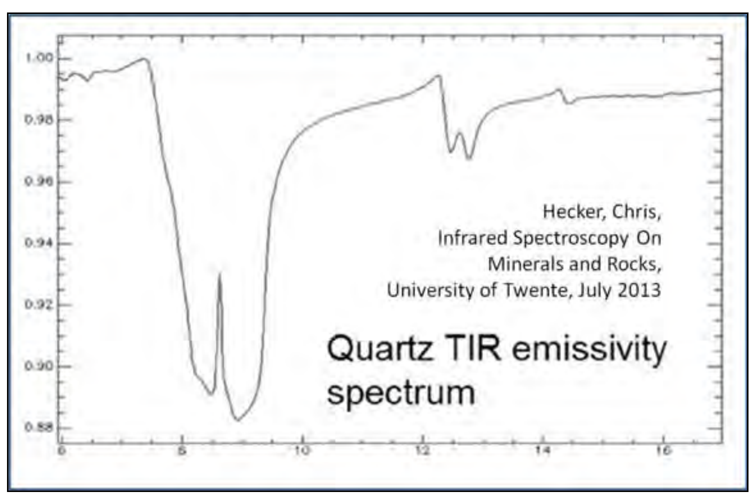

Figure 19 (above left). Visible light image; September 16, 2019, 05:21 UT; Darryl Wilson; 80 mm APO refractor, Celestron Skyris 274C.

Figure 20 (above right). Emissivity spectrum of quartz.

Emissivity

At the same temperature, the maria appear slightly brighter in the thermal image due to their 96% emissivity as compared to the 95% emissivity of the highlands. If two objects with different emissivities are at the same kinetic surface temperature, the one with the higher emissivity will appear brighter in the thermal image.

Emissivity is sometimes described as (1 - albedo) for an opaque object. That's true for any given region of the electromagnetic spectrum. The sharp reader has already noted that the albedo values quoted above for the maria and highlands are 7% and 16% respectively, but the values for emissivity are 96% and 95% respectively. Since 1 - 0.07 is not equal to 0.96, and 1 - 0.16 is not equal to 0.95, something seems amiss. The answer lies in the phrase "… any given region of the electromagnetic spectrum." Albedo is measured from a wavelength 0.4 microns to 0.7 microns (what the eye sees). Emissivity is a wavelength dependent function. In our case it is measured from 7 to 14 microns (what the camera sees). Emissivity = (1 - albedo) is only true if both numbers refer to the same spectral region.

So temperature differences are the primary cause of brightness differences in thermal images.

Radiometric Calibration

Brightness in the image is a function of both temperature and emissivity of the lunar surface. Unfortunately, for the images presented here, it is also influenced by the image process chain employed by the author. As described in the paper "How to Collect Lunar TIR Images" (Wilson, 2019), these images are radiometrically uncalibrated. That means that equal brightnesses in difference parts of the image do not represent equal temperatures. Consequently, these images cannot be used to measure temperatures on the lunar surface. Nevertheless, brighter areas in the image do represent areas that are warmer than their nearby surroundings. If they were calibrated, the maria would indeed be a little bit brighter. In fact, calibration would reveal an obvious global temperature trend decreasing steadily from a maximum at the subsolar point to a minimum at the terminator. The strongest image processing artifacts are visible either as an intense brightening at the limb in some scenes, such as portions of **Figure 5**, or as a vignetting effect near the corners, as in the upper right of **Figure 11**. They should both be ignored.

Thermal Equilibrium

For readers who are curious about the concept of a "highest possible temperature" for the lunar surface, a brief explanation is offered. Solar flux at the Earth's (and Moon's) distance from the Sun (F_{in}) is about 1,340 watts per square meter. The maximum temperatures recorded on the Moon are over 390 K. Application of **Equation 7** shows that the emitted flux (F_{out}) for the maria (ε = 0.96) at T=396.0 K is 1340 W / m^2. At a temperature of 396 K, the maria will radiate energy away as the same rate that the Sun is delivering it. Radiometric balance has been achieved and no further increase in temperature can occur. If it were to become hotter than that for any reason, the surface would radiate away energy until it cooled back to 396 K, just as your car's engine cools to ambient temperature after you turn it off.

Some Features Glow in the Lunar Night

A particularly interesting phenomenon is the night glow of some lunar features. The fact that the terminator appears to be in the same position in simultaneous visible and thermal images means that most of the lunar surface cools rapidly and almost uniformly after sunset to a temperature below the limit of detection. But not everything goes immediately into a deep freeze.

Careful inspection of thermal images of the waning Moon reveals bright (warm)

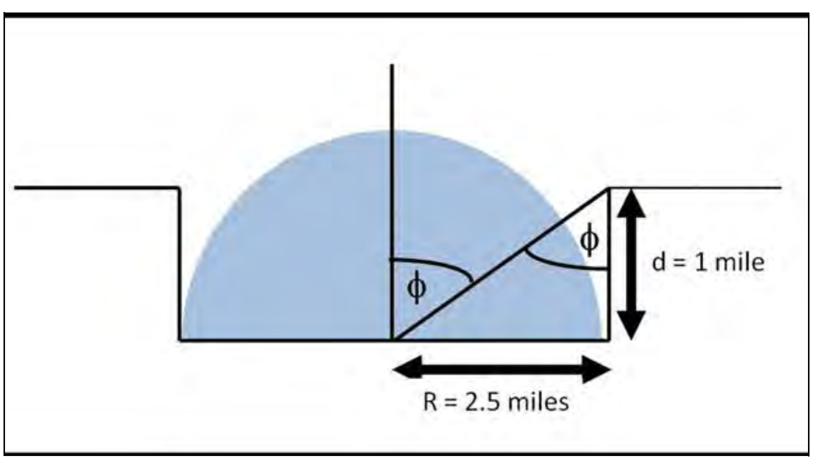

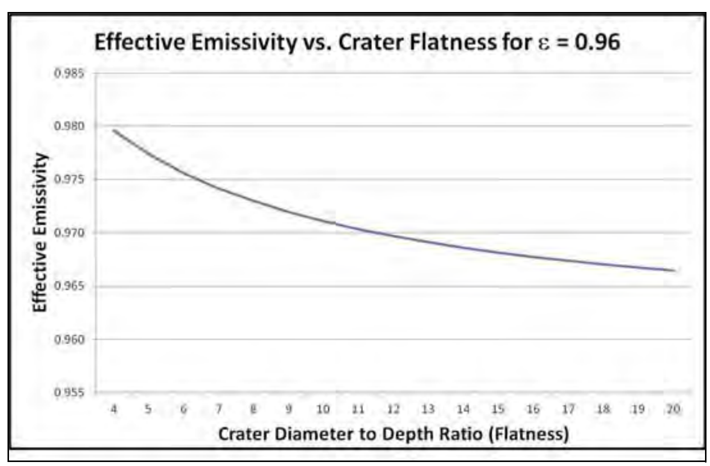

Figure 21 (above left). Partial sky visibility from crater floor.

Figure 22 (above right). Cavity effect on emissivity.

spots on the nighttime side of the terminator. Analysis reveals that the spots almost always correspond to craters in the roughly 6- to 12-mile diameter size range. Several can be seen in **Figure 11**. The simultaneous visible light reference image in **Figure 12** shows that the terminator moved past the craters many hours earlier. **Figure 18** shows that Proclus, Messier and Pickering, Gardner, Charmichael, Cauchy and many others of similar size remain warmer and continue to glow for days after sunset. **Figure 19**, taken three days earlier, shows the illuminated lunar surface for reference.

Why are craters the only features that glow? Why not mountain ranges, mountain peaks, or the maria? One might expect that the westward side of mountain ranges would remain warmer than surrounding areas long after sunset, but that is not observed.

Surface features that glow visibly after sunset must either be more emissive or warmer than their surroundings. Let's examine each of those possibilities in turn.

In the 7 – 14 micron region of the spectrum, emissivity over the lunar surface does not vary much. Almost uniformly high, it is typically about 95% for the highlands and about 96% for the maria in the TIR spectral range. **Figure 20** shows the emissivity of quartz (silicon dioxide) over the 7 – 14 micron range of the spectrum. Silicates on the lunar surface have similar emissivities, although the deep feature from 7.5 to 9.5 microns is attenuated in the regolith.

Since we just stated that the emissivity everywhere is about the same, it might seem obvious that temperature differences must be the cause of any glowing features that we can image. Before we accept that conclusion, we should investigate an unexpected, unintuitive aspect of emissivity.

The Cavity Effect

The appearance of small craters glowing in the lunar night may be due in part to something known as the "cavity effect". Concave areas in thermal images appear to have artificially higher emissivity than flat areas of the same material at the same temperature - and the deeper the concavity, the greater the effect. Most of the craters listed above are relatively smooth, deep concavities. **Equation 9**, the cavity effect equation, quantifies this. Let's use it to see what it might explain.

A 5-mile diameter, 1-mile deep crater is modeled by an open-ended cylinder with a diameter (d) of 5 miles and a depth (h) of 1 mile, as shown in **Figure 21**. The cavity exit port area (A) is

$$A = \pi r^2 = \pi * 6.25 = 19.6 \text{ square miles.}$$

The interior surface area (S) is

$$S = A + h * \pi * d = 19.6 + 15.7 = 35.3 \text{ square miles.}$$

The effective emissivity can be calculated with the cavity effect equation, as shown here.

$$\varepsilon_{eff} = \varepsilon / [\varepsilon (1 - A / S) + A / S] \qquad (9)$$

$$= 0.96 / [0.96 * (1 - 19.6 / 35.3) + 19.6 / 35.3]$$

$$\varepsilon_{eff} = 0.977$$

For the above example, the effective emissivity is increased by 1.8%.

Figure 22 plots the effective emissivity for a range of crater diameter-to-depth ratios if the regolith emissivity is 0.96. As crater diameters decrease from 50 miles down to 5 miles, their relative depth generally increases (diameter-to-depth decreases), and their apparent emissivity increases. The smallest craters exhibit

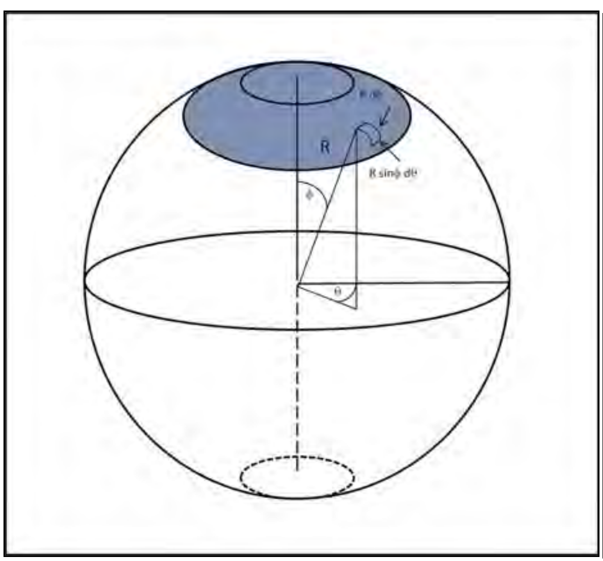

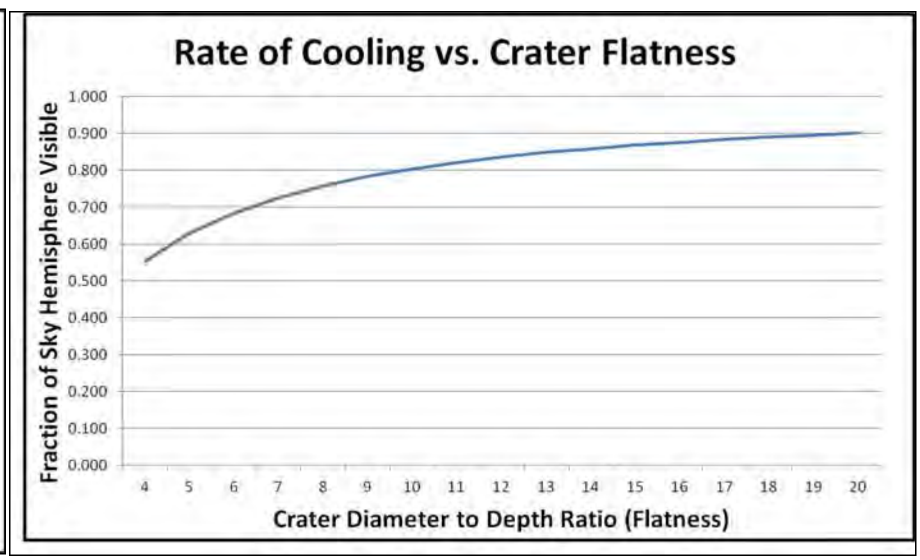

Figure 23 (above left). Visible sky fraction.

Figure 24 (above right). Rate of cooling inside crater.

about a 2% increase in radiative flux relative to the surrounding mare if the surface temperature everywhere is uniform. That should be sufficient to cause a detectable difference between the crater and the mare if both are warm enough to be imaged, but it doesn't go far enough. In order to explain what we see - visibly glowing craters surrounded by lunar surface so cold that our sensor registers nothing - we need something that can explain more than a 2% difference.

Radiative Cooling

What about temperature differences? As expressed in **Equation 7**, the quantity of thermal radiation emitted by a warm object is directly proportional to its emissivity, and to the fourth power of its temperature. Since the emitted flux is proportional to the fourth power of temperature, a temperature difference can potentially cause a much greater increase in radiative flux than a difference in emissivity.

Although this seems to be a promising possibility, there's a problem. We can see that late in the lunar afternoon, most of the small craters in the maria have about the same temperature as the surrounding surface. What could cause them to become warmer than the surrounding mare after the Sun sets and lunar night falls?

Mathematics offers a clue. Deeper in a relative sense, the interior of small craters is exposed to a smaller fraction of sky than large ones. Radiative cooling to the cold sky is the only cooling mechanism available to the surface after sunset, and it happens more slowly in small craters.

Geometric calculations show that the center point in a crater that is five miles in diameter and one mile deep, as illustrated in **Figure 21**, is exposed to less than 2/3 (62.9%) the area of the sky that a point on a flat surface would be. Therefore, a point on the mare surface will experience cooling at a 59% greater rate than a point near the center of the crater.

This would result in relatively higher temperatures within deep craters as the surface cools after sunset. Since the radiative flux is proportional to the fourth power of the temperature, a 2% temperature difference causes an 8.2% increase in flux. This is worthy of some further analysis.

The fraction of sky visible from the interior of a crater depends on the angle that the walls rise above the horizon. In **Figure 21**, the angle above the horizon is equal to 90 - ϕ. **Equation 10** is used to calculate ϕ.

Equation 11 is used to calculate area on the surface of a sphere (see **Figure 23**). We wish to calculate the fraction of the sky that is covered by the shaded area relative to the upper half of the sphere. We take advantage of circular symmetry of the crater, and normalize the radius to a value of 1.0 to arrive at **Equation 12**, which can be evaluated in fewer steps than **Equation 11**.

Combining **equations 10** and **12** results in **Equation 13**. It gives the fractional area of the sky visible as a function of the relative depth of the crater, independent of crater size (width). The effect of curvature on the lunar

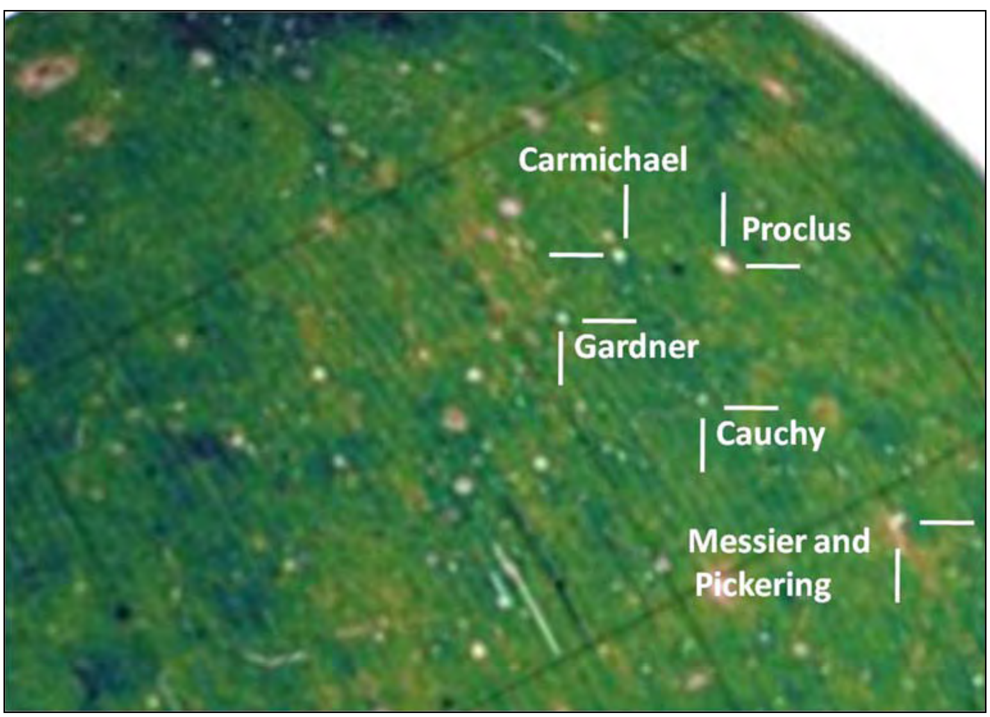

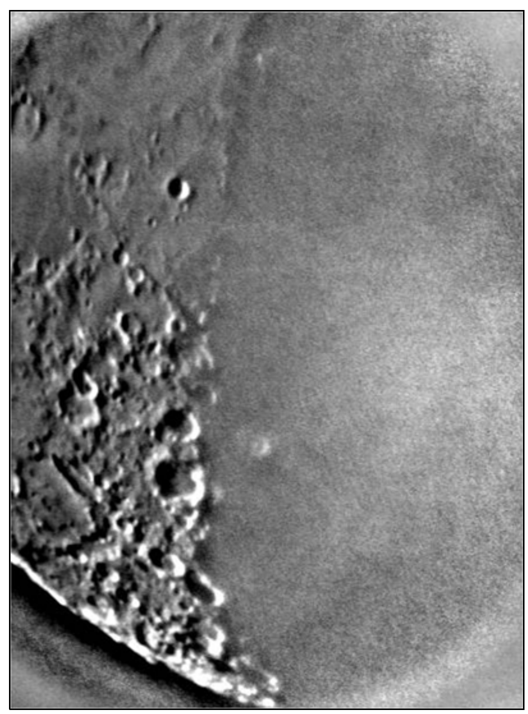

Figure 25 (above left). Thermal inertia map of same area as Figure 17.

Figure 26 (above right). Tycho radiates after sunset.

surface is small and can be ignored. It causes only about a 1% difference in visible sky for a 40-mile diameter, one-mile deep crater, and even less for smaller craters. If a crater is large enough for surface curvature to be important, more than 95% of the sky will be visible anyway and this effect will be unimportant. **Figure 24** plots the visible sky fraction, which is a proxy for the rate of cooling, as a function of the relative flatness of a crater (2*R/d). It shows that the deeper the crater, the more slowly it cools, and the effect is increasingly strong with greater depth. This may cause some craters to remain detectably warm long after the surrounding mare has cooled.

$$\phi = \text{atn}(R / d) \quad (10)$$

$$= \text{atn}(2.5 / 1)$$

$$= 68.2 \text{ deg.}$$

$$\text{area} = R^2 \int_0^{2\pi} \int_0^{\phi} \sin(\phi)\, d\phi\, d\theta \quad (11)$$

$$\text{frac. area} = \int_0^{\phi} \sin(\phi)\, d\phi \quad (12)$$

$$= \int_0^{68.2} \sin(\phi)\, d\phi$$

$$= -\cos(\phi)]_0^{68.2}$$

$$= (-\cos(68.2)) - (-\cos(0))$$

$$= (-0.371) - (-1)$$

$$= 0.629$$

$$\text{frac. area} = 1 - \cos(\text{atn}(R / d)) \quad (13)$$

Temperature differences between the interior of craters and the surrounding mare are probably more important than the cavity effect in causing the nighttime glows, but they both contribute in the same direction. These geometric effects at least partly, perhaps mostly, explain why mountain peaks, flat plains, and isolated walls apparently cool more rapidly to a point below the limit of detection and do not continue to visibly glow after sunset.

We have identified two likely contributors to the nightglow effect, but they don't seem to be sufficiently strong to account for our observations. Could there be another contributor?

Surface Materials Might Cause Glow

It is also possible that surface material differences are part of the cause. If the interiors of these craters are composed of exposed silicates, which are high thermal inertia materials, they would absorb more thermal energy during the day and remain significantly warmer into the lunar evening.

The paper referenced in the bibliography (list of references at the end of this paper) by Hayne (2017) discusses mapping of the lunar surface by the scientists who analyzed the LRO data. A subset of one of the P maps from their paper is reproduced in **Figure 25**. It has been cut to match the area of **Figure 18**.

Almost all of the hot spots in the TIR image correspond to high thermal inertia features in the P map. There are no prominent examples of hot spots that map to low P areas. Interestingly, many high thermal inertia features do not appear as hot spots. Apparently high thermal inertia alone is not enough to form a hot spot that glows after sunset.

A final piece of evidence that illustrates the strength of the thermal inertia effect concerns the crater Tycho. At 100 million years old, it is quite young relative to the timeframe required for space weathering. Consequently, its interior is largely composed of freshly exposed silicate surfaces with high thermal inertias. Unlike other craters in its size range, **Figure 26** shows that it maintains a detectable glow more than 24 hours after sunset.

The Final Word On Nighttime Glows

The final word is not yet in. Perhaps it awaits observations and analyses by a motivated amateur astronomer somewhere.

A multivariate analysis of the correlation between the relative depths of high thermal inertia craters, their individual mean thermal inertias, and their visibility in TIR imagery as hot spots might solve this puzzle. It should at least point to areas for further investigation.

A promising avenue is multispectral thermal imaging. Thermal narrowband filters might be used in conjunction with a TIR imager to collect distinct spectral bands of imagery. With appropriate processing, they could be used to map the abundance of exposed silicates on the surface. The correlation between the resulting map and the TIR images should help to explain the observations.

Opportunities for Amateur Observers

The history of astronomy shows that scientifically valuable knowledge always results from the application of a new observational technology. These remote sensing technologies are, collectively, responsible for almost all that we know and understand about the universe beyond Earth. In the hands of capable amateur astronomers, TIR imaging will certainly enable a new round of discoveries. Two possibilities are mentioned here.

First, you may be able to detect and characterize meteor impacts on the lunar surface. Visible light impacts usually last only a fraction of a second. The thermal signature from an impact may persist for minutes or hours, offering more opportunity for detection and analysis. With high quality observations, we could constrain the mass and velocity of the impactor, and surface material characteristics at the site of the impact.

Second, although the Moon is not volcanically active, outgassing may still occur. On the sunlit side of the Moon, TIR imaging could detect a cold gaseous plume as an ephemeral, amorphous dark feature against a hot surface background. Limb observations might also reveal outgassing due to the high contrast between the relatively warm gas and the cold background of space.

Either, or both, may be observable. Of course, outgassing may not even occur, but at least we now have the imaging technology to see it if it does. Professional astronomers are not looking for these events, so the door is open for an amateur to discover the first conclusive evidence of a lunar outgassing event.

A Historical Perspective on TIR Imaging

The invention of the telescope gave the ability to visually observe previously unsuspected detail in celestial bodies. The development of photography enabled recording of objects too faint to be seen visually. The discovery of spectroscopy gave information that identified the atomic and molecular species that constitute planets and stars. More recently, electronic imaging techniques that record radiation in the near-infrared (outside the visible spectrum) have been used to record methane distribution in Jupiter's atmosphere, surface features on Venus, and other kinds of information that had been thought to be unattainable.

TIR imaging is a new way to observe the Moon that offers exciting possibilities for unexpected discoveries and scientific research. It is potentially the most revolutionary advance in lunar observation techniques since CCD imaging and video image processing were introduced to amateurs more than 20 years ago.

A Final Thought

The author wishes to thank Dave Kriege (owner, Obsession Telescopes) for providing several insightful questions that were incorporated into this paper to illuminate key concepts.

He also thanks Shawn Dilles and Ken Poshedly for finding and fixing grammar errors, wordsmithing, and formatting that improved the quality and readability of the paper.

About the Author

Darryl Wilson is a retired scientist and has been an amateur astronomer since age 12. See the list of references here for other articles by him on thermal imaging.

References

Cook, Dr. Anthony (2019). “The Lunar Change Detection Program”. *The Lunar Observer*, December 2019: p. 36. Available at http://www.alpo-astronomy.org/lunarblog/wp-content/uploads/2019/12/tlo-december.pdf*FLIR Systems, Inc. (2020). Available at: https://www.flir.com/discover/rd-science/lunar-eclipse-when-viewed-in-thermal/

Miller, John Lester and Friedman, Ed. (2004). *Photonics Rules of Thumb*, 2nd ed., McGraw-Hill Companies, Inc., 2004, pp. 283. Available at: https://www.amazon.com/Photonics-Rules-Thumb-Optics-Electro-Optics/dp/0071385193

Paul O. Hayne, et. al. (2017) “Global Regolith Thermophysical Properties of the Moon from Radiometer Experiment” *Journal of Geophysical Research*: Planets, Vol. 122 No. 12, pp. 2371-2400. Available at either: https://doi.org/10.1002/2017JE005387, or at: https://agupubs.onlinelibrary.wiley.com/doi/epdf/10.1002/jgre.20586

Rukl, Antonin (1992). *Atlas of the Moon*, Kalmbach Publishing Co., Waukesha, WI: pp. 224. Available at: https://www.amazon.com/Atlas-Moon-Antonin-Rukl/dp/0600571904

Saari, J. M., Shorthill, R. W., and Deaton, T. K. (1966). "Infrared and Visible Images of the Eclipsed Moon of December 19, 1964", *Icarus*, Vol. 5 Nos. 1-6, pp. 635-659. Available at: https://doi.org/10.1016/0019-1035(66)90076-5

Salisbury, John W. and Hunt, Graham R. (1967). "Infrared Images: Implications for the Lunar Surface", October 24, 1966, *Icarus* Vol. 7, Nos. 1-3: pp. 47-58. Available at: https://doi.org/10.1016/0019-1035(67)90046-2

Sinton, W. M., "Eclipse Temperatures of the Lunar Crater Tycho" (1960). *Lowell Obs. Bull*. 5, pp. 25-26. Available at: http://articles.adsabs.harvard.edu//full/1962IAUS...14..469S/0000469.000.html.

Williams, J.-P., Paige, D.A., Greenhagen, B.T., and Sefton-Nash, E. (2017). "The Global Surface Temperatures of the Moon as Measured by the Diviner Lunar Radiometer Experiment", August 13, 2016, *Icarus*, Vol. 283, pp. 300 - 325. Available at: https://doi.org/10.1016/j.icarus.2016.08.012

Wilson, Darryl G. (2019). "Lunar Nighttime Thermal Analysis", *The Lunar Observer*, Nov. 2019 Issue, pp. 25-31. Available at: http://www.alpo-astronomy.org/lunarblog/wp-content/uploads/2019/11/2019-11-tlo.pdf

Wilson, Darryl, “Lunar Nighttime Thermal Analysis”, (2020). *Journal of the Assn. of Lunar & Planetary Observers*, Vol. 62, No. 3 (Summer 2020), pp. 47-51.

Wilson, Darryl G. (2020). "Lunar Nighttime Thermal Analysis", *Journal of the Assn of Lunar & Planetary Observers*, Vol. 62, No. 4: pp. 57-65.

Papers & Presentations

The Mysterious History of Mapping ‘Luna Incognita!’

By Richard P. Wilds
ALPO Member
astromaster@att.net

To read about ALPO's extensive efforts to map “Luna Incognita”, see John Westfall's 1990 article in JALPO Vol. 34 No. 4, which can be found on the ALPO website (http://alpo-astronomy.org) in the Section Galleries/Publication Section or by loading the link below into your browser: *http://www.alpo-astronomy.org/gallery3/index.php/Publications-Section/ALPO-Journals/DJALPO-Volume-34*

Abstract

There are activities that go on in astronomical research that even many astronomers have never heard about. Over the past several decades there have been discussions by several national space agencies about establishing a base and research facility near the lunar south pole. One proposed site is on one of the highest mountains in the solar system (perhaps Leibnitz B; see ***Figure 1****) to take advantage of water deposits in nearby deep, shadowed and cratered valleys. The following is a little known part of the story that has helped make these proposals a real possibility by mapping an obscure part of the Moon - luna incognita - that is virtually impossible to measure with certainty from the Earth.*

The story includes Cold War spies and the efforts of professional and amateur astronomers from all over the world observing thousands of grazing occultations of stars by the Moon. The story continues with dedicated satellite imaging missions to the Moon by NASA (the Lunar Reconnaissance Orbiter) and the Japan Aerospace Exploration Agency (Kaguya).

Discussion

We begin the story with astronomer Giovanni Domenico Cassini, who made detailed observations of the Moon and lunar motion. In 1693, while at the Paris Observatory, Cassini published three laws of lunar motion. The first law states that the Moon rotates on its axis at the same time that it takes to revolve around the Earth (which explains why the same lunar side always faces the Earth). The second law states that the Moon’s axis is tilted relative to the ecliptic.

But most relevant to us is the “Third Law of Lunar Motion”, which states that the ascending node of the lunar orbit on the ecliptic coincides with the descending node of the lunar equator on the ecliptic (Colombo, 1967). This third law provided first scientific explanation of why some areas around the lunar poles cannot be easily observed from the Earth. Known as the “‘Cassini Regions”, these areas were often represented as blank areas on lunar maps. Even after the Apollo Moon landings, part of the south polar region remained uncharted and this area was sometimes referred to as “luna incognita” (Westfall, 1978, 1990).

We pick up the story with Johann H. Schröter and his work on the Moon entitled *Selenotopographische Fragmente* which was published first in 1791 and then in 1802. Schröter attracted particular note for having claimed that some of the mountains that he had measured at the southern limb of the Moon were calculated to be higher than any mountains on the Earth. Mount Everest on Earth is approximately 29,000 feet above sea level, while there are at least three mountains on the Moon’s southern limb — Leibnitz B, M5 and Beta Doerfel (see **Figure 1**) — measured to be close to 33,000 feet above the “mean limb”, which is akin to sea level on planet Earth.

None of these come close to the 72,000 feet of Olympus Mons on Mars, but that is another story. Many astronomers have spent the last two centuries trying to check Schröter’s measurements, but found this to be a difficult task due to the problems with lighting near the lunar south pole and compounded by the

Online Readers

Your comments and questions about this report are appreciated. Please send them to the author by left-clicking your mouse on the e-mail address under the byline on this page in blue text.

Also left-click on any hyperlinks in blue text within the text of this paper and in the References section for additional information.

Table of Early Grazing Occultation Observations

Date	ZC Star	Magnitude	Observer Location
Sep 02, 1811	3353	3.8	Olomouc, Czechoslovakia
Mar 07, 1794	692sk5	0.9	Gdansk, Poland (Danzig)
Jan 23, 1706	657	5.4	Paris Observatory, France

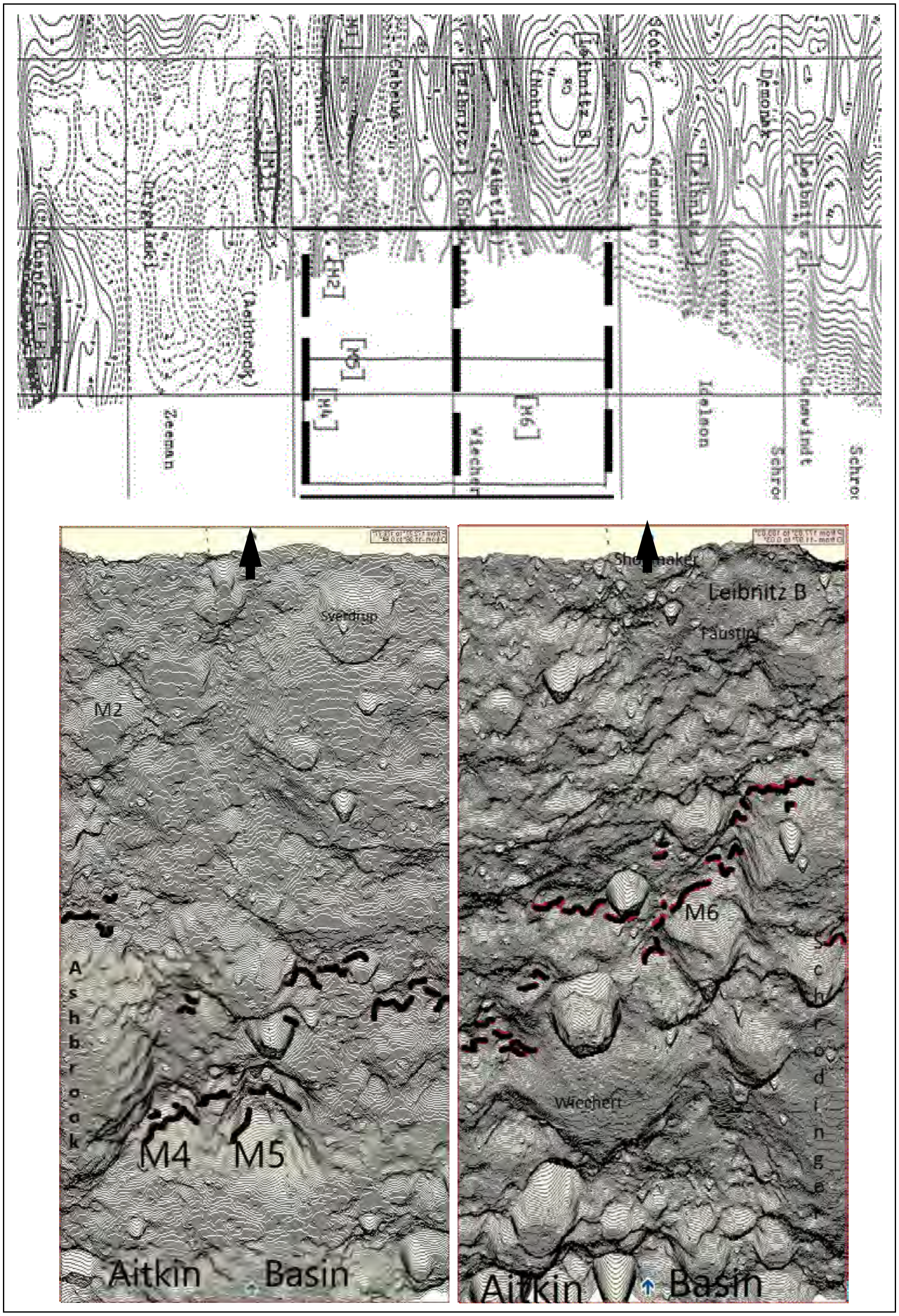

Figure 1.**Top:** Topographic map of the lunar south polar region mapped by Dr. Watts. The two squares outline the areas seen in the bottom image; annotations by this author indicate the location of mountains M2, M4, M5 and M6 (Watts, 1963 and Wilds, 2008).
Bottom: Insets of the area outlined above of part of the lunar south polar region, with arrows indicating the direction toward Earth. The base topographic data from the JAXA Kaguya Mission and NASA Lunar Reconnaissance Orbiter Missions as displayed from David Herald's Occult software, with the locations of mountains M2 - M6 noted. The bold black lines show elevation data derived from measurements acquired during the author's 1988 grazing occultation expedition to Moonlight, Kansas. Occultation measurements acquired over the last century on expeditions like this one have contributed greatly to mapping this area.

rough surface terrain of towering mountains and deep craters.

One approach to measuring terrain near the lunar poles is by timing lunar grazing occultations. Lunar occultations occur when the Moon passes in front of a star as seen by an observer on Earth. Grazing occultations represent the special case where the star appears to “skim” near the lunar surface, blinking on and off as its light path is blocked by protruding terrain. There have been a number of efforts over the years to use occultation events to study regions of the Moon (Hayn, 1907) (Przybyllok, 1908) (Taylor, 1920) (Weimer, 1952) (Nefediev, 1957) (Chugunov, 1979). All of these were early attempts failed to fully resolve the luna incognita due to the unavailability of critical work done by Dr. Watts, which I shall discuss later.

Though grazing occultations have been observed by chance since 1706, no one was able to predict any of these exciting events until well into the 20th Century. Some of the earliest events are listed in the table on the first page of this paper.

Over the next century and a half, many more grazing occultations were observed, but all accidentally. Dr. Thomas Van Flandern of the U.S. Naval Observatory compiled a list of these observations which he forwarded to Dr. David Dunham. From Dr. Dunham it has gone to David Herald, where it has been included in the *World Listing of Grazing Occultations* in the database of his Occult software (Herald, 2018).

In 1828, Friedrich Wilhelm Bessel published his mathematical methods for predicting these events and they have become known as *Besselian Elements*. These Besselian elements are now used on a regular basis in calculations of occultations in spherical astronomy.

Bessel first approached the problem of calculating eclipses and occultations by defining a fundamental plane with a z-axis from the Earth's center to the star to be observed. Then the Moon’s shadow is represented as a circle on the Besselian plane that is perpendicular to the z-axis, and the circle moves on the plane as the Moon moves.

Observers on the Earth’s surface can also be projected onto the plane, with multiple observers in different locations being represented as different points on this curve as the Earth rotates. The time of an occultation is found by calculating the intersection of the observer’s location with the lunar circle.

Today, by compensating for relativistic effects caused by interactions of the Earth-Moon system, occultations are routinely predicted with a high degree of accuracy (Smart, 1965) (Meeus, 1995) (Herald, 2018) (Limburg, 2002) (Riedel, 1997).

However, practical attempts to predict occultations were not made until the 1930’s when J.T. Foxell of the British Astronomical Association (BAA) Computing Section attempted to predict the grazing occultation of the star Regulus along the northern limb of the Moon. The BAA had 12 members willing to be led by graze leaders Dr. R.L. Waterfield and Dr. R.M. Fry. They met at the White Horse Inn in Bridge before deploying along the Canterbury-Dover Road on 6 April 1933.

The team included capable observers such as Dr. Hugh Percy Wilkins and the young and enthusiastic Patrick Moore, who would go on to become one of Britain’s leading practitioners of the art

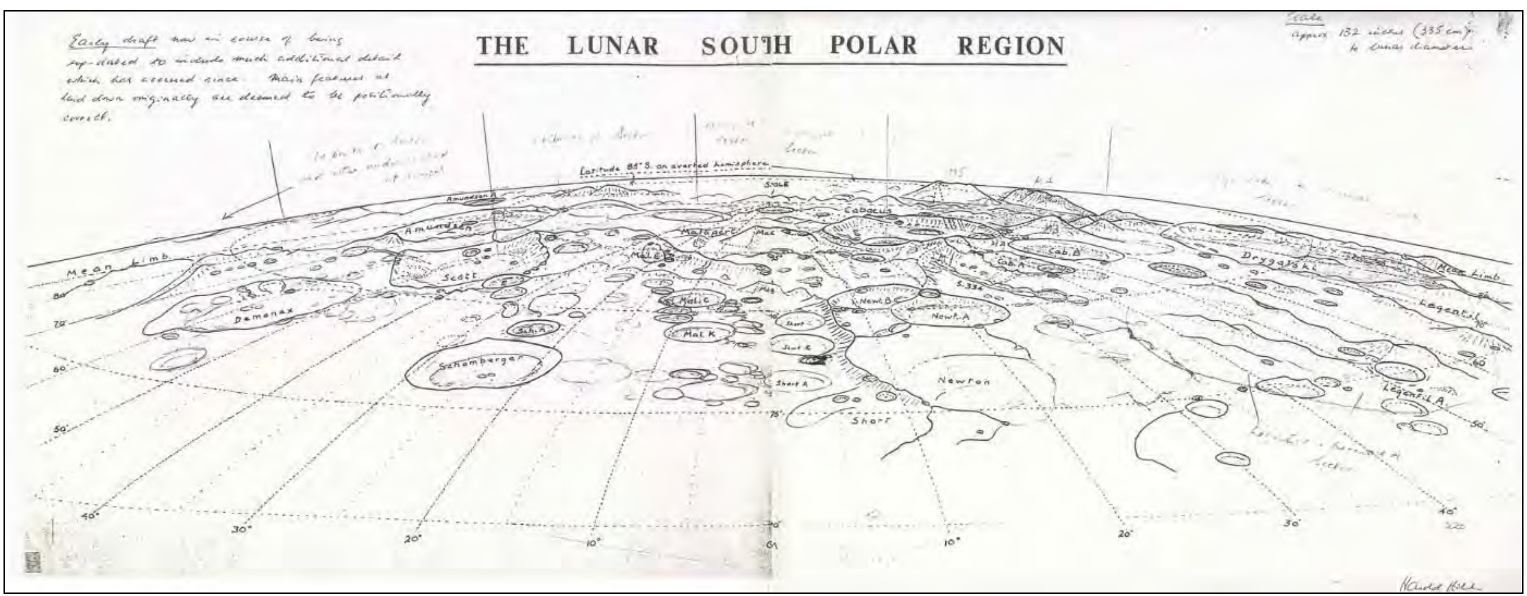

Figure 2. Harold Hills' “Working Drawing” of the Lunar South Pole Cassini Region.

of astronomical observing.
Unfortunately, this early effort met the fate of many such teams in that they were clouded out for just the few crucial minutes during the time of the event. While others were able to observe the occultation from other locations, the observations reporter, J.D. McNeile, did not find any success in the one-kilometer-wide path of the grazing occultation. The prediction was accurate enough to bring the team into the region of the "Mean Limb," but not enough to place observers in the exact locations needed to observe lunar limb topography with certainty (Brown, 1930) (Comrie, 1924) (Foxell, 1933) (Foxell, et. al., 1933) (Kelly, 1948).

Members of the BAA spent the rest of the century working on detailed drawings of the lunar south pole region even though many believed the lunar spacecraft of the 1960s would put an end to such work (Westfall, 1971). However, many like Harold Hill felt that meticulous drawings could still be helpful in dealing with the difficulties of the Cassini region. **Figure 2** shows the "working drawing" by Harold Hill. It very accurately shows the topography of the area involved in the grazing occultation shown in **Figure 3**, except that the drawing and the pictorial reduction below are reversed left-to-right with the mountains M4 and M5 to the right rather than the left and the plateau of M6 to the left instead of to the right.

Nevertheless, one can still easily see how much below the Mean Limb the terrain is between M5 and the M6 plateau – welcome to the Aitkin Basin!

However, other than the reversal due to the mirrors used in viewing, the Harold Hill drawing is remarkably similar and accurate in relation to charts made of the Cassini region that resulted from decades of effort by Dr. Chester Burleigh Watts - perhaps similar to the decades of effort that Harold Hill put into his drawings as well! (Arthur & Abineri, 1952) (Baum, 2010) (Bowker & Hughes, 1971) (Cattermole, 1964) (Hill, 1991) (Lenham & Abineri, 1955) (Whitaker, 1954) (Wilkins, 1947) (Wilkins & Moore, 1955).

Dr. Watts was involved with the United States Naval Observatory in making observations of solar eclipses along with regular positional observations of stars. One of the instruments he used in such efforts was a 5-inch, f/9.6, Alvan Clark refractor. Dr. Watts came up with the idea of using this instrument to obtain highly resolved arcs of the lunar limb. This would take an extended time and using observations from various locations in order to obtain arcs through the many years it would take to observe the lunar limb going through its many subtle wobbles known as librations and take advantage of parallax by observing from various parts of the Earth. The end of the war was a time that would allow Dr. Watts to begin his work (Watts, 1963) (Hockey, 2007) (Wilds 2007).

However, World War II had also started something else that the world had never seen – nuclear weapons. The United States came out of the war as the only nation with such weapons, but history shows that this monopoly would not last long. A bright young astronomer, Dr. John Aloysius O'Keefe, had made a name for himself in the Army Map Service during World War II and remained there after the war for a special secret mission. The world saw the rise of nuclear weapons and the missiles to deliver them in the years after World War II, but there was a problem that most people were not aware of in these years. The two main protagonists in what would become known as the Cold War were on completely different continents and found that they could not be certain that a missile fired from one continent would hit the intended target on the other because the datum used to map each continent were different and had never been connected. Throughout the 1950's, Dr. O'Keefe would led a secret team of astronomical observers armed with 12-inch reflector telescopes to observe solar eclipses and grazing occultations that crossed both Eurasia and North America in an attempt to connect the datum used on the maps of both continents.

Dr. O'Keefe's teams met with limited success due to the lack of detailed, accurate maps of the lunar limb and most observations by the team ended up being the less accurate total occultations of stars by the Moon. Therefore, Dr. O'Keefe pushed to provide more funding to support the work of Dr. Watts until his maps of the lunar limb were published in 1963 as the *Marginal Zone of the Moon* (Watts, 1963). This work was discussed by Joseph Ashbrook in the pages of *Sky & Telescope* magazine (Ashbrook, 1964), and the crater "Ashbrook" is appropriately found in this newly mapped *Cassini Region of the Moon* (Morrison, Martin, 1971) (Scott, 1988) (Dunham, 1971) (Gray, 1992) (Henriksen & Pamelia, 1955) (Henriksen et al., 1958) (Henriksen, 1962) (Ingalls, 1955) (O'Keefe & Mears, 1954) (O'Keefe, 1958) (Hockey, 2014) (Wilds, 2018). (*Editor's Note: Joseph Ashbrook was an active ALPO member from 1957 to 1977.*)

Dr. Watts' publication is comprised of 1,800 contour maps providing the elevation of the lunar limb and cover all libration ranges of the Moon. These maps enable the user to produce a profile of a specific region of the Moon as seen from a particular location on the Earth at an exact moment of time.

Today, however, users need only rely on the occultation prediction software program "Occult" to obtain the needed profile to observe any predicted event for any location on Earth.

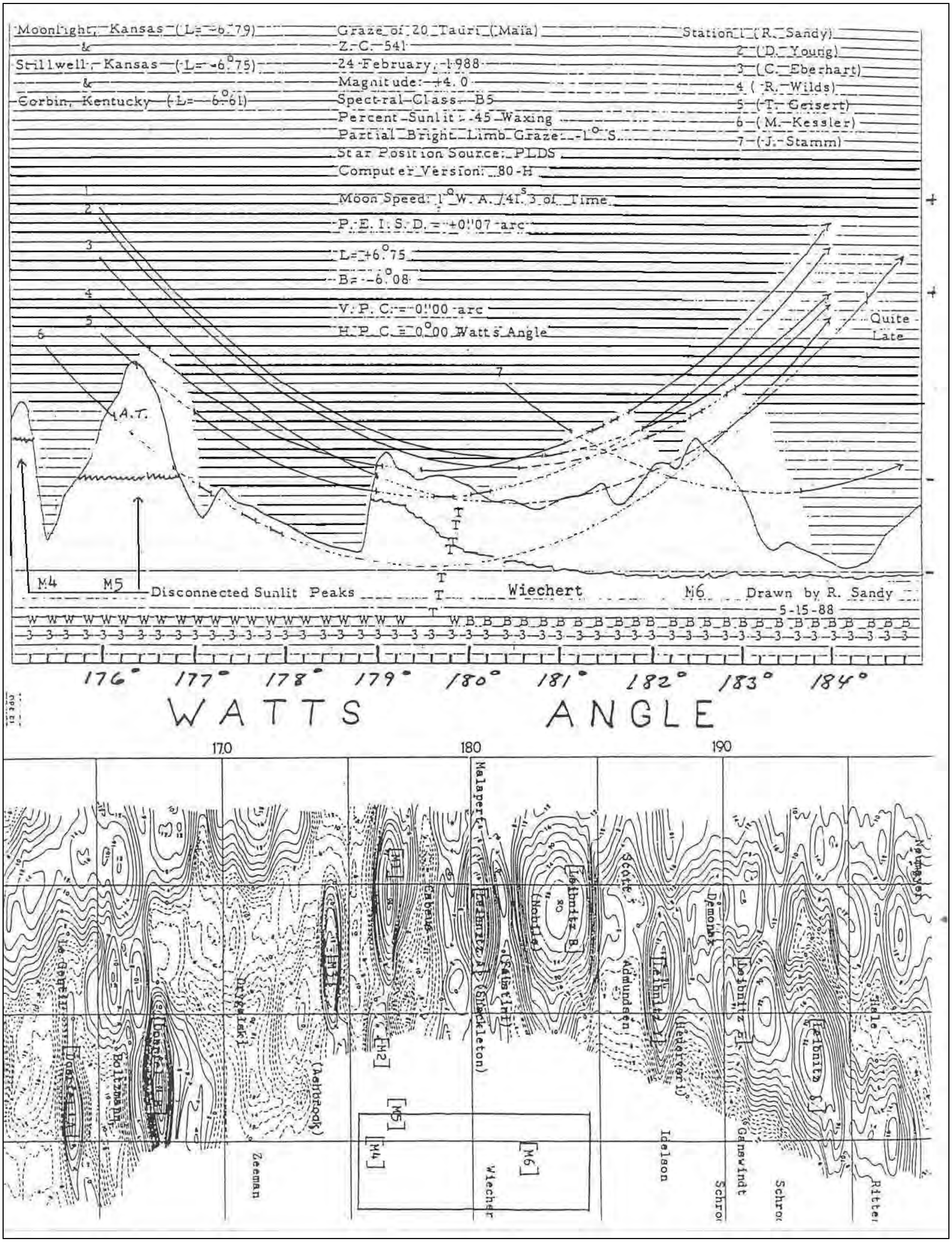

Figure 3. Pictorial Reduction by Bob Sandy and Watts P&D South Pole Annotated by Wilds (image courtesy of Springer International Publishing).

Dr. Watts also provided an index of just over 12 pages at the end of his publication known as the "P&D Charts".

An easy understanding of the Watts P&D charts can be had by comparing them directly to the libration zone maps in Antonin Rukl's *Atlas of the Moon* (Rükl, 1990; Watts, 1963; Van Flandern, 1970; Wilds, 1992-1999; Wilds, 2008; and Wilds, 2018).

Satellites eventually proved effective in accurately connecting continents in the Space Age and a single global datum known as the "World Geodetic System 1984" (WGS-84) has been internationally adopted. This standard datum is used by GPS satellites and provides accurate locations that are precise for most practical applications.

Dr. O'Keefe would leave the secrecy of the Army Map Service for a happier career with NASA, working with the scientific stations (Apollo Lunar Surface Experiments Package - ALSEP) that the Apollo astronauts set up at each landing site. At about the same time, two astronomers in different parts of the world would independently apply Besselian elements to the geometric problem of accurately predicting grazing occultations - Jean Meeus in Belgium and David Dunham in the United States (Meeus, 1960 and 1967) (Dunham 1964 and 1992). They had started their studies before the publication of Dr. Watts' work, but when it was published in 1963, they were quick to take advantage of his findings and use them to plan accurate locations to conduct occultation observing expeditions.

Teams of adventure-seeking professional and amateur astronomers spent the following decades leading thousands of grazing occultation expeditions around the world. They found that as advantageous as Dr. Watts' work was, it also had a number of problems that required corrections. This, of course, is typical with the first effort in a major advancement in science.

The largest problem was that Dr. Watts could not properly image the areas close to the lunar poles, in particular on the far side away from the Earth. These areas, known as "Cassini Regions", can easily be identified on the Watts P&D Charts as the large blank spot behind the lunar South Pole (Bell, 1971) (Fjermedal, 1989) (Povenmire, 1979) (Robinson & Povenmire, 2006) & (Wilds, 2018).

The problem with the north and south Cassini regions is that when the libration renders one of these areas in our line of sight, it is not lit by the Sun. The areas are only lit by the Sun when they are beyond the limb of the Moon as seen from Earth. Furthermore, the precession of the lunar rotational axis advances in unison with the precession of the axis of the lunar orbit, so that the illumination defect continues during the entire 18.6-year-long lunar precessional cycle. This makes producing a coherent map of the area extremely difficult.

This problem has been solved through a massive scientific team effort over many decades. As mentioned earlier, intrepid graze leaders led observing teams on expeditions to observe grazing occultations that crossed the unknown Cassini Region. The first efforts faced difficult challenges after discovering that the far side Cassini Region of the lunar South Pole not only contained some of the highest mountains on the Moon, but also unexpectedly contained some of the lowest lunar topography in the Aitkin Basin. This impact basin is similar to the Mare Imbrium/Montes Apenninus location for Apollo 15 which is easily observable from Earth. The extreme relief and rough terrain in this area makes placing observers for full coverage of the area extremely challenging. As time progressed our expeditions were able to produce increasingly accurate maps of this mysterious and extremely rough topography (Heiken, 1991).

The top portion of **Figure 3** shows the pictorial reduction made by Bob Sandy of data from several expeditions measuring the same occultation event. It includes observations obtained from an expedition led by the author to Moonlight, Kansas. (This is the same pictorial reduction chart shown as part of **Figure 1**). Sandy's data can be accessed in Walt "Rob" Robinson's "Archive of Pictorial Reductions for Past Grazes" website located at *http://lunar-occultations.com/iota/PRData/prdata.htm*).

In the bottom half of **Figure 3** are two of this author's annotated Watts P&D Charts, showing the grazing occultation region found deep in the blank area of the Cassini Region. This is only one of hundreds of expeditions led by the author, but it was easily the most beautiful, due to the mixture of the blue color of the bright Pleiades star Maia being seen up against the very bright sunlit peaks M4 and M5, due only to its blue color.

Then the author saw the spectacular beauty of the bright blue Maia star up against the dull tints of the faintly lit M6 plateau – one of the few times he has observed a grazing occultation and was actually able to see this lunar topography as the Moon passed the occulting star. (Wilds; 2008, 2018).

It should be noted that while collecting occultation timing data, it is not only the Moon that must be of concern; the observer must also be aware that the stellar position is also an issue. In this regard, our teams have also had to make an effort to improve our knowledge of stellar positional accuracy. As such, we have had to provide various star catalogues for lunar work that have increased in accuracy with improved technology from the first generation of "Zodiacal Star Catalogues" to the most recent Gaia satellite data releases (Robertson, 1967 and Sato, 1986).

The next chapter of our story comes with the missions of two lunar mapping satellite missions – the Japanese Kaguya Mission (2007-2009) and the U.S. Lunar Reconnaissance Orbiter Mission (2009-Present). These satellites carry high-resolution cameras and – more importantly for our purposes – laser altimeters that can collect millions of very accurate surface elevation measurements. These missions validated the decades-long work of the grazing occultation observers and were able to obtain new data from very deep craters and other areas that are otherwise not obtainable.

Occultation observers now have access to tools that would have been unimaginable when Dr. Watts first published his P&D Charts. One example is a new GPS Time Insertion Video technology promoted by the International Occultations Timing Association that allows observations to an accuracy of ~0.02-0.03 seconds. This translates into lunar topographic measurements equal to those made by Kaguya and LRO. All of these IOTA efforts, along with the Occult software of David Herald, will allow any observer the opportunity to partner with a number of International research efforts on numerous solar system targets such as the Moon, asteroids or mutual events among the moons of the planets of the outer solar system.

For more information, go to:

http://lunar-occultations.com/iota/iotandx.htm:

http://occultations.org/observing/recommended-equipment/

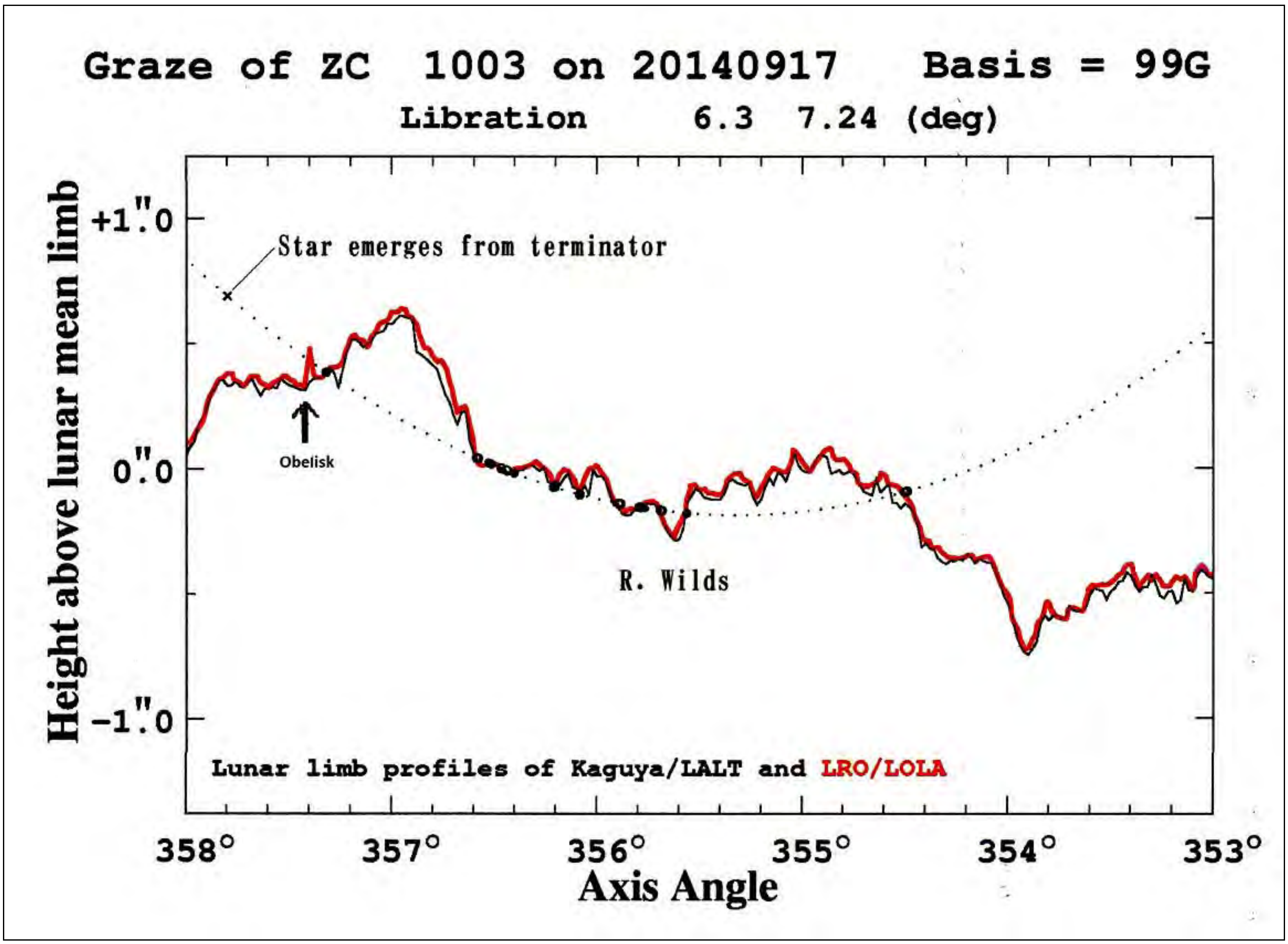

Figure 4. A recent *Pictorial Reduction of a Grazing Occultation* drawn by Dr. Mitsuru Sôma. (image courtesy Dr. Mitsuru Sôma, National Astronomical Observatory of Japan and Springer International Publishing). Color image available from the author.

http://occultations.org/observing/software/

Figure 4 is a recent pictorial reduction of a grazing occultation observed by this author showing how the new GPS time insertion video technology promoted by IOTA allows an observer to help correct even the Kayuga and LRO data. Note that the LRO obelisk anomaly shown to be false on the left side of the lunar limb. The new GPS video system allows observations to an accuracy of ~0.02 to 0.03 second, which translates into lunar topographic accuracy equal to that of Kayuga and LRO.

Conclusions

Today, the primary need for further grazing occultation observations, maintained in Dave Herald's *Occult Database*, is in finding the locations of small glitches in the lunar topography recorded by LRO laser altimeter. A prime example is the "obelisk anomaly" (see arrow, **Figure 4**) shown to be false by the absence of an occultation at its position during a recent grazing occultation observed by the author. Grazing occultation observations will continue to play a contributing role, since even modern, expensive and well-designed spacecraft are capable of the occasional error that will need to be smoothed out by future observations (Herald, 2018) (Dunham, 1992) (Gray, 2002) (Limburg, 2002) (Sôma, 1999, 2002) (Stevens, 1975) (Wilds, 2018).

The history of lunar occultations is marked by hundreds of years of research, involving not only advances in lunar cartography, astrometry and spherical geometry, but also progress in understanding the lunar orbit, its rotation and its precessions. It has been driven by its relevance to global mapping and to the aiming of intercontinental missiles as well as by pure science. In addition to helping to resolve luna incognita, it has produced new knowledge about individual stars and star systems when they are occulted.

References

Arthur, D.W.G. & Abineri, K.W. (1951). The Lunar Limb - South of Schomberger, *Journal of the British Astronomical Assn.*, Vol. 61, No. 2: pp. 45-47. Available to BAA members at: *https://britastro.org/downloads/3844*

Ashbrook, Joseph (1964). The Marginal Zone of the Moon, *Sky & Telescope*, Vol. 27, No. 2: p. 94. *https://skyandtelescope.org/wp-content/uploads/stindex-thru-Mar-2018.txt*

Baum, Richard (2010). Harold Hill and the South Polar Region of the Moon, *Journal of the British Astronomical Assn.*, Vol. 120, No. 2: pp. 86-97. Available to BAA members at: *https://britastro.org/downloads/3844*

Bell, Gertrude 'Trudy' E. (1971). *One Bright Star Within the Nether Tip: The History of Lunar Occultation Observations*. (Senior thesis), Univ. of Cal. Santa Cruz. Contact Dr. Bell at: *trudy.bell@worldnet.att.net*

Bowker, D.E. and Hughes, J.K. (1971). *Lunar Orbiter Photographic Atlas of the Moon*. NASA Report SP-206, Washington, D.C., pp. 42 + 675 pl. *https://ntrs.nasa.gov/citations/19730005152*

Brown, Ernest W. (1930). Practical Astronomy for Amateurs: How the Amateur Astronomer is Helping to Observe and Calculate the Moon's Motions, *Journal of the Royal Astronomical Society of Canada,* Vol. 24: pp. 177-183. *http://articles.adsabs.harvard.edu//full/1930JRASC..24..177B/0000177.000.html*

Cattermole, Peter J. (1964). A Chart of the Lunar Region South and South-East of Bailly. *Journal of the British Astronomical Assn.*, Vol. 74: pp. 104-108. Available to BAA members at: *https://britastro.org/downloads/3844*

Chugunov, I.G. (1979). System of Absolute Elevations in the Marginal Zone of the Moon Derived from Stellar Occultations, *The Moon and the Planets* Vol. 21: pp. 277-281. *http://articles.adsabs.harvard.edu/pdf/1979M%26P....21..277C*

Colombo, G. (1967). Cassini's Second and Third Laws, In: *Measure of the Moon*. Astrophysics and Space Science Library, Vol 8., Springer, Dordrecht: pp. 497. *https://doi.org/10.1007/978-94-010-3529-3_2*

Comrie, L. J. (1924). An Appeal for the Observation of Certain Lunar Occultations, *Journal of the British Astronomical Assn.*, Vol. 35: pp. 23-24. Available to BAA members at: h*ttps://britastro.org/downloads/3844*

Dunham, David W. (1964). Grazing Occultation Observations Made During 1963. (unpublished). E-mail: *dunham@starpower.net*

_____________ (1965). Grazing Occultation Observations Made during 1964 and early 1965. (unpublished). E-mail: *dunham@starpower.net*

______________ (1971). Geodetic Applications of Grazing Occultations, In: De Jager C. (eds) *Highlights of Astronomy*. International Astronomical Union, Vol 2. Springer, Dordrecht. Available at: *https://www.amazon.com/Highlights-Astronomy-U-International-Astronomical/dp/902770189X/ref=sr_1_5?dchild=1&keywords=Highlights+of+Astronomy+springer&qid=1612829199&s=books&sr=1-5*

______________ (1992). Lunar Occultation Prediction and Software News. IOTA *Occultation Newsletter*, Vol. V, No. 8: p. 206. Available at: *http://www.occultations.org/on/volume05/onv05n08.pdf*

Fjermedal, Grant (1989). *New Horizons in Amateur Astronomy.* Putnam, New York: pp. 144. Available at: *https://www.amazon.com/New-Horizons-Amateur-Astronomy-Satellites/dp/0399514864/ref=sr_1_5?dchild=1&keywords=Fjermedal%2C+Grant&qid=1612831169&s=books&sr=1-5*

Foxell, J.T. (1933). Occultation of Regulus, 1933 April 6. *Journal of the British Astronomical Assn.*, Vol. 43 No. 5: pp. 196-198. Available to BAA members at: *https://britastro.org/downloads/3844*

________, Notes: The Occultation of Regulus, 1933 April 6. *Journal of the British Astronomical Assn.*, Vol. 43, No. 9: pp. 303 & 397. Available to BAA members at: h*ttps://britastro.org/downloads/3844*

Foxell, J.T., et al. (1933). An Expedition to Observe The Occultation of Regulus, 1933

April 6. *Journal of the British Astronomical Assn.*, Vol. 43 No. 7: pp. 281-283 with additional notes on pp. 278-9. Available to BAA members at: https://britastro.org/downloads/3844

Gray, Bill J. (2002). *Guide 8.0 Computer Software*. Project Pluto, 168 Ridge Road, Bowdoinham, Maine 04008 USA. http://www.projectpluto.com, E-mail: Pluto@projectpluto.com.

Gray, Mike (1992). *Angle of Attack: Harrison Storms and the Race to the Moon*. W. W. Norton and Co., New York: pp. 308. Available at: https://www.amazon.com/Angle-Attack-Harrison-Storms-Race/dp/039332513X/ref=sr_1_1?dchild=1&keywords=Angle+of+Attack%3A+Harrison+Storms+and+the+Race+to+the+Moon&qid=1612829459&s=books&sr=1-1

Hayn, Friedrich (1907). Selenographische Koordinaten III, *Abh. d. K. Sachs. Ges. d. Wiss., Math.-Phys. Kl.* Vol. 30.

____________ (1914). Selenographische Koordinaten IV, *Abh. d. K. Sachs. Ges. d. Wiss., Math.-Phys. Kl.* Vol. 33.

Heiken, Grant H., Vaniman, D. T., and French, B. eds. (1991). *Lunar Sourcebook*. Cambridge University Press, pp. 736, Cambridge, U.K. Available at: https://www.lpi.usra.edu/publications/books/lunar_sourcebook/pdf/LunarSourceBook.pdf

Henriksen, S.W. and J. Pamelia Anderson (1955). A Rough Measurement of the Geodetic Relationship of Europe to North America Using Visually Observed Occultations, *Technical Report No. 18*. (Confidential) U.S. Army Map Service, Washington, DC. https://www.researchgate.net/publication/304045602_Oenopides_of_Chios

Henriksen, S.W., Genatt, S.H., Marchant, M.Q. and Batchlor, C.D. (1958). Surveying By Occultations, *The Astronomical Journal,* Vol. 63, pp. 291 – 295. http://articles.adsabs.harvard.edu/pdf/1958AJ.....63..291H

Henriksen, S. W. (1962). The Applications of Occultations to Geodesy, *Technical Report No. 46,* U.S. Army Map Service, Alexandria, Virginia: pp. 98.

Herald, David (2018). *Occult v4* Software. David Herald E-mail: DRHerald@bigpond.net.au

Hill, Harold (1991). *A Portfolio of Lunar Drawings*. Cambridge Press, New York: pp. 268. Available at: https://www.amazon.com/Portfolio-Drawings-Practical-Astronomy-Handbooks/dp/0521381134/ref=sr_1_1?dchild=1&keywords=A+Portfolio+of+Lunar+Drawings&qid=1612829656&s=books&sr=1-1

Hockey, Thomas, et al. (2007). *Biographical Encyclopedia of Astronomers Vol.I*. Springer, New York: pp. 1348. (See entries by Richard P. Wilds). http://link.springer.com/search?facet-creator=%22Richard+P.+Wilds%22

_______________ (2014). *Biographical Encyclopedia of Astronomers Vol. II*. Springer, New York: pp. 2496. (See entries by Richard P. Wilds). http://link.springer.com/search?facet-creator=%22Richard+P.+Wilds%22

Ingalls, Albert G. (1955). About Utilizing the Moon to Occult the Stars and Increase Telescope Resolution, *Scientific American,* Vol. 192 No.1: pp. 96-103. Available for purchase at: https://www.scientificamerican.com/article/the-amateur-scientist-1955-01/

Kelly, Howard L. (1948). The History of the British Astronomical Association: The First Fifty Years, *Memoirs of the British Astronomical Assn.*, pp.132. http://articles.adsabs.harvard.edu/pdf/1947MmBAA..36C...1

Lenham, A.P. and Abineri, K.W. (1955). Bailly, *Journal of the British Astronomical Assn.*, Vol. 66, No. 1: pp. 25-26. Available to BAA members at: https://britastro.org/downloads/3844

Limburg, Eric (2002). *Lunar Occultation Workbench (LOW) Computer Software v3.1*. Dutch Occultation Assn. Internet: http://www.doa-site.nl/ E-mail: EricLimburg@e-wire.net.au

Meeus, Jean (1960). Waarneming van een Rakende Sterbedekking, *De Meteoor*, Vol. 16, No. 31. E-mail: JMeeus@compuserve.com

__________ (1967). Le Calcul des Occultations Rasantes, *Extrait de Ciel et Terre*, Vol. 83, Nos. 1-2. http://articles.adsabs.harvard.edu/pdf/1967C%26T....83...29M

__________ (1995). *Astronomical Tables of the Sun, Moon and Planets*. Willmann-Bell, Richmond, Virginia: pp. 487. Available for purchase at: https://www.amazon.com/Astronomical-Tables-Sun-Moon-Planets/dp/094339645X

Morrison, L. V. and Martin, R.J. (1971). A digitized version of C. B. Watts' charts of the marginal zone of the Moon, In: *Earth, Moon and Planets*, Vol. 2: pp. 463-467. http://articles.adsabs.harvard.edu/pdf/1971Moon....2..463M

Nefediev, A. (1957). *Bulletin Engelhardt Obs.*, Vol. 30.

Occult Software: http://lunar-occultations.com/iota/occult4.htm

O'Keefe, John A. (1958). The Occultation Method of Long Line Measurements, *Bulletin Geodesique*, Vol. 32 No. 3: pp. 64-65. Available through Springer: https://doi.org/10.1007/BF02526744

O'Keefe, John A. and Donald D. Mears (1954). The 800-Inch Telescope, *Journal of the Royal Astronomical Society of Canada*. Vol. 48 No. 1: pp. 3-15. http://articles.adsabs.harvard.edu/pdf/1954JRASC..48....3O

Povenmire, Harold R. (1979). *Graze Observer's Handbook (Second Ed.).* Vantage Press, N.Y.: pp. 180. Available at: https://www.amazon.com/Graze-observers-handbook-Harold-Povenmire/dp/0934086001/ref=sr_1_1?dchild=1&keywords=Graze+Observer%27s+Handbook&qid=1612829750&s=books&sr=1-1

Przybyllok, E. (1908). *Mitt. d. Grosh. Sternwarte zu Heidelberg*, Vol. 11.

Riedel, Eberhard (1997). *Grazereg Computer Software v5.1*. Herrn Dr. Eberhard Riedel, E-mail: E_Riedel@msn.com

Robertson, James (1967). *Catalog of 3539 Zodiacal Stars for the Equinox 1950.0*. Nautical Almanac Office, U. S. Naval Observatory Vol. X, Part II. Washington.

Robinson, Walt and Hal Povenmire (2006). *Graze Observer's Handbook*. Canaveral Area Graze Observers. Available at: *https://www.bookfinder.com/search/?keywords=Graze+Observer%92s+Handbook&currency=USD&destination=us&mode=advanced&classic=off&lang=en&st=sh&ac=qr&submit=*

Rükl, Antonin (1990). *Atlas of the Moon.* Hamlyn, London: pp. 224. Available used at: *https://www.amazon.com/Astronomy-Atlas-Moon-Antonin-Rükl/dp/0913135178/ref=sr_1_1?dchild=1&keywords=rukl&qid=1612828808&s=books&sr=1-1*

Sadler, D.H. and Clemence, G.M. (1954). *Improved Lunar Ephemeris 1952-1959*. Nautical Almanac Office, United States Naval Observatory, Washington D.C.: pp. 422. Available at: *https://babel.hathitrust.org/cgi/pt?id=uc1.31822008888745&view=1up&seq=9*

Sato, Isao (1986). *Catalog of 3539 Zodiacal Stars for the Equinox J2000.0*. Lunar Occultation Observers Group, Japan.

Scott, David H. (1988). Position - Angle Discrepancy in Watts' Lunar Limb Charts - An Explanation, *Astronomical Journal,* Vol. 95, No. 5: pp.1567-1568. *http://articles.adsabs.harvard.edu/pdf/1988AJ.....95.1567S*

Smart, W.M. (1965). *Text Book on Spherical Astronomy*. Cambridge University Press, Cambridge, U.K.: pp. 430. Fifth and sixth editions available at: *https://www.amazon.com/Textbook-Spherical-Astronomy-W-Smart/dp/0521291801/ref=tmm_pap_title_0?_encoding=UTF8&qid=&sr=*

Sobel, Dava (1995). *Longitude*. Walker and Company, New York: pp. 208. Available at: *https://www.amazon.com/Longitude-Dava-Sobel/dp/B0028BX10K/ref=sr_1_2?crid=2IMP9R5YWZZJP&dchild=1&keywords=sobel+longitude&qid=1612828941&s=books&sprefix=sobel%2Cstripbooks%2C143&sr=1-2*

Sôma, Mitsuru (1999). Limb Profiles of the Moon Obtained from Grazing Occultation Observations. *Publications of the National Astronomical Observatory of Japan*, Vol. 5: pp. 99-119. E-mail: *Mitsuru.Soma@nao.ac.jp* Also *https://ui.adsabs.harvard.edu/abs/1999PNAOJ...5...99S/abstract*

____________ (2002). Limb Profiles of the Moon from Grazing Occultation Observations Collected at RGO. *Publications of the National Astronomical Observatory of Japan*, Vol. 6: pp. 75-105. *https://ui.adsabs.harvard.edu/abs/2002PNAOJ...6...75S/abstract*

Stevens, Berton (1975). The Automatic Computer Lunar Profile Plotting Program (ACLPPP), IOTA *Occultation Newsletter*, Vol. 1, No. 5 p. 46. Available at: *http://www.occultations.org/on/volume01/onv01n05.pdf*

Taylor, G. I. (1920). Tidal Friction and the Secular Acceleration of the Moon, *Monthly Notices of the Royal Astronomical Society Vol. 80 No.3: pp*. 308-309. *http://articles.adsabs.harvard.edu/pdf/1920MNRAS..80..308T*

Van Flandern, T.C. (1970). Some Notes on the Use of the Watts Limb-Correction Charts, *Astronomical Journal*, Vol. 75, No. 6: pp. 744-746. *http://articles.adsabs.harvard.edu/pdf/1970AJ.....75..744V*

Watts, C.B. (1963). The Marginal Zone of the Moon. *American Ephemeris and Nautical Almanac Astronomical Papers*, No. 17. U.S. Naval Observatory, Washington, D.C. *https://www.amazon.com/marginal-Astronomical-prepared-American-ephemeris/dp/B0007EYQUO*

Weimer, T. (1952). *Atlas de Profils Lunaire*. Observatoire de Paris, Paris, France.

Westfall, John E. (1971). Observing the Moon: The Spacecraft Versus the Telescope, *Journal of the Assn of Lunar & Planetary Observers*, Vol. 22 Nos. 11-12: pp. 187-192. *http://www.alpo-astronomy.org/gallery3/var/albums/Publications-Section/ALPO-Journals/DJALPO-Volume-22-1970-71/DJALPO%20Vol_%2022%20Nos_%2011-12%20February%201971.pdf?m=1546120170*

______________ (1972). Luna Incognita: The Last Frontier, *Journal of the Assn. of Lunar & Planetary Observers,* Vol. 23, Nos. 7-8: pp. 118-122. *http://www.alpo-astronomy.org/gallery3/var/albums/Publications-Section/ALPO-Journals/DJALPO-Volume-23-1971-72/DJALPO%20Vol_%2023%20Nos_%207-8%20February%201972.pdf?m=1546120314*

______________(1990). Mapping Luna Incognita, *Journal of the Assn of Lunar & Planetary Observers*, Vol. 34, No. 4: pp.149-159. Plus updated chart graciously supplied by Dr. Westfall. *http://www.alpo-astronomy.org/gallery3/index.php/Publications-Section/ALPO-Journals/DJALPO-Volume-34/DJALPO-Vol_-34-No_-4-November-1990*

_____________ (1997). A Lunar Polar Peek, *Sky & Telescope*, Vol. 93 No. 4: pp. 112-113.

Whitaker, E.A. (1954). The Lunar South Polar Regions, *Journal of the British Astronomical Assn.*, Vol. 64, No. 6: pp. 234-243. Available to BAA members at: *https://britastro.org/downloads/3844*

Wilds, Richard P. (1992-1999). Grazing Occultation Observations, *Occultation Newsletter*, International Occultation Timing Assn. Available at: *http://occultations.org/pub/newsletters/occultation-newsletter/*

______________ (2008). The Marginal Zone of the Moon. International Occultation Timing Assn. See: *http://iota.jhuapl.edu/watts.htm*

______________, (2018) Lunar Grazing Occultations. in: *Encyclopedia of Lunar Science*, Brian Cudnik (Ed.), Springer International Publishing. *https://doi.org/10.1007/978-3-319-05546-6_220-3*

Wilkins, H. Percy, ed. (1947). Tenth Report of the Lunar Section, *Memoirs of the British Astronomical Assn.,* pp. 1-20. *http://articles.adsabs.harvard.edu/pdf/1947MmBAA..36A...1*

_________________ (1950). Eleventh Report of the Lunar Section, *Memoirs of the British Astronomical Assn.,* pp. 18-20.

Wilkins, H. Percy and Moore, Patrick (1955). *The Moon*. Macmillan, New York: pp. 388. Available at: *https://www.bookfinder.com/search/?full=on&ac=sl&st=sl&ref=bf_s2_a1_t1_1&qi=ATlGVr0wsOUV2hKMtx8sSGva.JY_1497963026_1:4:4*

Papers & Presentations

ALPO Observations of Jupiter During the 2016-2017 Apparition

By: Richard W. Schmude, Jr., Coordinator, ALPO Jupiter Section
schmude@gordonstate.edu

To our hard-copy readers: This paper can be viewed in full-color in the online (pdf) version of this Journal.

Abstract

Forty eight observers from 16 different countries submitted nearly 900 images and drawings of Jupiter, and almost 400 light intensity estimates of Jupiter's albedo features during the apparition. A few of the highlights include an analysis of both the north-south and east-west dimensions of the Great Red Spot (GRS), a discussion of important developments in the context of 2016-2017 Jupiter reports on the British Astronomical Association (BAA) website, a summary of near-infrared brightness measurements and a brief description of a possible Jovian fireball.

Introduction

The characteristics of Jupiter for the 2016-2017 apparition are given in Table 1. Those who submitted observations, images or measurements of Jupiter either to the writer or to the ALPO website are included in Table 2. There were 882 images in the 2016-2017 ALPO Jupiter Section image gallery folder as of January 25, 2020. It may be examined at: *http://www.alpo-astronomy.org/gallery3/index.php/Jupiter-Images-and-Observations/Apparition-2016-2017* or go to *alpo-astronomy.org*, click on the ALPO Section Galleries link near the top-right corner of your screen, click on "Jupiter Images and Observations", then click on the "Apparition 2016-2017" folder.

This paper follows certain conventions. The planetographic (or zenographic) latitude is always used. Latitudes and longitudes were measured from images using WinJUPOS (Hahn, 2019). West refers to the direction of increasing longitude. The three longitude systems are described in (Rogers, 1995). The Greek letter λ, followed by a subscript Roman numeral describes the longitude system and value. For example, λ_{II} = 57° W means a system II longitude of 57° W. All dates and times are in Universal Time (UT). Unless stated otherwise, all data are based on visible or near infrared (wavelengths up to 1.0 micrometer) light images.

All methane band images were made in light with a wavelength near 0.89 µm. In all cases the drift rate is for the center of the feature. All dates, except where noted, are for the current apparition and, hence, years are not included. Normal belt abbreviations are used like NEB = North Equatorial Belt. See Table 3.

The north and south edges of a belt will have a small letter "n" or "s" following the abbreviation. For example the north edge of the North Equatorial Belt is the NEBn.

Table 1. Characteristics of the 2016-2017 Apparition of Jupiter[a]

First Conjunction Date	Sep. 26, 2016
Opposition Date	Apr. 7, 2017
Second Conjunction Date	Oct. 26, 2017
Brightness at Opposition (Stellar Magnitude)	-2.5
Equatorial Angular Diameter at Opposition	44.3 arc-seconds
Right Ascension at Opposition	13h 10m
Declination at Opposition	5.7° S
Planetographic Latitude of the Earth at Opposition	3.5° S
Planetographic Latitude of the Sun at Opposition	3.1° S

[a] Data are from the Astronomical Almanac (2015, 2016)

All Readers

Your comments, questions, etc., about this report are appreciated. Please send them to: *ken.poshedly@alpo-astronomy.org* for publication in the next Journal.

Online Features

Left-click your mouse on:

- The author's e-mail address in blue text to contact the author of this article.
- The references in blue text to jump to source material or information about that source material (Internet connection must be ON).

Observing Scales

Standard ALPO Scale of Intensity:
- 0.0 = Completely black
- 10.0 = Very brightest features
- Intermediate values are assigned along the scale to account for observed intensity of features

ALPO Scale of Seeing Conditions:
- 0 = Worst
- 10 = Perfect

Scale of Transparency Conditions:
- Magnitude of the faintest star visible near Jupiter when allowing for moonlight and twilight

Table 2. Individuals Submitting Observations During the 2016-2017 Apparition of Jupiter

Name, Location (Type of Observation)*	Name, Location (Type of Observation)	Name, Location (Type of Observation)
D. Arditti, UK (I)	T. Hansen, Germany (I)	D. Peach, UK (I)
C. Ashcraft, USA (I)	R. Hill, USA (I)	S. Pedranghelu, France (I)
T. Ashcraft, USA (I)	M. Hood, USA (I)	M. Phillips, USA (I)
V. Amadori, Italy (I)	R. Hueso, France (I)	S. Pogrebisskiy, UK (I)
T. Barry, Australia (I)	M. Kardasis, Greece (I)	J. Rogers, UK (U)
Y. Beletsky, UK (I)	K. Kell, Canada (I)	R. Schmude, Jr., USA (PP)
R. Bosman, The Netherlands (I)	S. Kowollik (Germany)	I. Sharp, Spain (I)
P. Budine, USA (D)	E. Kraaikamp, France (I)	C. Sprianu, Romania (I)
G. Chester, USA (I)	G. Lewis, UK (I)	M. Sweetman, USA (D, DN, I)
F. Colas, France (I)	O. C. Lopez, Venezuela (I)	G. Therin, France (I)
B. Combs, USA (I)	P. Masding (UK)	C. Triana, Columbia (I)
B. Cudnik, USA (D, TT)	P. Maxson, USA (I)	D. Tyler, UK (I)
V. da Silva Jr., Brazil (I)	J. Melka, USA (I)	G. Walker, USA (I)
M. Delcroix, France (I)	F. Mellilo, USA (I)	A. Wesley, Australia (I)
J. Ferreira, USA (I)	P. Miles, Australia (I, Pol)	J. Willinghan, USA (I)
C. Go, Philippines (I)	A. Pace, Malta (I)	C. Zannelli, Italy (I)

Key: D = drawing, I = image, Pol = polarization, PP = photoelectric photometry, TT = transit time, U = Jupiter update and V = video

Disk Appearance

Figures 1 and 2 illustrate the visible-light appearance of Jupiter during 2016-2017. Figure 3 shows Jupiter's appearance in methane band light.

Cudnik and Sweetman submitted almost 400 light intensity estimates of Jupiter's albedo features. These were made on the scale of 0 = black to 10 = white. Mean light intensities and standard deviations are summarized in Table 4. The largest change in this apparition was that the NTrZ darkened by 0.6 intensity units.

Table 5 lists belt latitudes measured from visible-light images. The NEBs shifted 1.0° north and the NEBn shifted 2.5° north compared to the previous apparition. The NTB grew wider and its growth was at its southern edge.

Table 6 lists latitudes for some features imaged in methane band light. The SEBs shifted 1.6° farther south and the NEBn shifted 1.9° farther north than noted in the previous apparition.

Was there a statistically significant difference in belt latitudes in visible and methane band wavelengths? A t-test was carried out at the 95% confidence level to give insights to this question. The results are summarized in Table 7. There was a statistically significant difference for both edges of the SEB along with the NEBs and NTBs. Since methane band light is sensitive to high altitude clouds, the results suggest the high altitude cloud environment may be different than at lower altitudes. More work is needed to better understand this difference.

Region I: The Great Red Spot (GRS)

The GRS was brighter in methane band light than any other feature. See Figures 3B-3J and 3O-3P. (The largest bright oval in these figures is the GRS). This is evidence it extended to higher altitudes than other cloud belts or oval storms (Rogers, 1995). Thin white extensions were often seen near the GRS. Two of these are visible in Figures 3H and 3P. Similar features were noted in the 2014-2015 apparition (Schmude, 2018).

The shape of the GRS also changed. It had a nearly elliptical shape with the major axis nearly parallel to the equator in Figure 3F, but the major axis was not parallel to the equator in Figures 3E and 3I. (The major axis in an ellipse is the longest dimension.) A second shape change is illustrated in Figures 3B and 3G. Its southern border is flatter in Figure 3B than in Figure 3G. Similar shape changes were noted in the previous apparition (Schmude, 2020).

Figure 4 shows images of the GRS in visible and methane band light. Figure 4P shows a Juno spacecraft image of the GRS. As in the previous apparition

(Schmude, 2020) the GRS had several irregularities and a few of these are discussed.

In visible light, the GRS had a dark central bar (see figures 4C - 4F, 4H - 4J and 4M). This bar has grown shorter since 1951. For example, it was nine degrees of longitude long on September 24, 1951 (Humason, 1961) but was only around three to four degrees long in 2017.

A second irregularity is the dark outer border around the GRS. It is best seen in Figure 4E. It is more distinct at the south end than at the north end (see figures 4F and 4M). A dark GRS border was drawn in 1881 by Henry Corder (Peek, 1981).

Small bright ovals and streaks were also imaged within the GRS (see figures 4F, 4I and 4P). Similar features were imaged in the previous apparition (Schmude,

Table 3. Names and Abbreviations of Belts and Zones on Jupiter

Belt and zone name	Abbreviated form	Current name	Abbreviated form
South Polar Region	SPR	South Polar Current	SPC
South Polar Belt	SPB	South South South South Temperate Current	S^4TC
South South South Temperate Zone	S^3TZ	South South South Temperate Current	S^3TC
South South Temperate Belt	SSTB	South South South Temperate Current jetstream	S^3TC jetstream
South Temperate Zone	STZ	South South Temperate Current	SSTC
South Temperate Belt	STB	South Temperate Current	STC
South Tropical Zone	STrZ	South Temperate Belt North jetstream	STBn jetstream
South Equatorial Belt	SEB	South Tropical Current	STrC
South Equatorial Belt Zone	SEBZ	South Equatorial Belt Current, barges	SEBC, barges
Equatorial Zone	EZ	South Equatorial Belt revival	SEB revival
Equatorial Band	EB	North Equatorial Current	NEC
North Equatorial Belt	NEB	North Intermediate Current	NIC
North Tropical Zone	NTrZ	North Tropical Current, barges	NTrC, barges
North Temperate Belt	NTB	North Tropical Current	NTrC
North Temperate Zone	NTZ	North Temperate Current B	NTC-B
North North Temperate Belt	NNTB	North Temperate Current	NTC
North North Temperate Zone	NNTZ	North North Temperate Current Jetstream	NNTC jetstream
North North North Temperate Belt	N^3TB	North North Temperate Current	NNTC
North North North Temperate Zone	N^3TZ	North North North Temperate Current	N^3TC
North Polar Region	NPR	North North North North Temperate Current	N^4TC
Great Red Spot	GRS	North Polar Current	NPC

2020). A white streak cuts into the north (bottom) edge of the GRS in Figure 4E. Figure 4P also shows a white streak cutting into the western (right) edge. Similar streaks were imaged in the previous apparition (Schmude, 2020).

There were also faint dark arcs visible within the bright methane-band images of the GRS (figures 4K and 4N). These arcs are best seen in the digital version of this paper. This is evidence that not all parts of the GRS extend to high altitudes.

Sweetman describes the GRS as being very dark in visible light on several dates (May 13, 27, June 4, 16, 23 and 28). This is consistent with its low mean light intensity of 3.7. This is even darker than the value in the previous apparition (Schmude, 2020) and is much darker than in 2014-2015 (Schmude, 2018).

The mean longitude of the GRS within 15 days of opposition, April 7.9, was 267.7° W with a standard deviation of 1.8°. This mean is based on 22 measurements. The mean longitude is just over 14° west of the predicted longitude based on a quadratic equation reported elsewhere (Schmude, 2016). Therefore, the GRS may be accelerating in a retrograde (westward) direction.

The mean latitude of the GRS was 22.6° S with a standard deviation of 0.7°. This value is based on 52 measurements made between October 23, 2016 and July 9, 2017. The mean latitude is the same as in the previous apparition (Schmude, 2020). The reported latitude is near the mean value of 22.4° S (Rogers, 1995). Interestingly, Peek (1981) reports the mean GRS latitude between 1908 and 1930 was 21.8° S with a standard deviation of 1.0°.

The GRS had a mean east-west length of 14.0° with a standard deviation of 1.1°. This is consistent with Rogers (2017b). It had a mean north-south length of 10.0° with a standard deviation of 0.6°. These values are similar to those in the previous apparition (Schmude, 2020), but are smaller than the 1979-2005 lengths (Rogers, 2008). Between 1927 and 2017, the GRS east-west dimension shrunk at a mean rate of 0.19°/year. This is based on an analysis of images published elsewhere (Peek, 1981), (Humason, 1961), (ALPO Archives) and in the cited reports. This is shown in Figure 5 and the rate is similar to the corresponding value reported for 1979 - 2006 (Rogers, 2008). The north-south dimension shrunk at 0.06°/year based on images made between 1952

Table 4. Mean Intensities of Jovian Features for the 2016-2017 Apparition

Feature	Intensity	Standard Deviation	Number
NPR	5.9	0.54	41
NTB	5.2	0.86	36
NTrZ	7.4	0.80	37
NEB	3.5	0.45	41
EZn	9.0	0.28	40
EB	7.6	0.68	19
EZs	9.0	0.28	40
SEB	3.7	0.72	41
STrZ	9.5	0.63	40
GRS	3.7	0.86	15
SPR	5.9	0.40	41

Table 5. Planetographic Latitudes of Belts on Jupiter (based on images made in visible wavelengths in April 2017)*

Feature	South Edge	North Edge
South Polar Belt (SPB)	68.3° S (1.1°, 15)	63.4° S (1.2°, 16)
South Equatorial Belt (SEB)	22.3° S (0.9°, 17)	7.5° S (0.82°, 18)
North Equatorial Belt (NEB)	7.8° N (0.9°, 18)	20.6° N (0.8°, 18)
North Temperate Belt (NTB)	23.8° N (0.5°, 18)	31.6° N (1.0°, 18)

* Standard deviations are in parentheses followed by the number of measurements.

Table 6. Planetographic Latitudes of Belts on Jupiter (based on methane-band images made at a wavelength of 0.889 m in April 2017)

Feature	South Edge	North Edge
South Polar Cap (SPCn)	–	68.4° S (0.8°, 18)
South Equatorial Belt	21.2° S (1.1°, 18)	5.3° S (1.3°, 18)
North Equatorial Belt	9.0° N (1.0°, 18)	21.0° N (0.7°, 18)
North Temperate Belt	24.6° N (0.7°, 18)	31.3° N (0.6°, 18)
North Polar Cap (NPCs)	67.7° N (2.4°, 18)	–

* Standard deviations are in parentheses followed by the number of measurements.

(Humason, 1961) and 2017 (ALPO Archives). I would like to state a word of caution, though: If the north and south limbs are not distinct, the accuracy of latitude measurements is lost. Therefore, images were restricted to the years 1952, 2000, 2016 and 2017. In the latter three years, WinJupos was used allowing for accurate grid placement.

Figure 5 shows the System II longitudes of the GRS. The mean drift rate was 0.077°/day or 2.3°/30 days. This is similar to the rate of 2.2°/year (Rogers, 2017d), but is much higher than the mean drift rate for 1990 - 2015 (Schmude, 2019). The GRS has undergone significant drift rate changes in the past (Rogers, 1995) and may be starting a new trend.

Region II: South Polar Region (SPR) to the South Tropical Zone (STrZ)

The mean light intensity of the SPR was 5.9, which is the same as the NPR. Sweetman reports the SPR was dark or very dark on several dates between May 13 and July 2; however, on April 16, 22 and 30, he reports it being hazy or fuzzy. He reports it lacked a sharp northern border on June 16.

A wide zone often separated the SPR from a belt. For example, on April 8 at λ_{II} = 300° W, the zone had a latitude range of 54° S to 45° S and the belt had a latitude range of 45° S to 36° S. The latitudes shifted with longitude (compare figures 1F and 1H).

Figure 5 shows Oval BA longitudes. Its mean System II drift rate was -0.3814°/day or -11.4°/30 days. This is similar to what it was in the previous apparition and the values reported by Rogers (2017b). Rogers (2017b) also suggests Oval BA may have oscillated with a period of two months. The data in Figure 5 suggests about a 1.0° oscillation in longitude with a period close to that reported by Rogers (2017b). According to the linear equations in Figure 5, Oval BA was at the same System II longitude as the GRS (λ_{II} = 255.3°) on Nov. 2, 2016, which is nearly the same day (Nov. 1) reported by Rogers (2017b).

Figure 6 shows close-up images of Oval BA. Three of the characteristics of this oval are discussed:

First, Oval BA apparently undergoes changes in shape like the GRS and Neptune's Great Dark Spot (Schmude, 2008). Figures 6D and 6K show an elliptical shaped Oval BA with a major axis tilted to the southwest at right with respect to the Equator while Figure 6E shows the reverse.

A second characteristic of Oval BA is that it is not as bright as the GRS in methane band light (see figures 3B-3E). This is consistent with the GRS extending to higher altitudes than Oval BA.

Finally, the orange ring in Oval BA

Table 7. Statistical Comparison of Belt Latitudes in Visible and Methane Band Light

Features*	Statistically significant**
SEBs (visible light) & SEBs (CH_4 light)	Yes
SEBn (visible light) & SEBn (CH_4 light)	Yes
NEBs (visible light) & NEBs (CH_4 light)	Yes
NEBn (visible light) & NEBn (CH_4 light)	No
NTBs (visible light) & NTBs (CH_4 light)	Yes
NTBn (visible light) & NTBn (CH_4 light)	No

Table 8: Dimensions of the Orange Ring in Oval BA for the 2015-2016 and 2016-2017 Apparitions. (The standard deviation and number of measurements are in parentheses.)

Apparition	Outer dimension		Inner dimension	
	East-West	North-South	East-West	North-South
2015-2016	5.5° (0.61°, 13)	4.5° (0.36°, 14)	2.5° (0.36°, 13)	1.9° (0.44°, 14)
2016-2017	6.2° (1.0°, 11)	4.8° (0.53°, 11)	3.1° (0.56°, 11)	2.4° (0.42°, 11)

Table 9. Measured Sizes of the Tiny White Ovals Following the GRS on March 7, 2017 (All measurements were made from Figure 4Q.)

Location	East-West by North-South Dimension (degrees of longitude or latitude)
274.6° W, 15.2° S	1.8° by 1.3°
277.4° W, 21.1° S	2.2° by 1.7°
284.3° W, 16.3° S	1.3° by 1.0°
296.5° W, 15.3° S	1.4° by 0.8°
314.5° W, 15.2° S	1.3° by 1.1°
297.9° W, 16.2° S (Just forming?)	0.4° by 0.4°

persisted though the apparition (see figures 6B-6C and 6G). This feature has been imaged before (Schmude, 2017, 2018, 2020). It has a different shape in figures 6B and 6C. It was also not visible in near-infrared light (see Figure 6H). The mean inner and outer dimensions of it are defined in Figure 7 and summarized in Table 8. T-tests were carried out at the 95% confidence level for the dimensions in the table. There is no statistical difference between the outer dimensions of the ring for the two years but there is a statistical difference for the inner dimensions.

Region III: South Equatorial Belt (SEB)

The SEB was very active. Rogers (2017*e*) reports that a "mid-SEB outbreak" begun on Dec. 29. Essentially, a bright feature developed near λ_{II} = 208° W and it expanded eastward. Figure 1E shows this outbreak at an early stage and Figure 1L shows it at a later stage. On April 22 (λ_{II} = 91° W) and May 17, (λ_{II} = 151° W) Sweetman describes the SEB as "broken", which is consistent with the "mid-SEB outbreak". A second SEB change was the development of tiny white ovals. Damian Peach imaged five or six tiny white ovals following the GRS on March 7 (see Figure 4Q). The measured positions and sizes for March 7 are summarized in Table 9. The mean east-west by north-south dimensions for these ovals are 1.4° of longitude by 1.1° of latitude. The SEB had a light intensity value of 3.7, which is a bit higher than in the previous apparition. This may be the result of the "mid-SEB outbreak".

Region IV: Equatorial Zone (EZ)

The EZ was consistently bright in visible and methane band light (figures 1 - 3). Cudnik usually drew a faint band (Equatorial Band or EB) across the center of this zone (Figure 2L); however, Sweetman usually did not draw it (Figure 2G). He did, however, note a streak near the center of the EZ on June 11 (Figure 2I) and June 23. Sweetman also noted two bright ovals in the EZ on April 15. According to Cudnik and Sweetman, there was no difference in light intensity between the southern and northern portions of the EZ (see Table 4).

Region V: North Equatorial Belt (NEB)

According to Rogers (2017c), the NEB underwent an expansion event, which probably started in late 2016. Figure 1B shows the NEB being thin on the left and thick on the right. An expansion would explain the large north-south width near opposition (12.8°) compared to two years earlier (Schmude, 2018). After this expansion, white ovals were present inside this belt and visible near its northern edge. (figures 1N and 1O).

Table 10. Measured Magnitudes of Jupiter in the J and H Filters During the 2016-2017 Jupiter Apparition

Date	α (degrees)	Measured Magnitude	Date	α (degrees)	Measured Magnitude
2017			**2017**		
Jan. 12.477	10.4	H = –1.722	May 26.088	8.4	H = –2.022
Jan. 12.461	10.4	J = –2.207	May 26.101	8.4	J = –2.559
Jan. 27.459	10.0	J = –2.303 [a]	May 26.121	8.4	H = –2.072
Jan. 27.470	10.0	H = –1.788	May 26.136	8.4	J = –2.545
Feb. 1.461	9.8	J = –2.356	Jul. 5.078	10.7	H = –1.733
Feb. 1.472	9.8	H = –1.818	Jul. 5.088	10.7	J = –2.218
Mar. 20.425	3.7	J = –2.650	Jul. 5.101	10.7	H = –1.716
Mar. 20.437	3.7	H = –2.107	Jul. 5.112	10.7	J = –2.177
Apr. 8.444	0.31	H = –2.168	Jul. 13.096	10.7	J = –2.227
Apr. 9.052	0.37	H = –2.074	Jul. 13.115	10.7	H = –1.686
Apr. 9.064	0.37	J = –2.586	Jul. 13.128	10.7	J = –2.228
Apr. 26.116	3.6	H = –2.160	Jul. 13.140	10.7	H = –1.738
Apr. 26.125	3.6	J = –2.642	Aug. 2.069	9.9	J = –2.099
May 20.106	7.6	H = –2.026	Aug. 2.078	9.9	H = –1.624
May 20.116	7.6	J = –2.511	Aug. 17.064	8.8	H = –1.473

[a] Large scatter in data

Sweetman often reported the NEB as "broken" (May 24, 27 and 28). On June 4, he reports this belt having a moderately dark brown color.

Region VI: North Tropical Zone (NTrZ) to the North Polar Region (NPR)

The mean light intensity of the NTrZ was 7.4 compared to 8.0 in the previous apparition. This is a statistically significant drop based on a t-test at the 95 % confidence level. The drop may be due to the fact that the NTrZ was narrower than in the previous apparition.

The NTB was over twice as wide as in the previous apparition (Schmude, 2020). This increase took place as a result of a "NTBs jet outbreak" (Rogers, 2017a). The outbreak started around Sept. 15 with the development of a super-fast moving bright plume. Rogers reports System I drift rates of between 154 and 169°/30 days. This is equivalent to rotation periods of between 9h 46m 44s to 9h 47m 04s, which is over three minutes faster than the Equatorial Current! Both amateur and professional astronomers imaged one or more bright plumes in October (Figure 1A). This outbreak eventually led to the expansion of the NTB (Rogers (2017a).

A second belt north of the NTB was often visible (figures 1A - 1E, 1L, 1P). On January 19, it extended from 36° N to 40° N. This is consistent with it being the NNTB (Rogers, 1990; 1995).

The NPR underwent change. First, it may have darkened. Its light intensity dropped compared to the previous apparition, but the difference is not statistically significant. A second NPR change was the development of a thin and bright north polar haze cap that was visible on a few dates in methane band light (see Figure 8). Note the straight border in this figure is different from the usual bright limb seen in Figure 3. This haze cap was less bright than the corresponding cap in the South Polar Region.

Photoelectric Photometry

The writer continued his near-infrared brightness study of Jupiter during 2016-2017. Comparison star magnitudes are from Henden (2002). The procedure described in Hall and Genet (1988) was used in evaluating magnitudes. Secondary extinction coefficients were assumed to equal zero. These measurements are summarized in Table 10.

The reduced magnitudes (Shepard, 2017) are computed in the same way as is described elsewhere (Schmude, 2018). They were then plotted against the phase angle and fit to linear equations. The correlation coefficient is not statistically significant for either filter (Larson and Farber, 2006). Therefore, it is concluded any change in the reduced magnitudes for phase angles less than 11° for the apparition were small. The mean reduced magnitude for the J filter is -9.57 with respective standard deviations and standard errors of estimate of 0.042 and 0.046 magnitudes. The mean reduced magnitude for the H filter is -9.07 with respective standard deviations and standard errors of estimates of 0.041 and 0.043 magnitudes. These values are close to those measured in the three previous apparitions (Schmude, 2020).

Jupiter Meteor

T. Riessler (Germany) and S. Pedranghelu (France) imaged the development of a bright spot on May 26, 2017 in Jupiter's North Polar Region (King, 2017). The mean of the reported locations of the bright spot is 51.1° N, λ_I = 164.1° W (ALPO Japan Latest Jupiter website). There was no evidence of a visible dark area. Therefore, the estimated upper limit of any dark spot is ~1000 km. The writer estimated the flash was equal to a star of magnitude 5. If one uses the procedure and assumptions described in (Schmude, 2020), the impacting object would have had a mean diameter of 12 meters.

Acknowledgements

The writer would like to thank Gordon State College for a Faculty Development Grant in 2014, which enabled the purchase of an SSP-4 photometer.

References

ALPO Archives (A collection of photographs & other Jupiter observations). Or the GRS East-West direction, photographs by C. Capen, C. Chapman, D. C. Parker, D. Peach, T. Pope, J. Sussenbach, and images recorded at the Lick and Hale Observatories were used. For the GRS North-South dimension, photographs by D. Peach, observers cited in the 2015-2016 and 2016-2017 apparition reports, and those taken at the Hale Observatory were used.

ALPO Japan Latest Jupiter website at *http://alpo-j.asahikawa-med.ac.jp/Latest/Jupiter.htm*

Astronomical Almanac for the Year 2016, U. S. Govt. Printing Office, Washington DC, 2015. *https://bookstore.gpo.gov/products/sku/008-054-00242-1*

Astronomical Almanac for the Year 2017, U. S. Govt. Printing Office, Washington DC, 2016. *https://bookstore.gpo.gov/products/sku/008-054-00254-4*

Hahn, G. A. (2019) see *http://jupos.privat.t-online.de/index.htm*

Hall, D. S., Genet, R. M. "Photoelectric Photometry of Variable Stars, Second, Revised and Expanded Edition, Willmann-Bell, Inc. Richmond, VA, 1988. *www.alibris.com/Photoelectric-Photometry-of-Variable-stars-A-Practical-Guide-for-the-Smaller-Observatory-Douglas-S-Hall/book/5109450*.

Henden, A. A. "JHK Standards for Small Telescopes". *Journal of the American Assn. of Variable Star Observers*, 31, pp. 11-20, 2002. *http://adsabs.harvard.edu/full/2002JAVSO..31...11H*

Humason, M. L. Photographs of Planets with the 200-inch Telescope, in: "Planets and Satellites". (G. P. Kuiper and B. M. Middlehurst - editors) pp. 572-574, plates 9 & 14, 1961. *https://www.amazon.com/Planets-Satellites-System-Gerard-Kuiper/dp/0226459276/ref=sr_1_6?dchild=1&keywords=%22Planets+and+Satellites%22&qid=1610126135&s=books&sr=1-6*

JPL Horizons at: *https://ssd.jpl.nasa.gov/horizons.cgi* .

King, B. (2017) "New Impact Flash Seen on Jupiter". *https://skyandtelescope.org/astronomy-news/new-impact-flash-seen-at-jupiter/*

Larson, R., Farber, B. "Elementary Statistics Picturing the World", 3rd edition, Pearson, Upper Saddle River, NJ, 2006.

Peek, B. M. "The Planet Jupiter", 2nd edition, Faber and Faber, London, 1981. *https://www.amazon.com/Planet-Jupiter-B-M-Peek/dp/B0000CJX4K*

Rogers, J. H. "The pattern of jetstreams on Jupiter: correlation with Earth-based observations and consequences for belt nomenclature". *Journal of the British Astronomical Assn,* 100, No. 2, pp. 88-90, 1990. *http://absabs.harvard.edu/full/1990JBAA..100...88R*.

Rogers, J. H. "The Giant Planet Jupiter" Cambridge University Press, Cambridge, 1995. *http://www.amazon.com/Planet-Jupiter-Practical-Astronomy-Handbooks/dp/0521410088*

Rogers, J. H. "The accelerating circulation of Jupiter's Great Red Spot". *Journal of the British Astronomical Assn,* 118, No. 1, pp. 14-20, 2008. *http://www.britastro.org/jupiter/JBAA-118-1_GRS-paper.pdf*

Rogers, J. and Adamoli, G. "Jupiter in 2015/16: Final Report" (2016) at *https://britastro.org/sites/default/files/FINAL_2015-16_Main-text.pdf*

Rogers, J. H. "Jupiter in 2016/17, Report No. 1: Start of the 2016 NTBs Outbreak" (2017a). *https://britastro.org/node/8102*

Rogers, J. H. "Jupiter in 2016/17, Report No. 4: The Apparition up to 2017 January" (2017b). *https://britastro.org/node/8892*

Rogers, J. H. "2016-17, Report No. 11: Update on the NEB Expansion Event" (2017c). *https://britastro.org/node/10609*

Rogers, J. H. "Jupiter in 2016/17, Report No. 14" (2017d). *https://britastro.org/node/10891*

Rogers, J. H. "Jupiter in 2016-17, Report No. 17: Summary of the mid-SEB Outbreak" (2017e). *https://britastro.org/node/16772*

Schmude, R. W. Jr. "ALPO Observations of Jupiter During the 2012-2013 Apparition". *Journal of the Assn of Lunar & Planetary Observers,* Vol. 58, No. 3, pp. 60-74, 2016a. *http://alpo-astronomy.org/gallery3/var/albums/Publications-Section/ALPO-Journals/DJALPO-2016/DJALPO58-3-Summer2016.pdf?m=1529263025*

Schmude, R. W. Jr. "ALPO Observations of Jupiter During the 2013-2014 Apparition" *Journal of the Assn of Lunar & Planetary Observers,* Vol. 59, No. 2, pp. 41-60, 2017. *http://alpo-astronomy.org/gallery3/var/albums/Publications-Section/ALPO-Journals/DJALPO-2017/DJALPO59-2-Spring2017.pdf?m=1529266043*

Schmude, R. W. Jr. "ALPO Observations of Jupiter During the 2014-2015 Apparition" *Journal of the Assn of Lunar & Planetary Observers,* Vol. 60, No. 3, pp. 53-74, 2018. *http://alpo-astronomy.org/gallery3/var/albums/Publications-Section/ALPO-Journals/DJALPO-2018/JALPO60-3-Summer-2018.pdf?m=1545337354*

Schmude, R. W. Jr. "The 2015-2016 Apparition of Jupiter" *Journal of the Association of Lunar & Planetary Observers*, Vol. 62, No. 2, pp. 55-67, (2020).

Schmude, R. W. Jr. "Observing Jupiter in the 21st Century", Second Edition. The Astronomical League: Humble Independent School District and the Insperity Observatory (2019). *https://store.astroleague.org/index.php?main_page=product_info&products_id=160*

Shepard, M. K. "Introduction to Planetary Photometry." (Cambridge: Cambridge University Press) 2017. *https://www.amazon.com/Introduction-Planetary-Photometry-Michael-Shepard/dp/110713174X*

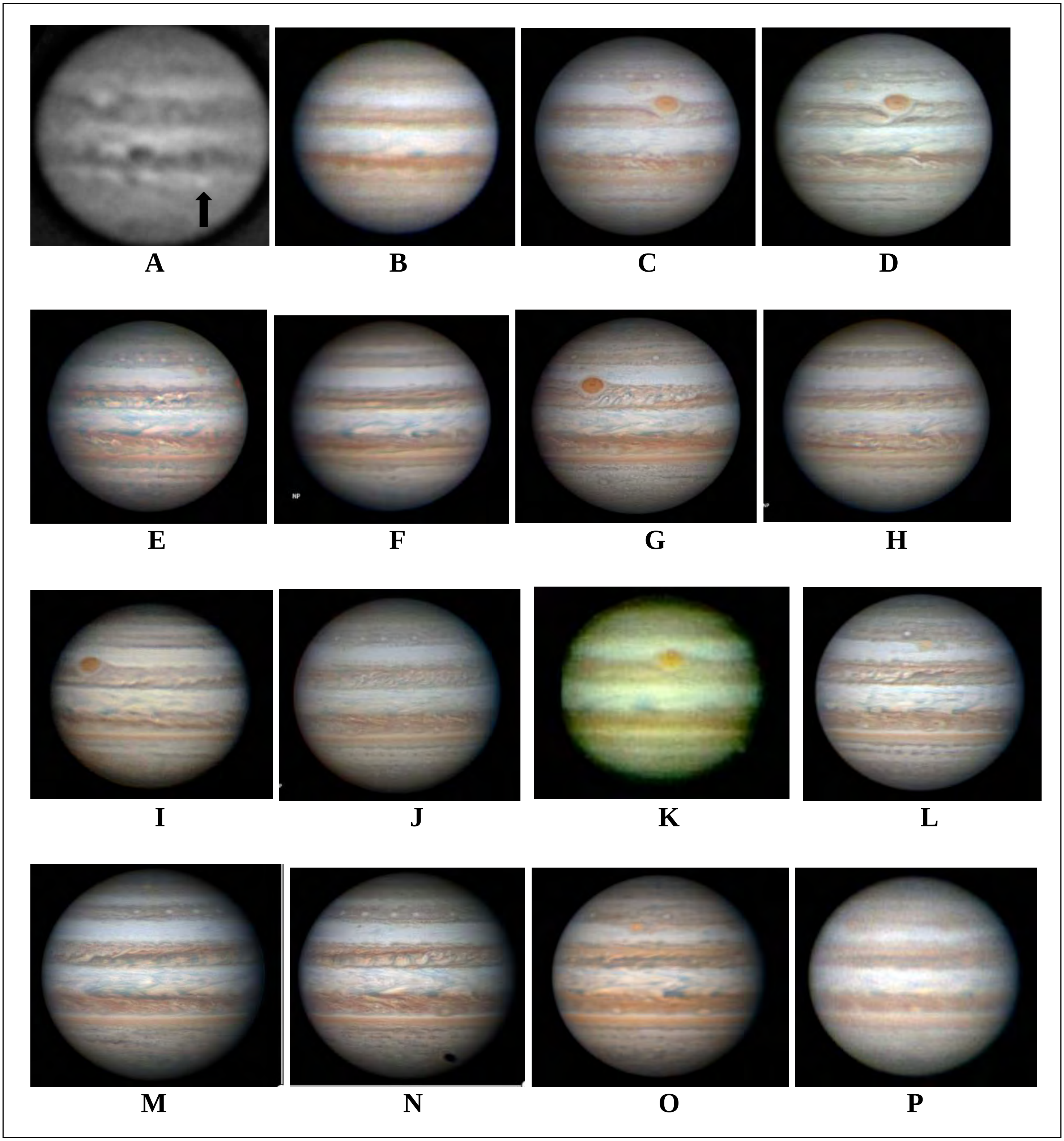

Figure 1. Visible light images of Jupiter made during the 2016-2017 apparition. South is at the top in all images. **A**: Oct. 23 (20:23.7 UT) by A. Wesley; **B**: Nov. 30 (13:37 UT) by P. Maxson; **C**: Dec. 13 (6:35.0 UT) by T. Hansen; **D**: Dec. 30 (6:00 UT) by I. Sharp; **E**: Jan. 19 (10:38.5 UT) by B. Combs; **F**: Feb. 11 (10:33.5 UT) by M. Hood; **G**: Feb. 28 (6:30.1 UT) by D. Peach; **H**: March 20 (6:25.1 UT) by M. Hood; **I**: April 8 (23:56.3 UT) by G. Lewis; **J**: April 21 (4:52.1 UT) by M. Hood; **K**: May 1 (6:49 UT) by R. Hill; **L**: May 16 (11:42.7 UT) by A. Wesley; **M**: June 3 (12:01 UT) by C. Go; **N**: June 18 (10:37 UT) by C. Go; **O**: July 8 (0:37.5 UT) by D. Peach & Chiliscope Team; **P**: Aug. 15 (2:33 UT) by P. Maxson.

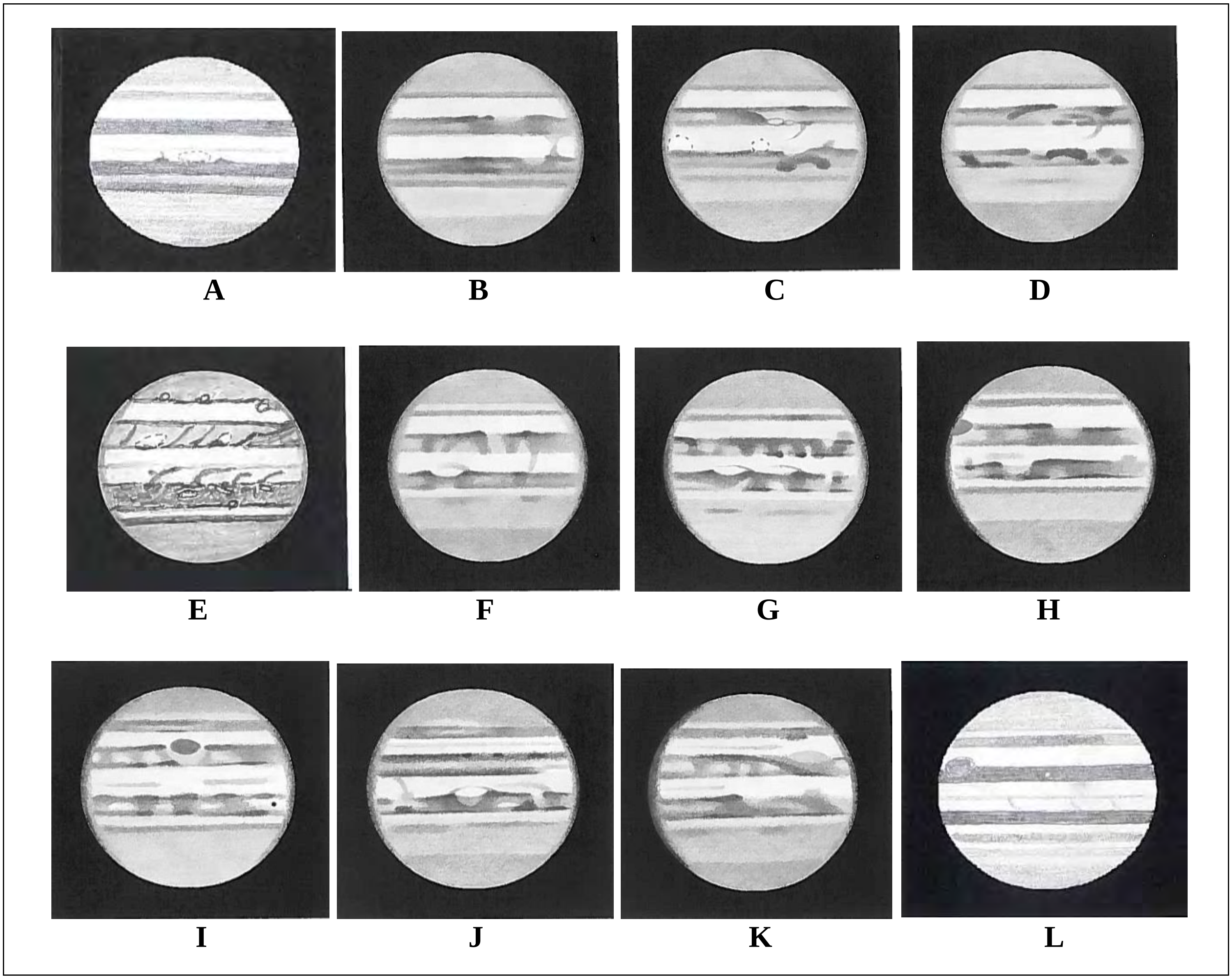

Figure 2. Drawings of Jupiter. South is at the top in all images. **A**: Nov. 24 (12:30 UT) by B. Cudnik, λ_I = 77° W, λ_{II} = 121° W; **B**: April 10 (9:52 UT) by M. Sweetman, λ_I = 19° W, λ_{II} = 98° W; **C**: April 15 (9:48 UT) by M. Sweetman, λ_I = 89° W, λ_{II} = 130° W; **D**: April 22 (9:32 UT) by M. Sweetman, λ_I = 103° W, λ_{II} = 91° W; **E**: May 4 (0:35 UT) by P. Budine, λ_I = 231° W, λ_{II} = 130° W; **F**: May 14 (7:48 UT) by M. Sweetman, λ_I = 270° W, λ_{II} = 91° W; **G**: May 21 (7:29 UT) by M. Sweetman, λ_I = 288° W, λ_{II} = 56° W; **H**: May 27 (7:08 UT) by M. Sweetman, λ_I = 143° W, λ_{II} = 225° W; **I**: June 11 (5:41 UT) by M. Sweetman, λ_I = 298° W, λ_{II} = 265° W; **J**: June 17 (5:31 UT) by M. Sweetman, λ_I = 158° W, λ_{II} = 80° W; **K**: July 1 (6:00 UT) by M. Sweetman, λ_I = 225° W, λ_{II} = 215° W; **L**: August 13 (1:45 UT) by B. Cudnik, λ_I = 11° W, λ_{II} = 231° W.

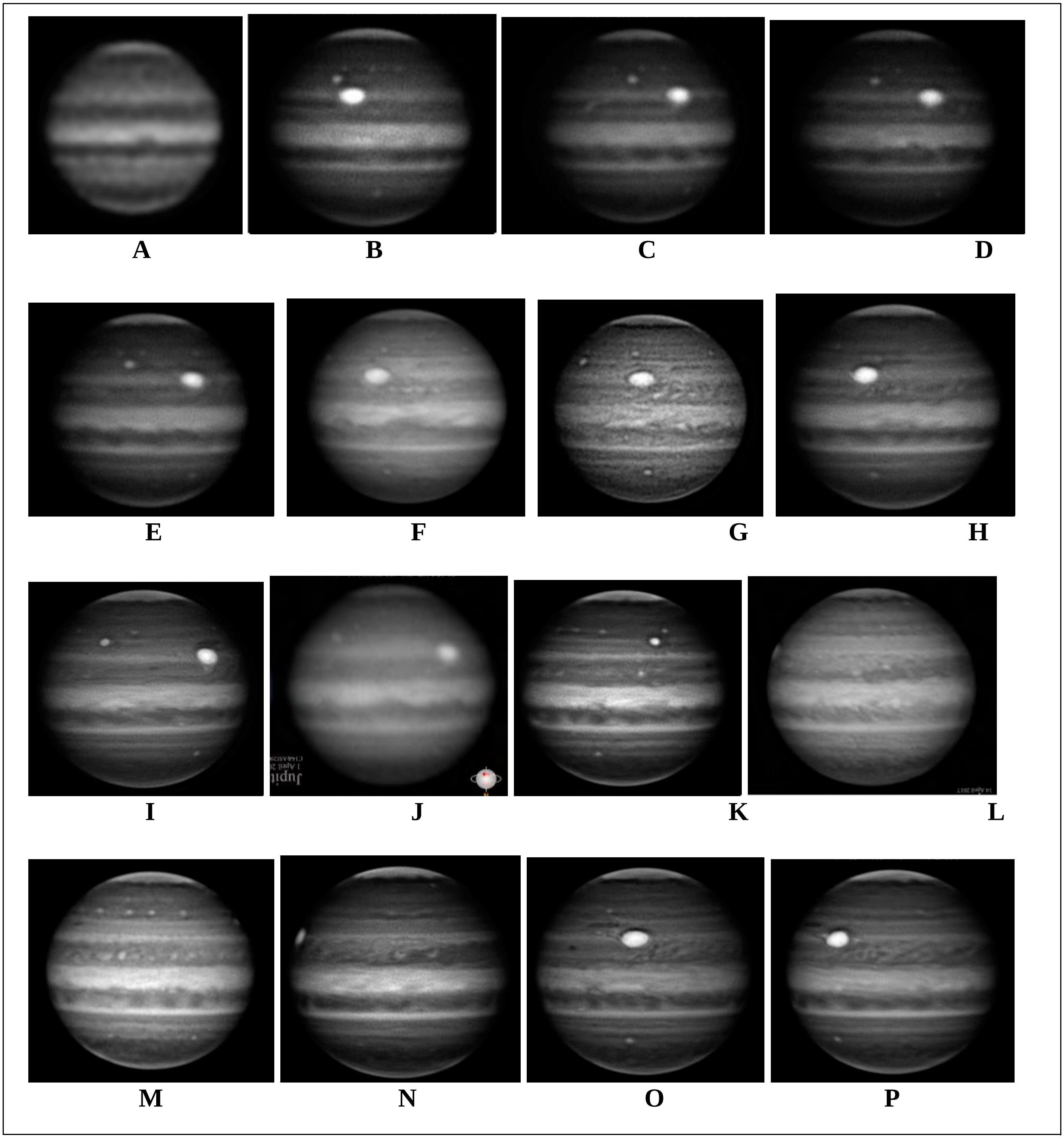

Figure 3. Methane band images of Jupiter. South is at the top in all images. **A**: Oct. 29 (19:01.6 UT) by A. Wesley; **B**: Nov. 30 (21:28 UT) by C. Go; **C**: Dec. 31 (21:14 UT) C. Go; **D**: Jan. 12 (21:16 UT) by C. Go; **E**: Jan. 24 (21:02 UT) by C. Go; **F**: Feb. 2 (4:51 UT) by C. Sprianu; **G**: Feb. 10 (10:42 UT) by P. Maxson; **H**: March 2 (17:48 UT) by C. Go; **I**: March (16:56 UT) by C. Go; **J**: April 1 (21:07.3 UT) by M. Kardasis; **K**: April 7 (14:29 UT) by C. Go; **L**: April 14 (19:55.2 UT) by M. Kardasis; **M**: April 24 (12:00.2 UT) by A. Wesley; **N**: April 30 (13:02 UT) by C. Go; **O**: May 2 (12:50 UT) by C. Go; **P**: May 14 (13:32 UT) by C. Go.

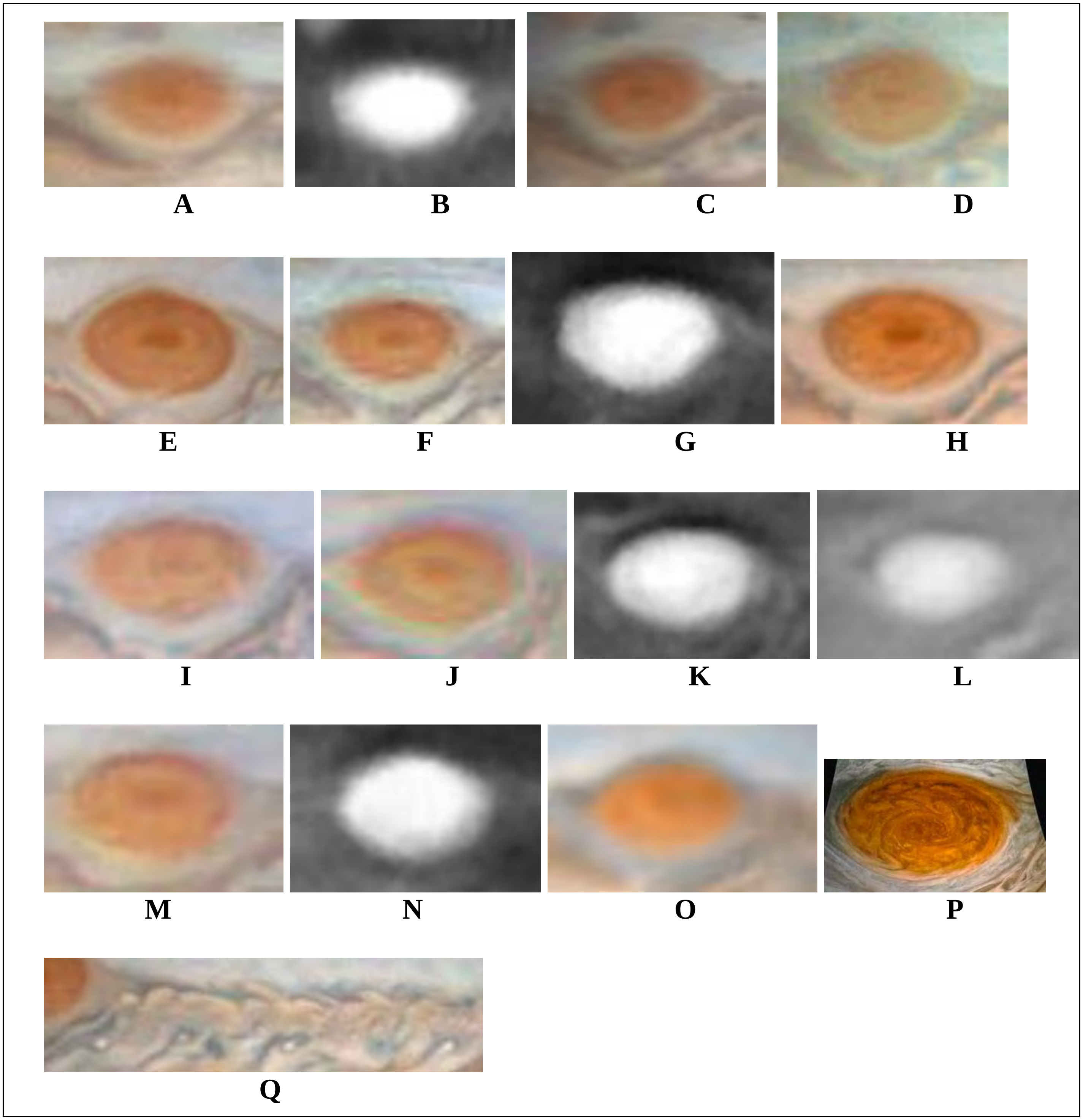

Figure 4. Images of the Great Red Spot. South is at the top in all images. All images were color images except where noted. **A**: Nov. 30 (21:14 UT) by C. Go; **B**: Nov. 30 (21:28 UT) by C. Go, made in methane band light; **C**: Dec. 5 (21:06 UT) by C. Go; **D**: Dec. 11 (6:03 UT) by I Sharp; **E**: Feb. 25 (7:48.2 UT) by D. Peach; **F**: March 24 (15:44 UT) by C. Go; **G**: March 24 (15:54 UT) by C. Go in methane band light; **H**: April 5 (5:46.9 UT) by D. Peach; **I**: April 13 (21:56.7 UT) by C. Zannelli; **J**: April 22 (4:15.2 UT) by M. Hood; **K**: April 22 (14:23 UT) by C. Go in methane band light; **L**: April 28 (19:49 UT) by M. Kardasis in methane band light; **M**: May 16 (4:11.3 UT) by M. Hood; **N**: June 24 (11:00 UT) by C. Go in methane band light; **O**: July 8 (23:09.4 UT) by D. Peach and the Chiliscope Team; **P**: July 11 (3:10 UT) by the Juno spacecraft Image Credit: Enhanced by Jason Major based on images courtesy of NASA/JPL-Caltech/SwRI/MSSS; **Q**: March 7 (7:30 UT) by D. Peach and the Chiliscope Team.

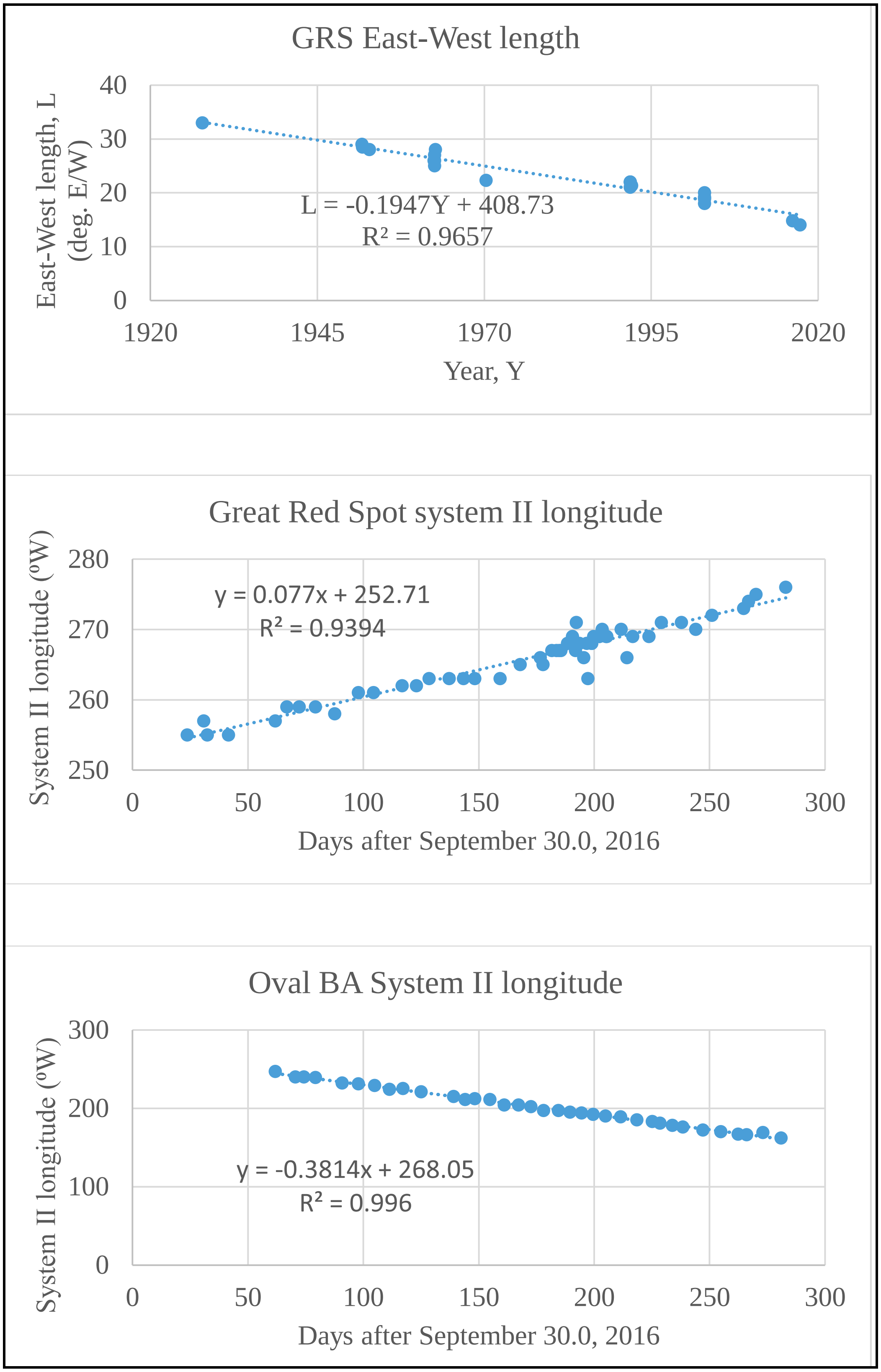

Figure 5. Top: Graph of the longitude of the Great Red Spot versus the number of days after Nov. 30.0, 2017. Middle: Graph of the longitude of the Oval BA versus the number of days after Nov. 30.0, 2017. Bottom: Graph of the latitude of Oval BA versus the number of days after Nov. 30.0, 2017.

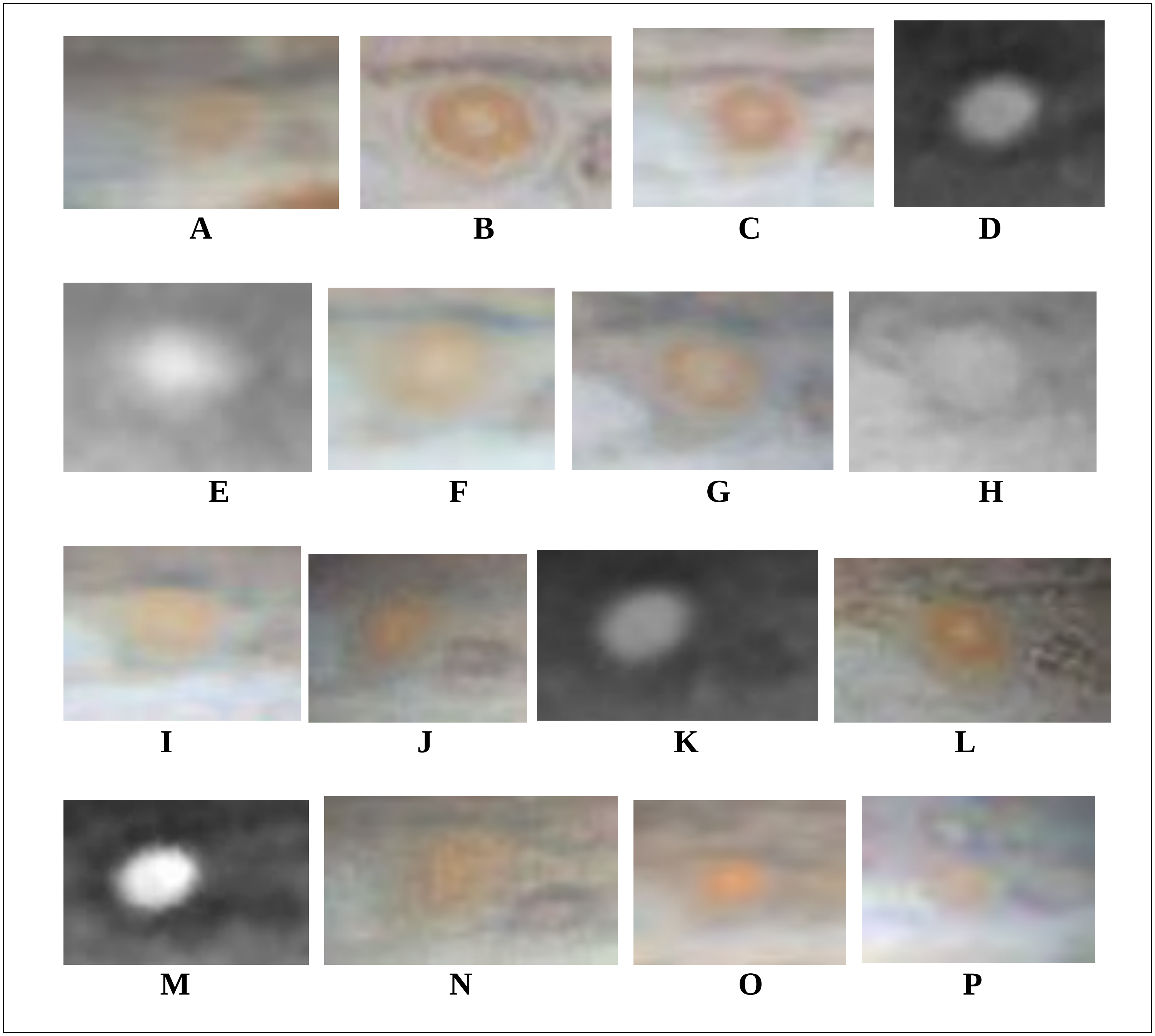

Figure 6. Images of Oval BA. South is at the top in all images. Unless otherwise noted, images were in color and made in visible light. **A**: Nov. 30 (21:14 UT) by C. Go; **B**: Feb. 25 (6:38.5 UT) by D. Peach; **C**: March 16 (7:02.5 UT) by D. Peach; **D**: March 21 (16:56 UT) by C. Go in methane band light; **E**: Feb. 24 (10:40 UT) by P. Maxson in methane band light; **F**: April 7 (15:30.3 UT) by A. Wesley; **G**: April 29 (12:15.9 UT) by A. Wesley; **H**: May 6 (12:53.6 UT) by A. Wesley made in near infrared light; **I**: May 16 (11:42.7 UT) by A. Wesley; **J**: May 26 (11:11 UT) by C. Go; **K**: June 9 (22:10 UT) by M. Delcroix, E. Kraaikamp, D. Peach, G. Therin, C. Sprianu, R. Hueso & F. Colas; **L**: June 11 (21:57.4 UT) by D. Peach, E. Kraaikamp, F. Colas, M. Delcroix, R. Hueso, C. Sprianu and G. Therin; **M**: June 14 (11:03 UT) by C. Go in methane band light; **N**: June 19 (10:37 UT) by C. Go; **O**: July 8 (0:37.5 UT) by D. Peach & the Chiliscope Team; **P**: Aug. 5 (2:34 UT) by P. Maxson.

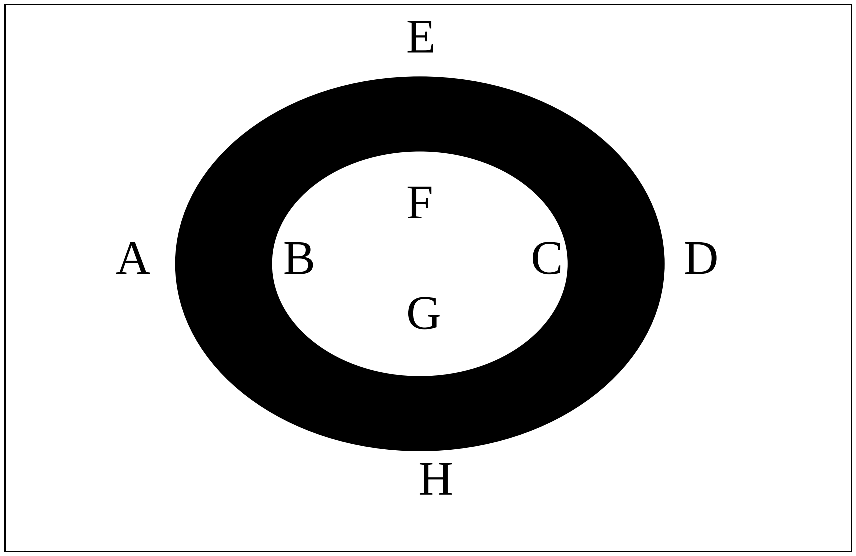

Figure 7. A representation of the ring in Oval BA. The outer east-west dimension is A-D and the inner north-south dimension is F-G and so forth. The East-west direction is horizontal and the north-south dimension is vertical.

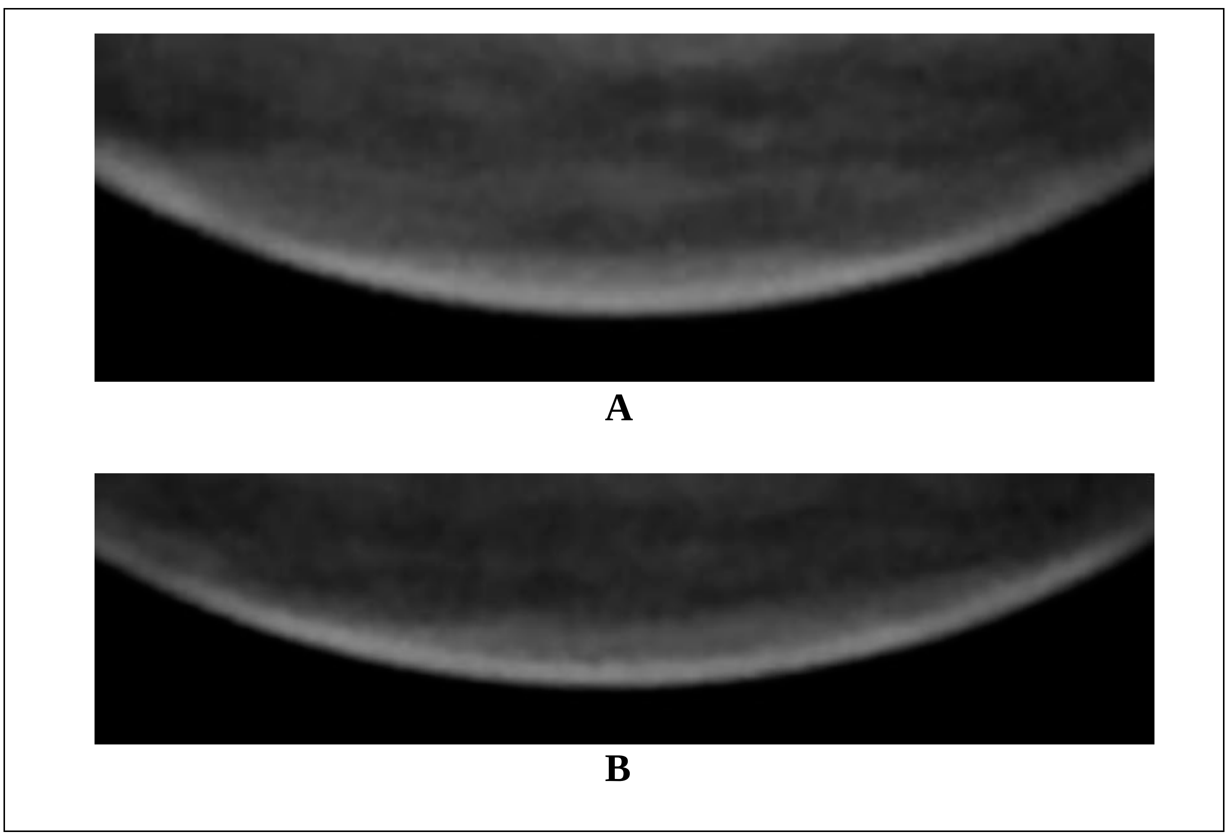

Figure 8. North is at the bottom in both images. A: April 16 (14:04 UT) by C. Go in methane band light. Note the faint linear bright area near the bottom; B: April 17 (13:35 UT) by C. Go in methane band light. Note the faint linear bright area near the bottom, which is not parallel to the equator.

Papers & Presentations:

ALPO Observations of Saturn During the 2016 - 2017 Apparition

By Julius L. Benton, Jr.,
Coordinator, ALPO Saturn Section
jlbaina@msn.com

This paper includes a gallery of Saturn images submitted by a number of observers.

Please note that when a visual observer records or suspects a specific feature on Saturn, it is important to secure future observations quickly if we wish to obtain the period of rotation. For this purpose we encourage observers to use these facts: In System I (EZ plus NEB or SEB), 7 rotations are accomplished in close to 3 Earth-days, while in System II (rest of planet), 9 rotations require close to 4 such days.

A complete set of Saturn Observing Forms are available for downloading at http://www.alpo-astronomy.org/publications/ALPO Section Publications/SaturnReportForms - All.pdf

See the *ALPO Observing Section Publications* in the ALPO Resources section of this Journal for hardcopy availability.

Abstract

The ALPO Saturn Section received 234 visual observations and digital images for the 2016-17 apparition spanning the period from January 22, 2017 through November 21, 2017. Observations were submitted by 24 observers in Australia, Brazil, Colombia, Greece, Italy, New Zealand, Philippines, South Africa, Spain, United Kingdom and the United States. Instruments utilized for the observations ranged in aperture from 9.0 cm (3.5 in.) up to 106.0 cm (41.7 in.). Imaging during 2016-17 revealed a considerable amount of discrete activity within Saturn's northern hemisphere. Such features included recurring white spots within the Equatorial Zone, northern half (EZn), the Equatorial Zone, southern half (EZs), North Tropical Zone (NTrZ), the North Temperate Zone (NTeZ), and occasional white spots in the North Equatorial Belt Zone (NEBZ), North Equatorial Belt, northern component (NEBn), and the North North Temperate Zone (NNTeZ). Small sporadic dark spots were occasionally detected in the Equatorial Band (EB) during 2016-17 with a possible dark spot in the North Polar Region (NPR).

All Readers

Your comments, questions, etc., about this report are appreciated. Please send them to: ken.poshedly@alpo-astronomy.org for publication in the next Journal.

Online Features

Left-click your mouse on:

• The author's e-mail address in blue text to contact the author of this article.
• The references in blue text to jump to source material or information about that source material (Internet connection must be ON).

Observing Scales

Standard ALPO Scale of Intensity:
0.0 = Completely black
10.0 = Very brightest features
Intermediate values are assigned along the scale to account for observed intensity of features
Ring B has been adopted (for most apparitions) as the standard on the numerical sequence. The outer third is the brightest part of Ring B, and it has been assigned a constant intensity of 8.0 in integrated light (no filter). All other features on the globe and in the rings are estimated using this standard of reference.

ALPO Scale of Seeing Conditions:
0 = Worst
10 = Perfect

Scale of Transparency Conditions:
Magnitude of the faintest star visible near Saturn when allowing for daylight and twilight

IAU directions are used in all instances (so that Saturn rotates from west to east).

Table 1. Geocentric Phenomena in Universal Time (UT) for Saturn During the 2016-17 Apparition

Conjunction	2016	Dec	10^d
Opposition	2017	June	15^d
Conjunction		Dec	21^d
Opposition Data			
Visual Magnitude		0.0	
Constellation		Ophiuchus	
Declination		22.0°	
B		+26.5°	
B'		+26.7°	
Globe	Equatorial Diameter	18.3"	
	Polar Diameter	16.3"	
Rings	Major Axis	41.5″	
	Minor Axis	18.5″	

Table 2. 2016-17 Apparition of Saturn: Contributing Observers

	Observer	Location	No. of Observations	Telescopes Used
1.	Abel, Paul G.	Leichester, UK	1	50.8 cm (20.0 in.) DAL
2.	Barry, Trevor	Broken Hill, Australia	36	40.8 cm (16.0 in.) NEW
3.	Benton, Julius L.	Wilmington Island, GA, USA	2 2 8 4 2	11.5 cm (4.0 in.) REF 14.0 cm (5.5 in.) REF 15.0 cm (5.9 in.) REF 18.0 cm (7.1 in.) MAK 18.0 cm (7.1 in.) MAK
4.	Carvalho, Pablo	Ribeirão Preto, Brazil	1	40.8 cm (16.0 in.) NEW
5.	Collins, Maurice	Palmerston, New Zealand	4 2	11.0 cm (4.3 in.) REF 20.3 cm (8.0 in.) SCT
6.	da Silva, Vlamir	San Paolo, Brazil	6	20.3 cm (8.0 in.) SCT
7.	Edwards, Peter	West Sussex, UK	1	35.6 cm (14.0 in.) SCT
8.	Foster, Clyde	Centurion, South Africa	44	35.6 cm (14.0 in.) SCT
9.	Go, Christopher	Cebu City, Philippines	11	35.6 cm (14.0 in.) SCT
10.	Hill, Rik	Tucson, AZ, USA	2 2	9.0 cm (3.5 in.) MAK 20.3 cm (8.0 in.) MAK
11.	Hood, Mike	Kathleen, GA, USA	6	35.6 cm (14.0 in.) SCT
12.	Kardasis, Manos	Athens, Greece	3	35.6cm (14.0 in.) SCT
13.	Malagón, Carlos	Alhurin de la Torre, Spain	1	30.5 cm (12.0 in.) RC
14.	Maxson, Paul	Phoenix, AZ, USA	55	25.0 cm (8.8 in.) DAL
15.	Melillo, Frank J.	Holtsville, NY, USA	4	25.4 cm (10.0 in.) SCT
16.	Melka, Jim	St. Louis, MO, USA	6	45.0 cm (17.7 in.) NEW
17.	Peach, Damian	Norfolk, UK	8 5	35.6 cm (14.0 in.) SCT 106.0 cm (41.7 in.) CAS
18.	Rosolina, Michael	Friars Hill, WV, USA	1	35.6 cm (14.0 in.) SCT
19.	Sweetman Michael E.	Tucson, AZ, USA	12	10.2 cm (4.0 in.) REF
20.	Tatum, Randy	Henrico, VA, USA	1	20.3 cm (8.0 in.) SCT
21.	Triana, Charles	Bogota, Colombia	2	25.4 cm (10.0 in.) SCT
22.	Walker, Gary	Macon, GA, USA	2	25.4 cm (10.0 in.) REF
23.	Wesley, Anthony	Murrumbateman, Australia	1	36.8 cm (14.5 in.) NEW
24.	Zannelli, Carmelo	Palermo, Italy	1	35.6 cm (14.0 in.) SCT
	TOTAL OBSERVATIONS		**234**	
	TOTAL OBSERVERS		**24**	

Instrumentation Abbreviations:
NEW = Newtonian, SCT = Schmidt-Cassegrain, MAK= Maksutov-Cassegrain, REF = Refractor,
DAL = Dall-Kirkham, CAS = Cassegrain

Continuing interest has resulted in routine amateur images of the extraordinary hexagonal feature at Saturn's North Pole at different wavelengths. Views of the major ring components, including Cassini's and Encke's divisions, were very favorable this apparition due to the increased inclination of Saturn's rings towards Earth since the immediately preceding 2015-16 apparition.

The tilt of Saturn's ring system towards Earth, B, attained a maximum value of +26.9º on October 26, 2017, thereby affording observers advantageous views during the apparition of the northern hemisphere of the globe and northern face of the rings. The ALPO Saturn Section's dedicated team of visual observers and those who routinely imaged the planet at various wavelengths continued active participation in our Pro-Am efforts in support of the Cassini mission.

A summary of visual observations and digital images of Saturn contributed during the 2016-17 apparition is provided, including results of determined efforts to try to image the curious bi-colored aspect and azimuthal brightness asymmetries of the rings.

Accompanying this report are references, drawings, photographs, digital images, graphs and tables.

Introduction

This report is derived from an analysis of 34 visual observations, descriptive notes, visual numerical relative intensity estimates, and digital images contributed to the ALPO Saturn Section by 24 observers from January 22, 2017 through November 21, 2017, referred to hereinafter as the 2016-17 "observing season" or apparition of Saturn. Examples of submitted drawings and images are included with this report,

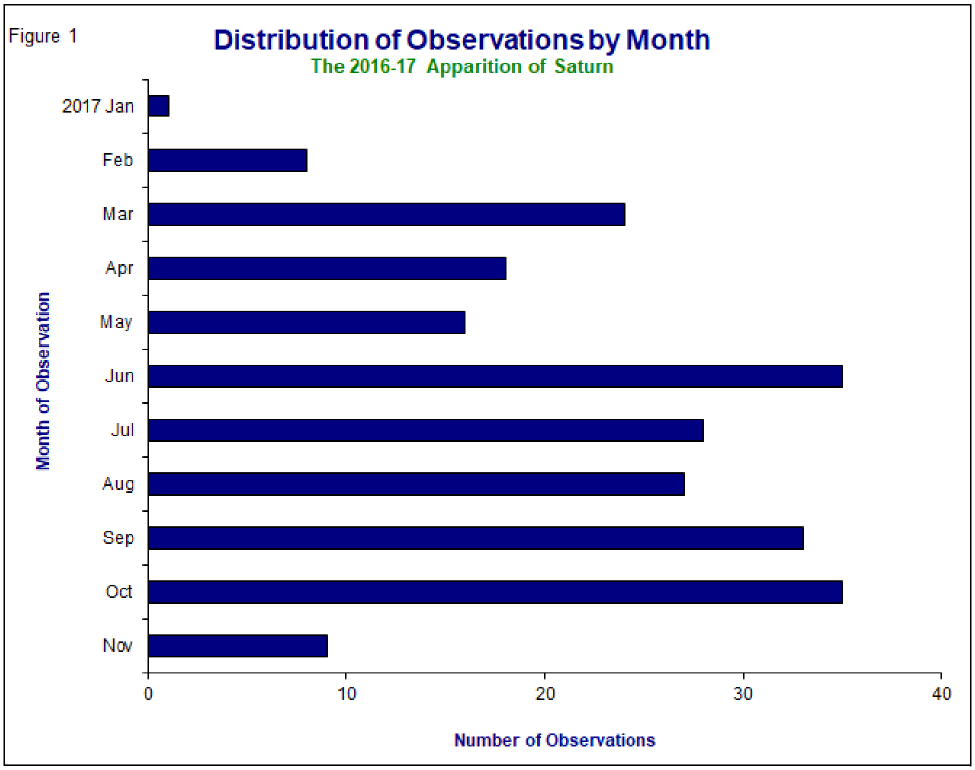

Figure 1. Number of observations by month during the 2016-17 Apparition of Saturn, opposition occurring on June 15, 2017 submitted to the ALPO Saturn Section.

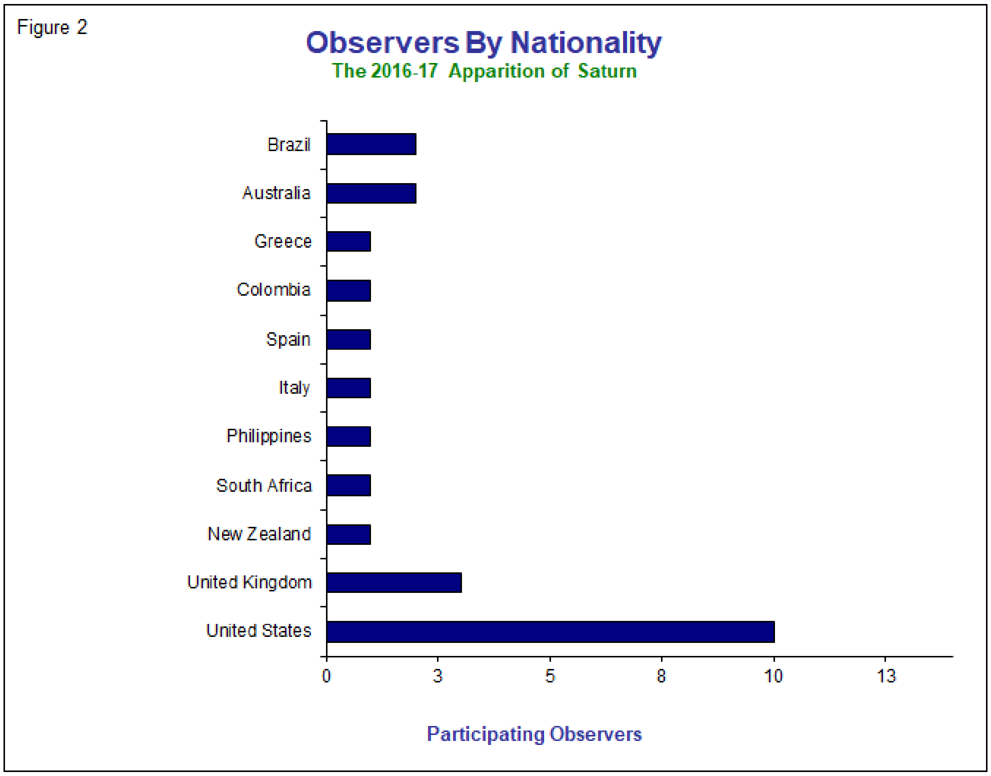

Figure 2. Number of observers by nationality during the 2016-17 Apparition of Saturn, submitted to the ALPO Saturn Section.

integrated as much as feasible with topics discussed in the text. All times and dates all given in Universal Time (UT).

Table 1 provides geocentric data in Universal Time (UT) for the 2016-17 apparition. The numerical value of **B**, or the Saturnicentric latitude of the Earth referred to the ring plane (+, when north), varied within the extremes of +26.4° (April 17, 2017) and +26.9° (October 26, 2017). The value of **B'**, the saturnicentric latitude of the Sun, varied within the range of +26.6° (November 21, 2017) to +26.8° (May 27, 2017).

Table 2 lists the 24 individuals who sent 234 reports to the ALPO Saturn Section during this apparition, including their observing sites, number of observations, telescope apertures, and type of instrument. *Figure 1* is a histogram of the distribution of observations by month whereby 36.8% were made prior to opposition, 0.9% at opposition (June 15, 2017), and 62.4% thereafter. Although many observers tend to view Saturn most frequently at or near opposition, when the planet is well placed high in the evening sky, coverage favored a wider period of time on either side of opposition during this apparition (92.3% of all observations took place from early March 2017 through late October 2017). To achieve the best overall coverage, observers are urged to begin viewing and imaging Saturn as soon as the planet becomes visible in the eastern sky before sunrise after conjunction with the Sun. Our main objective is to keep up a well-balanced observational surveillance of the planet for as much of its mean synodic period of 378d as possible (this period refers to the elapsed time from one conjunction of Saturn with the Sun to the next, which is slightly longer than a terrestrial year).

Figure 2 and *Figure 3* show the ALPO Saturn Section observer base and the international distribution of all observations submitted during the 2016-17 apparition. The United States accounted for 41.7% of the participating observers and 45.7% of the submitted

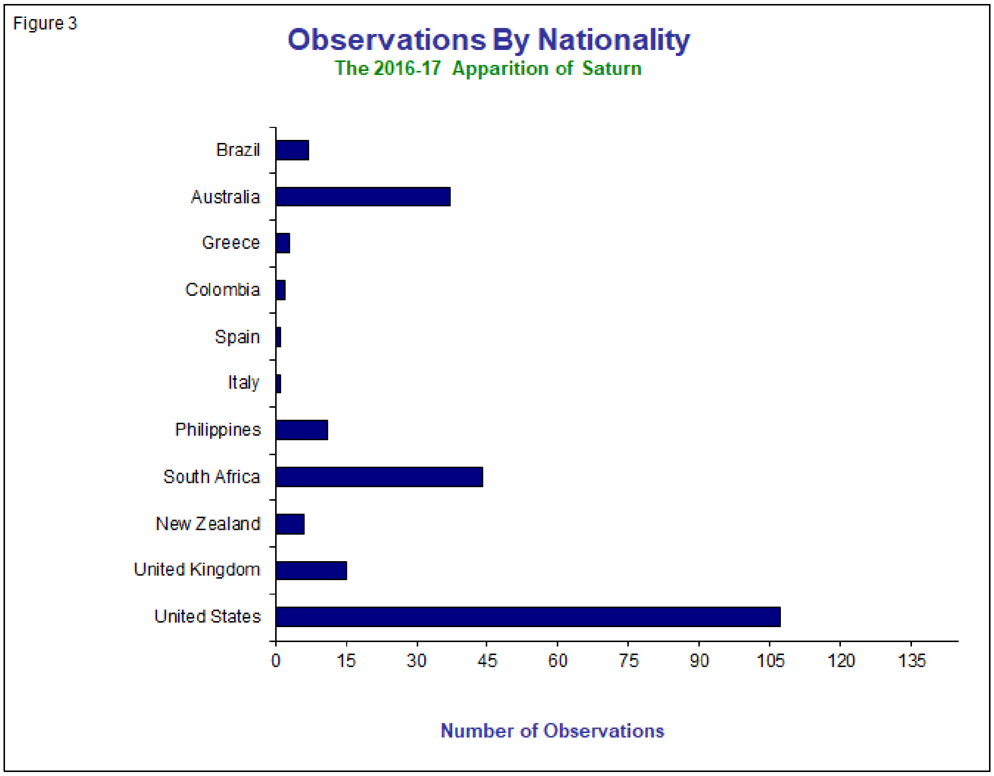

Figure 3. Number of observations by nationality during the 2016-17 Apparition of Saturn, submitted to the ALPO Saturn Section.

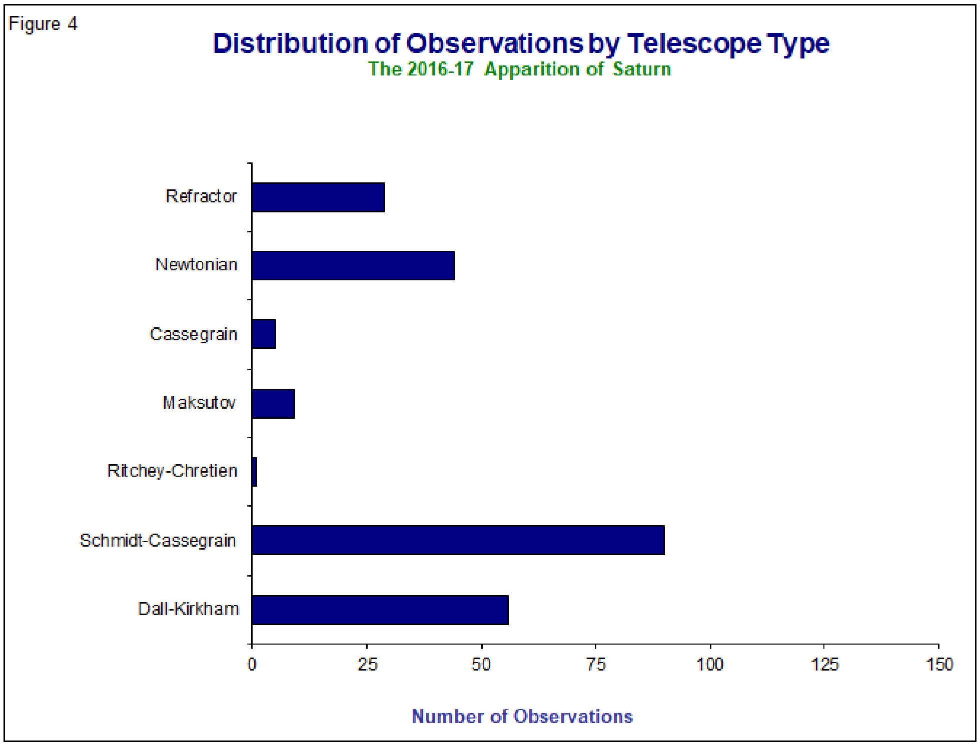

Figure 4. Number of observations grouped by optical type of telescope during the 2016-17 Apparition of Saturn, submitted to the ALPO Saturn Section.

Table 3. Visual Numerical Relative Intensity Estimates and Colors for the 2016-17 Apparition of Saturn

Globe/Ring Feature	# Estimates	2016-17 Mean Intensity & Standard Error	Intensity Difference Since 2015-16	Average Estimated Color
Zones				
EZn	25	7.72 ± 0.04	+0.30	Bright Yellowish-White
NPR	25	3.89 ± 0.06	-0.04	Very Dull Gray
Globe N of Rings	25	5.22 ± 0.13	+0.10	Light Yellowish-Gray
NTeZ	5	6.04 ± 0.04	-0.30	Yellowish-White
NTrZ	5	5.60 ± 0.09	+0.60	Dull Yellowish-Gray
Belts				
EB	2	4.50 ± 0.41	-0.50	Very Light Brown
NEBw (whole)	22	3.55 ± 0.05	0.00	Dull Yellowish-Brown
NEBn	1	3.50 ± 0.00	0.00	Dull Yellowish-Brown
NEBs	1	3.20 ± 0.00	-0.20	Dull Yellowish-Brown
Rings				
A (whole)	32	5.12 ± 0.10	0.00	Dull Grayish-White
A (Outer Half)	2	5.55 ± 0.04	+0.20	Dull Grayish-White
A (Inner Half)	2	5.70 ± 0.00	+0.10	Dull Grayish-White
Encke's (A5)	2	0.65 ± 0.11	0.00	Grayish-Black
Cassini's (A0 or B10)	16	0.00 ± 0.00	0.00	Black
B (outer 1/3)	26	**8.00 ± 0.00 STD**	0.00	Brilliant White
B (inner 2/3)	16	7.00 ± 0.00	0.00	Yellowish-White
Ring C (ansae)	30	1.25 ± 0.10	-0.30	Very Dark Gray
Crape Band	22	2.20 ± 0.11	+0.20	Very Dull Gray
Sh G on R	20	0.00 ± 0.00	0.00	Black shadow

Notes:
For nomenclature, see text and Figure 5. A letter with a digit (e.g., A0 or B10) refers to a location in the ring specified in terms of units of tenths of the distance from the inner edge to the outer edge. Visual numerical relative intensity estimates (visual surface photometry) are based upon the ALPO Intensity Scale, where 0.0 denotes complete black (shadow) and 10.0 refers to the most brilliant condition (very brightest Solar System objects). The adopted scale for Saturn uses a reference standard of 8.0 for the outer third of Ring B, which appears to remain stable in intensity for most ring inclinations. All other features on the Globe or in the rings are compared systematically using this scale, described in the Saturn Handbook, which is issued by the ALPO Saturn Section. The "Intensity Difference Since 2014-15" is in the same sense of the 2015-16 value subtracted from the 2016-17 value, "+" denoting an increase (brightening) and "-" indicating a decrease (darkening). When the apparent change is less than about 3 times the standard error, it is probably not statistically significant.

observations. International cooperation remained excellent this observing season, with 58.3% of all observers residing in Australia, Brazil, Colombia, Greece, Italy, New Zealand, Philippines, South Africa and United Kingdom, whose total contributions represented 54.3% of the observations.

Figure 4 graphs the number of observations by instrument type in 2016-17. About one-third (33.3%) of all observations were made with telescopes of classical design (refractors and Newtonians), while the remaining 66.7% were completed with catadioptrics (Schmidt-Cassegrains, Maksutov-Cassegrains, Ritchey-Chretiens, and Dall-Kirkhams). Telescopes with apertures ranging from 9.0 cm (3.5 in.) through 106.0 cm (41.7 in.) were utilized for recording observations this apparition. Readers are reminded, however, that there are numerous past instances where smaller instruments of good quality have

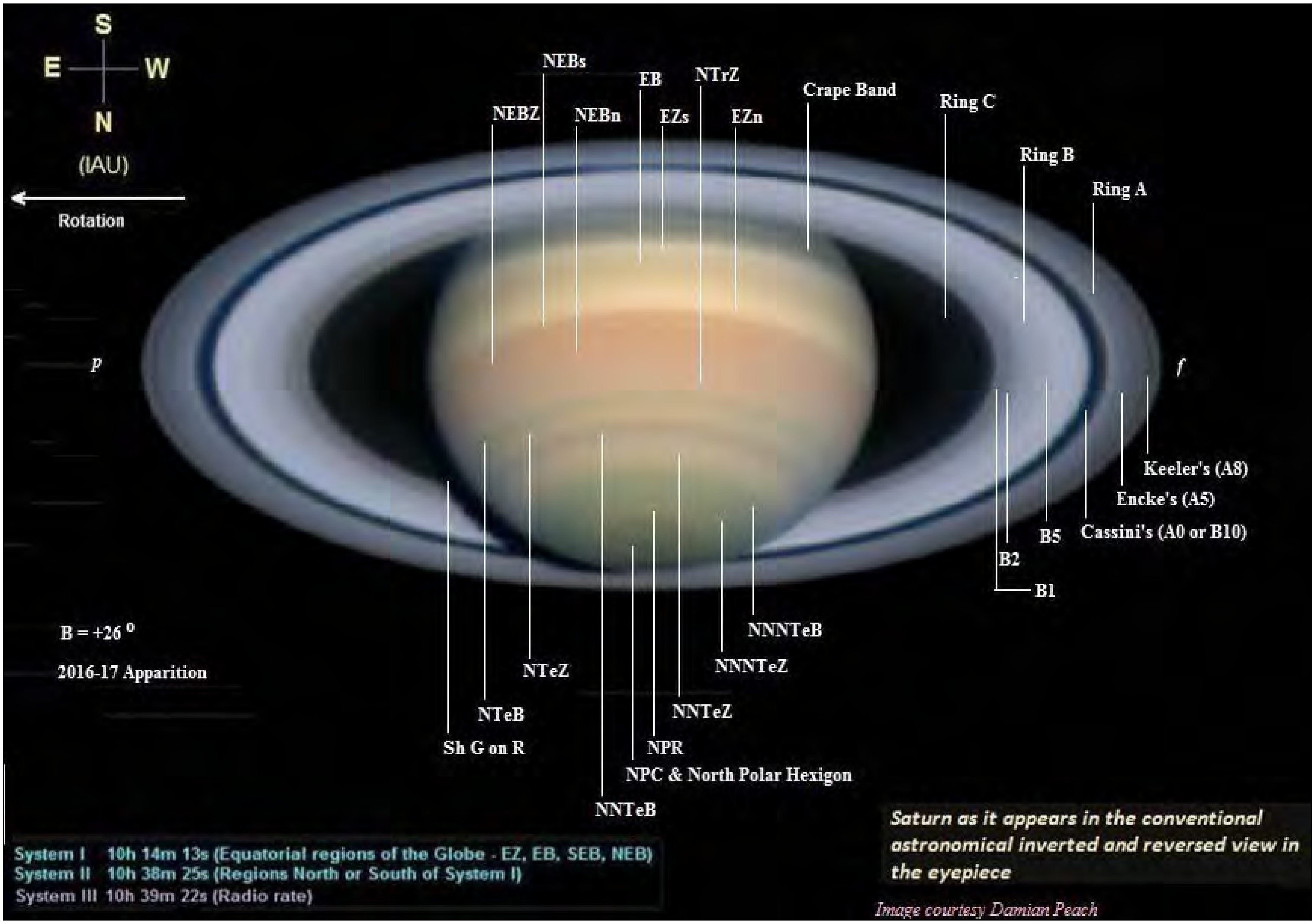

Figure 5. Saturn nomenclature, where A = Ring A, B = Band or Ring B or saturnicentric latitude of Earth, C = Ring C or Cap, E = Equatorial, f = following (celestial east), G = Globe, n = north component, N = North, p = preceding (celestial west), P = Polar, R = Ring(s) or Region, s = south component, S = South, Te = Temperate, Tr = Tropical, Z = Zone. The ring Ansae (not labeled) are the easternmost and westernmost protrusions of the Ring System. Note that "Gap" is also called "Division" or "Complex." South is at the top in this inverted view, similar to the orientation seen through an inverting telescope in Earth's Northern Hemisphere.

been successfully utilized for many of our Saturn observing programs.

The ALPO Saturn Section truly appreciates all of the digital images, visual drawings, descriptive reports, and supporting data submitted by observers listed in *Table 2* for the 2016-17 apparition. Without this dedicated teamwork, this report would not have been possible. Those wishing to join us in our various Saturn observing programs using visual methods in the form of drawings, estimates of visual numerical relative intensity, latitude estimates, and Central Meridian (CM) transit timings, as well as performing routine digital imaging, are encouraged to do so in upcoming observing seasons.

The domestic and international flavor of our observational work is most encouraging and valuable, and we strive to maintain participation by observers everywhere. All methods of recording observations are crucial to the success of our programs, whether one's preference is sketching Saturn at the eyepiece or simply writing descriptive reports, making visual numerical relative intensity and latitude estimates, or pursuing systematic digital imaging.

The ALPO Saturn Section especially emphasizes the ongoing need for more experienced observers to carry out regular visual numerical relative intensity estimates in integrated light and with standard color filters. Such estimates, which are simple to do, are greatly needed for maintaining our data to enable a recurring comparative analysis of belt, zone, and ring component brightness fluctuations over many apparitions. The ALPO Saturn Section is at all times happy to receive observations from novices, and the author is always delighted to offer assistance as one becomes acquainted with our programs. The 234 observations submitted to the ALPO Saturn Section during 2016-17 were used to prepare this report. Drawings, digital images, tables, and graphs are included so readers can refer to them as they study the content of this report. As applicable, contributors are cited in the text for drawings or images

General Caption Note for Illustrations 1-37. *B = saturnicentric latitude of the Earth; B' = saturnicentric latitude of the Sun; CMI, CMII and CMIII = central meridians in longitude Systems I, II and III; IL = integrated light; S = Seeing on the Standard ALPO Scale (from 0 = worst to 10 = perfect); Tr = Transparency (the limiting naked-eye stellar magnitude). Telescope types as in Table 2; feature abbreviations are as in Figure 5. In all figures, south is at the top and IAU east is to the left.*

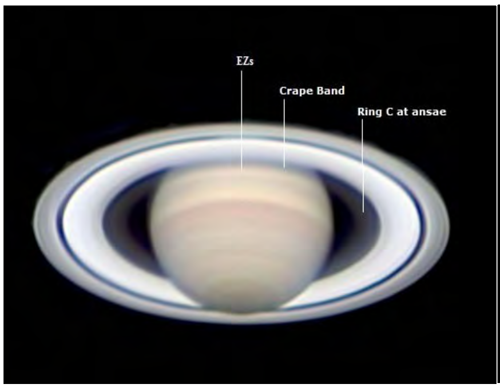

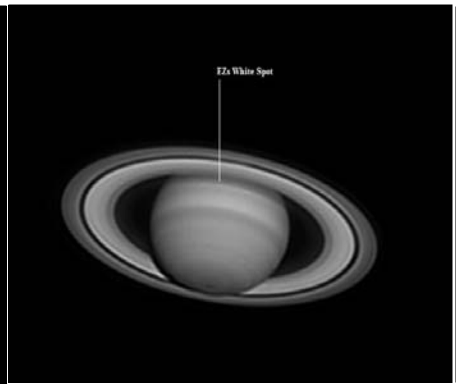

Illustration 001. (Above left) 2017 June 15, 05:06 UT. Digital image by Mike Hood. 35.6 cm (14.0 in.) SCT with RGB filters. S=5 and Tr=6.0. CMI = 38.1°, CMII = 294.2°, CMIII = 99.8°, B = +26.6°, B´ = +26.7°. The yellowish-white EZs is visible northward of the where the rings traversed the globe of Saturn. Various belts and several brighter zones of Saturn's northern hemisphere are also visible in this excellent image. The Crape Band and Ring C at ansae are shown. Saturn is at opposition in this image with a noticeable Seeliger Effect.

Illustration 002. (Above middle) 2017 March 25, 01:47 UT. Digital image by Clyde Foster. 35.6 cm (14.0 in.) SCT using a 685nm IR filter. S (not specified), Tr (not specified). CMI = 161.2°, CMII = 1190.5°, CMIII = 95.2°, B = +26.4°, B´ = +26.7°.. Small EZs white spot is barely visible.

Illustration 003. (Above right) 2017 March 26, 15:30 UT Digital image by Vlamir da Silva. 20.3 cm (8.0 in.) SCT NEW with RGB filters. S (rated as average), Tr (not specified). CMI = 48.1°, CMII = 26.6°, CMIII = 289.5°, B = +26.4°, B´ = +26.7°. The EB is quite apparent in this image.

Illustration 004. (Bottom left) 2017 August 6, 02:16 UT. Digital image by Jim Melka. 45.0 cm (17.7 in.) NEW with RGB filters. S=5.0 (not specified), Tr =6.0. CMI = 86.2°, CMII =143.6°, CMIII = 234.6°, B = +26.8°, B´ = +26.7°. The light brown EB looks wider in this image.

Illustration 005. (Bottom middle) 2017 June 16, 19:34 UT. Digital image by Clyde Foster. 35.6 cm (14.0 in.) SCT using RGB filters. S (not specified), Tr (not specified). CMI = 311.5°, CMII = 155.7°, CMIII = 3119.5°, B = +26.7°, B´ = +26.7°. Elongated fuzzy EB dark spot is near the W limb of Saturn.

Illustration 006. (Bottom right) 2017 June 19, 20:03 UT. Digital image by Clyde Foster. 35.6 cm (14.0 in.) SCT using a 685nm IR filter. S (not specified), Tr (not specified). CMI = 341.6°, CMII = 88.3°, CMIII = 248.4°, B = +26.6°, B´ = +26.7°. The EB dark spot is near the CM.

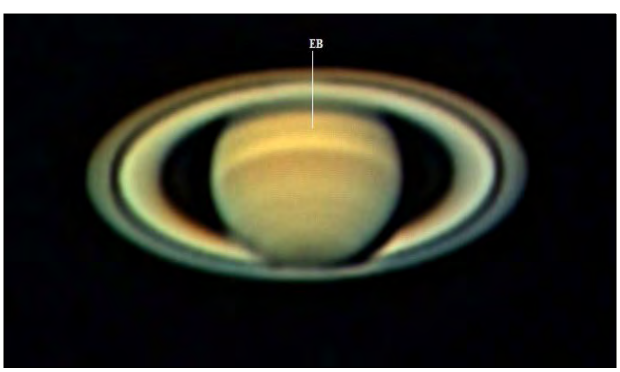

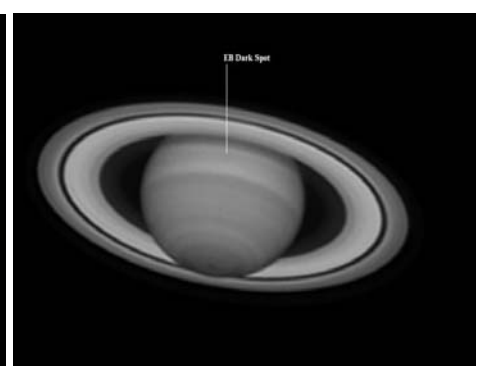

provided herein as examples of notable features or phenomena occurring within Saturn's belts and zones, along with dates and times of those observations for easy reference back to the relevant tables that list instrumentation employed, seeing, transparency, CM data, and so forth. In addition, captions associated with illustrations provide useful information.

The numerical value of **B** (the Saturnicentric latitude of the Earth referred to the ring plane) attained a maximum value of +26.9° during the 2016-17 apparition, with the Earth situated north of the rings as they continued to attain their near-maximum tilt toward our line of sight this observing season, affording optimum views of the north face of the rings and regions of the northern hemisphere of Saturn, with the planet's summer solstice occurring in 2016-17. The rings primarily hid features of the southern hemisphere as they crossed in front of the globe.

Minor fluctuations in intensity of Saturn's atmospheric features (see Table 3) may be attributable to the varying inclination of the planet's rotational axis relative to the Earth and Sun, although photometric work in past years suggests that small oscillations of about ±0.10 in the visual magnitude of Saturn likely happen over the span of a decade or so. Transient and longer-lasting atmospheric features seen or imaged in various belts and zones on the globe may also play a role in what appear to be subtle brightness variations.

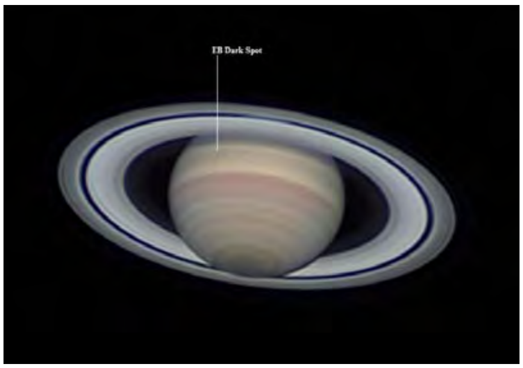

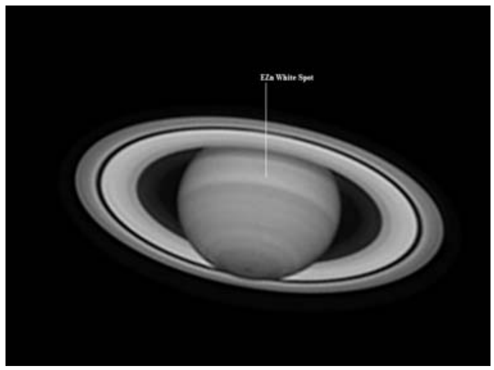

Illustration 007. (Above left) 2017 June 25, 19:35 UT. Digital image by Clyde Foster. 35.6 cm (14.0in.) SCT using RGB filters. S (not specified), Tr (not specified). CMI = 351.4°, CMII = 365.0°, CMIII = 67.8°, B = +26.6°, B´ = +26.7°. The EB dark spot is about halfway between the CM and E limb of Saturn.

Illustration 008. (Above middle) 2017 June 24, 20:03 UT. Digital image by Clyde Foster. 35.6 cm (14.0in.) SCT using a 685nm IR filter. S (not specified), Tr (not specified). CMI = 243.5°, CMII = 188.7°, CMIII = 342.7°, B = +26.6°, B´ = +26.7°. A diffuse white spot appears in the EZn near the CM.

Illustration 009. (Above right) 2017 July 18, 07:14 UT. Digital image by Clyde Foster. 35.6 cm (14.0in.) SCT using RGB filters. S (not specified), Tr (not specified). CMI = 256.8°, CMII = 164.1°, CMIII = 289.8°, B = +26.7°, B´ = +26.7°. The EZn white spot is approaching the CM.

Illustration 010. (Bottom left) 2017 August 18, 16:20 UT. Digital image by Clyde Foster. 35.6 cm (14.0in.) SCT using RGB filters. S (not specified), Tr (not specified). CMI = 109.5°, CMII = 83.3°, CMIII = 171.2°, B = +26.8°, B´ = +26.7°. The EZn white spot is headed toward the CM.

Illustration 011. (Bottom middle) 2017 August 22, 11:42 UT. Digital image by Trevor Barry. 40.6 cm (16.0 in.) NEW with 685nm IR filter. S = 5.5, Tr (not specified). CMI = 83.5°, CMII = 194.3°, CMIII = 17.6°, B = +26.8°, B´ = +26.7°. The EZn white spot is midway between the W limb and the CM.

Illustration 012. (Bottom right) 2017 August 23, 10:17 UT. Digital image by Trevor Barry. 40.6 cm (16.0 in.) NEW with a red filter. S = 5.5, Tr (not specified). CMI = 156.1°, CMII = 250.5°, CMIII = 73.1°, B = +26.8°, B´ = +26.7°. The fuzzy EZn white spot is approaching the E limb of the planet.

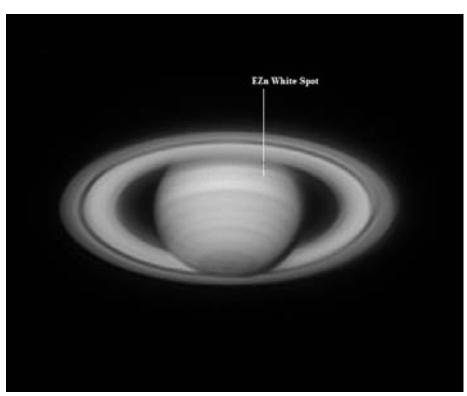

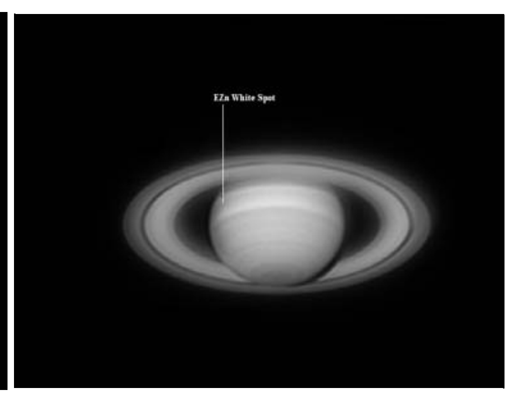

Regular photoelectric photometry of Saturn, in conjunction with carefully executed visual numerical relative intensity estimates, is strongly encouraged. The intensity scale routinely employed by Saturn observers is the standard *ALPO Standard Numerical Relative Intensity Scale*, where 0.0 denotes a total black condition (for example, complete black shadow) and 10.0 is the maximum brightness of a feature or phenomenon (for example, an unusually bright EZ or dazzling white spot). The numerical scale is normalized by setting the outer third of Ring B at a "standard" intensity of 8.0. The arithmetic sign of an intensity change is determined by subtracting a feature's 2015-16 intensity from its 2016-17 value. Suspected variances of ±0.10 mean intensity points are usually insignificant, while reported changes in intensity that do not equal or exceed roughly three times the standard error are probably not important.

It is important to evaluate contributed digital images of Saturn captured with different apertures using systematic filter techniques to understand the level of detail seen and how such phenomena compares with impressions by visual observers of the globe and rings. Moreover, it remains worthwhile to establish any correlation with spacecraft imaging and results from professional observatories.

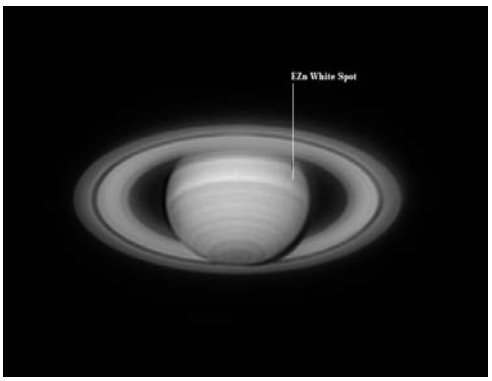

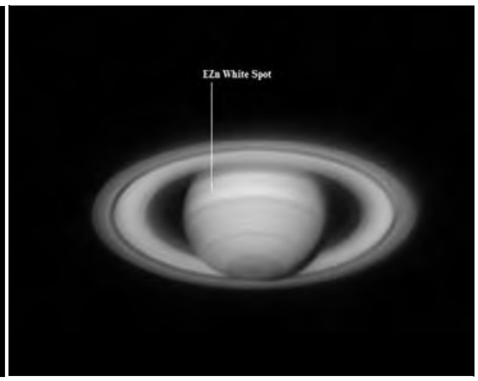

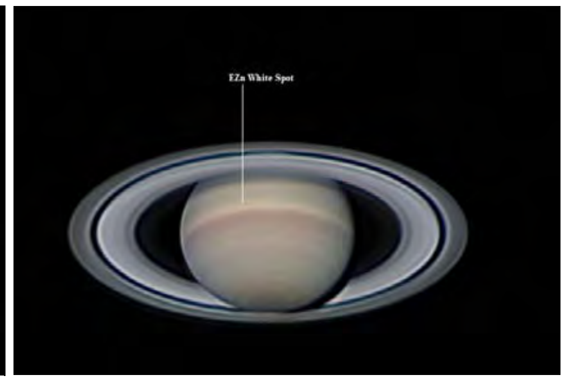

Illustration 013. (Above left) 2017 August 25, 10:26 UT. Digital image by Trevor Barry. 40.6 cm (16.0 in.) NEW with a red filter. S = 5.5, Tr (not specified). CMI = 51.6°, CMII = 167.3°, CMIII = 247.0°, B = +26.8°, B´ = +26.7°. The fuzzy EZn white spot is near the W limb of Saturn.

Illustration 014. (Above middle) 2017 September 26, 18:58 UT. Digital image by Trevor Barry. 40.6 cm (16.0 in.) NEW with a 685nm IR filter. S = 4.5, Tr (not specified). CMI = 51.6°, CMII = 167.3°, CMIII = 247.0°, B = +26.8°, B´ = +26.7°. The EZn white spot is between the CM and E limb of Saturn.

Illustration 015. (Above right) 2017 September 28, 16:48 UT. Digital image by Clyde Foster. 35.6 cm (14.0in.) SCT using RGB filters. S (not specified), Tr (not specified). CMI = 178.0°, CMII = 267.0°, CMIII = 305.4°, B = +26.9°, B´ = +26.6°. The less well defined EZn white spot is just beyond the CM.

Illustration 016. (Bottom left) 2017 October 02, 16:20 UT. Digital image by Clyde Foster. 35.6 cm (14.0in.) SCT using a 685nm IR filter. S (not specified), Tr (not specified). CMI = 298.2°, CMII = 358.7°, CMIII = 292.3°, B = +26.9°, B´ = +26.6°. The EZn white spot is approaching the CM.

Illustration 017. (Bottom middle) 2017 November 01, 09:52 UT. Digital image by Trevor Barry. 40.6 cm (16.0 in.) NEW with a 685nm IR filter. S = 4.0, Tr (not specified). CMI = 195.1°, CMII = 275.3°, CMIII = 273.1°, B = +26.9°, B´ = +26.6°. The EZn white spot is almost on the CM.

Illustration 018. (Bottom right) 2017 November 07, 09:37 UT. Digital image by Trevor Barry. 40.6 cm (16.0 in.) NEW with a red filter. S = 5.0, Tr (not specified). CMI = 211.1°, CMII = 97.9°, CMIII = 88.4°, B = +26.9°, B´ = +26.6°. The EZn white spot is halfway between the CM and E limb of the planet.

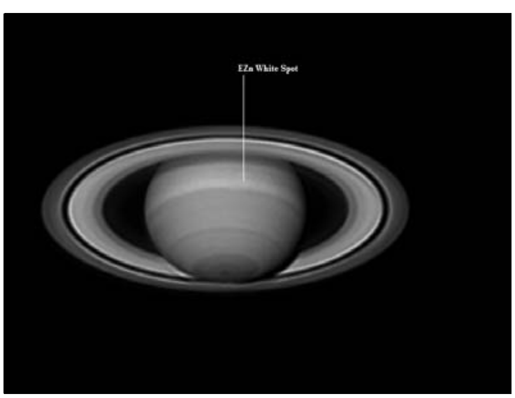

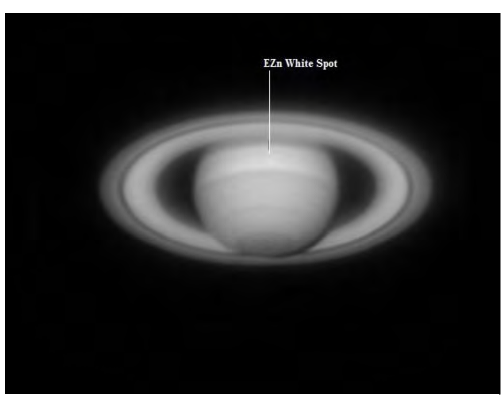

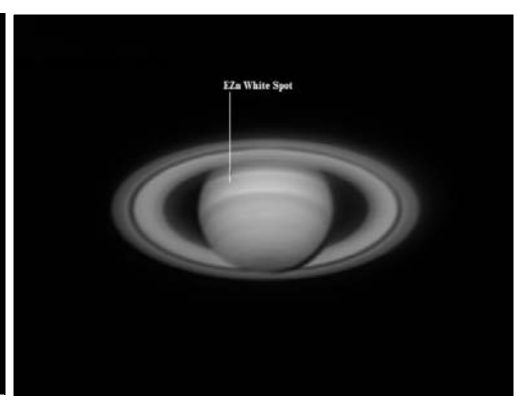

In addition to routine visual studies, such as drawings and visual numerical relative intensity estimates, Saturn observers are asked to systematically image the planet every possible clear night, as applicable. This allows documentation of individual features on the globe and in the rings, their motion and morphology (including changes in intensity and hue), to facilitate comparisons with images taken by professional ground-based observatories and spacecraft monitoring Saturn at close range.

Furthermore, comparing images taken over several apparitions for a given hemisphere of the planet's globe provides information on long-term seasonal changes suspected by observers using visual numerical relative intensity estimates. Images and systematic visual observations by amateurs are being relied upon for providing initial alerts of interesting large-scale features on Saturn that professionals may not already know about but can subsequently examine with considerably larger and more specialized instrumentation.

Particles in Saturn's atmosphere reflect different wavelengths of light in very distinct ways, which causes some belts and zones to appear especially prominent, while others look very dark, so imaging the planet with a series of color filters may help shed light on the dynamics, structure, and composition of its atmosphere.

In the UV and IR regions of the electromagnetic spectrum, it is possible to determine additional properties as well as the sizes of aerosols present in different atmospheric layers not otherwise accessible at visual wavelengths, as well as useful data about the cloud-covered satellite Titan. UV wavelengths shorter than 320nm are effectively blocked by the Earth's stratospheric ozone (O_3), while CO_2 and H_2O-vapor molecules absorb in the IR region beyond 727nm. The human eye is insensitive to UV light short of 320nm and can detect only about 1.0% at 690nm and 0.01% at 750nm in the IR (beyond 750nm visual sensitivity is essentially zero).

Although most of the reflected light from Saturn reaching terrestrial observers is in the form of visible light, some UV and IR wavelengths that lie on either side and in close proximity to the visual region penetrate to the Earth's surface, and imaging Saturn in these near-IR and near-UV bands has provided some remarkable results in the past. The effects of absorption and scattering of light by the planet's atmospheric gases and clouds at various heights and with different thicknesses are often evident. Indeed, such images sometimes show differential light absorption by particles with dissimilar hues intermixed with Saturn's white NH_3 clouds.

In the next few paragraphs, our discussion of features on Saturn's globe proceeds in the usual south-to-north order (traditional astronomical inverted and reversed view).

For clarity, the relative positions of major belts and zones can be identified by referring to the nomenclature diagram

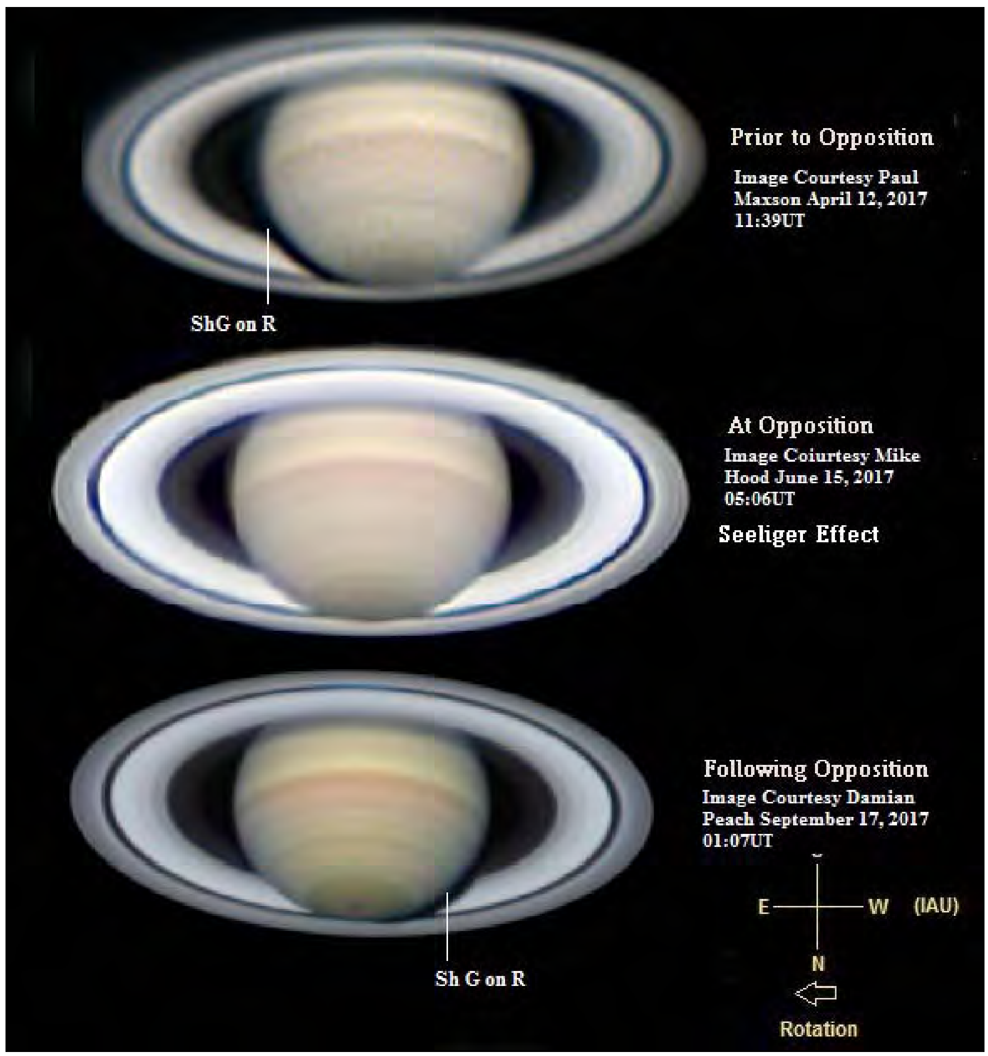

Figure 6. Saturn nomenclature, where A = Ring A, B = Band or Ring B or saturnicentric latitude of Earth, C = Ring C or Cap, E = Equatorial, f = following (celestial east), G = Globe, n = north component, N = North, p = preceding (celestial west), P = Polar, R = Ring(s) or Region, s = south component, S = South, Te = Temperate, Tr = Tropical, Z = Zone. The ring Ansae (not labeled) are the easternmost and westernmost protrusions of the Ring System. Note that "Gap" is also called "Division" or "Complex." South is at the top in this inverted view, similar to the orientation seen through an inverting telescope in Earth's Northern Hemisphere.

shown in *Figure 5*. If no reference is made to a global feature in this report, observers did not report the area during the 2016-17 apparition.

It has been customary in past Saturn apparition reports to compare the brightness and morphology of atmospheric features between observing seasons, and this practice continues with this report so readers are aware of very subtle, but nonetheless recognizable, variations that may be occurring seasonally on planet.

Saturn's Globe: The Southern Hemisphere

Saturn's southern hemisphere was obstructed from our view during 2016-2017, where the rings crossed in front of this pare of the globe, with the exception of the yellowish-white Equatorial Zone (EZs) appearing just south of the Equatorial Band (EB).

Equatorial Zone—Southern Half (EZs). Higher resolution images revealed a portion of the yellowish-white Equatorial Zone (EZs) just northward of the where the rings traversed the globe of Saturn [refer to *Illustration 001*]. Visual observers provided descriptions of the EZs but regrettably provided no visual numerical relative intensity estimates during 2016-17. The only report of discrete atmospheric phenomena associated with the EZs in 2016-17 came from Clyde Foster who thought he had imaged a vague small white spot on March, 25, 2017 at 01:47 UT using a 685nm IR filter [refer to *Illustration 002*].

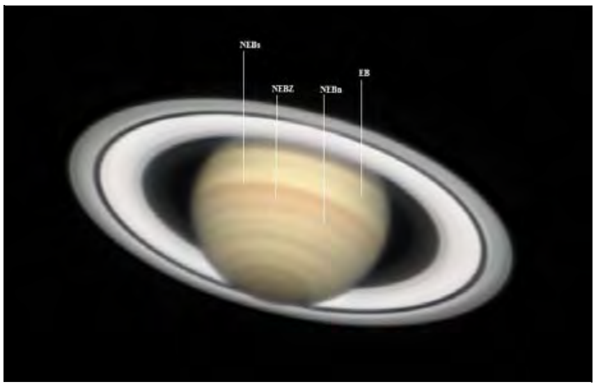

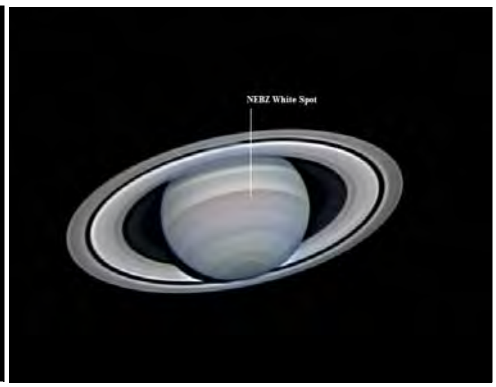

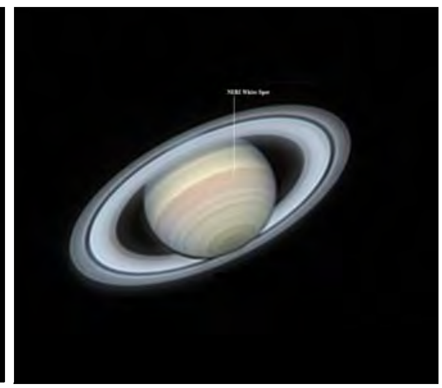

Illustration 019. (Above left) 2017 June 13, 23:59 UT. Digital image by Carmelo Zannelli. 35.6 cm (14.0-in) SCT with RGB filters. S (not specified), Tr (not specified). CMI = 93.7°, CMII =28.9°, CMIII = 196.0°, B = +26.6°, B´ = +26.7°. The NEBn, NEBZ, and NEBs are obvious in this image. The light brown EB looks wider.

Illustration 020. (Above middle) 2017 March 12, 02:48 UT. Digital image by Clyde Foster. 35.6 cm (14.0in.) SCT using RGB filters. S (not specified), Tr (not specified). CMI = 210.5°, CMII = 108.3°, CMIII = 28.6°, B = +26.5°, B´ = +26.7°. A small NEBZ white spot is apparent between the NEBs and NEBn.

Illustration 021. (Above right) 2017 May 24, 15:14 UT. Digital image by Trevor Barry. 40.6 cm (16.0 in.) NEW with a red filter. S = 6.5, Tr (not specified). CMI = 177.9°, CMII = 51.0°, CMIII = 242.6°, B = +26.5°, B´ = +26.7°. The NEBZ white spot is located midway between the W limb and CM.

Illustration 022. (Bottom left) 2016 June 11, 14:55 UT. Digital image by Christopher Go. 35.6 cm (14.0 in.) SCT with RGB filters. S = 8.0, Tr = 4.5. CMI = 244.2, CMII = 256.3° CMIII = 66.3°, B = +26.6°, B´ = +26.7°. The NEBZ and NEBn white spots are captured in this excellent detail image, with both features near the CM. Shown also are Cassini's division (A0 or B10), Encke's complex (A5), Keeler's Gap (A8), and "intensity minima" (B1, B2 and B5).

Illustration 023. (Bottom middle) 2016 June 13, 14:34 UT Digital image by Christopher Go. 35.6 cm (14.0 in.) SCT with RGB filters. S = 8.0, Tr = 4.5. CMI = 87.2°, CMII = 36.5° CMIII = 204.1°, B = +26.6°, B´ = +26.7°. The NEBZ and NEBn white spots are both E of the CM.

Illustration 024. (Bottom right) 2017 April 25, 19:07 UT. Digital image by Christopher Go. 35.6 cm (14.0 in.) SCT with RGB filters. S = 8.0, Tr = 4.5. CMI = 306.9°, CMII = 31.4° CMIII = 257.9°, B = +26.4°, B´ = +26.7°. The NEBn white spot is between the W limb of Saturn and the CM.

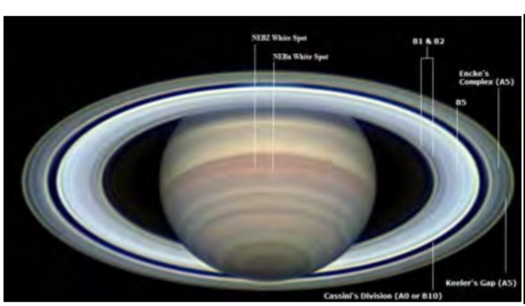

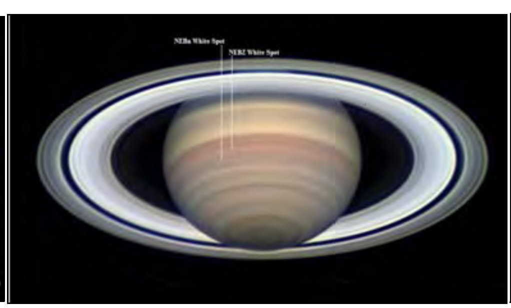

Saturn's Globe: The Northern Hemisphere

Equatorial Band (EB). Only two visual numerical relative intensity estimates of the very light brown Equatorial Band (EB) were submitted during 2016-2017. Despite the limited number of these estimates, the belt was portrayed on several drawings in integrated light and noticeable on many of the digital images submitted during the observing season [refer to *illustrations 003 and 004*]. Clyde Foster imaged a small elongated dark spot with a 685nm IR filter within the EB on June 16, 2017 at 19:34 UT, plus he captured another image of a dark spot in the EB near the CM on June 19, from 20:03 UT employing a 685nm IR filter. Clyde Foster recorded a subsequent image of an EB dark spot on June 25, 2017 at 19:35 UT he imaged another possible dark spot in the EB using a 685nm IR and RGB filters [refer to *illustrations 005, 006, and 007*]. Other than these images of EB dark spots, there was no other activity reported in the EB during the 2016-17 apparition.

Equatorial Zone—Northern Half (EZn). With the numerical value of **B** ranging between +26.4° (April 17, 2017) and +26.9° (October 26, 2017), the northern half of the Equatorial Zone (EZn) was seen and imaged to best advantage in 2016-17.

Based on limited visual numerical relative intensity estimates and numerous digital images, the bright yellowish-white Equatorial Zone (EZn) displayed a negligible brightness variation of +0.30 mean intensity points since 2015-2016), and it was always the brightest zone on Saturn's globe in 2016-2017. The first report to the ALPO Saturn Section of a small white spot in the EZn came from Clyde Foster on June 24, 2017 at 20:03 UT with a 685nm IR filter, he again imaged an EZn white spot on July 18, 2017 between 17:14 UT and 17:24 UT

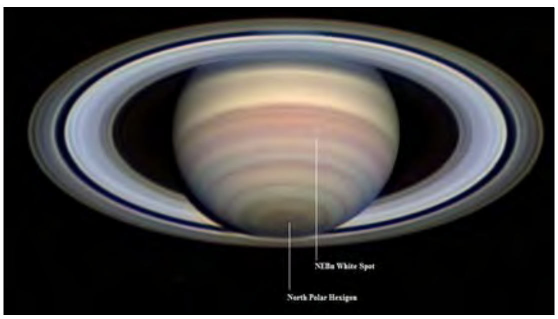

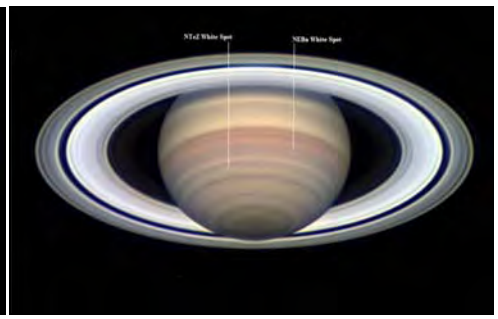

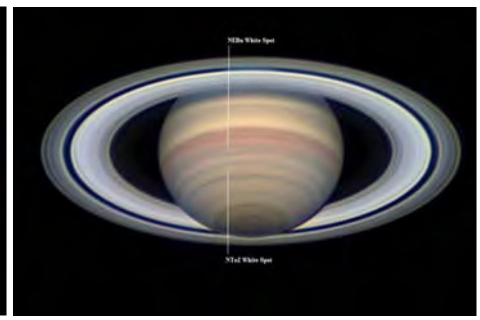

Illustration 025. 2017 April 29, 18:36 UT. Digital image by Christopher Go. 35.6 cm (14.0 in.) SCT with RGB filters. S = 8.0, Tr = 4.5. CMI = 306.9°, CMII = 31.4° CMIII = 257.9°, B = +26.4°, B´ = +26.7°. The NEBn white spot is getting nearer the CM. The interesting north polar hexagon is clearly visible.

Illustration 026. 2017 June 16, 14:51 UT. Digital image by Christopher Go. 35.6 cm (14.0 in.) SCT with RGB filters. S = 8.0, Tr = 4.5. CMI = 306.9°, CMII = 31.4° CMIII = 257.9°, B = +26.4°, B´ = +26.7°. The NEBn and NTeZ white spots are both visible.

Illustration 027. 2017 June 24, 14:22 UT. Digital image by Christopher Go. 35.6 cm (14.0 in.) SCT with RGB filters. S = 8.0, Tr = 4.0. CMI = 43.5°, CMII = 156.2° CMIII = 150.7°, B = +26.6°, B´ = +26.7°. The slightly elongated NEBn white spot and NTeZ white spot are both E of the CM.

Illustration 028. 2017 July 29, 12:54 UT. Digital image by Christopher Go. 35.6 cm (14.0 in.) SCT with RGB filters. S = 6.5, Tr = 3.0. CMI = 306.9°, CMII = 31.4° CMIII = 257.9°, B = +26.4°, B´ = +26.7°. The NEBn white spot has apparently faded from view. A curious fuzzy NPR dark spot appears near the W limb.

Illustration 029. 2017 June 12, 14:48 UT. Digital image by Trevor Barry. 40.6 cm (16.0 in.) NEW with a red filter. S = 6.0, Tr (not specified). CMI = 177.9°, CMII = 51.0°, CMIII = 242.6°, B = +26.5°, B´ = +26.7°. The NTrZ white spot is located between the W limb and CM, plus a few less prominent white spots nearby the CM.

Illustration 030. 2017 July 12, 17:08 UT. Digital image by Clyde Foster. 35.6 cm (14.0in.) SCT using RGB filters. S (not specified), Tr (not specified). CMI = 299.8°, CMII = 356.6°, CMIII = 33.8°, B = +26.9°, B´ = +26.6°. The NTrZ white spot is approaching the CM.

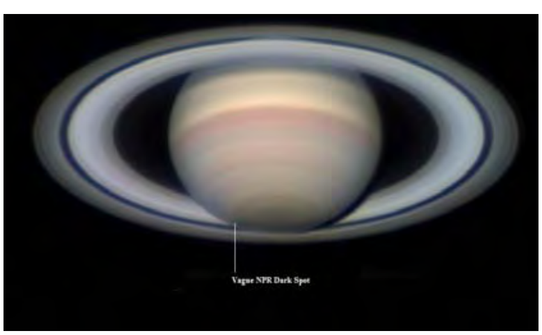

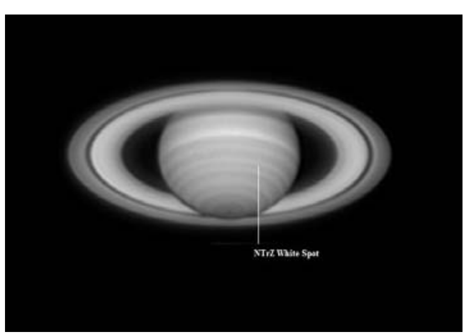

with a 685nm IR filter [refer to *illustrations 008 and 009*].

On August 18, 2017, Clyde Foster provided another image of an EZn white spot at 16:20 UT with RGB filters [refer to *Illustration 010*]. Trevor Barry employing a 685nm IR filter imaged a probable recurring EZn white spot on August 22, 2017 at 11:42 UT, as well as on August 23, 2017 at 10:17 UT using a red filter [refer to *illustrations 011 and 012*]. Trevor Barry recorded an EZn white spot yet again on August 25, 2017 at 10:26 UT with a red filter [refer to *Illustration 013*]. As the 2016-2017 apparition progressed, Trevor Barry captured another image of an EZn white spot on September 26, 2017 at 18:58 UT using a 685nm IR filter [refer to *Illustration 014*]. Two days later on September 28, 2017 from 16:48 UT Clyde Foster using RGB filters imaged an EZn white spot; employing a 685nm IR filter, he recorded another image of an EZn white spot on October 2, 2017 at 16:20UT [refer to *illustrations 015 and 016*].

The final images of an Zn white spot during 2016-2017 was provided by Trevor Barry using a 685nm IR filter on November 1, 2017 from 09:52 UT measured at saturnigraphic latitude +4.4o as well as another image with a red filter on November 7, 2017 from

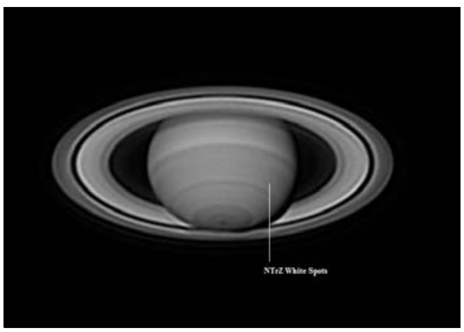

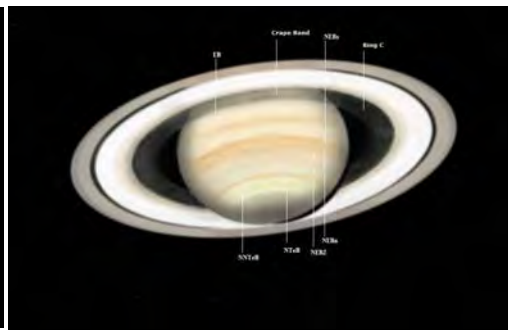

Illustration 031. 2017 September 28, 16:44 UT. Digital image by Clyde Foster. 35.6 cm (14.0in.) SCT using a 685nm IR filter. S (not specified), Tr (not specified). CMI = 175.6°, CMII = 264.7°, CMIII = 303.2°, B = +26.9°, B´ = +26.6°. The NTrZ white spot is between the W limb approaching the CM. A few subtle nearby white mottlings within the NTrZ are strongly suspected.

Illustration 032. 2017 July 19, 22:06 UT. Drawing by Paul G. Abel. 50.8 cm (20.0in) DAL at Integrated Light. S = 6.5 (interpolated), Tr = rated as average to poor. CMI = 66.6°, CMII = 140.7°, CMIII = 342.8°, B = +26.0°, B´ = +26.4°. The NNTeB and NTeB are both labeled, along with other features represented in this excellent colorful drawing. The Crape Band and Ring C at both the ansae are noted as well.

Illustration 033. 2017 August 02, 02:42 UT. Digital image by Gary Walker. 25.4 cm (10.0 in.) REF with RGB filters. S=5.5, Tr=4.5. CMI = 161.8°, CMII = 310.7°, CMIII = 58.6°, B = +26.8°, B´ = +26.7°. The narrow NTeB is indicated on the image.

Illustration 034. 2017 May 31, 14:42 UT. Trevor Barry. 40.6 cm (16.0 in.) NEW with RRG filters. S = 5.5, Tr (not specified). CMI =310.0°, CMII = 317.6°, CMIII = 140.9°, B = +26.5°, B´ = +26.7°. The NTeZ white spot is noted, as well as several important northern hemisphere belts and zones are visible and labeled on this image, namely the NNTeZ, NNTeB, NNNTeZ, NNNTeB.

Illustration 035. 2017 August 12, 19:11 UT. Manos Kardasis. 35.6cm (14.0 in.) SCT with 885nm IR filter. S = 4.5, Tr = not specified. CMI = 184.3°, CMII = 248.1°, CMIII = 83.1°, B = +26.8°, B´ = +26.7 The Sh on G is visible across the globe just N of the rings and slightly S of thr Crape Band. The ring shadow is geometrically to the N of the rings as shown in this image, but care must be taken not to confuse the ring shadow with the Crape Band across the globe.

Illustration 036. 2017 August 16, 11:21 UT. Trevor Barry. 40.6 cm (16.0 in.) NEW with RRG filters. S = 5.0, Tr (not specified). CMI =45.7°, CMII = 90.9°, CMIII = 181.4°, B = +26.8°, B´ = +26.7°. Saturnian satellites Enceladus, Tethys, and Dione are visible in this image.

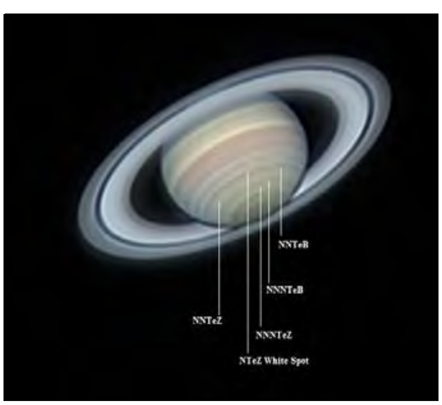

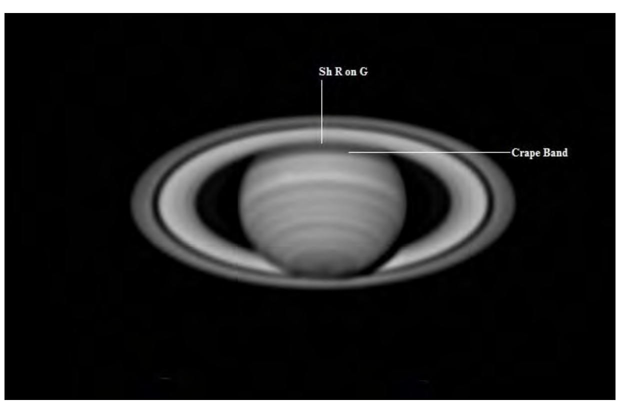

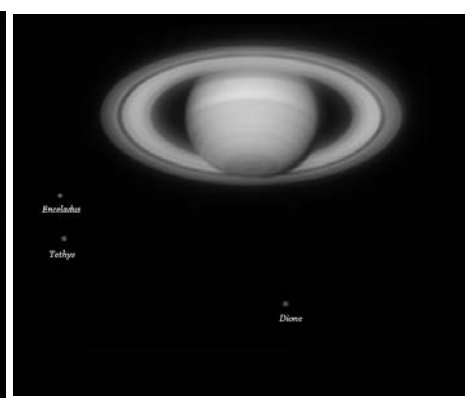

09:37 UT at saturnigraphic latitude +4.9° [refer to *illustrations 017 and 018*]. Based on the digital images provided by the aforementioned observers during 2016-2017, it appears likely that the EZn white spot represented a long-term white spot that persisted for much of this apparition.

North Equatorial Belt (NEB). The rather broad and dull yellowish-brown NEB (considered as a whole feature and abbreviated as "NEBw") was frequently reported by visual observers and imaged regularly throughout the 2016-2017 apparition. Visual observers reported the NEBw as a singular belt most of the observing season as opposed to it being separated into the NEBs and NEBn components with the NEBZ lying between the two components. The NEBw showed no change in appearance or intensity since 2015-2016, usually displaying a lighter-to-darker southward progression in intensity across its broad width, consistent also with its form on most digital images in 2016-2017.

Observational results revealed a grayish-brown NEBs appearing generally thinner and darker than the slightly wider grayish-brown NEBn, often with a narrow yellowish-gray NEBZ lying in between [refer to *Illustration 019*]. In terms of atmospheric activity associated with the NEB, Clyde Foster imaged a small NEBZ white spot using a 685nm IR filter on March 12, 2017 at 02:48 UT [refer to *Illustration 020*].

Trevor Barry utilizing RGB filters, also furnished an image of a small, ill-defined relatively short-lived yellowish-white oval immersed within the NEBZ on May 24, 2017 at 15:14 UT [refer to *Illustration 021*]. An NEBZ white spot was imaged with RGB filters by Christopher Go on June 11, 2017 at 04:55 UT [refer to *Illustration 022*], plus he imaged the apparent recurring NEBZ white spot yet again on June 13, 2017 at 14:34 UT with RGB filters [refer to *Illustration 023*]. Christopher Go imaged a small NEBn white spot on April 25, 2017 at 18:35 UT using RGB filters, plus he recorded the NEBn white spot again on April 29, 2017 at 1836 UT [refer to *illustrations 024 and 025*]. Three additional RGB images by Christopher Go at 14:34 UT on June 13, 2017, June 16, 2017 at 15:51 UT, and on June 24, 2017 at 14:22 UT showed a slightly more elongated NEBn white spot [refer to *illustrations 023, 026 and 027*]. Christopher Go's RGB image on July 29, 2017 at 12:54 UT suggested that the NEBn white spot had faded so much that it was no longer detectable [refer to *Illustration 028*].

There were no other reports of NEBn white spot activity during the remainder of the 2016-2017 observing season. No discrete activity was reported in the dull yellowish brown NEBs during this apparition, although a singular visual numerical relative intensity estimate suggested a negligible darkening by -0.2 mean intensity points since 2015-2016.

North Tropical Zone (NTrZ). Visual numerical relative intensity estimates in 2016-2017 rated the NTrZ third in order of brightness compared with the EZn and NTeZ. The yellowish-white NTrZ was apparent on most images in good seeing conditions throughout the observing season.

In terms of specific NTrZ atmospheric phenomena, several observers imaged NTrZ white features, considered by some to possibly be a "fossil" of the massive white storm that occurred in 2010. It should be pointed out that the white spot features addressed in our foregoing discussion of white spots imaged or observed at the north edge of the NEBn, the features were all situated in their latitudinal proximity close to the domain of the adjacent NTrZ during 2016-2017, leading to some confusion among observers when attempting to describe their observational results.

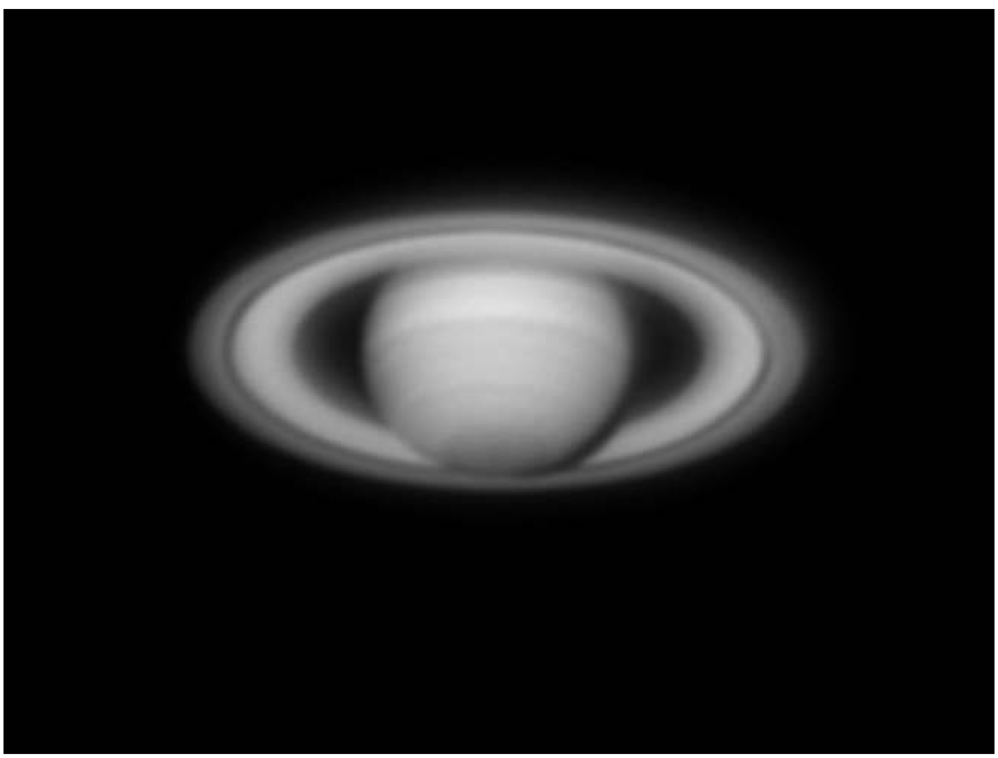

Illustration 037. 2017 September 15, 11:55:46 UT. Trevor Barry. 40.6 cm (16.0 in.) NEW with 685nm IR filter. S = 5.0, Tr (not specified). CMI =186.7°, CMII = 342.4°, CMIII = 36.7°, B = +26.9°, B´ = +26.7°. Image of Saturn on the date of the impact of the *Cassini* spacecraft with the planet, marking the time of the confirmed loss of signal and thus “end of mission” on this date.

For example, consider an image by Trevor Barry at 12:44 UT on June 12, 2017 using a red filter, which shows a discrete NTrZ white spot (and perhaps others nearby within the NTrZ), as well as an RGB image by Clyde Foster on July 12, 2017 at 17:08 UT [refer to *illustrations 029 and 030*]. Lastly, notice another image of NTrZ white spots captured using a 685nm IR filter by Clyde Foster on September 28, 2017 at 16:44 UT [refer to *Illustration 031*].

North Temperate Belt (NTeB). The grayish-brown NTeB was occasionally seen by visual observers during the observing season, although no visual numerical relative intensity estimates were provided. When seen, the belt was described as somewhat duskier in appearance and perhaps slightly wider since 2015-2016.

Several visual drawings and digital images of Saturn during the apparition also showed a slightly wider NTeB; for instance, consider the integrated light drawing by Paul Abel on July 19, 2017 at 22:06 UT, as well as the image using RGB filters taken by Gary Walker on August 2, 2017 at 02:42 UT [refer to *illustrations 032 and 033*]. No truly discernable spot activity within the NTeB was reported in 2016-2017.

North Temperate Zone (NTeZ). Although there were only a small number of visual numerical relative intensity estimates of the dull yellowish-gray NTeZ received for this apparition, the rather insignificant darkening of the NTeZ by -0.3 mean intensity points since the previous 2015-16 apparition in of no real consequence. Nevertheless, the NTeZ was frequently apparent on drawings submitted during the apparition as well as captured on the majority of digital images received.

The NTeZ was a bit more conspicuous than the NTrZ on most images, and in order of brightness, it ranked second when compared with the EZn. Observers who routinely imaged Saturn detected possible recurring atmospheric white spot activity in the NTeZ during 2016-2017. For instance, the initial image of discrete phenomena in the NTeZ occurred in the form of a small white spot observed by Trevor Barry using RGB filters at 14:42 UT on May 31, 2017 [refer to *Illustration 034*].

Christopher Go recorded an NTeZ white spot on June 16, 2017 at 14:51 UT with RGB filters, and he imaged the NTeZ white spot again using RGB filters on June 24, 2017 at 14:22 UT [refer to *illustrations 026 and 027*]. There were no additional images of NTeZ white spots submitted for the remainder of the apparition.

North North Temperate Belt (NNTeB). The very dull gray NNTeB was difficult to detect even on the best images taken in good seeing conditions in 2016-2017.

For example, consider the RGB image by Trevor Barry at 14:42 UT on May 31, 2017 [refer to *Illustration 034*]. Visual observers did not report the NNTeB during the 2016-2017 apparition, while those attempting to capture images of NNTeB **were not convinced that discrete phenomena in the NNTeB truly existed.**

North North Temperate Zone (NNTeZ). During 2016-2017, the often yellowish-white NNTeZ, second only to the EZn in overall brightness, was not reported visually but was barely obvious on many of the best images taken with moderate-to-larger apertures during the observing season [refer to *Illustration 034*].

Although several observers suspected small white and dark features during the observing season, definitive corroboration of discernible atmospheric detail within the NNTeZ was not forthcoming from observers when imaging Saturn.

North North North Temperate Belt (NNNTeB). The very narrow dull gray NNNTeB displayed no definitive confirmed activity in the form of dark and white spots in good seeing during 2016-2017 [refer to *Illustration 034*].

North North North Temperate Zone (NNNTeZ). Visual observers did not call attention to the yellowish-gray NNNTeZ during the 2016-2017 apparition, but it was frequently seen in higher resolution images at RGB and various other wavelengths [refer to *Illustration 034*].

North Polar Region (NPR). Visual observers frequently reported the very dull gray NPR, and it was quite evident on digital images contributed during the 2016-2017 apparition. Visual numerical relative intensity estimates suggested only a trivial (-0.04) dimming in mean intensity of the NPR since 2015-2016. Christopher Go suspected a diffuse dark spot at the southern edge of the NPR in his RGB image on July 29, 2017 at 12:54 UT [refer to *Illustration 028*].

The NPR was otherwise devoid of any reported activity by visual observers or those imaging Saturn during the 2016-2017 observing season. The always-intriguing dark North Polar hexagon within the NPR was easily recognizable on many of the best images from this apparition, such the one by Christopher Go taken on April 23, 2016 at 19:14 UT [refer to *Illustration 025*].

Shadow of the Globe on the Rings (Sh G on R). The Sh on G was visible to observers as a geometrically regular black shadow on either side of opposition during 2016-2017. Any presumed variation of this shadow from a totally black intensity (0.0) during an apparition is merely a consequence of poor seeing conditions or the presence of extraneous light. Digital images of the Sh G on R showed the feature as completely black.

It should be noted that the globe of Saturn casts a shadow on the rings toward the left (or IAU East) prior to opposition, and on neither side at opposition (no observable shadow), and toward he right (or IAU West) after opposition. Figure 6 includes selected digital images by several ALPO Saturn observers to help illustrate this phenomenon.

Latitude Estimates of Features on the Globe. Observers did not submit latitude estimates of features on Saturn's globe during 2016-2017, employing the convenient visual method originated by the late ALPO founder Walter Haas. Several of the sharpest images in good seeing, however, were measured to ascertain as accurately as possible the saturnigraphic latitude of specific discrete phenomena discussed in this report.

Readers are encouraged to try the historically accurate and effective Haas visual technique to estimate latitudes. It merely involves determining as accurately as possible the fraction of the polar semi diameter of Saturn's globe subtended on the central meridian (CM) between the limb and the feature whose latitude is desired.

As a control on the accuracy of this method, observers should include in their estimates the position on the CM of the projected ring edges and the shadow of the rings. The actual latitudes can then be calculated from the known values of **B** and **B'** and the dimensions of the rings, but this test cannot be effectively applied when **B** and **B'** are near their maximum attained numerical values.

Experienced observers have used this visual convenient procedure for many years with very reliable results, especially since filar micrometers are virtually non-existent, and even if available, they tend to be very expensive, not to mention sometimes cumbersome to use properly.

A detailed description of the technique can be found in the author's book entitled *Saturn and How to Observe It*, published by Springer and available from booksellers worldwide.

Saturn's Ring System

This section addresses visual studies of Saturn's ring system with the accustomed comparison of mean intensity data between apparitions, as well as interpretations of digital images of the rings contributed during 2016-2017.

With the ring tilt toward Earth increasing to as much as +26.9° (October 26, 2017), the major ring components were much easier to see and image as the rings progress toward their theoretical maximum inclination of +27.0° during the 2016-17 apparition.

Ring A. Visual numerical relative intensity estimates suggested that the dull greyish-white Ring A (taken as a whole) was unchanged in appearance in 2016-2017 when compared with the immediately preceding apparition. Visual observers described Ring A as being largely homogeneous (as opposed to being subdivided into inner and outer halves), but digital images of Saturn in 2016-17 often showed inner and outer halves of Ring A, with the inner half somewhat lighter than the outer half.

Visual numerical relative intensity estimates suggested only a very minor increase in brightness of the inner half of Ring A by +0.10 mean intensity points compared with 2015-2016, while the outer half of Ring A was negligibly lighter by +0.20 mean intensity points since last apparition. Visual observers reported the very dark gray Encke's division (A5) at the ansae during the observing season in good seeing and with larger apertures, but there was a minimal number of visual numerical relative intensity estimates (see Table 3).

Many of the higher resolution images revealed Encke's division (A5) and Keeler's gap (A8), but the latter was seldom described by visual observers except those with the largest instruments used [refer to *Illustration 022*].

Ring B. The outer third of Ring B is the traditional standard of reference for the "ALPO Saturn Visual Numerical Relative Intensity Scale," with an assigned value of 8.0.

Under circumstances of greater ring tilt during the 2016-2017 apparition, visual observers reported that the outer third of Ring B appeared brilliant white with no variation in intensity, and compared with other ring components and atmospheric phenomena of Saturn's globe, it was always the brightest intrinsic feature on Saturn.

The inner two-thirds of Ring B during this apparition, described as yellowish-white and uniform in intensity, displayed no variation in visual numerical intensity compared with 2015-2016. Digital images confirmed most visual impressions during this observing season, with those of the highest resolution in favorable seeing exhibited several "intensity minima" across the breadth of Ring B [refer to *Illustration 022*].

Cassini's Division (A0 or B10). Visual observers regularly saw Cassini's division (A0 or B10) in 2016-2017, and visual numerical relative intensity estimates averaged out at a difference of +0.10 since the previous apparition, but any suspected deviation of Cassini's Division from a totally black intensity (that is, intensity of 0.0) was almost certainly a result of poor seeing, scattered light, or insufficient aperture.

Indeed, most visual observers viewing Saturn in good seeing conditions, and those submitting digital images, described or depicted it as a totally black gap at both ansae and usually traceable all the way around Saturn's ring system (except, of course, where the globe blocked views of the rings). This was also true for most of the high-resolution images submitted [refer to *Illustration 022*].

Ring C. The very dark gray Ring C was observed at the ansae on most digital images during 2016-2017 and splayed on drawings made by visual observers [refer to *illustrations 001 and 036*]. Intensity estimates during this apparition suggested that Ring C (at the ansae) was slightly lighter by +0.30 mean intensity points since 2015-2016.

The Crape Band (Ring C across the globe of Saturn) was reported by visual observers, appearing very dull gray with uniform intensity, displaying a subtle increase by +0.20 mean intensity since 2015-2016, and it was routinely evident on drawings and most digital images [refer to *illustrations 001 and 032*].

Opposition Effect. The Seeliger "opposition effect" was reported by a handful of observers on opposition date (June 15, 2017), which is a readily noticeable brightening of Saturn's ring system during a very brief interval on either side of opposition when the phase angle between Sun, Saturn, and the Earth is $\leq$0.3°.

This ring brightening is due to coherent back scattering of sunlight by µ-sized icy particles that make up the rings, scattering light far more efficiently than the particles of Saturn's atmosphere. The Seeliger effect is exhibited on the opposition date image shown in *Figure 6*.

Shadow of the Rings on the Globe (Sh R on G). The Sh R on G, when normally seen or imaged under the correct geometric circumstances in 2016-2017, was designated by observers in good seeing as a fully black shadow situated where the rings crossed Saturn's globe. Those very few instances when the shadow appeared as grayish-black, a departure from an overall black (0.0) intensity, occurred for the same reason as previously noted in our discussion regarding the Sh G on R.

When **B** and **B'** are both positive, and the value of **B** is *greater* than that of **B'**, the geometric circumstances that occurred from January 22, 2017 (the earliest observation this apparition) through January 27, 2017 and then again from July 26, 2017 thru November 21, 2017 (the last observation during 2016-17), the ring shadow (Sh R on G) was positioned to the north of the projected rings [refer to *Illustration 035*]. Care must be taken not to confuse the ring shadow with the nearby Crape Band.

When **B** and **B'** are both positive, and the value of **B** is *less* than of **B'**, the shadow of the rings on the globe (Sh R on G) is cast to their south, circumstances that occurred starting January 31, 2017 through July 25, 2017.

It should be pointed out that, since the rings blocked views of the southern hemisphere of the globe, it was not favorable to see the Sh R on G during that time period.

Terby White Spot (TWS). The TWS is an apparent brightening of the rings immediately adjacent to the Sh G on R. There were only a handful of instances when visual observers suspected this spurious feature during 2016-17. The TWS is an artificial contrast effect and not an intrinsic feature of Saturn's rings, but it is helpful to try to find any correlation that might exist between the visual numerical relative intensity of the TWS and the varying tilt of the rings, including its brightness and visibility using variable-density polarizers, color filters and digital images.

Bicolored Aspect of the Rings and Azimuthal Brightness Asymmetries. The bicolored aspect of the rings is an observed difference in coloration between the East and West ansae (IAU system) when systematically compared with alternating W47 (where W denotes the Wratten filter series), W38, or W80A (all blue filters) and W25 or W23A (red filters).

Michael E. Sweetman reported a bicolored aspect where the East ansa was considered brighter than the West ansa with a W80A (blue) blue filter, but both ansae appeared of equal brightness with a W23A (light red) filter in good seeing on July 1, 2017 from 07:48UT to 08:15UT. This observation was the only instance when a bicolored aspect was reported during 2016-2017, although in recent years observers have been systematically attempting to document the presence of the bicolored aspect of the rings using digital imagers.

In the past, there have been rare instances when the phenomenon was allegedly photographed, and of particular importance would be images of the bicolored aspect at the same time it is sighted visually, especially when it occurs independent of similar effects on the globe of Saturn (which would be expected if atmospheric dispersion were a contributing factor). Such simultaneous visual observations cannot be stressed enough so that more objective confirmation of the bicolored aspect of the rings can occur.

Professional astronomers are well-acquainted with Earth-based sightings of azimuthal variations in the rings (initially confirmed by Voyager spacecraft), which probably is a consequence of light-scattering by denser-than-average clumps of particles orbiting in Ring A. ALPO Saturn observers are encouraged to try to image any azimuthal brightness asymmetries in Ring A, preferably at the same date that visual observers report it. There were no reports of this phenomenon during 2016-2017.

Saturn's Satellites

Many of the planet's satellites show tiny fluctuations in visual magnitude as a result of their varying orbital positions relative to the planet and due to asymmetries in distribution of surface markings on a few. Despite close proximity sensing by spacecraft, the true nature and extent of all of the observed satellite brightness variations is not completely understood and merits further investigation.

Visual Magnitude Estimates and Photometry. ALPO Saturn Section observers in 2016-17 conducted no systematic visual magnitude estimates of Saturn's satellites using suggested ALPO Saturn Section methodology.

Although photometry has largely replaced visual magnitude estimates of

Saturn's moons, visual observers should still try to establish the comparative brightness of a satellite relative to reference stars of calibrated brightness when the planet passes through a field of stars that have precisely known magnitudes. To do this, observers need to employ a good star atlas that goes faint enough and an accompanying star catalogue that lists reliable magnitude values. A number of excellent computer star atlases exist that facilitate precise plots of Saturn's path against background stars for comparative magnitude estimates.

The methodology of visually estimating satellite magnitudes is simple. It starts with selection of at least two stars with well-established magnitudes and those that have about the same color and brightness as the satellite. One of the stars chosen should be slightly fainter and the other a little brighter than the satellite so that the difference in brightness between the stars is roughly 1.0 magnitude. This makes it easy to divide the brightness difference between the two comparison stars into equal magnitude steps of 0.1.

To estimate the visual magnitude of the satellite, simply place it along the scale between the fainter and brighter comparison stars. In the absence of suitable reference stars, however, a last resort alternative is to use Saturn's brightest satellite, Titan, at visual magnitude 8.4. It is known to exhibit only subtle brightness fluctuations over time compared with the other bright satellites of Saturn that have measured amplitudes.

Some observers have begun using digital imagers with adequate sensitivity to capture the satellites of Saturn together with nearby comparison stars, thereby providing a permanent record to accompany visual magnitude estimates as described above.

Images of the positions of satellites relative to Saturn on a given date and time are worthwhile for crosschecking against ephemeris predictions of their locations and identities. It is important to realize, however, that the brightness of satellites and comparison stars on digital images will not necessarily be the same as visual impressions because the peak wavelength response of the CCD chip is typically different from that of the eye.

Observers who have photoelectric photometers may also contribute measurements of Saturn's satellites, but they are notoriously difficult to measure owing to their faintness compared with the planet itself. Rather sophisticated techniques are required to correct for scattered light surrounding Saturn and its rings.

Images of Saturn's Satellites. During the 2016-2017 apparition, several observers made attempts to capture images of several of the satellites of Saturn. For example, in the image provided by Trevor Barry on August 16, 2017 at 11:21 UT using a 685nm IR filter, Enceladus, Tethys, and Dione are seen [refer to *Illustration 036*]. It would be interesting to see if other observers can achieve similar results in future apparitions.

Spectroscopy of Titan. Since 1999 observers have been urged to attempt spectroscopy of Titan whenever possible as part of a cooperative professional-amateur project. Although Titan has been studied by the Hubble Space Telescope (HST), very large Earth-based instruments, and at close range the ongoing *Cassini-Huygens* mission, opportunities continue for amateurs to contribute systematic observations using appropriate instrumentation.

Thanks to the *Cassini-Huygens* mission starting in 2004 and ending in 2017), we now know that Titan is a very dynamic world with transient and long-term variations. From wavelengths of 300nm to 600nm, Titan's hue is dominated by a reddish methane (CH_4) atmospheric haze, and beyond 600nm, deeper CH_4 absorption bands appear in its spectrum. Between these CH_4 wavelengths are “portals” to Titan's lower atmosphere and surface, so regular monitoring in these regions with photometers or spectrophotometers is a useful complement to professional work.

Long-term studies of Titan's brightness from one apparition to the next is meaningful in helping shed light on Titan's known seasonal variations. Observers with suitable equipment are being asked to participate in these professional-amateur projects, and further details can be found on the Saturn page of the ALPO website at http://www.alpo-astronomy.org/ as well as directly from the ALPO Saturn Section.

Simultaneous Observations

Simultaneous observations, or studies of Saturn by individuals working independently of one another at the same time and on the same date, offer unparalleled chances for verification of ill-defined or traditionally controversial phenomena. Such corroborating observations are valuable and helpful to strengthen the objectivity of the data received.

The ALPO Saturn Section strongly encourages such efforts to increase the likelihood of solid conformational work, and accordingly, the ALPO Saturn Section has organized a simultaneous observing team so that several individuals in reasonable proximity to one another can maximize opportunities for viewing and imaging Saturn on any given night using similar equipment and methodology. These efforts significantly reinforce the level of confidence in the data submitted for each apparition.

Pro-Am Opportunities

ALPO Saturn Section involvement in professional-amateur (Pro-Am) projects continued in 2016-2017 in support of the ongoing *Cassini* mission with ALPO observers submitting images of discrete phenomena on the globe of Saturn.

Readers of this Journal should remember the combined efforts of amateurs and professionals in keeping track of the dynamic, brilliant NTrZ white storm raging on Saturn during the well-observed 2010-2011 apparition.

Pro-Am cooperation in the *Cassini* mission continued during the 2016-2017 apparition as NASA's unprecedented close-range surveillance of the planet ended after nearly thirteen years. *Cassini* began imaging Saturn at close range on April 1, 2004, and entered orbit on 1 July 2004. It concluded its remarkable odyssey on September 15, 2017, when it plunged into Saturn's atmosphere. For years to come, however, planetary scientists will be carefully studying the vast database of images and results gleaned from the *Cassini* mission. ALPO Saturn observers who were participating in our on-going Pro-Am activities made attempts to image Saturn on the date of the impact of the *Cassini* spacecraft with Saturn.

For example, given that the confirmed loss of signal and thus "end of mission" was at 11:55:46 UT on September 15, 2017, Trevor Barry contributed a 685nm IR image while monitoring Saturn continuously for six full minutes, covering three minutes on either side of the predicted loss of signal, thereby imaging the planet from 11:53:40 UT through 11:57:46 UT with subsequent processing of the data to produce an image with the midpoint of precisely 11:55:46 UT, although the actual impact was not detected because the impact zone had already rotated out of view [refer to *Illustration 037*].

Ever since Cassini started observing Saturn at close range in April 2004 and until the mission ended in 2017, digital images at wavelengths ranging from 400nm to 1μ were actively sought by the professional community from amateurs. Pro-Am cooperation continues as a project of high significance, even though the mission has concluded. Advanced observers continue to be encouraged to submit images using classical broadband filters (for instance, Johnson system: B, V, R and I) with apertures upwards of 30.5 cm (12.0 in.) or larger, in addition to imaging through an 890-nm narrow band CH_4 (methane) filter.

Therefore, to sustain our Pro-Am work following closure of the *Cassini* mission, ALPO Saturn observers are asked to pursue diligent systematic patrol of the planet every clear night for individual features, keeping track of their motions, locations and morphology. These reports provide input concerning interesting large-scale targets to alert the professional community as our Pro-Am endeavors continue for years to come.

In addition, visual observers with apertures ranging upwards from about 15.2 cm (6.0 in.) can play a very meaningful role by making routine visual numerical relative intensity estimates and recording suspected variations in belt and zone reflectivity's (that is, intensity) and color. Up until the time that the mission concluded, the *Cassini* team combined ALPO Saturn Section images with data from the Hubble Space Telescope and from other professional ground-based observatories for in depth study.

As a means of facilitating and stimulating active Pro-Am observational cooperation, readers are asked to contact the ALPO Saturn Section with any questions as to how they can share their observational reports, drawings, and images of Saturn and its satellites with the professional community. The author is always pleased to offer guidance to novices, as well as observers that are more experienced. A meaningful resource for novices to learn how to observe and develop skill in recording data on Saturn is the ALPO Lunar & Planetary Training Program, and it is recommended that beginners take advantage of this valuable educational resource.

Conclusions

Although the number of visual numerical relative intensity estimates was fewer than usual during 2016-2017, features of Saturn's globe seemed marginally lighter in appearance compared with the immediately preceding apparition. Saturn's southern hemisphere during 2016-17 was blocked from our view by the rings with the exception of the yellowish-white Equatorial Zone (EZs) just to the south of where the Equatorial Band (EB) crossed the globe.

Activity within Saturn's northern hemisphere throughout the 2016-2017 apparition included features such as recurring white spots within the Equatorial Zone, northern half (EZn), the Equatorial Zone, southern half (EZs), North Tropical Zone (NTrZ), the North Temperate Zone (NTeZ), and occasional white spots in the North Equatorial Belt Zone (NEBZ), North Equatorial Belt, northern component (NEBn), and the North North Temperate Zone (NNTeZ). Small sporadic dark spots were occasionally detected in the Equatorial Band (EB) during 2016-2017 as was a possible poorly defined dark spot in the North Polar Region (NPR). Nearly all of these atmospheric features were successfully imaged by observers at various wavelengths as exemplified in the images provided in this report.

Observations of the major ring components, including Cassini's and Encke's divisions, plus occasional views of Keeler's division (A8) and "intensity minima" in Ring B, were even more favorable this apparition because of the improved inclination of Saturn's rings toward Earth since the last apparition. One observer used standard visual procedures for trying to confirm any bi-colored aspect of the rings during the 2016-2017 observing season, but there were no other reports of the phenomenon by visual observers, and its presence on digital images was not noticeable.

ALPO Saturn Section observers studying the planet by visual methods or through routine digital imaging of the planet at various wavelengths kept active participation alive in our Pro-Am efforts supporting the ongoing Cassini mission during the 2016-2017 observing season. Digital imaging, which now occurs as routinely as visual studies of Saturn, frequently divulges minute detail on the globe and in the rings below the normal visual threshold. With a combination of both observational methods, opportunities markedly increase for detecting changes on Saturn during any given apparition. Because of their sensitivity, digital imagers help detect outbursts of activity that visual observers might ultimately try to study with their telescopes. This helps establish limits of visibility of discrete features in integrated light and at various wavelengths.

With regard to Saturn's satellites, during the 2016-2017 apparition observers did not submit magnitude estimates.

Acknowledgements

The author truly appreciates all of the efforts by dedicated observers mentioned in this report in submitting their excellent drawings, digital images, descriptive reports, simultaneous observations, and visual numerical relative intensity estimates during 2016-2017. Regular systematic observational work highly enriches our pursuits and reinforces Pro-Am collaboration we try to better understand Saturn as a planet. Observers everywhere are encouraged to join us in our activities in upcoming apparitions.

References

Alexander, A.F. O'D. (1962). *The Planet Saturn*. London: Faber and Faber. http://www.amazon.com/planet-Saturn-history-observation-discovery/dp/B0006AYB=82U

Benton, J.L. Jr, (2005). *Saturn and How to Observe It*. London: Springer-Verlag. http://www.amazon.com/Saturn-Observe-Astronomers-Observing-Guides/dp/1852338873/ref=sr_1_1/105-9507435-7968466?ie=UTF8&s=books&qid=1183915123&sr=1-1

__________ (1996). *Visual Observations of The Planet Saturn: Theory and Methods (The Saturn Handbook)*. Savannah, GA: Review Publishing Company, 1996 (Eighth Revised Edition — now available in pdf format: http://alpo-astronomy.org/gallery3/index.php/Publications-Section/ALPO-Monographs/ALPO-Monograph-14-Theory-and-Methods-for-Visual-Observations-of-Saturn

___________ (2014). "ALPO Observations of Saturn during the 2010-2011 Apparition", *Journal of the Assn of Lunar & Planetary Observers*, Vol. 56, No. 2: pp. 31-66. http://www.alpo-astronomy.org/gallery3/var/albums/Publications-Section/ALPO-Journals/DJALPO-2014/DJALPO56-2-Spring2014.pdf?m=1521160755

___________ (2015). "ALPO Observations of Saturn during the 2011-2012 Apparition", *Journal of the Assn of Lunar & Planetary Observers*, Vol. 57 No. 2: pp. 48-74. http://www.alpo-astronomy.org/gallery3/var/albums/Publications-Section/ALPO-Journals/DJALPO-2015/DJALPO57-2-Spring2015.pdf?m=1521160812

___________ (2016). "ALPO Observations of Saturn during the 2012-13 Apparition", *Journal of the Assn of Lunar & Planetary Observers*, Vol. 58 No. 4: pp. 53-80. http://www.alpo-astronomy.org/gallery3/var/albums/Publications-Section/ALPO-Journals/DJALPO-2016/DJALPO58-4-Autumn2016.pdf?m=1529263065

___________ (2018). "ALPO Observations of Saturn during the 2013-14 Apparition", *Journal of the Assn of Lunar & Planetary Observers*, Vol. 60 No. 4: pp. 74-92. http://www.alpo-astronomy.org/gallery3/var/albums/Publications-Section/ALPO-Journals/DJALPO-2018/JALPO60-4-Autumn-2018.pdf?m=1545337392

___________ (2019). "ALPO Observations of Saturn during the 2014-15 Apparition", *Journal of the Assn of Lunar & Planetary Observers*, Vol. 61 No. 4: pp. 64-84. http://www.alpo-astronomy.org/gallery3/var/albums/Publications-Section/ALPO-Journals/DJALPO-Volume-61-%282019%29/JALPO61-4-Autumn-2019.pdf?m=1578161895

___________ (2020). "ALPO Observations of Saturn During the 2015-16 Apparition", *Journal of the Assn of Lunar & Planetary Observers*, Vol. 63 No. 4, pp. 68-88.

Lissauer, Jack J, and de Pater, Imke (2013). *Fundamental Planetary Science*. New York: Cambridge University Press. http://www.amazon.com/dp/052161855X/?tag=mh0b-2-&hvadid=4162391626&ref=pr_sl_7lqawqcmqg_e

United States Naval Observatory, Astronomical Almanac. Washington: U.S. Government Printing Office.. 2016 edition available at: https://bookstore.gpo.gov/products/sku/008-054-00242-1

2017 edition available at: https://www.amazon.com/Astronomical-Almanac-Year-Companion-Online/dp/0707741661

ALPO Resources

People, publications, etc., to help our members

Board of Directors

http://www.alpo-astronomy.org/main/board.html

- Executive Director; Julius L. Benton, Jr., Associates in Astronomy, P.O. Box 30545, Wilmington Island, Savannah, GA 31410; jlbaina@msn.com (preferred) and jbenton55@comcast.net
- Associate Executive Director; Carl Hergenrother, 4101 North Sunnywood Place, Tuscon, AZ 85749; chergen@lpl.arizona.edu
- Member of the Board; Sanjay Limaye, University of Wisconsin, Space Science and Engineering Center, Atmospheric Oceanic and Space Science Bldg. 1017, 1225 W. Dayton St., Madison, WI 53706; sanjayl@ssec.wisc.edu
- Member of the Board; Ken Poshedly, 1741 Bruckner Ct., Snellville, GA 30078-2784; ken.poshedly@alpo-astronomy.org
- Member of the Board; Timothy J. Robertson, 195 Tierra Rejada Rd., #148, Simi Valley, CA 93065; cometman@cometman.net
- Member of the Board; Richard W. Schmude, Jr., 109 Tyus St., Barnesville, GA 30204; schmude@gordonstate.edu
- Member of the Board, Secretary/Treasurer; Matthew Will, P.O. Box 13456, Springfield, IL 62791-3456; matt.will@alpo-astronomy.org

Publications Section

http://alpo-astronomy.org/gallery3/index.php/Publications-Section

- Coordinator; Ken Poshedly (ALPO-Member-Discussion e-mail group moderator & *The Strolling Astronomer* production); 1741 Bruckner Ct, Snellville, GA 30078-2784; ken.poshedly@alpo-astronomy.org
- Assistant Coordinator; (Editor, *The Strolling Astronomer)*; Shawn Dilles, 9517 Center St., Vienna, VA 22181; shawn.dilles@alpo-astronomy.org
- Assistant Coordinator (Book reviews, *The Strolling Astronomer*); Robert A. Garfinkle, FRAS, 32924 Monrovia St., Union City, CA 94587-5433; ragarf@earthlink.net
- Assistant Coordinator (Indexer, *The Strolling Astronomer*); Michael Mattei, 11 Coughlin Rd., Littleton, MA 01460-2108; micmatt@hughes.net

Interest Sections

Outreach Section

Lunar & Planetary Training Program

http://www.alpo-astronomy/training

- Coordinator; Timothy J. Robertson, 195 Tierra Rejada Rd., #148, Simi Valley, CA 93065; cometman@cometman.net

YouTube Channel & Podcasts

https://soundcloud.com/observersnotebook

- Coordinator; Timothy J. Robertson, 195 Tierra Rejada Rd., #148, Simi Valley, CA 93065; cometman@cometman.net

Youth Activities Program

http://www.cometman.net/youth/

- Acting Coordinator; Pam Shivak, 4225 NW 32nd St., Cape Coral, FL 33993; pamelashivak@yahoo.com

Online Section

http://www.alpo-astronomy.org/

- Coordinator (ALPO website); Larry Owens, 4225 Park Brooke Trace, Alpharetta, GA 30022; larry@ceastronomy.org
- Assistant Coordinator (ALPO social media); Steven Siedentop, 1475 Holly Lake Circle; Snellville, GA 30078; sdsiedentop@gmail.com
- Acting Assistant Coordinator; Jim Tomney, 404 Dixie Dr., Towson, MD 21204; jim@tomney.com

Observing Sections

Eclipse Section

http://www.alpo-astronomy.org/eclipseblog

- Coordinator; Keith Spring, 2173 John Hart Circle, Orange Park, FL 32073; star.man13@hotmail.com

Mercury/Venus Transit Section

http://www.alpo-astronomy.org/transit

- Coordinator; Keith Spring, 2173 John Hart Circle, Orange Park, FL 32073; star.man13@hotmail.com

Meteors Section

http://www.alpo-astronomy.org/meteor

- Coordinator; Robert D. Lunsford, 14884 Quail Valley Way, El Cajon, CA 92021-2227; lunro.imo.usa@cox.net
- Assistant Coordinator; Robin Gray, P.O. Box 547, Winnemuca, NV 89446; sevenvalleysent@yahoo.com

Meteorites Section

http://www.alpo-astronomy.org/meteorite

- Coordinator; Dolores Hill, Lunar and Planetary Laboratory, University of Arizona, Tucson, AZ 85721; dhill@lpl.arizona.edu

Comets Section

http://www.alpo-astronomy.org/comet

- Coordinator; Carl Hergenrother, 4101 North Sunnywood Place, Tuscon, AZ 85749; chergen@lpl.arizona.edu
- Acting Assistant Coordinator; Michel Deconinck, Aquarellia Observatory, 5 rue des Aires, F83630 Artignosc-sur-Verdon, France; trialogmdc@yahoo.fr

Solar Section

http://www.alpo-astronomy.org/solar

- Coordinator & Scientific Advisor; Richard Hill, 10130 E. King Manor Dr., Tucson, AZ 85730; rhill@lpl.arizona.edu
- Assistant Coordinator; Pam Shivak, 4225 NW 32nd St., Cape Coral, FL 33993; pamelashivak@yahoo.com
- Acting Assistant Coordinator (new observers and ALPO Solar Section Online Image Archive contact; primary moderator ALPO Solar Section Yahoo email list); Kim Hay, 76 Colebrook Rd., RR #1, Yarker, Ontario, K0K 3N0 Canada; cdnspooky@gmail.com

Mercury Section

http://www.alpo-astronomy.org/Mercury

- Coordinator; Frank J. Melillo, 14 Glen-Hollow Dr., E-#16, Holtsville, NY 11742; frankj12@aol.com

Venus Section

http://www.alpo-astronomy.org/venus

- Coordinator; Julius L. Benton, Jr., Associates in Astronomy, P.O. Box 30545, Wilmington Island, Savannah, GA 31410; jlbaina@msn.com (preferred) and jbenton55@comcast.net

ALPO Resources

People, publications, etc., to help our members

Lunar Section

Lunar Topographical Studies Program

http://moon.scopesandscapes.com/ALPO_Lunar_Program.htm

Lunar Selected Areas Program

http://moon.scopesandscapes.com/alpo-sap.html

Lunar Banded Craters Program

http://moon.scopesandscapes.com/alpo-bcp.htm

- Coordinator; David Teske, 2162 Enon Rd., Louisville, MS 9501; drteske@yahoo.com
- Assistant Coordinator; Wayne Bailey, 14120 S. Mica Place, Tucson, AZ 85736; wayne.bailey@alpo-astronomy.org
- Assistant Coordinator; William Dembowski, 219 Old Bedford Pike, Windber, PA 15963; dembowski@zone-vx.com
- Acting Assistant Coordinator; Alberto Anunziato, Boulevard Racedo 773, 3100-Parana-Entre Rios, Argentina albertoanunziato@yahoo.com.ar

Lunar Domes Studies Program

- Coordinator; Raffaello Lena, Cartesio 144 D, 00137 Rome, Italy; raffaello.lena@alpo-astronomy.org
- Assistant Coordinator; Jim Phillips, 101 Bull St., Charleston, SC 29401-1712; thefamily90@gmail.com

Lunar Meteoritic Impacts Search Program

http://www.alpo-astronomy.org/lunar/lunimpacts.htm

- Coordinator; Brian Cudnik, 11851 Leaf Oak Drive, Houston, TX 77065; cudnik@sbcglobal.net

Lunar Transient Phenomena Program

http://www.alpo-astronomy.org/lunar/LTP.html; also http://www.LTPresearch.org

- Coordinator; Dr. Anthony Charles Cook, Institute of Mathematical and Physical Sciences, University of Aberystwyth, Penglais, Aberystwyth, Ceredigion. SY23 3BZ, United Kingdom; tony.cook@alpo-astronomy.org
- Assistant Coordinator; David O. Darling, 416 West Wilson St., Sun Prairie, WI 53590-2114; DOD121252@aol.com

Mars Section

http://www.alpo-astronomy.org/Mars

- Coordinator; Roger J. Venable, MD, P.O. Box 117, Chester, GA 31012; rjvmd@hughes.net
- Assistant Coordinator (photometry and polarimetry); Richard W. Schmude, Jr., 109 Tyus St., Barnesville, GA 30204; schmude@gordonstate.edu
- Assistant Coordinator; Jim Melka, 14176 Trailtop Dr., Chesterfield, MO 63017; jtmelka@yahoo.com

Minor Planets Section

http://www.alpo-astronomy.org/minor

- Coordinator; Frederick Pilcher, 4438 Organ Mesa Loop, Las Cruces, NM 88011; fpilcher35@gmail.com
- Scientific Advisor: Alan W. Harris, 4750 Walnut St, Suite 205, Boulder, CO 80301; harrisaw@att.net
- Scientific Advisor; Dr. Petr Pravec, Ondrejov Observatory, Astronomical Institute, Academy of Sciences, Cz-25 165 Ondrejov, Czech Republic; ppravec@asu.cas.cz
- Asteroid Photometry Coordinator; Brian D. Warner, Center For Solar System Studies, 446 Sycamore Ave, Eaton, CO 80615; brian@MinorPlanetObserver.com

Jupiter Section

http://www.alpo-astronomy.org/jupiter

- Section Coordinator - Open
- Assistant Coordinator, Apparition Reports; Richard W. Schmude Jr., 109 Tyus St., Barnesville, GA 30204; schmude@gordonstate.edu
- Assistant Coordinator, John McAnally, 2124 Wooded Acres, Waco, TX 76710; CPAJohnM@aol.com
- Assistant Coordinator, Jupiter Section Yahoo email list; Craig MacDougal, 821 Settlers Road, Tampa, FL 33613; macdouc@verizon.net

Saturn Section

http://www.alpo-astronomy.org/saturn

- Coordinator; Julius L. Benton, Jr., Associates in Astronomy, P.O. Box 30545, Wilmington Island, Savannah, GA 31410; ; jlbaina@msn.com (preferred) and jbenton55@comcast.net

Remote Planets Section

http://www.alpo-astronomy.org/remote

Coordinator; Richard W. Schmude, Jr., 109 Tyus St., Barnesville, GA 30204; schmude@gordonstate.edu

Exoplanets Section

http://www.alpo-astronomy.org/saturn

- Acting Coordinator; Jerry Hubbell, 406 Yorktown Blvd, Locust Grove, VA 22508; jerry.hubbell@alpo-astronomy.org

****

ALPO Publications

The Monograph Series

http://www.alpo-astronomy.org/publications/Monographs page.html

Publications too lengthy for publication in *The Strolling Astronomer*. All are available ONLY online as a pdf files. NONE are available any longer in hard copy format. There is NO CHARGE for any of the ALPO monographs.

- **Monograph No. 1.** *Proceedings of the 43rd Convention of the Association of Lunar and Planetary Observers. Las Cruces, New Mexico, August 4-7, 1993. 77* pages. File size approx. 5.2 mb.
- **Monograph No. 2**. *Proceedings of the 44th Convention of the Association of Lunar and Planetary Observers. Greenville, South Carolina, June 15-18, 1994. 52* pages. File size approx. 6.0 mb.
- **Monograph No. 3**. *H.P. Wilkins 300-inch Moon Map.* 3rd Edition (1951). Available as one comprehensive file (approx. 48 megabytes) or five section files (Part 1, 11.6 megabytes; Part 2, 11.7 megabytes; Part 3, 10.2 megabytes; Part 4, 7.8 megabytes; Part 5, 6.5 mb)
- **Monograph No. 4.** *Proceedings of the 45th Convention of the Association of Lunar and Planetary Observers. Wichita, Kansas, August 1-5, 1995.127* pages. Hard copy $17 for the United States, Canada, and Mexico. File size approx. 2.6 mb.
- **Monograph No. *5.*** *Astronomical and Physical Observations of the Axis of Rotation and the Topography of the Planet Mars. First Memoir; 1877-1878.*

ALPO Resources

People, publications, etc., to help our members

By Giovanni Virginio Schiaparelli, translated by William Sheehan. 59 pages. File size approx. 2.6 mb.

- **Monograph No. *6.*** *Proceedings of the 47th Convention of the Association of Lunar and Planetary Observers, Tucson, Arizona, October 19-21, 1996.20* pages. File size approx. 2.6 mb.

- **Monograph No. 7.** *Proceedings of the 48th Convention of the Association of Lunar and Planetary Observers. Las Cruces, New Mexico, June 25-29, 1997.76* pages. File size approx. 2.6 mb.

- **Monograph No. 8**. *Proceedings of the 49th Convention of the Association of Lunar and Planetary Observers. Atlanta, Georgia, July 9-11,1998.122* pages. File size approx. 2.6 mb.

- **Monograph Number 9**. *Does Anything Ever Happen on the Moon?* By Walter H. Haas. Reprint of 1942 article. 54 pages. File size approx. 2.6 mb.

- **Monograph No. 10.** *Observing and Understanding Uranus, Neptune and Pluto*. By Richard W. Schmude, Jr. 31 pages. File size approx. 2.6 mb.

- **Monograph No. 11**. *The Charte des Gebirge des Mondes* (Chart of the Mountains of the Moon) by J. F. Julius Schmidt, this monograph edited by John Westfall. Nine files including an accompanying guidebook in German. Note files sizes:
  Schmidt0001.pdf, approx. 20.1 mb;
  Schmidt0204.pdf, approx. 32.6 mb;
  Schmidt0507.pdf, approx. 32.1 mb;
  Schmidt0810.pdf, approx. 31.1 mb;
  Schmidt1113.pdf, approx. 22.7 mb;
  Schmidt1416.pdf, approx. 28.2 mb;
  Schmidt1719.pdf, approx. 22.2 mb;
  Schmidt2022.pdf, approx. 21.1 mb;
  Schmidt2325.pdf, approx. 22.9 mb;
  SchmidtGuide.pdf,approx. 10.2 mb

- **Monograph No. 12.** *Solar Activity from 2014 through 2016* (subtitled *An unorthodox analysis of solar activity during three years, on the way to solar minimum*) by Theo Ramakers. Documents the research done to evaluate the relationship between the Wolf number indicator used to identify solar activity in many amateur solar reports and the size of the areas which Active Regions occupy during times of high solar energy."

- **Monograph No. 13.** *A Manual for Observing the Moon: The ALPO Lunar Selected Areas Program* by Dr. Julius Benton. Second update to original 1994 edition. Intended for serious enthusiasts who want to seriously contribute to lunar science through participation in the specialized efforts of the ALPO Lunar Selected Areas Program (which now includes the Dark Haloed Craters Program (DHCP) and the Bright and Banded Craters Program (BBCP). The handbook includes fundamental methods and techniques for conducting systematic observations of specific types of lunar features, including remarks on the lasting value of current lunar visual observations by amateur astronomers with Earth-based telescopes.

- **Monograph No. 14.** *Theory and Methods for Visual Observations of Saturn* by Dr. Julius Benton. Intended for the individual who seeks to gain an understanding of the observational theory and methodology involved in pursuing a worthwhile program of observing Saturn, its ring system, and accompanying satellites. The methods and techniques presented will hopefully be instructive and helpful to the observer who wishes to produce the most useful and reliable data possible for analysis, whether one is conducting a purely visual program or utilizing digital imagers to capture images of Saturn at various wavelengths.

- **Monograph No. 15.** *A Guide for Visual Observations of the Planet Venus* by Dr. Julius Benton. Update to the original 2016 edition. Intended for the individual who seeks to gain an understanding of the observational theory and methodology involved in pursuing a worthwhile program of observing the planet Venus. This small (65-page) handbook has been written for the amateur astronomer who wants to pursue an organized program of systematic visual observations of this planet, a beautiful but exceedingly difficult object to observe.

ALPO Observing Section Publications

Order the following directly from the appropriate ALPO section recorders; use the address in the listings pages which appeared earlier in this booklet unless another address is given.

- **Solar:** *Guidelines for the Observation of White Light Solar Phenomena*, *Guidelines for the Observing Monochromatic Solar Phenomena* plus various drawing and report forms available for free as pdf file downloads at *http://www.alpo-astronomy.org solarblog*.

- **Lunar & Planetary Training Section:** *The Novice Observers Handbook* $15. An introductory text to the training program. Includes directions for recording lunar and planetary observations, useful exercises for determining observational parameters, and observing forms. Available as pdf file via e-mail or send check or money order payable to Timothy J. Robertson, 195 Tierra Rejada Rd., #148, Simi Valley, CA 93065; e-mail *cometman@cometman.net*.

- **Lunar:** (1) *The ALPO Lunar Selected Areas Program Handbook* (hardcopy, $17.50). Includes full set of observing forms. (2) *Observing forms*: Send a SASE for a hardcopy of forms. Both the Handbook and individual observing forms are available for download (as pdf files) at *moon.scopesandscapes.com/alpo-sap.html*. Use of observing forms will ensure that all requested information is included with observations, but are not required. Various lists and forms related to other Lunar section programs are also available at *moon.scopesandscapes.com*. NOTE: Observers who wish to make copies of the observing forms may instead send a SASE for a copy of forms available for each program. Authorization to duplicate forms is given only for the purpose of recording and submitting observations to the ALPO lunar SAP section. Observers should make copies using high-quality paper.

- **Lunar**: *The Lunar Observer*, official newsletter of the ALPO Lunar Section, published monthly. Free at *http://moon.scopesandscapes.com/tlo.pdf* or

ALPO Resources

People, publications, etc., to help our members

send SASE to: Wayne Bailey, 17 Autumn Lane, Sewell, NJ 08080.

- **Venus (Benton):** Introductory information for observing Venus, the comprehensive *ALPO Venus Handbook*, as well as all observing forms and ephemerides, can be conveniently downloaded as pdf files at no cost to ALPO members and individuals interested in observing Venus as part of our regular programs at *http://www.alpo-astronomy.org/venus*.

- **Mars:** Free resources are on the ALPO website at *www.alpo-astronomy.org* . Click on "Mars Section" in the left column; then on the resulting webpage, look for links to resources in the right column including "Mars Observing Form", and "Mars Links". Under "Mars Links", click on "Mars Observers Cafe", and follow those links to The New "Internet Mars Observer's Handbook."

- **Minor Planets (Derald D. Nye):** *The Minor Planet Bulletin*. Published quarterly; free at *http://www.minorplanetobserver.com/mpb/default.htm*. Paper copies available only to libraries and special institutions at $24 per year via regular mail in the U.S., Mexico and Canada, and $34 per year elsewhere (airmail only). Send check or money order payable to "Minor Planet Bulletin", c/o Derald D. Nye, 10385 East Observatory Dr., Corona de Tucson, AZ 8564I-2309.

- **Jupiter:** *(1) Jupiter Observer's Handbook*, from the Astronomical League Sales, temporarily out of stock. (2) *ALPO_Jupiter*, the ALPO Jupiter Section e-mail network; to join, send a blank e-mail to *ALPO_Jupiter-subscribe@yahoogroups.com* (3) *Jupiter Observer's Startup Kit*, $3 from Richard Schmude, Jupiter Section Coordinator.

- **Saturn (Benton):** Introductory information for observing Saturn, including all observing forms and ephemerides, can be conveniently downloaded as pdf files at no cost to ALPO members and individuals interested in observing Saturn as part of our regular programs at *http://www.alpo-astronomy.org/saturn*. The former *ALPO Saturn Handbook* was replaced in 2006 by *Saturn and How to Observe It* (authored by Julius L. Benton) and it can be obtained from book sellers such as *Amazon.com*.

- **Meteors:** (1) *The ALPO Guide to Watching Meteors* (pamphlet). $3 per copy (postage & handling); check/money order to Astronomical League Sales, 9201 Ward Parkway, Suite 100, Kansas City, MO 64114; phone 816-DEEP-SKY (816-333-7759); e-mail *leaguesales@astroleague.org*. (2) *The ALPO Meteors Section Newsletter*, free (except postage), published quarterly (March, June, September and December). Send stamps, check or money order for first class postage to cover desired number of issues to Robert D. Lunsford, 14884 Quail Valley Way, El Cajon, CA 92021-2227.

Back Issues of The Strolling Astronomer

Online Issues

All issues of this Journal are available for downloading via the ALPO website through Vole 61(2019).
All indexes have been posted except for volume 61 (2019) and volume 62 (2020). The missing items will be posted as soon as possible.

To download online Journals:

1. Go to alpo-astronomy.org, then click on the "ALPO Section Galleries" link near the top of the right corner.
2. Next, click on the Publications Section icon, then click on the ALPO Journals icon.
3. Choose either the folder of indexes or the desired volume of Journals according to year.
4. Finally, click on the desired Journal to view or download.

Note that the newest four issues are available for downloading only by ALPO members.

Hard-Copy Issues

Some hard-copy back issues listed below may be out of stock with no guarantee of availability. Issues are sold on a first-come, first-served basis. Back issues are $4 each, and $5 for the current issue. Discounts available on orders over $30. Contact Secretary/Treasurer Matthew Will to order hard copies (see address under "Board of Directors,"):

$4 each:
Vol. 16 (1962) Nos. 3-4
Vol. 17 (1963) Nos. 1-2
Vol. 19 (1965) Nos. 3-4
Vol. 29 (1981-83) Nos. 1-2 and 11-12
Vol. 30 (1983-84) Nos. 1-2, 7-8, 9-10
Vol. 32 (1987-88) Nos. 3-4, 10-12
Vol. 33 (1989) Nos. 10-12
Vol. 34 (1990) Nos. 1 and 3
Vol. 35 (1991) Nos. 1, 2, and 4
Vol. 36 (1992-93) Nos. 1, 2, 3, and 4
Vol. 37 (1993-94) Nos. 1, 2, 3, and 4
Vol. 38 (1994-96) Nos. 1, 2, 3, and 4
Vol. 39 (1996-97) Nos. 1, 2, 3, and 4
Vol. 40 (1998) Nos. 2 and 3
Vol. 41 (1999) Nos. 1, 2, and 3
Vol. 42 (2000) Nos. 1 and 4
Vol. 43 (2001) Nos. 1, 2, 3, and 4
Vol. 44 (2002) Nos. 1, 2, 3, and 4
Vol. 45 (2003) Nos. 1, 2, and 3
Vol. 46 (2004) Nos. 1, 2, 3, and 4
Vol. 47 (2005) Nos. 1, 2, 3, and 4
Vol. 48 (2006) Nos. 1, 2, 3, and 4
Vol. 49 (2007) Nos. 1, 2, 3, and 4
Vol. 50 (2008) Nos. 1, 2, 3, and 4
Vol. 51 (2009) Nos. 1, 2, 3, and 4
Vol. 52 (2010) Nos. 1, 2, 3, and 4
Vol. 53 (2011) Nos. 1, 2, 3, and 4
Vol. 54 (2012) Nos. 1, 2, 3, and 4
Vol. 55 (2013) Nos. 1, 2, 3 and 4
Vol. 56 (2014) Nos. 1, 2, 3 and 4
Vol. 57 (2015) Nos. 1, 2, 3 and 4
Vol. 58 (2016) Nos. 1, 2, 3 and 4
Vol. 59 (2017) Nos. 1, 2, 3 and 4
Vol. 60 (2018) Nos. 1, 2, 3 and 4
Vol. 61 (2019) Nos. 1, 2, 3 and 4
Vol. 62 (2020) Nos. 1, 2, 3 and 4
Vol. 63 (2021) No. 1

$5: Vol. 63 (2021) No. 2 (current issue)

THE ASSOCIATION OF LUNAR & PLANETARY OBSERVERS (ALPO)

The Association of Lunar & Planetary Observers (ALPO) was founded by Walter H. Haas in 1947 and incorporated in 1990 as a medium for advancing and conducting astronomical work by both professional and amateur astronomers who share an interest in Solar System observations. We welcome and provide services for all individuals interested in lunar and planetary astronomy. For the novice observer, the ALPO is a place to learn and to enhance observational techniques. For the advanced amateur astronomer, it is a place where one's work will count and be used for future research purposes. For the professional astronomer, it is a resource where group studies or systematic observing patrols add to the advancement of astronomy.

Our Association is an international group of students that study the Sun, Moon, planets, asteroids, meteors, meteorites and comets. Our goals are to stimulate, coordinate, and generally promote the study of these bodies using methods and instruments that are available within the communities of both amateur and professional astronomers. We hold a conference each summer, usually in conjunction with other astronomical groups.

We have "sections" for the observation of all the types of bodies found in our Solar System. Section coordinators collect and study submitted observations, correspond with observers, encourage beginners, and contribute reports to our quarterly Journal at appropriate intervals. Each section coordinator can supply observing forms and other instructional material to assist in your telescopic work. You are encouraged to correspond with the coordinators in whose projects you are interested. Coordinators can be contacted either via e-mail (available on our website) or at their postal mail addresses listed in our Journal. Members and all interested persons are encouraged to visit our website at *http://www.alpo-astronomy.org*. Our activities are on a volunteer basis, and each member can do as much or as little as he or she wishes. Of course, the ALPO gains in stature and in importance in proportion to how much and also how well each member contributes through his or her participation.

Our work is coordinated by means of our quarterly periodical, the *Journal of the Assn. of Lunar & Planetary Observers* (known also as *The Strolling Astronomer*). Membership dues include a subscription to our Journal. Two versions of our Journal are distributed — a hardcopy (paper) version and an online (digital) version in portable document format (pdf) at considerably reduced cost.

Membership rates and terms are listed below (effective January 1, 2019).

- ..*$US18 – 4 issues of the digital Journal only; all countries, e-mail address required
- ..*$US32 – 8 issues of the digital Journal only; all countries, e-mail address required
- ..*$US45 – 4 issues of the paper Journal only; US, Mexico and Canada
- ..*$US84 – 8 issues of the paper Journal only; US, Mexico and Canada
- ..$US46 – 4 issues of the paper Journal only, all other countries
- ..$US86 – 8 issues of the paper Journal only, all other countries
- ..*$US75 – Sustaining Membership level, 4 issues of the digital and paper Journal, all countries
- ..*$US150 – Sponsoring Membership level, 4 issues of the digital and paper Journal, all countries
- ..*$US250 – Patron Membership level, 4 issues of the digital and paper Journal, all countries
- ..*$US500 – Benefactor Membership level, 4 issues of the digital and paper Journal, all countries
- ..*$US1,000 – Provider Membership level, 4 issues of the digital and paper Journal, all countries
- ..*$US2,500 – Funder Membership level, 4 issues of the digital and paper Journal, all countries
- ..*$US10,000 – Universal Membersship level, lifetime issues of the digital and paper Journal, all countries

For your convenience, you may join online via the via the Internet or by completing the form at the bottom of this page.

To join or renew online, simply left-click on this Astronomical League web page link:
http://www.astroleague.org/store/index.php?main_page=product_info&cPath=10&products_id=39

Afterwards, e-mail the ALPO membership secretary at *matt.will@alpo-astronomy.org* with your name, address, the type of membership and amount paid.

If using the form below, please make payment by check or money order, payable (through a U.S. bank and encoded with U.S. standard banking numbers) to "ALPO" There is a 20-percent surcharge on all memberships obtained through subscription agencies or which require an invoice. Send to: ALPO Membership Secretary, P.O. Box 13456, Springfield, Illinois 62791-3456 USA.

Please Print:
Name____
Street Address____
____
City, State, ZIP ____
E-mail Address____
Phone Number____
Please share your observing interests with the ALPO by entering the appropriate codes on the line below.
Interest____

Interest Abbreviations
0 = Sun 1 = Mercury 2 = Venus 3 = Moon 4 = Mars 5 = Jupiter 6 = Saturn 7 = Uranus 8 = Neptune 9 = Pluto A = Asteroids C = Comets D = CCD Imaging E = Eclipses & Transits H = History I = Instruments M = Meteors & Meteorites P = Photography R = Radio Astronomy S = Computing & Astronomical Software T = Tutoring & Training Program (including Youth)

Ready to Resume Travel in a Safer 2021?

Book a *Sky & Telescope* Astronomy Tour

African Stargazing Safari
Jul. 3-8, 2021
skyandtelescope.org/botswana2021

Iceland Aurora Adventure
October 2-9, 2021
skyandtelescope.org/iceland2021

Great Observatories of the American West
October 3-16, 2021
skyandtelescope.org/observatories2021

Mt. Wilson telescope image: Heven729 / Wikimedia Commons / CC-BY-SA 4.0

2021 Flight Into Totality
December 2-5, 2021
skyandtelescope.org/2021eclipseflight

Dan McGlaun / eclipse2024.org

©Vladgalenko / dreamstime.com

©Jeremy Richards / dreamstime.com

For the latest on all *S&T* tours,
in 2021 and beyond, visit:
skyandtelescope.org/astronomy-travel

SKY & TELESCOPE